Conception, Synthèse et Caractérisation de *Bis*-Azobenzènes - Leurs Applications Synthétiques et leur Incorporation dans des Polymères

Par

Hui Xiao

Thèse présentée au Département de chimie en vue

de l'obtention du grade de docteur ès science (Ph.D.)

FACULTÉ DES SCIENCES,

UNIVERSITÉ DE SHERBROOKE

Sherbrooke, Québec, Canada, Mars 2018

DESIGN, SYNTHESIS AND CHARACTERIZATION OF *BIS*-AZOBENZENES - THEIR SYNTHETIC APPLICATIONS AND INCORPORATION INTO POLYMER

by

Hui Xiao

A Thesis

Presented to the Department of Chimie

in Partial Fulfillment of the Requirements for the Degree of

Doctor of Philosophy (Ph.D.)

FACULTÉ DES SCIENCES

UNIVERSITÉ DE SHERBROOKE

Sherbrooke, Québec, Canada, Mars 2018

Mars 2018

le jury a accepté la thèse de madame Hui xiao
dans sa version finale

Membres du jury

Professeur Yves Dory
Directeur de recherche
Département de chimie

Professeur Yue Zhao
Codirecteur de recherche
Département de chimie

Professeur Jean-François Morin
Évaluateur externe
Département de chimie
Université Laval

Professeur Claude Spino
Évaluateur interne
Département de chimie

Professeur Pierre D. Harvey
Évaluateur interne
Département de chimie

Professeur Serge Lacelle
Président-rapporteur
Département de chimie

RÉSUMÉ

En raison de la commutation induite par la lumière entre leurs isomères trans et cis, les azobenzènes affichent une gamme étendue d'applications. On y retrouve des polymères sensibles aux stimuli, des indicateurs acido-basiques, des systèmes colorés, des cristaux liquides et des matériaux aux applications biomédicales. Dans les dernières décennies, de nombreuses recherches sur les azobenzènes ont été menées et ils sont devenues un sujet de plus en plus important. En particulier, la méthodologie de synthèse des dérivés d'azobenzène est devenue mature. Cependant, une méthode synthétique générale pour l'obtention des composés *bis*- et *tris*-azobenzène en une seule étape est encore manquante, et l'étude du *bis*-azobenzène est presque vierge, y compris les propriétés et les applications en solution.

Dans cette thèse, nous nous concentrons sur la conception et la préparation de *bis*-, *tris*- et de petits dérivés cycliques de l'azobenzène. Ce premier volet est suivi d'une étude plus poussée de leurs propriétés en solution. Nous explorons également la préparation et l'application de matériaux polymères d'azobenzène, réagissant à plusieurs stimulations.

Le premier chapitre décrit une stratégie efficace pour la synthèse des dérivés bis- et *tris*-azobenzène. Dans cette voie de synthèse, les *bis*- et *tris*-azobenzènes peuvent être obtenus dans un pot réactionnel, avec des produits secondaires *mono*-azobenzène. En modifiant les conditions de réaction, les rendements des composés azobenzène dépendent principalement des substituants sur les phénols et les sels de diazonium, et du rapport molaire des produits de départ. Par rapport à l'aniline non substituée, l'utilisation d'anilines avec des groupes électroattracteurs, conduisant à des sels de diazonium déficients en électrons, favorise la formation de monoazobenzènes plutôt que de *bis*-azobenzènes. En revanche, les anilines à groupements donneurs d'électrons ne sont pas efficaces au cours de la première étape conduisant à la formation de monoazobenzènes et favorisent ainsi la génération de

bis-azobenzènes. De grandes quantités d'anilines (excès de plus de deux et trois fois) sont le meilleur choix pour obtenir des *bis*- et *tris*-azobenzènes avec de bons rendements.

Dans le chapitre 2, nous décrivons une nouvelle méthode de cyclisation des *mono*- et *bis*-azobenzènes, sans lumière ultraviolette, pour former des hétérocycles à sept chaînons. Les produits de départ contiennent des groupes *ortho*-fluoro et orthophénol sur les cycles phényle des systèmes azobenzène. Le rôle du substituant fluoro est double. Il favorise la stabilité de la forme *cis* de l'azobenzène et agit comme un groupe partant lorsque son atome de carbone voisin est attaqué par le phénolate. La nature des solvants s'est avérée avoir un effet prononcé sur la réaction de cyclisation spontanée en stabilisant le complexe intermédiaire σ. La vitesse de cyclisation peut être accélérée sous l'irradiation UV et en utilisant des solvants plus polaires. En raison des tautomérisations céto-énol et des cyclisations en compétition, nous avons observé que l'évolution des spectres d'absorption UV-vis et de la couleur des solutions au fil du temps était compliqué. Il a été révélé que, pour les *ortho*-hydroxyl azobenzènes avec un atome d'*ortho*-fluor dans les solvants polaires, l'isomérisation et la cyclisation *trans*-*cis* se produisaient à la lumière du jour et que la tautomérisation céto-énol se produisait dans l'obscurité.

Dans le chapitre 3, nous avons étudié une classe de nouveaux copolymères biosensibles (photo- et thermo-) en modifiant le poly(*N*-isopropylacrylamide) (PNIPAM) avec des portions bis-azobenzène. Les copolymères ont été préparés à partir d'une copolymérisation radicalaire de *N*-isopropylacrylamide (NIPAM) et de *bis*-azobenzènes portant des substituants donneurs ou accepteurs d'électrons. Il a été constaté que les fragments *bis*-azobenzène pouvaient influencer le point de trouble de la solution aqueuse de copolymère en raison de la photoisomérisation des *bis*-azobenzènes et de la conformation de la chaîne polymère lors des photoréactions. En changeant les substituants sur les fragments *bis*-azobenzène, les solutions de copolymères présentaient un décalage du point de trouble

opposé après les photoréactions des chromophores. Lorsque les substituants sur l'azobenzène ont une influence «push-pull», les chaînes polymères préfèrent l'agrégation après l'irradiation UV, ce qui diminue le point de trouble. En revanche, le point de trouble passe à une température plus élevée lors de l'irradiation par la lumière UV lorsque les *bis*-azobenzènes portent des donneurs, ce qui est dû au fait que l'isomère cis est plus hydrophile que l'isomère trans. Cependant, l'effet de la photo-isomérisation de l'azobenzène sur le décalage du point de trouble semble être plus important sur les groupes pendants *mono*-azobenzène contenant du PNIPAM.

Mots-clés: azobenzènes, isomérisation, cyclisation, tautomérisation, polymérisation

ABSTRACT

Owing to the light-induced switching between their *trans*- and *cis*-isomers, azobenzenes display a wide range of applications including stimuli-responsive polymers, acid-base indicators, colorful systems, liquid crystals, and bio-medicals. In the past decades, much research on azobenzenes has been carried out and they have become a growing research topic. Particularly, the synthetic methodology of azobenzene derivatives has become mature. However, a general synthetic method of furnishing the *bis*- and *tris*-azobenzene compounds in one step is still lacking, and the study of *bis*-azobenzene is nearly blank including the solution properties and applications.

In this thesis, we focus on the design, and preparation of *bis*-, *tris*- and small cyclic azobenzene derivatives; followed by a further investigation of their properties in solution. We also explore the preparation and applications of azobenzene-based stimuli-responsive polymeric materials.

The first chapter describes an efficient strategy for the synthesis of *bis*- and *tris*-azobenzene derivatives. In this synthetic pathway, the *bis*- and *tris*-azobenzenes could be obtained in one pot, together with *mono*-azobenzene side products. By modifying the reaction conditions, the yields of the azobenzene compounds were mainly dependent on the substituents on the phenols and diazonium salts, and the molar ratio of starting materials. Compared with the unsubstituted aniline, the use of anilines with electron-withdrawing groups, leading to electron-deficient diazonium salts, favors the formation of *mono*-azobenzenes, rather than *bis*-azobenzenes. Whereas, anilines with electron-donating groups are not efficient during the first step leading to the formation of *mono*-azobenzene and thus favor the generation of *bis*-azobenzenes. Large amounts of anilines (over two-fold and three-fold excess), are the best choice to obtain *bis*- and *tris*-azobenzenes in good

yields.

In Chapter 2, we describe a novel method for the cyclization of *mono*- and *bis*-azobenzenes without ultraviolet light to form seven-membered heterocycles. The starting materials contain *ortho*-fluoro atom and *ortho*-phenol groups on the phenyl rings of the azobenzene systems. The role of the fluoro substituent is twofold. It promotes the stability of the *cis*-form of the azobenzene and it acts as a leaving group when its carbon atom neighbor is attacked by the phenolate. The nature of solvents was found to have a pronounced effect on the spontaneous cyclization reaction by stabilizing the σ intermediate complex. The cyclization rate could be accelerated under the UV irradiation and by using more polar solvents. Due to the competing *keto*-*enol* tautomerizations and cyclizations, we observed complicated changes in UV-vis absorption and color of solutions over time. It was revealed that, for *ortho*-hydroxyl azobenzenes with *ortho*-fluorine atom in polar solvents, the *trans*-to-*cis* isomerization and cyclization happened under daylight, and *keto*-*enol* tautomerization occurred in the dark.

In Chapter 3, we studied a class of novel dual-responsive (photo- and thermo-) copolymers by modifying Poly(*N*-isopropylacrylamide) (PNIPAM) with *bis*-azobenzene moieties. The copolymers were prepared from a free radical copolymerization of *N*-isopropylacrylamide (NIPAM) and *bis*-azobenzenes bearing electron-donating or electron-accepting substituents. It was found that *bis*-azobenzene moieties could influence the cloud point of aqueous copolymer solution due to the photoisomerization of *bis*-azobenzenes and the conformation of polymer chain upon the photoreactions. Varying substituents on *bis*-azobenzene moieties, the copolymer solutions displayed an opposite cloud point shift after the photoreactions of the chromophores. When the substituents on azobenzene have push-pull feature, the polymer chains prefer aggregation after UV irradiation, which decreases the cloud point. By contrast, the cloud point shifts to higher temperature upon UV light irradiation when the

bis-azobenzenes bears the donors, which is caused by *cis*-isomer being more hydrophilic than the *trans*-isomer. However, the effect of photoisomerization of azobenzene on the cloud point shift appears to be greater on PNIPAM containing *mono*-azobenzene pendent groups.

Keywords: azobenzenes, isomerization, cyclization, tautomerization, polymerization

ACKNOWLEDGEMENT

First of all, I would like to express my special gratitude to my supervisor, Prof. Yves Dory, for giving me the opportunity to study in his laboratory at the Université de Sherbrooke, for his continuous guidance and encouragement during my Ph.D. Without his guidance, none of the achievements presented in this thesis would have been possible. I also would like to thank my co-supervisor Prof. Yue Zhao for his guidance and discussions he provided throughout my studies. I am grateful to what they have taught me during my years in Sherbrooke. I really learned a lot from Prof. Dory and Prof. Zhao, not limited to the scientific aspects. It is a great pleasure to convey my gratitude to them in my humble acknowledgment.

I would like to thank two members of my doctoral committee, Prof. Serge Lacelle and Prof. Claude Spino. I also would like to thank Prof. Jean-François Morin (Université Laval) and Prof. Pierre D. Harvey for being part of the jury of my thesis, and all other professors and staff working in the Department of Chemistry for their help during my studies in the Université de Sherbrooke.

I would like to thank all group members, both present and past, in the Chemical Medicinal and Supermolecular Laboratory of Prof. Dory and Polymers and Liquid Crystals Laboratory of Prof. Zhao, including Ms. Xia Tong, Dr. Bing Yu, Dr. Xin Zhao, Dr. Shengwei Guo, Dr. Qiang Yan, Dr. Hu Zhang, Dr. Guo Li, Dr. Rong Yang, Dr. Weizhen Fan, Mr. Xili Lu, Mr. Jun Xiang, Mr. Feijie Ge, Mr. Liangliang Dong, Ms. Amélie Auge, Mrs. Yaoyu Xiao, Mr. Zhichao Jiang, Mr. Lu Yin, Mr. Farhad Farnia, Mr. Ricardo Amadio Da Silva Lemos, Dr. Hojjat Seyed-Jamali, Dr. Thị Thanh Hà Đào, Mrs Thi Minh Hue Tran, Mr. Thomas Marmin, Mr. Vahid Dianati, Ms. Dominique Bella Lee, Ms. Pauline Navals, Mr. Jean-louis Beaudeau for the joyful working atmosphere as well as countless helps and

discussions. Especially, I thank Ms. Xia Tong for her great support in all characterization work and great assistance in starting all my measurements in the lab. I am also grateful to all my other friends inside and outside of Sherbrooke for their generosity and encouragement that made my entire study enjoyable and memorable.

I sincerely thank the Chinese Scholarship Council (CSC) for awarding me a scholarship that made my studies in Sherbrooke possible. I would like to thank all the members of the Education Office of the Chinese Embassy in Canada, especially Mr. Shaohua Liu and Mr. Jianjun Zhai for all their help during my stay in Canada. I am also grateful to the financial support from several sources including Natural Sciences and Engineering Research Council of Canada (NSERC) that helped support my research.

Finally, I would like to thank my family for all their love and support throughout my time in Canada, especially my parents and my brother. Without your endless encouragement and support, none of this would have been possible.

TABLE OF CONTENT

LIST OF SCHEMES

LIST OF FIGURES

LIST OF TABLES

INTRODUCTION

I.1 Azobenzene molecules

I.1.1 Their structures

The azobenzene compounds (Ph-N=N-Ph) contain azo groups -N=N- separating the aryl rings,[1] that can be substituted with electron withdrawing or electron donating groups. Some azobenzene examples (**1**-**4**) are shown in Figure 1.[2] These groups can be used to modulate the color of the azobenzenes, which possess many applications in the industry as coloring agents. These aspects will be discussed more thoroughly later.

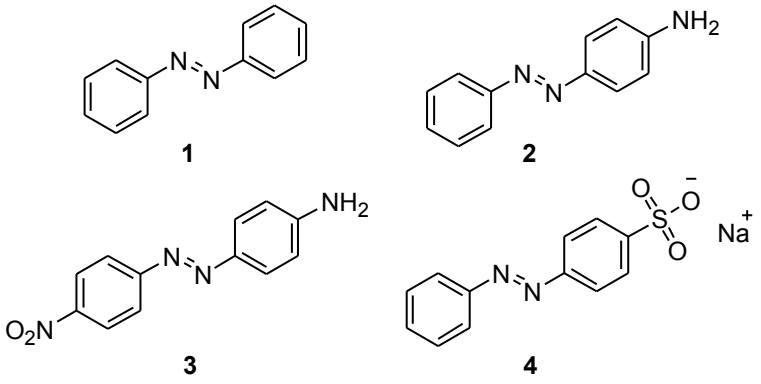

Figure 1. Structures of selected azobenzenes

I.1.1.1 Linear azobenzenes

In our knowledge, azobenzene molecules are man-made objects which do not exist in nature. Such synthetic azobenzenes are ubiquitous, which can be found almost everywhere in our daily life. Linear azobenzenes can be rather simple substituted molecules like **5** (Figure 2).

They can also incorporate naphtalene cores (**6**, **7**) and some are more complex structures as well (**8**). These four examples can be used as acid-base indicator (methyl red, **5**),[3] food additive (Sudan I, **6**),[4] Papanicolaou stain (Orange G, **7**),[5] diagnostic tools (Congo Red, **8**)[6] respectively.

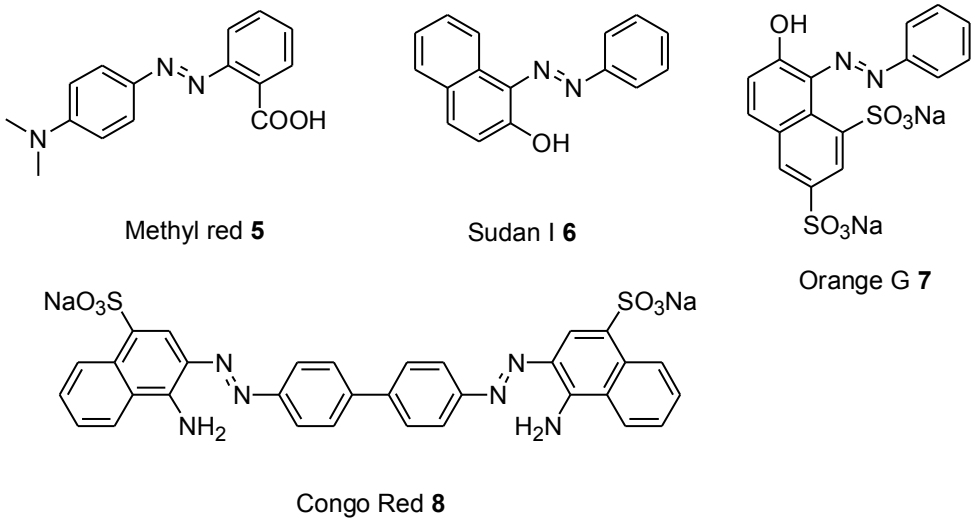

Figure 2. Chemical structures of linear azobenzene derivatives

I.1.1.2 Cyclic azobenzenes

Some azo groups are also found in small heterocyclic compounds, like **9-11**, shown in Figure 3. Many derivatives based on these simple cores have been synthesized.[7,8] Azobenzenes can also be part of much larger cycles, like cyclopeptides as in macrocycle **12** or in large crown ethers like **13**.[9]

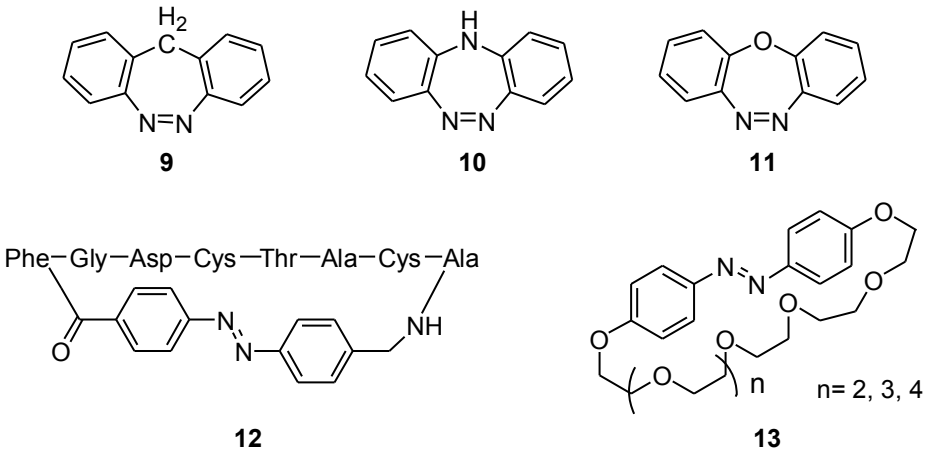

Figure 3. Chemical structures of cyclic azobenzene derivatives

I.1.2 Their discovery

The simplest azobenzene Ph-N=N-Ph was first discovered by Eilhard Mitscherlich in 1861.[10] A century later, in 1937, a study of the influence of light on the conformation of the N=N double bond was reported by Hartley.[11] It was then understood that the azo bonds can either be *trans*- or *cis*-state. This transformation is a reversible process controlled by light. However, this is not the case for alkene bonds, whose geometry (*trans*- or *cis*-) is locked.

I.1.3 Their applications

Nowadays, azobenzenes of all sorts are one of the most popular dyes in practical use. They were, in fact, investigated primarily for that purpose, because they are highly colored compounds, especially red, orange, and yellow. Moreover, they are prepared easily and cheaply. Other applications have also been discovered especially in the field of pharmacology and polymeric materials.

I.1.3.1 Dyes and pigment

As already mentioned, azobenzene compounds find numerous applications as coloring molecules. They can be used as dyes when they are soluble, or as pigments when they are not.[12] Such pigments (**14**, **15** in Figure 4) are important for paints, including artist's paints.[13] Since pigments are insoluble, they are often applied as finely ground solid particles mixed with a liquid. They have excellent coloring properties and tend to be very bright. Some typical azobenzene dyes are displayed in Figure 2. Noteworthy, it is even possible to create all possible colors from red to purple in solution as seen in Figure 5 for compounds **16-19**.[9,14] Up to date, approximately 60% of the world production of industrial dyes are constituted of azobenzenes.

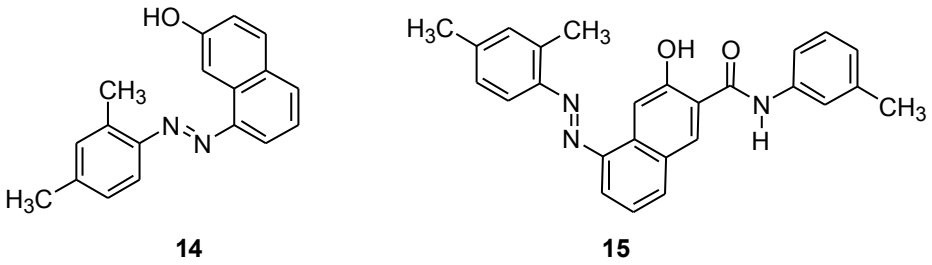

14 **15**

Figure 4. Chemical structures of azobenzene pigments

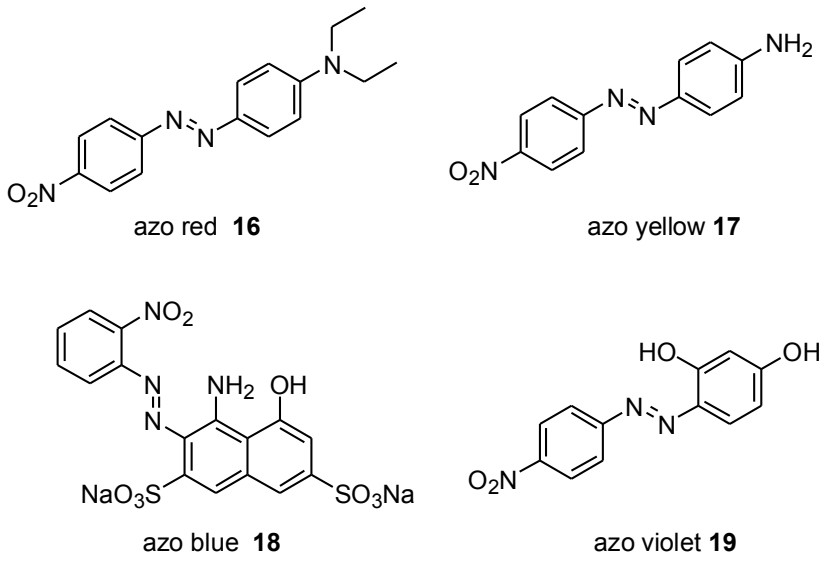

Figure 5. Chemical structures of azobenzene dyes

I.1.3.2 Drugs

The azobenzene compounds can not only be used in the industrial field, they can also find applications in medicinal area, as drug.[15] The first known drug belonging to that family was Trypan red (**20**), discovered by Paul Ehrlich as a mean to kill Trypanosomes.[16] A few years later, while looking for ways to fight bacterial infections, Gerhard Domagk investigated azobenzenes at Bayer laboratories in Germany. Prontosil **21**[15] proved to be very effective against streptococcus in Figure 6. He even used it to treat his own daughter, who was infected and who might have been amputated of an arm. Prontosil, as the first sulfonamide drug, revolutionized medicine, and Domagk was awarded the Nobel Prize in medicine in 1939 for his work.

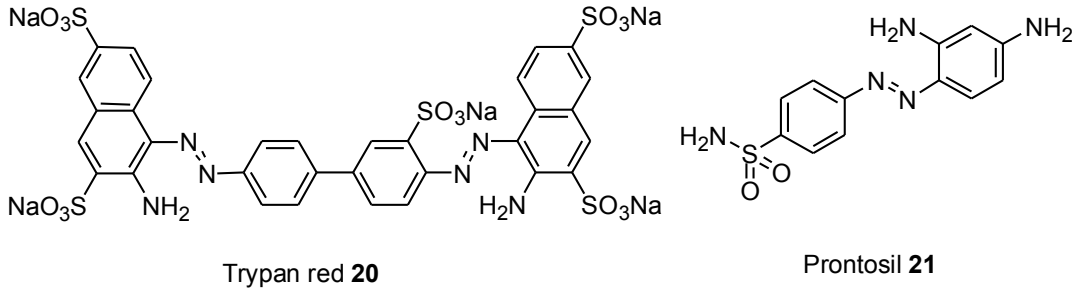

Figure 6. Chemical structures of Trypan red and Prontosil

In addition, a few small 7-membered heterocycles have also found applications as drugs or lead toward drugs. For example, the perfluorinated ring systems **22** and **23** (Figure 7) have been identified as 17a-hydroxylase-$C_{17,20}$-lyase and testosterone-5a-reductase inhibitors. Such inhibitors could find applications as cures for prostate cancer.[17]

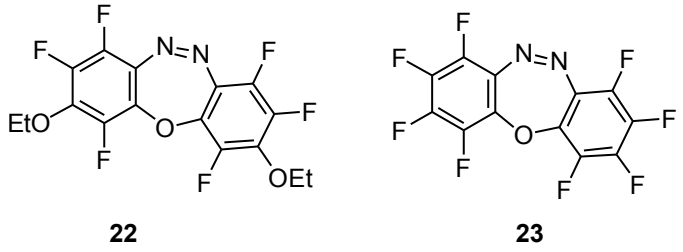

Figure 7. Biologically active small heterocycles containing azobenzenes

It is interesting to notice that, as a rule, small heterocycles having the generic formula **24-26** (Figure 8)[7,8,17-23] are topologically similar (biomimetics) to numerous biologically active compounds like some 5-oxa-10,11-diazadibenzo[*a*,*d*]cycloheptenes, **24c**, dibenzo[*b*,*f*][1,4]oxazepine, **25c**, and dibenzo[*b*,*f*]oxepine, **26c**. Therefore, it can be inferred that many molecules having the same scaffold as in **24**-**26** are likely to display valuable pharmacological properties.

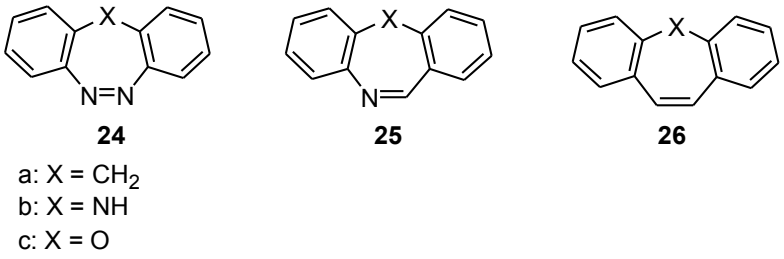

24 **25** **26**

a: X = CH_2
b: X = NH
c: X = O

Figure 8. Chemical structures of seven atoms heterocycles

I.1.3.3 Other applications

The azobenzene compounds have been attracted a great deal of attention in both industry and academia, due to their widespread applications ranging from large scale photo-switching devices[24] to *nano* scale cell biology (Figure 9).[25] Some of their noteworthy applications include, but not limited to, radical reaction initiators,[26] therapeutic agents,[27] photochemical molecular switchs,[28] ion channels (Figure 10).[29,30] Furthermore, azobenzene compounds appear to be powerful chemical tools to study living systems,[31-33] molecular machines,[34] surface-relief gratings,[35] birefringence,[36] rotors (Figure 11),[37] and so on. Some new applications have recently been reviewed.[38-41] For example, some azobenzene structures have been used in the photo pharmaceuticals area as red-light addressable units,[38,39] mesomorphic switches,[40] and electrochemical devices.[41] Hence the exploration of more efficient synthetic pathway to enlarge the diversity of azobenzene compounds is still very much in demand.[42,43]

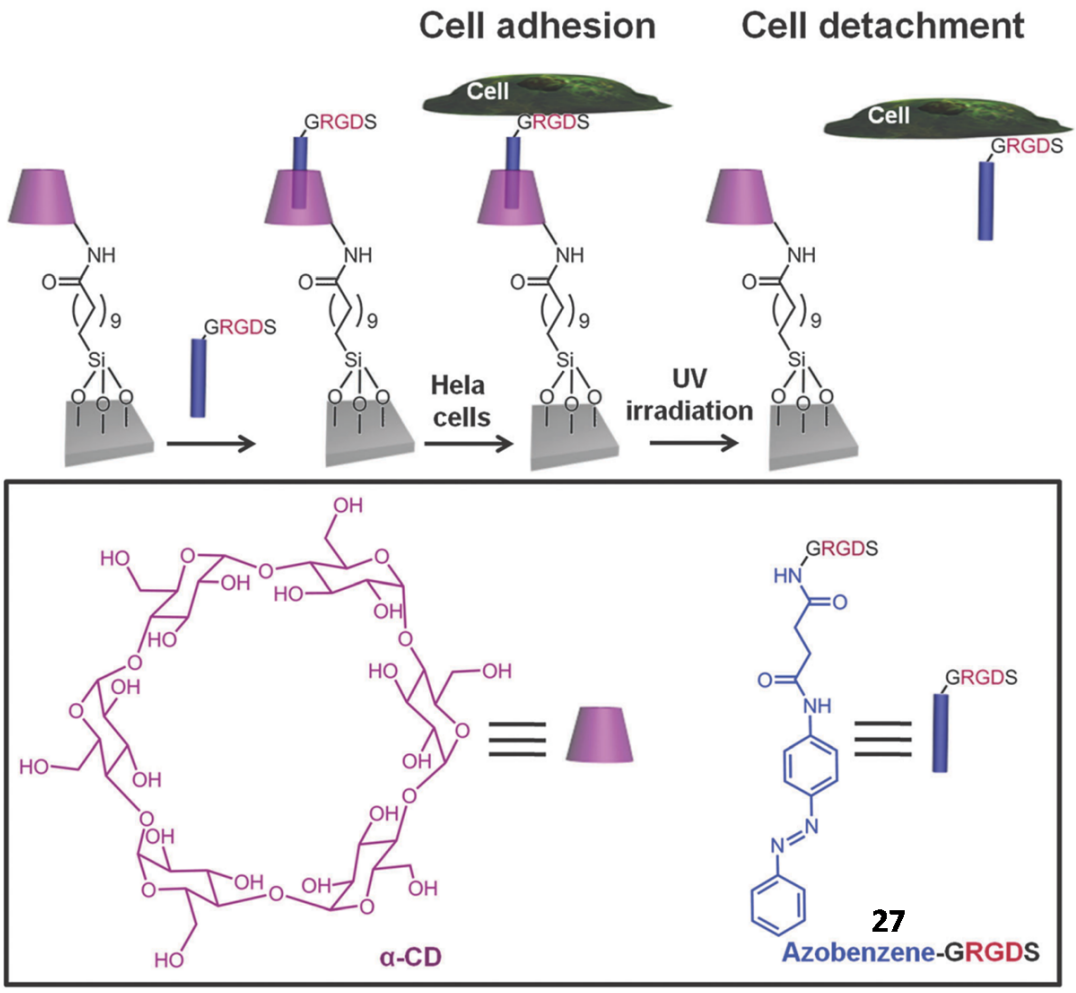

Figure 9. Schematic representation of an α-CD (cyclodextrine) terminated-silane SAM (self-assembled monolayers) which can form a complex with an azobenzene-GRGDS (Gly-Arg-Gly-Asp-Ser) peptide. Hela cells are cultured on the substrate when the azobenzene is in its *trans*-conformation. Upon UV irradiation at 365 nm, the *trans*-azobenzene undergoes isomerization to the *cis*-isomer. The *cis*-azobenzene is no longer recognized by the cyclodextrine. Consequently, the azobenzene-GRGDS and the cells both are detached from the substrate.[25]

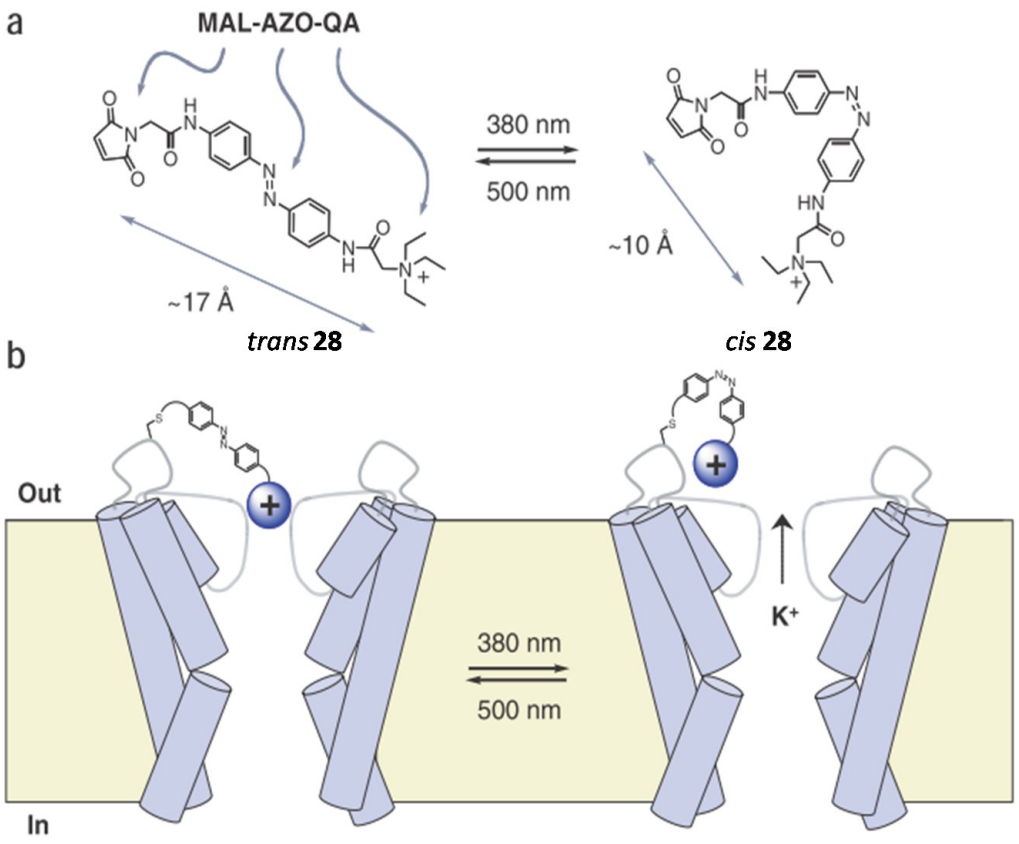

Figure 10. Photoisomerization process controlling ionic currents through modified Shaker channels. a) The shape of MAL-AZO-QA (**28**) (MALeimide-AZObenzene-Quaternary Ammonium) is controlled by light. In its *trans* geometry the molecule is very long, whereas it becomes much shorter in its *cis* form. b) The molecule is then attached to a cysteine residue of the channel rim, by Michael addition of the thiol (from Cys) onto the alkene of **28**. In its extended geometry, the ammonium part can act as a cork blocking the channel entrance. Upon irradiation (380 nm), the "stopper" is removed, and potassium cations can move freely across the channel. The process is reversible through irradiation at the proper wavelengths. Adapted with permission from reference 29.

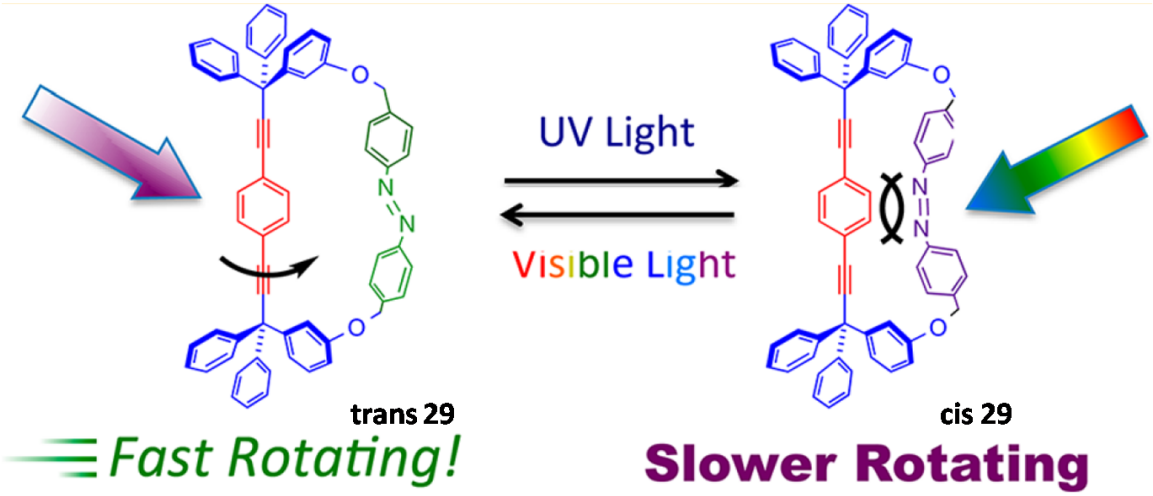

Figure 11. An idealized model of an azobenzene bridged molecular gyroscope where a change from *trans*- to *cis*-azobenzene configurations modulates the rotational motion of the central phenylene, through steric hindrance. Adapted with permission from reference 37.

I.2 Synthetic Methodology of azobenzene derivatives

I.2.1 Synthetic methods of *mono*-azobenzene derivatives

There are several synthetic methods for azobenzene derivatives, including:[44] (i) Azobenzene coupling reaction involving diazonium salts; (ii) Coupling of primary arylamines with nitroso compounds (Mills reaction); (iii) Oxidation reactions of aromatic primary amines; (iv) Reductive coupling of aromatic nitro derivatives; (v) Dehydrogenation of arylhydrazines; (vii) Copper-catalyzed arylation.

I.2.1.1 Azobenzene coupling reaction involving diazonium salts

The azobenzene coupling reaction *via* diazonium salts is one of the most useful methods for the preparation of azobenzene derivatives. It is carried out in acidic media, which involves firstly, the formation of the diazonium salt **31** by diazotization reaction at low temperature.

Then, this reactive intermediate can subsequently react with an electron-rich aromatic nucleophile **32** *via* an electrophilic coupling reaction (Scheme 1). Finally, it produces the azobenzene derivatives **33**.[45-53]

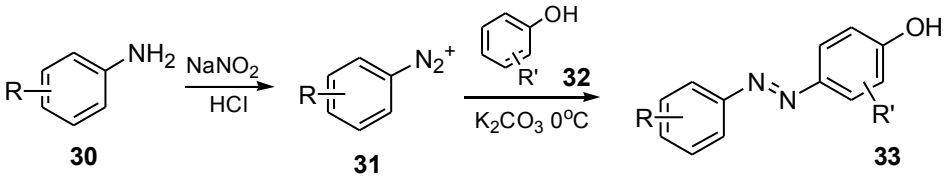

Scheme 1. Synthesis of azobenzene derivatives **33** using coupling reaction between freshly prepared diazonium salts **31** and phenols **32**

For coupling reaction, the pH of the solution acts as a very important factor for both aniline **30** and phenol **32** solutions. For the first step, the acidic medium is necessary to form the nitrous acid, with which the free aniline can react. The acidic conditions also stabilize the resulting diazonium salt product simultaneously. During the second step, the conditions are switched to become basic. In this new environment, the phenol reactant **32** produces the corresponding phenoxide ion which is then activated enough to attack the diazonium moiety of **31**. The resulting intermediate re-aromatizes readily to produce the desired azobenzene **33**.

There is a region-chemical issue during the attack of the phenolate onto the diazonium salt **31**. Only two sites are reactive on **32**, they are the *para*- and *ortho*-positions. Most of the time, the *para*-position leads to the major adducts for steric reasons. Obviously, if the *para*-position is already occupied, the phenolate will attack from its *ortho*-position.

This method presents many advantages, such as the use of simple agents, like cheap acids (eg. HCl, H_2SO_4) and bases (eg. NaOH, K_2CO_3). Moreover, this sequence of reactions offers an entry to the preparation of symmetrical or asymmetrical azobenzenes.

I.2.1.2 Coupling of primary arylamines with nitroso compounds (Mills reaction)

The diazonium route gives access to asymmetrical molecules only, unless both rings bear *para* hydroxyl groups. For the synthesis of asymmetrical as well as symmetrical azobenzene derivatives, there is another more general way.[54-66] This method, known as the Mills reactions, consists in coupling a nitrosobenzene **34** and an aniline **35** (Scheme 2).

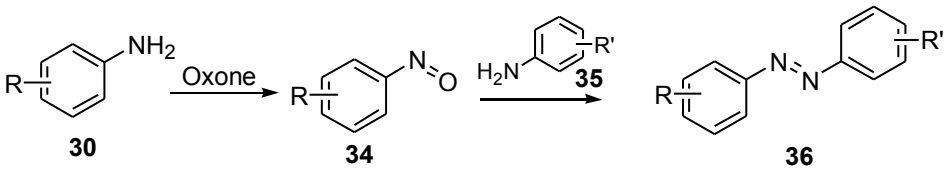

Scheme 2. Synthesis of asymmetric and symmetric azobenzenes by the Mills reaction

The oxidation of the aniline **30** into the nitroso precursor **34** can be carried out with mild oxidants such as oxone (potassium peroxymonosulfate, $KHSO_5 \cdot 0.5KHSO_4 \cdot 0.5K_2SO_4$). This type of reaction usually happens in a biphasic medium and can be catalyzed by either an acid or a base.[66] Then, **34** is condensed with a second aniline **35** in a subsequent step yielding the product **36** with concomitant elimination of water. The overall procedure is simple and high yield. Because of the lack of self-reactivity of the reacting species **34** and **35**, the method is absolutely ideal for the synthesis of asymmetrical azobenzenes. Obviously, the procedure is also perfectly adapted to the creation of symmetrical molecules. For the Mills reaction, it is notable that the different electron-withdrawing and electron-donating groups in the *ortho*-, *meta*-, and *para*-positions of both the aromatic amines and the aromatic nitroso compounds have no influence on the reaction efficiency.

I.2.1.3 Oxidation reaction of aromatic primary amines

Symmetrical azobenzene derivatives **38** (Scheme 3) can be obtained by the oxidation of

primary aromatic anilines **30** under mild conditions such as H_2O_2,[67] metal oxides (MnO_2,[68] Ag_2O,[69]), metal salts (Ag_2CO_3,[70] $NaBO_3$,[71] $Pb(OAc)_4$,[72,73] $BaMnO_4$,[74] $[Ag(C_5H_5)_2]MnO_4$,[75] bis(2,2'-bipyridyl)copper(II)permanganate),[76] nickel peroxide (Ni_2O_3).[77] Sometimes, the reactions are carried out *via* the hypervalent iodide regents like $PhI(OAc)_2$,[78] Galvinoxyl / $K_3Fe(CN)_6$ / KOH,[79] manganese (III) tetraphenylporphyrin,[80] and even aerobic oxidation (O_2-K-tBu,[81] mercury(II) oxide,[82] O_2-Cu_2Cl_2-pyridine.[83]). The most classical reaction employs HgO-I_2.[84] In this procedure, the anilines **30** are oxidized by HgO / I_2 to give the corresponding symmetrical hydrazines **37**, which are even further oxidized to afford the symmetrical azobenzene compounds **38**. The process is summarized in Scheme 3.

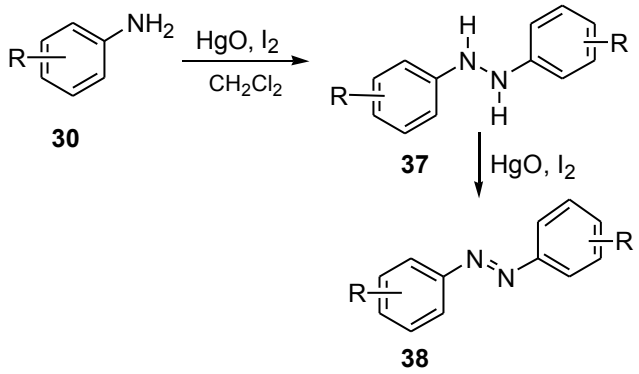

Scheme 3. Synthesis of symmetrical azobenzene derivatives by oxidation reactions

I.2.1.4 Reductive coupling of aromatic *nitro* derivatives

There is another way to synthesize symmetrical azobenzene derivatives *via* a reduction pathway involving nitro compounds by typically metal-catalyzed transfer hydrogenation. The nitrobenzenes **39** are reduced with lead powder in methanol under triethylammonium formate to firstly provide the nitroso derivative **34** and the corresponding hydroxylamine **40**. These two molecules lead to the *N,N*'-dihydroxy intermediate **42**, dehydration of this intermediate is to generate symmetrical azobenzene compounds **38** (Scheme 4).[85]

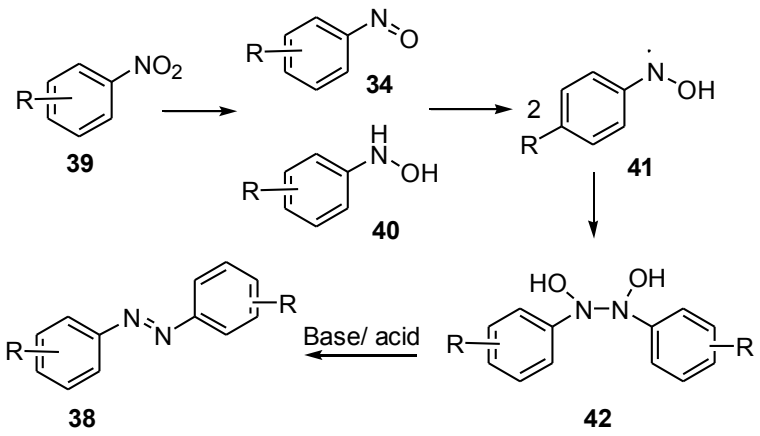

Scheme 4. Synthesis of symmetrical azobenzene derivatives by reductive coupling

I.2.1.5 Dehydrogenation of arylhydrazine

There is one of the most important methods for preparing azobenzene derivatives starting from hydrazo compounds **43** (Scheme 5). They undergo stoichiometric oxidation with H_2O_2 / $TiCl_3$[70] or other oxides such as periodate resin,[86] basic alumina / O_2,[87,88] HgO,[89,90] $Pb(OAc)_4$,[91] $FeCl_3 \cdot 6H_2O$,[92] ammonium persulphate,[93] polycationic ultraresins,[94] PEG (Polyethylene glycol)-NO_2[95] and arylsulfonyl peroxides.[96] In general, their yields are between 72% and 99%. So far, the detailed mechanism has not been clarified, but it had been suggested that radicals **44** is formed as an intermediate during the dehydrogenation leading to the corresponding azobenzenes **36**.

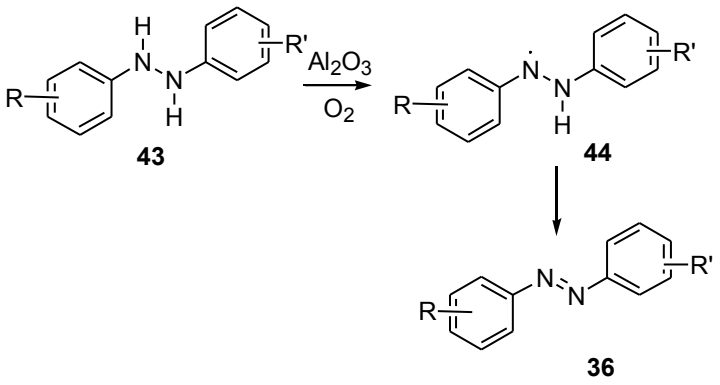

Scheme 5. Dehydrogenation of arylhydrazine

I.2.1.6 Copper-catalyzed arylation

Additionally, to the aforementioned methods, it is certainly worth mentioning Cu-catalyzed arylation of *bis*-Boc monoaryl-hydrazines **45**, that yields firstly the *bis*-Boc (*tert*-butyloxycarbonyl) diaryl-hydrazines **46**, then finally oxidized to afford azobenzenes **36** by CuI / Cs_2CO_3 (Scheme 6).[97]

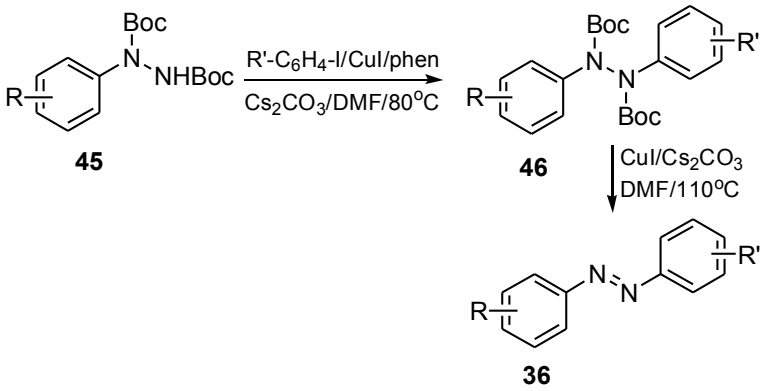

Scheme 6. Synthesis of azobenzene derivatives from *bis*-Boc aryl hydrazines

The various syntheses of azobenzene derivatives described in the literature can be summarized in a retrosynthetic scheme (Scheme 7). The azobenzene core structure can be

the result of a bond formation between one phenyl ring and one N atoms (retrosynthesis route A) or between the two N atoms (route B) leading to single-bonded N-N intermediates. Route A comprehends the diazonium reaction leading directly to azobenzene molecules, as well as the copper-catalyzed formation of hydrazines. Secondly, Route B exhibits Mills reaction, oxidation reaction of aromatic primary amines and reductive coupling of aromatic *nitro* derivatives. Finally, route C is a retrosynthetic pathway linking single-bonded N-N precursors to double-bonded N=N azobenzenes (dehydrogenation of arylhydrazine). Noteworthy, all of the above methods are one-pot reactions.

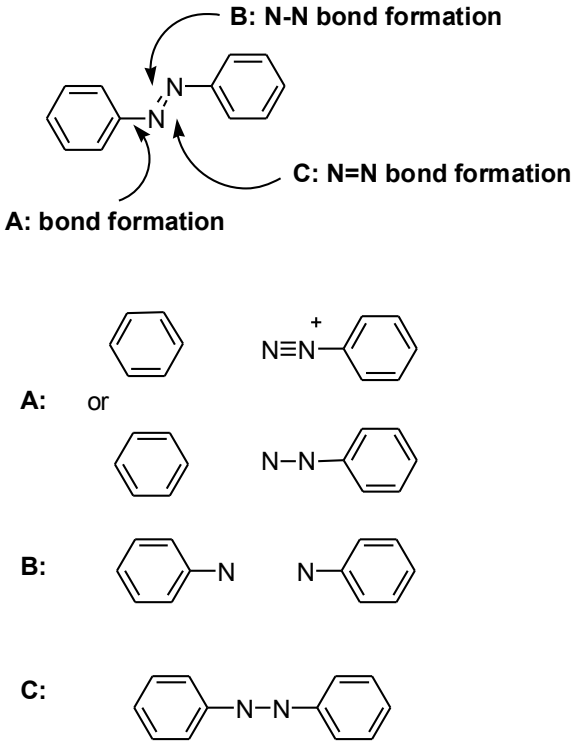

Scheme 7. The retrosynthetic pathways to the syntheses of azobenzene derivatives

I.2.2 Synthesis of *bis*-azobenzene derivatives

As mentioned above, there are a lot of ways to synthesize the *mono*-azobenzenes. Of course, there are many *bis*-azobenzenes[98-105] that can be synthesized. Schemes 8 and 9 show two

preparations of *bis*-azobenzenes **49** and **51**, which two azo moieties are remote from each other.[98,99]

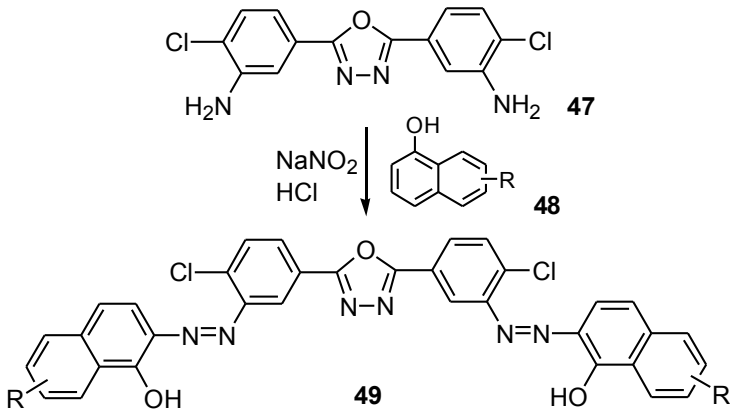

Scheme 8. Synthesis of *mono*-chloro-*s*-triazine *bis*-azobenzenes

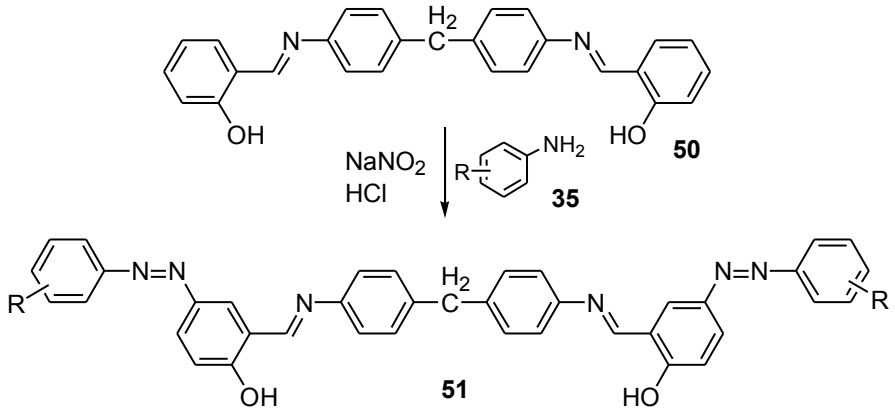

Scheme 9. Synthesis of bismethine *bis*-azobenzenes

Nevertheless, in this work we are going to limit the term "*bis*-azobenzenes" to molecules where both azobenzene groups belong to the same central aryl ring. We may consider two sorts of such *bis*-azobenzenes, namely the symmetrical ones and the asymmetrical ones. Accordingly, these two types can be prepared following different strategies. A lot of methods have been reported for the synthesis of azobenzene derivatives. However, these methods were originally devised to prepare *mono*-azobenzenes in a one-pot procedure.

Retrosynthetically, for the preparation of *bis*-azobenzene derivatives, we can consider six approaches (A-F) as shown in Scheme 10.

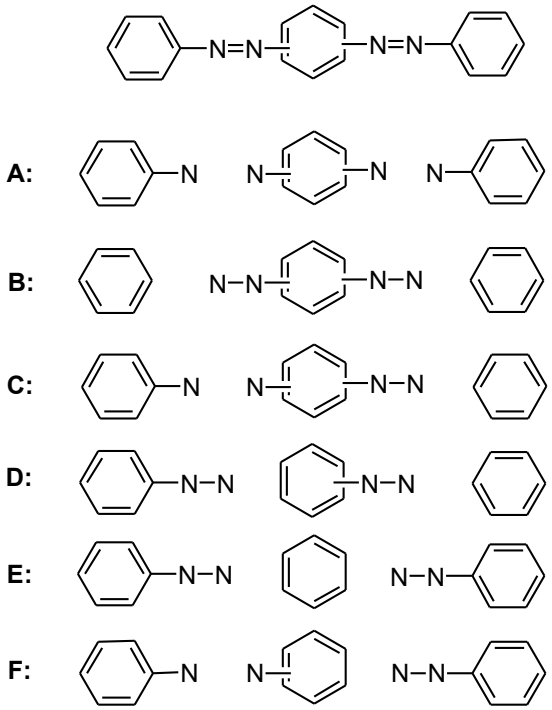

Scheme 10. The retrosynthetic pathways to the syntheses of *bis*-azobenzenes

All these methods can, in principle, open the door to symmetrical and asymmetrical azobenzenes. Nonetheless, routes A-D are more suitable to the preparation of the former molecules. A literature search revealed no synthesis based on retrosyntheses E-F; so, to the best of our knowledge, these approaches still need exploration. Rijeesh *et al*.[106,107] and Wegner *et al*.[108,109] have followed path A or path B to prepare azobenzenes (see parts **I.2.2.1** and **I.2.2.2**). Consider the retrosynthetic path C, Blackburn *et al*.[107] also prepare the asymmetrical *bis*-azobenzenes (see part **I.2.2.2**). Regarding the retrosynthetic path D, Jin, M *et al*.[110] have been using it to make unsymmetrical azobenzenes in a stepwise fashion taking advantage of two successively formed diazonium salts (see part **I.2.2.2**).

I.2.2.1 Synthesis of symmetrical *bis*-azobenzene derivatives

As shown in Scheme 11 and following retrosynthesis A, Rijeesh *et al*.[106] reported that the *bis*-amine **52** and nitrosobenzenes **34** afford *bis*-azobenzenes **53** under basic conditions (*t*-BuOK in *t*-BuOH). In addition, Blackburn *et al*.[107] considered the retrosynthetic route B, generating symmetrical *bis*-azobenzenes **56** *via* simultaneous diazonium coupling reactions from *bis*-amine **54** (Scheme 12).

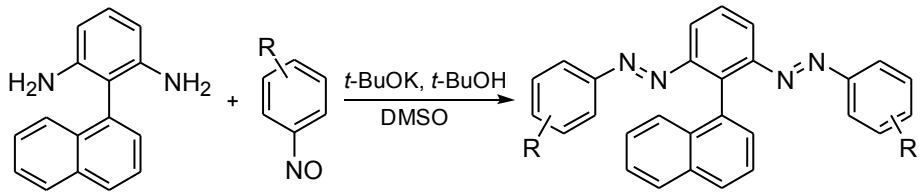

52 **34** **53**

Scheme 11. Synthesis of *bis*-azobenzene derivatives *via* simultaneous Mills reactions

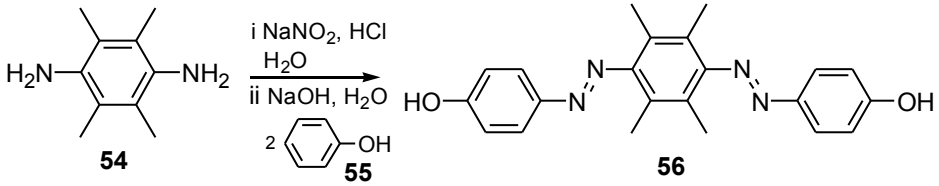

54 **55** **56**

Scheme 12. Synthesis of *bis*-azobenzene derivatives *via* simultaneous diazonium coupling reactions

I.2.2.2 Synthesis of asymmetrical *bis*-azobenzene derivatives

Wegner *et al*.[108,109] reported that the asymmetrical *bis*-azobenzenes **59** were obtained *via* two successive Mills reactions, following again the retrosynthesis path A (Scheme 13). On the other hand, Blackburn *et al*.[107] followed the retrosynthetic route C to prepare the asymmetrical *bis*-azobenzenes **62** (Scheme 14). Jin, M *et al*.[110] considered the retrosynthetic

route D while generating several asymmetrical *bis*-azobenzenes **67** *via* two diazonium coupling reactions (Scheme 15).

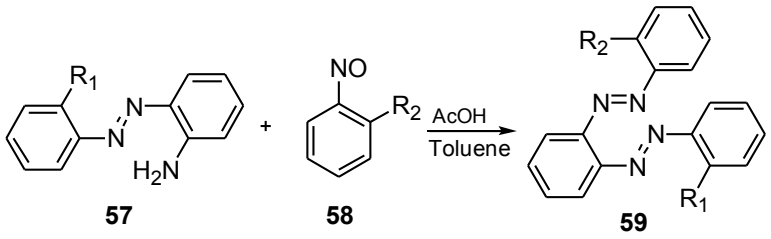

Scheme 13. Synthesis of *bis*-azobenzene derivatives with successive Mills reactions

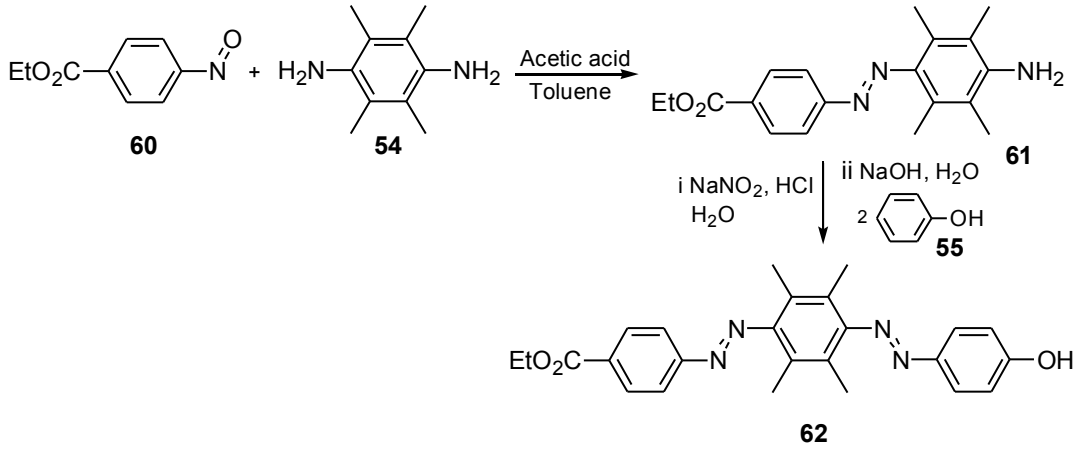

Scheme 14. Synthesis of *bis*-azobenzene derivatives with Mills reaction and then diazonium coupling reaction

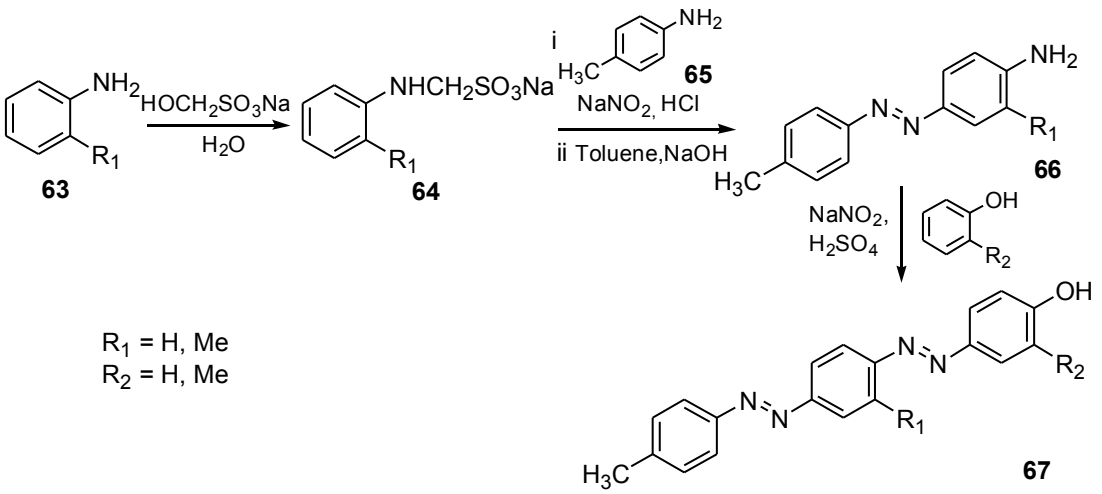

Scheme 15. Synthesis of *bis*-azobenzene derivatives with successive diazonium coupling reactions

I.2.3 Synthesis of cyclic azobenzene derivatives

The synthesis of cyclic azobenzenes can be divided into two branches according to their modes of cyclization: 1) by forming the azobenzene moiety; or 2) by forming a bond not directly linked to the azobenzene group.

I.2.3.1 Cyclization through formation of the azobenzene group

Many cyclic azobenzenes are obtained by forming the Ph-N=N-Ph moiety from *dinitro*-compounds following the chemistry described in Scheme 16.[7,111-117] Thus, this method was used by Reuter *et al*[113] to prepare switchable gels containing azobenzene macrocycles. In the same way, Biernat and his group[115] reported that the macrocyclic azobenzenes **69** could be made from *bisnitro*-compound **68** (Scheme 16). On the other hand, Brase[118] prepared the cyclic azobenzenes **71** by solid-phase synthesis (Scheme 17). In this way, the *macro*-cyclization of its precursor **70** still led to the formation of the azobenzene group.

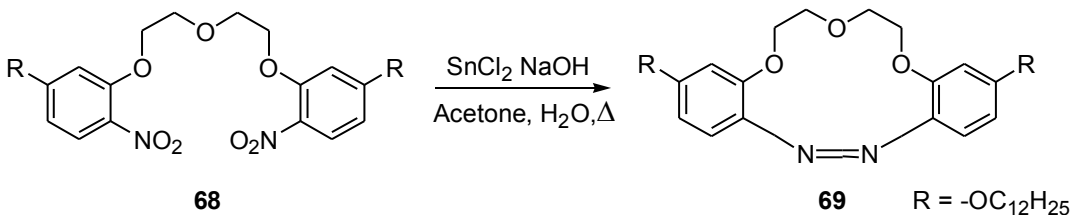

Scheme 16. Synthesis of macrocyclic azobenzene

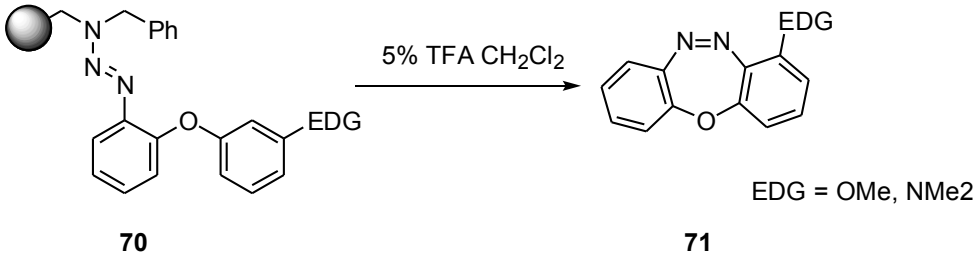

Scheme 17. Synthesis of seven atoms cyclic azobenzenes

I.2.3.2 Cyclization away from the -N=N- bond

Many methods can be used to synthesize cyclic azobenzene derivatives by cyclizing in sites remote from the -N=N- region. For example, two ether bonds were created during the formation of the cyclic azobenzenes **74** via two Mitsunobu reactions (Scheme 18),[111,119] when already has azobenzene bond. Zhu's group[119] described smart cyclic azobenzenes **76** that can be prepared by click coupling at the cyclization step (Scheme 19).

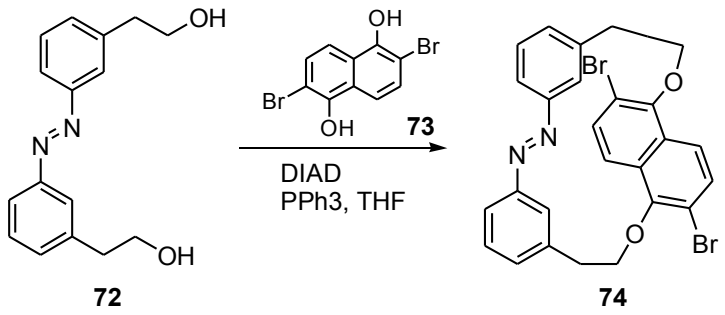

Scheme 18. Synthetic route to a cyclic azobenzene *via* Mitsunobu ether formation

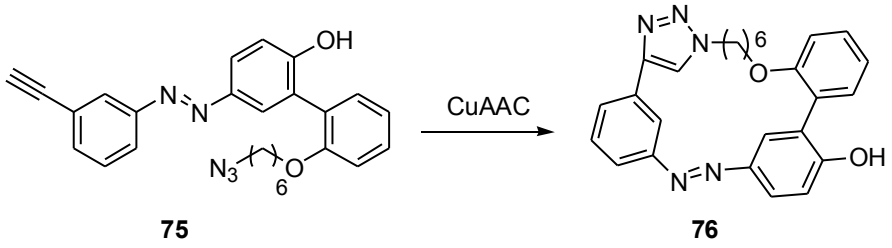

Scheme 19. Synthetic routes to cyclic azobenzenes *via* click reaction

As previously described, many kinds of azobenzene compounds have been synthesized, including linear azobenzenes and cyclic azobenzenes. However, for the preparation of the *bis*-azobenzenes and small cyclic azobenzenes, there still exist a gap to reach.

I.3. Properties of azobenzene compounds

I.3.1 Photo-isomerization of azobenzene compounds

One of the unique properties of azobenzene derivatives is that they display photo-isomerization which results in large structural change. In general, upon absorption of UV light (～ 350 nm), the rod-like *trans*-isomer is converted to the bent *cis*-isomer (Figure 12). This process is accompanied by a substantial variation of the dipole moment from 0D in the elongated *trans*-form to 3D in the bent *cis*-form. The photo-isomerization of

azobenzene is reversible; that is, once the UV irradiation ceases, the metastable *cis*-isomer can return to the more stable *trans*-state either through absorption of visible light (～ 450 nm) or thermal relaxation.[120]

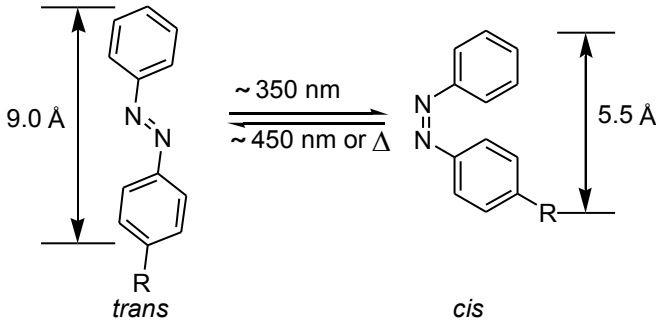

Figure 12. The reversible transformation between *trans*-form and *cis*-form upon irradiation with UV light or visible light / heat

There are four possible pathways for azobenzene photoisomerization from *trans*-isomer to *cis*-isomer including rotation, inversion, concerted inversion and inversion-assisted rotation (Scheme 20).[9,121-125] Some factors will influence the isomerization mechanism, such as wavelength of irradiation,[126] solvent effect,[127] nature of the substituents on the phenyl rings,[121] temperature,[128] pressure,[129] etc. Although, there are a lot of reports about photo-isomerization of azobenzene, the exact mechanism of photo-isomerization is still a matter of debate.

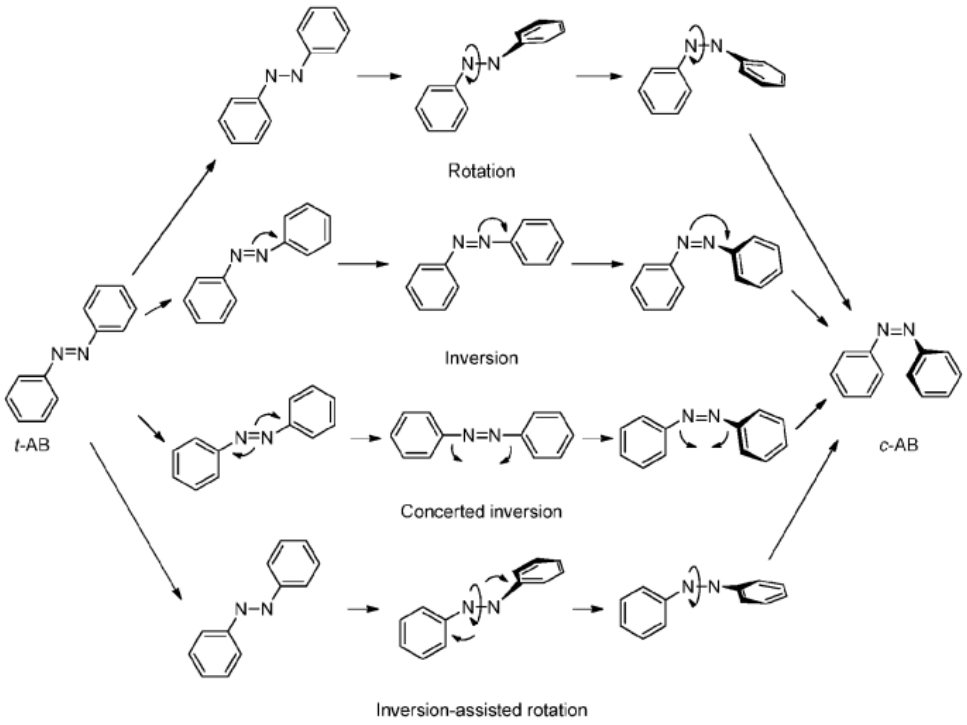

Scheme 20. Proposed mechanisms for the *trans*-to-*cis* isomerization of azobenzene. Adapted with permission from reference 9.

I.3.2 *Keto-enol* tautomerization of hydroxyl azobenzenes

For the *ortho*- and *para*-hydroxyl azobenzenes, the *keto-enol* tautomerization is common phenomenon for them in suitable solvents, which belongs to the prototropic tautomerism. It is an exchange of a proton between *keto*-form **77** and *enol*-form **78** in Scheme 21.[130] The *keto-enol* tautomerization attracts a lot of attention, which is attributed to its sensitivity to the environment. A very small change will induce the shift of equilibrium.

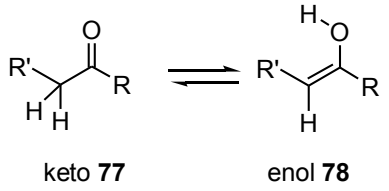

keto **77** enol **78**

Scheme 21. Tautomerization between *keto* and *enol* species

For hydroxy-substituted azobenzenes,[131-133] the tautomerism would arise by the removal of hydrogen from hydroxyl group, and the addition of hydrogen to a different part of the molecule (-N=N-). The hydroxy-substituted azobenzenes could undergo intramolecular proton transfer for *ortho*-HO-azobenzene **79** (Scheme 22), while *para*-OH-azobenzene **81** (Scheme 23) should give rise to an intermolecular mechanism through intermolecular hydrogen transfer.[134] There are many factors that take effect on the tautomeric equilibrium between the *enol*- and *keto*-forms of azobenzene molecules, in particular, pH,[135] solvent,[136] hydrogen bonding,[137,138] ionic state,[139] temperature,[140] substituents.[141,142] Noteworthy, the equilibrium between the *enol*-species and *keto*-species is too rapid to be observed by NMR. Therefore, for the monitoring of the *keto-enol* tautomerization, UV-vis absorption spectroscopy is the best tool.

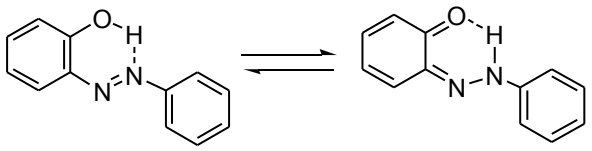

azo **79** hydrozone **80**

Scheme 22. Intramolecular *keto-enol* tautomerization of *ortho*-azobenzene

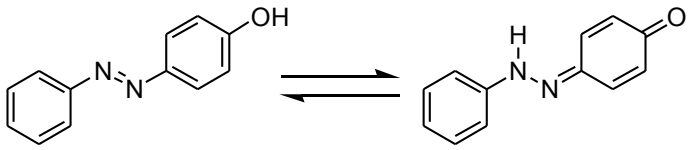

azo **81** hydrozone **82**

Scheme 23. Intermolecular *keto-enol* tautomerization of *para*-azobenzene

I.4 Background of stimuli-responsive polymers

Stimuli-responsive polymers can change their properties upon changing the environmental conditions. They are of considerable interest and have been extensively studied in various fields, such as polymer vesicles,[143-147] thermosensitive water-soluble copolymers,[148-152] *nano*-capsules,[153-156] cross-linked and degradable block copolymer micelles,[157,158] self-assembled hydrophilic homopolymers,[159] etc. Consequently, they have a wide range of applications such as, drug release, gene delivery, cell and tissue engineering.[160-169] The purpose of this part is not to show a comprehensive overview of the very extensive field of stimuli-responsive polymers. Here, we just provide a brief introduction to thermal and photo-responsive polymers, which are related in the present work.

I.4.1 Stimuli-responsive polymers

I.4.1.1 Thermo-responsive polymers

As previously known, the thermo-responsive polymer is sensitive to heat. It exhibits a phase transition at a certain temperature, which undergoes a sudden change in the solvation state upon the heating or cooling. There are two terms naming this critical temperature. One is lower critical solution temperature (LCST) at which polymer gets insoluble upon heating. The other one is upper critical solution temperature (UCST),[170] which is opposite to LCST, polymer becomes soluble upon heating at this temperature. For LCST, the simple

explanation is that the phase transition occurs as a result of changing intermolecular interactions and with a balance between the dissolution processes and the collapsed state of polymer chains, accompanied by a conformational coil-to-globule transition.

Above the LCST, the polymers undergo a sharp transition from coil to globule and form *inter*- and *intra*- chain association, resulting in hydrophobic aggregating and even precipitating from the aqueous solution, while below the LCST, the polymer chains are hydrophilic, well dissolved and show a coil conformation due to hydrogen bonds between hydrophilic groups and water.[171] The intermolecular interactions that lead to transition between the hydrated polymer and dehydrated polymer are the dominant factor for the determination of LCST behavior. The most widespread thermo-sensitive polymers include poly(N-isopropylacrylamide) (PNIPAM) with LCST 31-33 °C,[172] poly(methyl vinyl ether) (PMVE) around 37 °C,[173,174,] poly(N-vinly caprolactam) (PVCa),[173,175] with an LCST over the range of 30 °C to 40 °C, poly(2-ethyl-2-oxazoline) (PEtOx) whose LCST is between 61 and 64 °C,[173,176,177] poly(ethylene oxide)-poly(propylene oxide)-poly(ethylene oxide) (PEO-PPO-PEO),[178-180] and poly[2-(dimethylamino)ethyl methacrylate] (PDMAEMA)[181-185] owning LCST around 40 °C. Their chemical structures are shown in Figure 13.

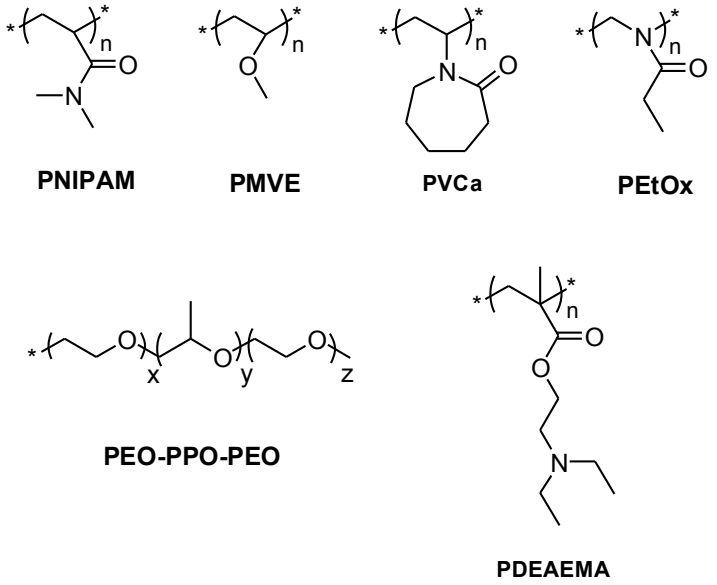

Figure 13. Chemical structures of representative thermo-responsive polymer

The phase transition of the thermo-responsive polymers can be tailored by varying a number of factors such as molecular weight,[186,187] composition of monomers,[188] end group polarity,[189-191] chain architecture,[192-194] branching,[195,196] and molecular weight dispersity.[197] It can also be affected by other environmental stimuli, for example, ionic strength,[198] pH,[198-201] electric field,[202] polyelectrolyte,[203] salts,[204] and surfactants.[205] At the molecular level, the phase transition is accompanied by a conformational change of the polymer chain from a disordered, random coil to a more ordered, collapsed globule.[206-208] Many applications of the thermosensitive polymers were reported in the literature including the design of biomaterials as drug delivery vehicles,[208-210] and chromatographic supports.[211]

I.4.1.2 Light-responsive polymers

Light-responsive polymers are one of the stimuli-responsive systems that have attracted much attention owing to their high accuracy and easy controllability. Light-responsive polymers have been widely developed by a variety of wavelengths from deep ultra-violet to

infrared.[212,213] There are highly investigated light-responsive molecules including azobenzene,[214] spiro-oxazine,[215] spiropyran,[216] and coumarin,[217] displayed in Figure 14.

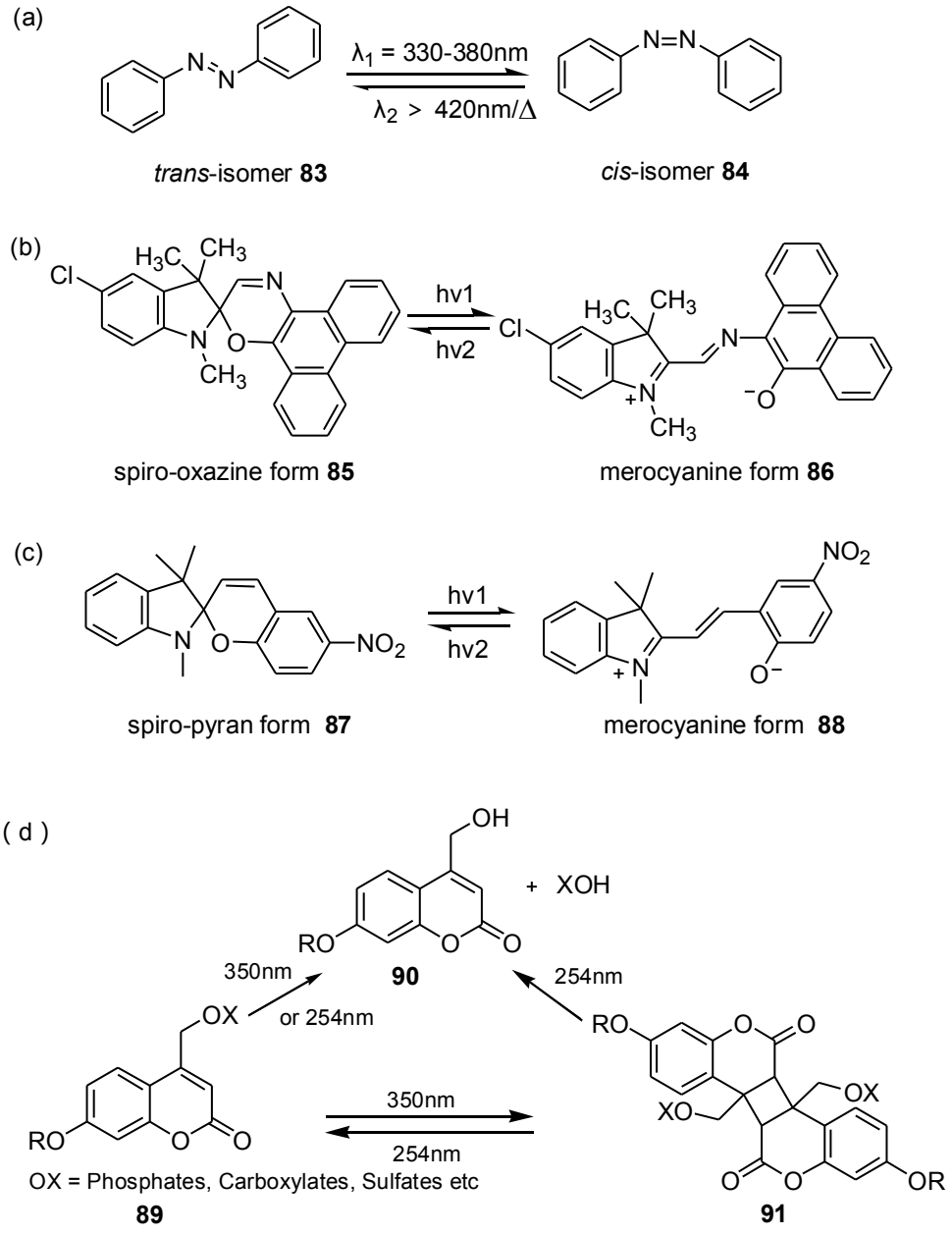

Figure 14. Schematic illustration of light-induced isomerization and photochemical reaction. (a) *Trans-cis* photoisomerization of azobenzene groups. (b) Photo-induced the

change between spiro-oxazine and merocyanine form. (c) Photo-induced the change between spiro-pyran and merocyanine form. (d) Photo-induced photo-dimerization and cleavage.

I.4.1.3 Other responsive polymers

For stimuli-responsive polymers, the external stimuli play a very important role in activating the response and modifying the polymers' properties in different environments. Many researchers have already demonstrated a sharp change in properties upon a small or modest change in external stimuli, including: pH,[218-233] gas (for example, CO_2),[234-241] ultrasound,[242] redox agents,[243-249] enzyme,[250-252] electric / magnetic fields,[253,254] and ion strength.[255] These smart polymers can be suitable for numerous engineering and industrial applications. In what follows, we provide some background information about the common stimuli and the specific stimuli-responsive functional groups used in this thesis.

I.4.2 Stimuli-responsive polymers based on azobenzene

Polymers containing azobenzene moieties are photo-responsive which is due to the photo-isomerization between the *cis*-isomers and the *trans*-isomers of azobenzenes on alternating irradiation with UV / visible light. The *inter*-conversion of azobenzene moieties between the two isomers can be achieved by either photo-chemical or thermal approach without any side reactions. Noteworthy, this isomerization is accompanied by a change in the dipole moment of azobenzene.

I.4.2.1 Side-chain and main-chain azobenzene polymers

Up to date, the photo-responsive properties of side-chain azobenzene polymeric systems have been much studied. Jiang and co-workers[256] pointed out the reversible photo-induced

micellization and micelle to hollow sphere transition of azobenzene polymers, shown in Figure 15. Watanabe *et al*.[257, 258] reported light-controlled reversible responsive copolymer containing side-chain azobenzene moieties.

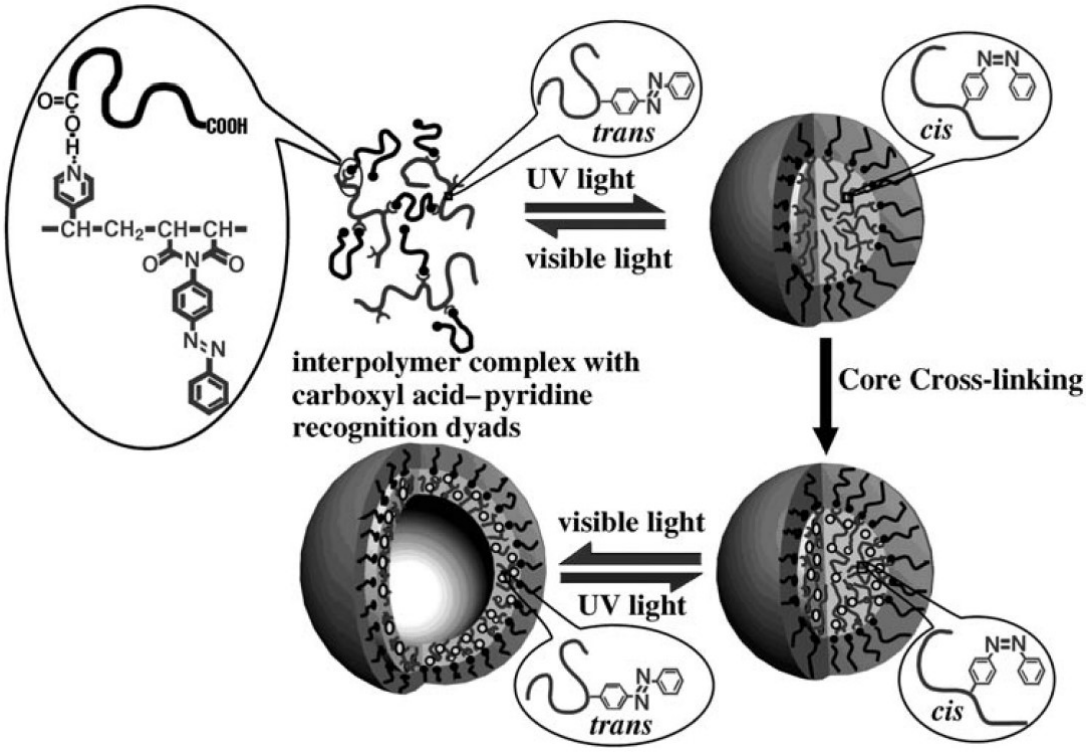

Figure 15. Illustration of the reversible photo-induced micellization and micelle to hollow sphere transition of azobenzene based polymers. Adapted with permission from reference 256.

For main-chain azobenzene polymers, they show good mechanical properties. Blair *et al.*[259,260] reported a monolayer of main-chain azobenzene polymers (Figure 16), which stress at the interface with the substrate was found to decrease upon irradiation with UV light and increase again when the layer was in the darkness, Moreover, the cycle can be repeated for many times.

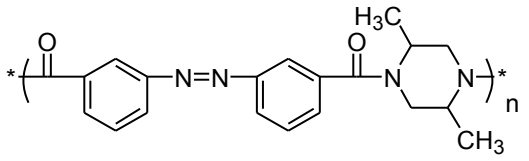

Figure 16. Chemical structure of main-chain azobenzene polymer

I.4.2.2 Polymers based on azobenzenes in solid state and solutions

Since azobenzene compounds exhibit a reversible photo-isomerization process between its *trans*- and *cis*-isomers upon exposure to light, the propertities of azobenzene-based polymers can be modulated by light. In solid state, the azobenzene-based polymers can be used for a wide variety of applications such as data storage and photo-switching,[261,262] optical devices,[263-267] photo-induced mechanical motion,[268-274] liquid crystalline displays, [275] and phase change and separate.[276] In polymer solutions, many phenomena related to photo-isomerization of azobenzene have also been discovered including, polypeptide order,[276] drug delivery,[278] micelles.[279]

I.4.2.3 *Multi*-stimuli-responsive polymers based on azobenzene moieties

The azobenzene not only can provide the photo-responsive properties of polymers, but also can affect other stimuli-responsive properties of polymers through the photoisomerization of azobenzene moieties incorporated in the polymer structures. On one hand, there are many reports showing that azobenzenes can be used to manipulate the thermal-responsive phase transition temperature due to the photo-isomerization of azobenzenes which can be easily adjusted and controlled. For example, Takeshi *et al*.[280] studied the tunable LCST of azobenzene-containing polymers induced by the photo-isomerization. Zhao *et al*.[281] reported that a variety of doubly photo-responsive copolymers containing azobenzene isomers, which can affect the LCST of thermo-polymers with light irradiation (Figure 17).

Watanabe *et al.*[282] showed that the UCST of polymer also depends on the photo-isomerization state of azobenzenes. On the other hand, the azobenzenes can be used for the enzyme-responsive polymers, whose micellar assembly can be disrupted by light.[283]

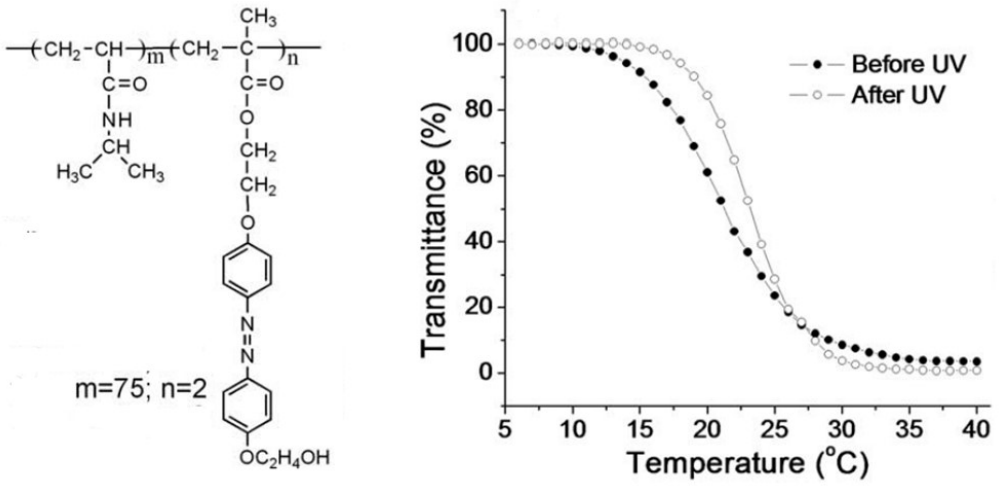

Figure 17. Transmittance *versus* temperature for aqueous solutions before and after UV light-induced photoisomerization of azobenzene groups. Adapted with permission from reference 281.

I.5 Objectives of the Thesis

Although many works about the *mono*-azobenzene compounds, ranging from synthesis, characterization, functionalization to applications, have already been reported, there are still unresolved issues and challenges about synthesis of *bis*-azobenzenes, cyclization of azobenzenes and their applications.

The overall objectives of this thesis are to design, prepare *bis*-azobenzene and small cyclic azobenzenes derivatives, then to investigate them in various solvents and to construct stimuli-responsive materials from them, and finally, to explore their potential applications. We carried out a number of studies in this thesis in order to contribute to reach the different

targets. The realized research work can be divided into three parts. The first part, which is the most important, is about the synthesis of *bis*-azobenzene and even *tris*-azobenzene derivatives (Chapter 1). The second part is a study of the preparation of cyclic azobenzene derivatives and their behaviors in solution (Chapter 2). The third part is to explore the properties of polymers densely populated with *bis*-azobenzene groups (Chapter 3).

The first chapter of this thesis deals more precisely with design of new synthetic routes to prepare efficiently *bis*-azobenzenes and even *tris*-azobenzenes. Although the synthesis of simple azobenzenes and *bis*-azobenzenes is already known in the literature, our research efforts focus on synthesizing these particular azobenzene architectures in one step or in a one-pot reaction. This part is to study the synthesis of *meta*-*bis*-azobenzene derivatives including various factors on the reactions.

In Chapter 2, we present a novel synthetic method for the creation of small cyclic molecules containing a *cis* azobenzene group. The critical cyclization step is triggered by *trans*-to-*cis* isomerization of specifically activated fluoro-azobenzenes under the daylight, while taking advantage of the ease at which the *cis*-isomer can be generated. The formation of the desired cyclic azobenzene is achieved through the elimination of HF under very mild conditions. The favorable geometries of the precursors are explored as well as the precise reaction conditions, particularly the effect of solvents and duration of reaction. Through the rational design of chemical structures and control of external conditions, we intend to manipulate the reaction pattern. Therefore, in order to achieve this, a thorough investigation of the effect of solvents and various external conditions on many of our *mono*- and *bis*-azobenzenes is to be studied. The various substitution patterns are also taken into account, as well as the polarity of solvents. The corresponding variations are then investigated by the means of UV-vis absorption spectroscopy, mass spectrometry, ^{1}H NMR and ^{19} F NMR, etc. Meanwhile, these studies aimed at understanding the evolution of color

changes over time are carried out.

In Chapter 3, we focus on stimuli-responsive polymers whose comonomers are NIPAM (*N*-isopropylacrylamide) and *bis*-azobenzene derivatives prepared by us. By using these *bis*-azobenzene moieties in the polymer, we wanted to know if their high concentration could tune the phase transition of thermal-responsive polymer and if its *trans-cis* photoisomerization has an impact on the phase transition. Meanwhile, we take a comparison of them with polymers containing *mono*-azobenzenes. Our study demonstrated that the solution behavior of our *bis*-azobenzene based polymers of a new kind display stimulus responsitivity either by heating or by UV light exposure, as a result of the photoisomerization of *bis*-azobenzene moieties.

Finally, in the last part of the thesis, a general discussion is presented on the accomplishment and significance of the conducted research. An opinion is given on the perspectives of *bis*-azobenzene-based polymers showed in the present thesis and we propose future avenues that are worth being pursued.

CHAPTER 1 ONE-POT SYNTHESIS OF *BIS*-AZOBENZENES *via* THE COUPLING REACTION OF DIAZONIUM SALTS

1.1 Introduction

This chapter deals with *bis*-azobenzenes where the two azobenzene groups share one aryl ring.

1.1.1 The structures of *bis*-azobenzenes

Bis-azobenzenes can be classified into three families according to their substitution pattern. Thus, one can consider the *ortho*-*bis*-azobenzene family, the *meta*-*bis*-azobenzene family and the *para*-*bis*-azobenzene family based on the three core ring systems **92**, **93** and **94** respectively (Figure 18).

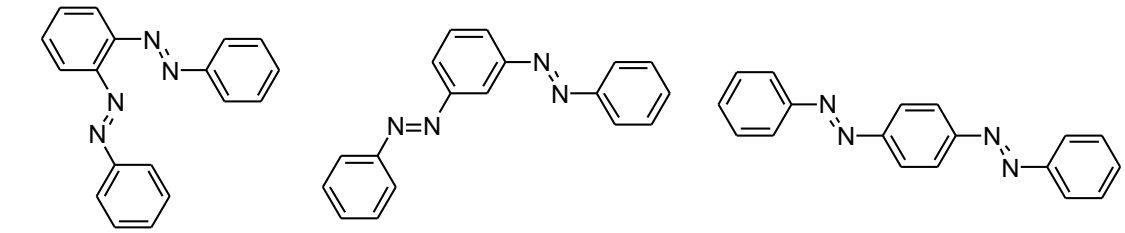

Figure 18. Chemical structures of *ortho*-, *meta*- and *para*-*bis*-azobenzene

1.1.2 Their appeal

This type of compounds is known to possess very appealing properties, such as photo-switching,[109] liquid crystal behavior,[284] opto-mechanical properties,[285] etc. It is also clear that their *trans*-*cis* isomerizations provides more possibilities on isomers than single

azobenzenes. Indeed, a single azobenzene is obviously either *trans* or *cis*, with no additional choice. In the case of *bis*-azobenzene, the whole story becomes much more complicated. Each system can adopt three states according to azobenzene geometry, namely *trans-trans*, *trans-cis* and *cis-cis*. However, many more conformations can be considered because of the relative geometries of each isolated *mono*-azobenzene system inside the entire *bis*-azobenzene molecule. For example, there exist 5 possibilities for the simple *ortho-bis*-azobenzene molecule **92**, as shown in Figure 19. There can be photochemical or thermal inter-conversion between these shapes. The conformationally wealthiest family is certainly the *meta-bis*-azobenzene **93** with a total of 9 conformations (Figure 20). The *trans-cis* photoisomerization of some derivatives belonging to this family have been thoroughly studied.[286] Finally, one considers the *para-bis*-azobenzene system based on the simplest representative **94** (Figure 21), there are 6 combinations.

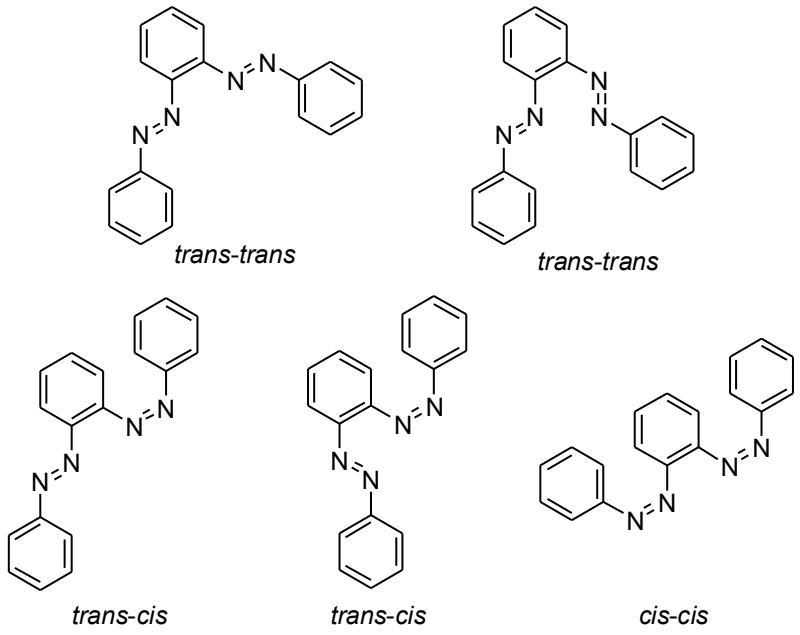

Figure 19. Five conformational possibilities for the simple *ortho-bis*-azobenzene, **92**

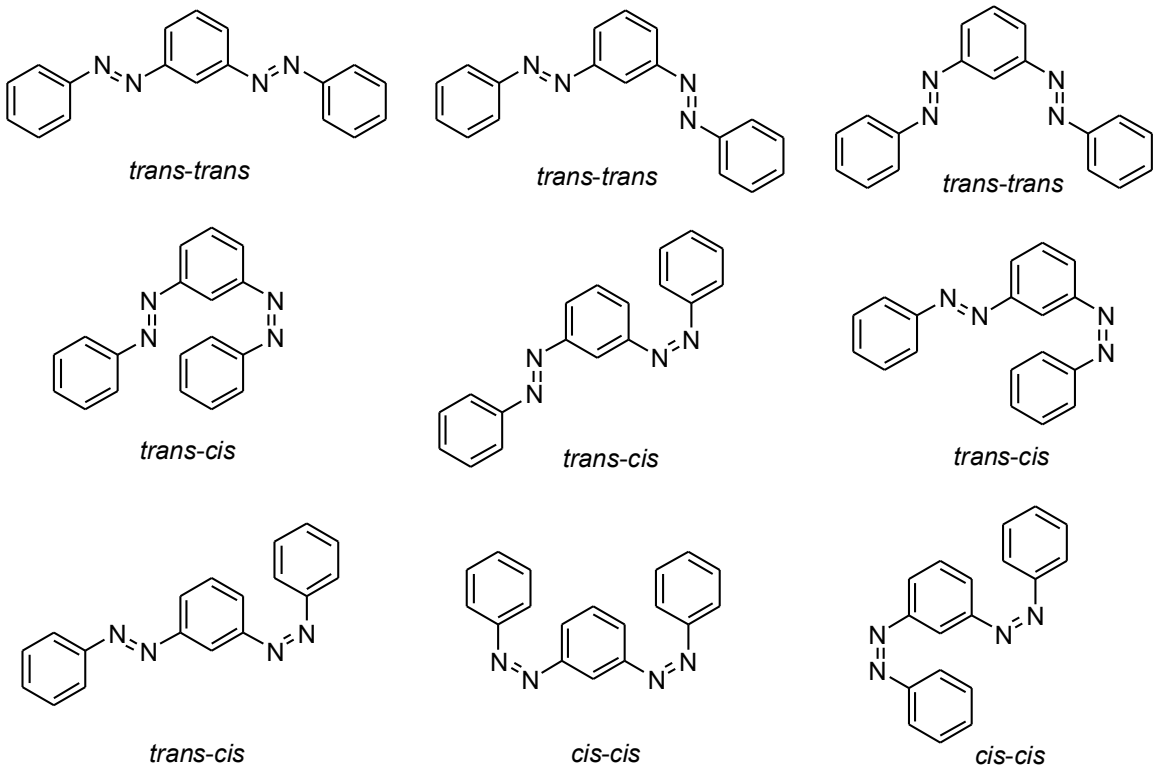

Figure 20. Nine conformational possibilities for the simple *meta-bis*-azobenzene, **93**

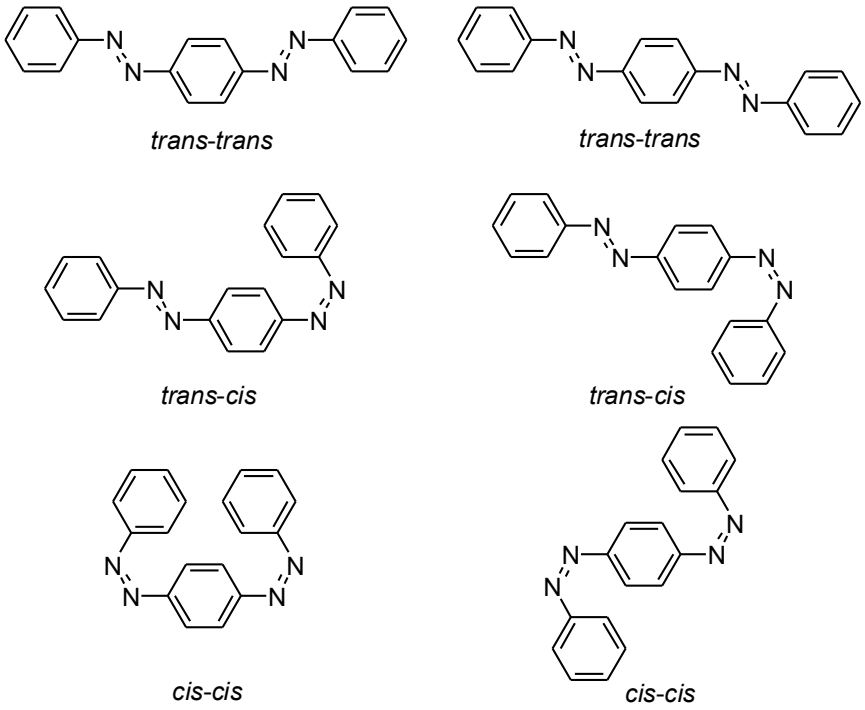

Figure 21. Six possible combinations of *para-bis*-azobenzene, **94**

There still exists one parameter to take into account, the conjugation of the whole system. In the case of *ortho*- and *para*-*bis*-azobenzenes like **92** and **94**, the π-electrons are fully delocalized over the three aryl rings and the azobenzene groups.[109] Such is not the case for the *meta*-*bis*-azobenzene **93**, where the two *mono*-azobenzene parts do not "see" each other electronically. There are consequences to these connectivity matters, which influence the absorption spectra (Figure 22).[109] The photo-isomerization properties of *meta*-*bis*-azobenzenes are very similar to the monomeric azobenzene. Obviously, all these above considerations make these systems very interesting indeed.

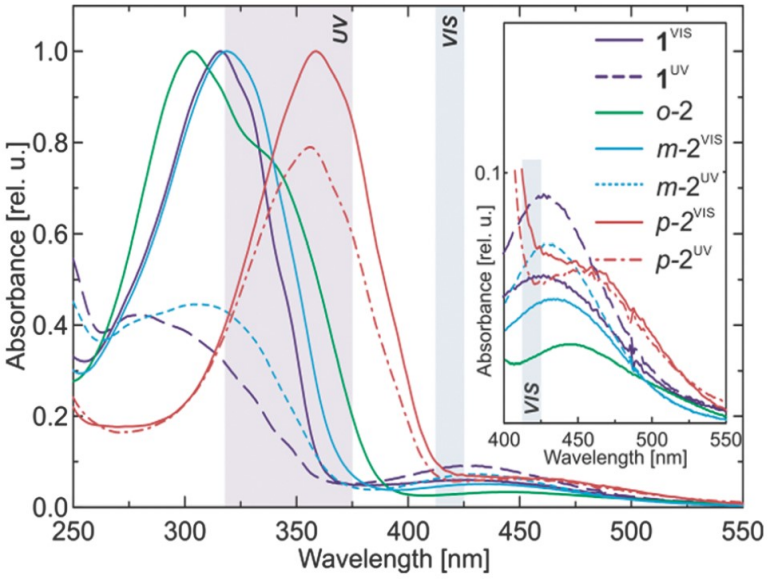

Figure 22. Absorption spectra of the investigated compounds in the photo-stationary states after visible (vis) or UV irradiation, **1**: *mono*-azobenzene; ***o*-2**: *ortho*-*bis*-azobenzene; ***m*-2**: *meta*-*bis*-azobenzene; ***p*-2**: *para*-*bis*-azobenzene.[109]

1.1.3 Their synthesis

Therefore, we became interested in introducing these *bis*-azobenzene structures into polymers (for example, with acrylate) to ultimately see if their photo-switching properties

could influence the opto-chemical behavior of the resulting materials. So, the *bis*-azobenzene requires a handle that can be used as an anchor onto the polymer main chain. A phenol can fulfill this role, as it is very interesting for two reasons: it is a group easily introduced and it is normally used in the synthesis of azobenzene following the diazonium salt coupling (Scheme 1). However, the diazonium salt coupling will only lead to *meta*-*bis*-azobenzene (Scheme 24).

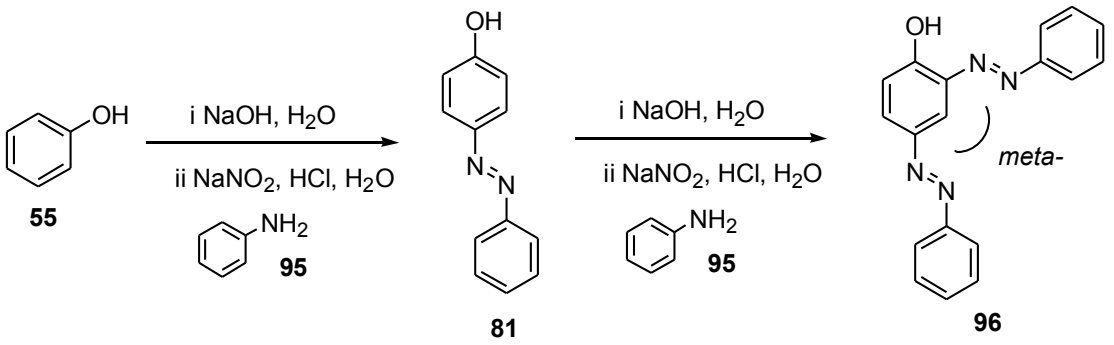

Scheme 24. Synthesis of *meta*-*bis*-azobenzene with diazonium salts coupling reaction

Even though several methods (in the introduction) have already been introduced for the synthesis of azobenzenes, none of them is truly appropriate for the preparation of *bis*-azobenzenes in one step. To the best of our knowledge, the existing procedures for *bis*-azobenzene compounds synthesis consist of one step for each azobenzene bond formation. For instance, in 2015, Rijeesh, K *et al*.[106] carried out the research to synthesize *bis*-azobenzene derivatives starting from two amines (Scheme 11). Wegner and co-workers[108] reported a *bis*-azobenzene preparation *via* Mills reaction using both continuous methodology and separated reaction steps (Scheme 13). In another research conducted by Jin, M *et al*,[110] the *bis*-azobenzene compounds were prepared *via* the diazonium coupling reaction in two steps (Scheme 15). Although efforts have already been devoted to the development of *bis*-azobenzene synthesis, a general method for furnishing

the *bis*-azobenzene compounds in one procedure start from one aniline group is still lacking.

As already mentioned, we have selected the diazonium salts coupling route, because it provides a phenol group as a straightforward way to attach the resulting *bis*-azobenzenes to polymers. Moreover, this most useful and classical synthetic methods based on the azobenzene coupling reaction *via* diazonium salts, presents many other advantages, such as the use of simple agents, like cheap acids (eg. HCl, H_2SO_4) and bases (eg. NaOH, K_2CO_3). In addition, this procedure is an efficient and versatile way towards the preparation of symmetrical or asymmetrical azobenzene compounds with high yields and short reaction times. Noteworthy, this synthetic pathway tends to be *para*-selective (Scheme 24), but not always since some *ortho*-adducts may also be formed. Herein, we wish to report a novel synthetic methodology for the preparation of *bis*-azobenzene and even *tris*-azobenzene compounds in one-pot reaction. We also disclose and discuss the effect of all the important parameters on the reaction yields, particularly the various molar ratios of starting materials, substituents on the phenols. The electron-donating or electron-withdrawing nature of the functionalities present on the aniline rings may also exert some influence. These electronic effects will be reviewed as well.

1.2 The reactants

1.2.1 The phenols

The phenol has a twofold usage: 1) in its phenolate form, it will couple with the diazonium salts partners, and 2) following this first step, it will provide a chemical anchor for later coupling as an ether, for example.

A brief study was carried out to verify whether a single phenol, like phenol itself, could easily lead to *bis*-azobenzene derivatives. This was accomplished with the simplest diazonium salt prepared from aniline (Scheme 25). The reactants ratio [aniline] / [phenol] was set at 2:1. Under these conditions, the *para-mono*-azobenzene **81** was by far the major compound (72% yield), with hardly any desired *bis*-azobenzene **96** (10% yield). This preliminary result clearly indicates that a single phenol group does not provide sufficient activation to form *bis*-azobenzene products.

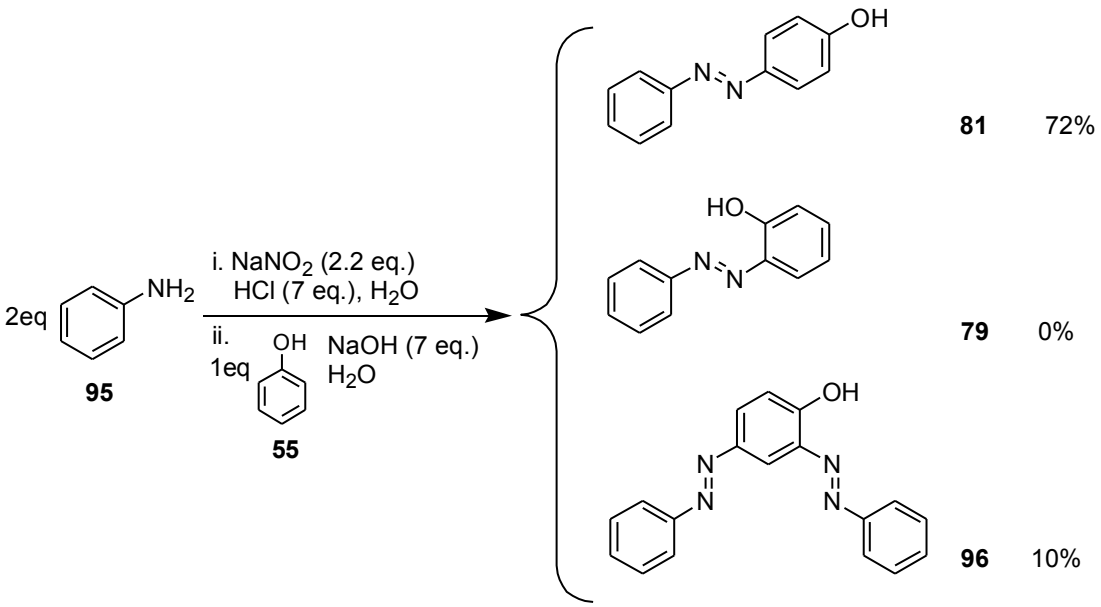

Scheme 25. Synthesis of azobenzene derivatives from a simple phenol **55**

Therefore, it appears necessary to add activating groups to **55**. In order for the activation to be effective, the additional electron-donating groups must be located *meta*- to the original phenol functionality, in order to activate their *ortho*- and *para*-positions during the coupling with diazonium salts. Accordingly, two phenol derivatives **97**, **98** were selected for further investigation (Schemes 26). *Meta*-methoxyphenol **97** gave very encouraging results, since as much as 85% of *bis*-azobenzene **101** was obtained. In fact, this adduct is so much

favored that very little *mono*-substituted azobenzenes **99** (8% with phenol *para* to the azo group) and **100** (3% with phenol *ortho* to the azo group) are generated. This same trend is also observed in the case of another *meta*-phenol **98** originally chosen for its potential use as click precursor. Nevertheless, possibly as a result of its increased steric hindrance, less *bis*-azobenzene **104** is formed. Although **104** is still the major product (58%), the two *mono*-azobenzenes **102** and **103** are now formed in substantial amounts (18% and 9% respectively).

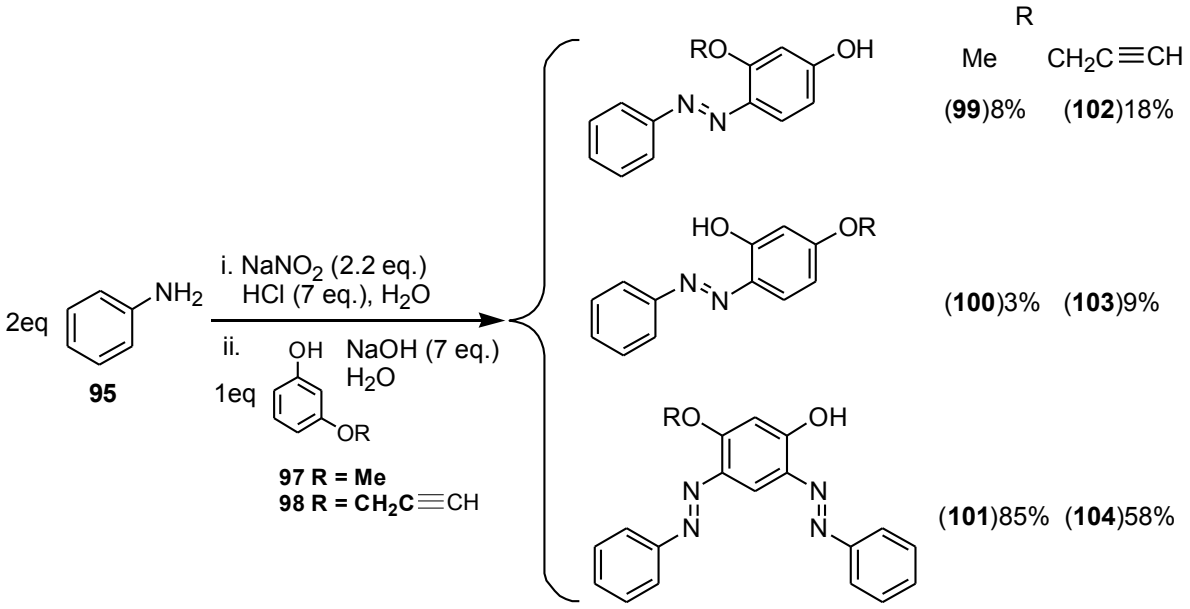

Scheme 26. Synthesis of azobenzene derivatives from *meta*-activated phenols **97** and **98**

To confirm that the additional ether groups, as in **97** and **98**, are behaving as expected, we also used the $\boldsymbol{C}_3$ symmetric triphenol **105** (phloroglucinol) with the same diazonium salt issued from aniline **95** (Scheme 27). The same methodology, as described above, was applied (3 equivalents of aniline **95** versus 1 equivalent of **105**), then the *bis*-azobenzene **106** was obtained with a reasonable yield of 57% and there was also as much as 33% of the fully symmetrical ($\boldsymbol{C}_3$) *tris*-azobenzene **107**.

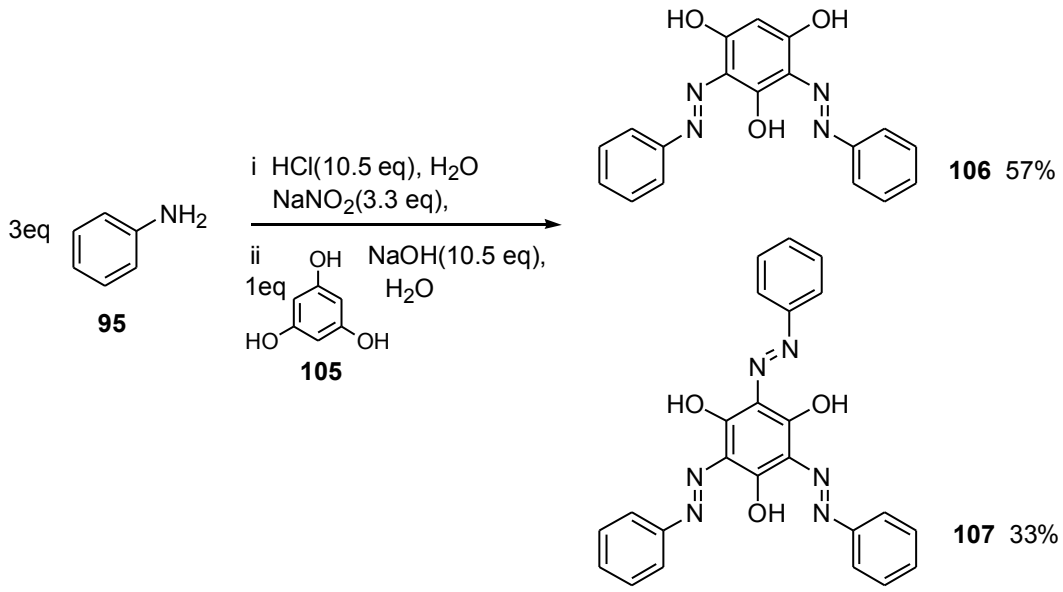

Scheme 27. Synthesis of *bis*-azobenzene and *tris*-azobenzene derivatives from phloroglucinol **105**

Consequently, the *meta*-methoxyphenol **97** was retained for the rest of this investigation, as it proved more selective than the two other activated phenols **55** and **98**.

1.2.2 The anilines

Having chosen *meta*-methoxy phenol **97** as our activated phenol species, it became necessary to select the appropriate diazonium salt partners. It was expected that substitution of these salts might influence, to some degree, the outcome of the reaction. Whatever the diazonium salt used (different R substituents), we can expect to always collect up to three azobenzene products (Scheme 28), two *mono*-azobenzenes, **111** and **112**, in which the free phenol group is either in *para* position or in *ortho* position *versus* the azo functionality, respectively.[287] The third product is the desired *bis*-azobenzene molecule **115**. This later product can be generated from both *mono*-azobenzenes **111** and **112**, whose corresponding phenolates **113** and **114** are formed *in situ* with NaOH and can then undergo coupling with

the same diazonium salt, present in excess quantity in the reaction medium.

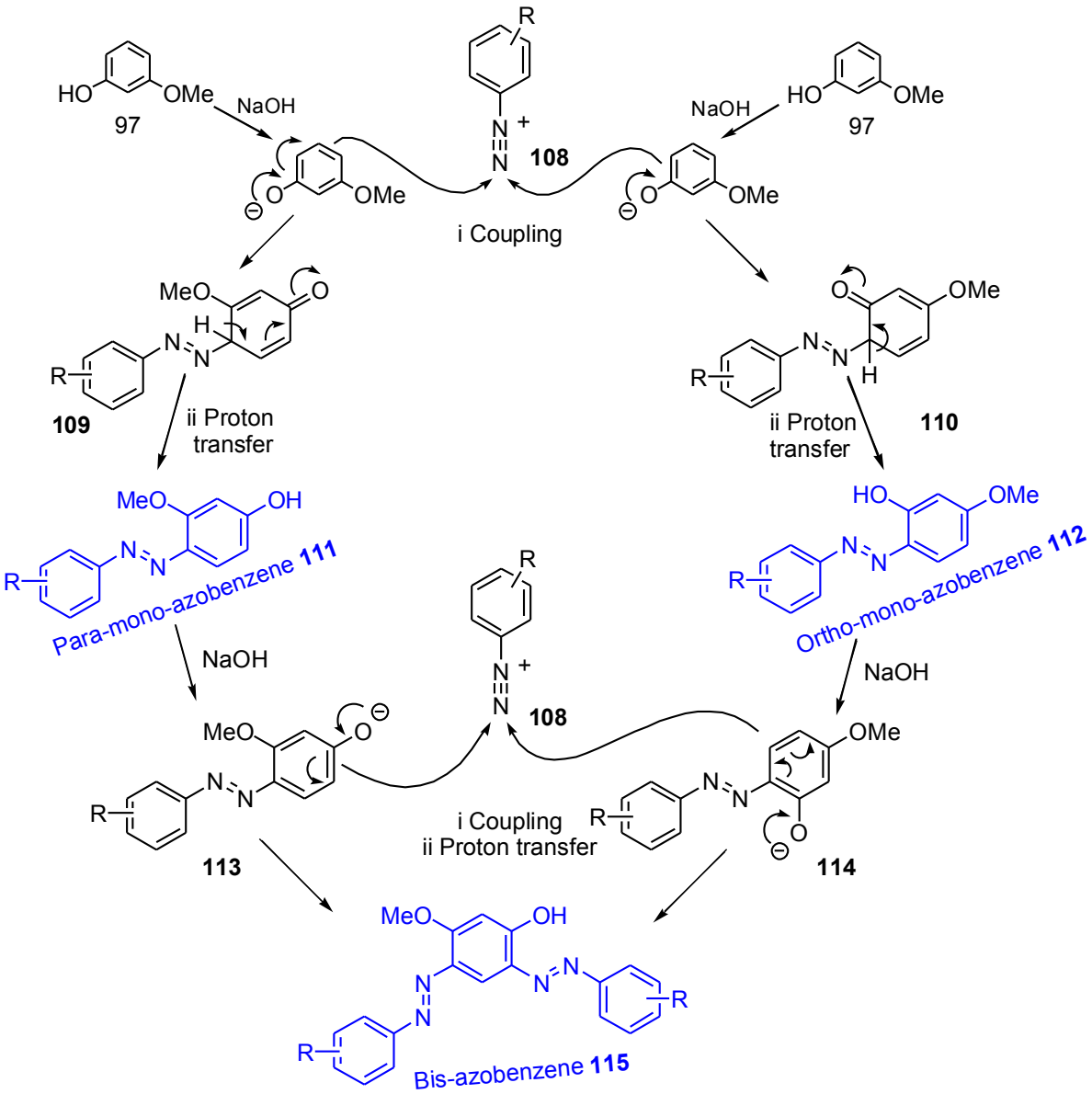

Scheme 28. Proposed mechanistic pathways

The case of the unsubstituted aniline **95**, with *meta*-methoxy phenol **97** has already been studied, and it will be used as a reference (Scheme 26). The obvious next step of our investigation was to consider electron-rich and electron-deficient anilines.

1.2.2.1 Electron rich anilines

Two ether groups were added to the simple aniline, in *para* and *ortho* positions in order to feed electrons to the diazonium group itself. The first aniline studied **116** was the most activated one (or deactivated of course), with two methyl ethers (Scheme 29).

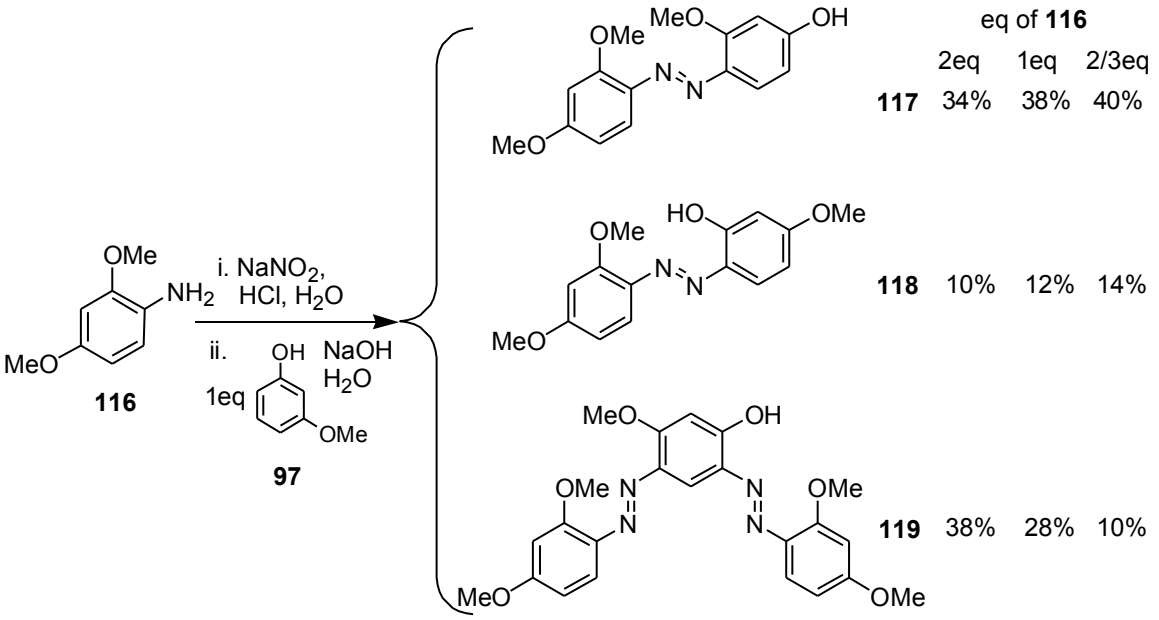

Scheme 29. Synthesis of azobenzene derivatives from aniline **116** with two methyl ethers

To gain a deeper understanding of the course of the reaction, the number of equivalents of aniline *versus* that of phenol ([aniline] / [phenol]) were set at 2 / 1, 1 / 1 and 2 / 3 in three separate experiments. Clearly, the first condition (2 / 1 ratio) is the only one that truly favors the appearance of *bis*-azobenzene adduct **119**, whereas the two other conditions increasingly favor the formation of *mono*-azobenzenes **117** and **118**. The results revealed that such was indeed the case, since the yield of *bis*-azobenzene **119** varied as expected. **119** was obtained in 38% yield under the more favorable conditions for its formation, it then went down to 28%, then even 10% in the less favorable [aniline] / [phenol] smaller ratios. The formation of the *mono*-azobenzenes followed the opposite trend, with 44%, 50% then

54%. In all cases, the proportion of *para*-azobenzenes was always the largest, accounting for around 76% of the mixtures of *mono*-azobenzenes. By comparing this result with the reference scenario with unsubstituted aniline **95** (Scheme 26), it immediately appears that electron donating groups strongly deactivate the diazonium salt during the coupling stage. Indeed, as much as 85% of *bis*-azobenzene **101** had been produced under identical conditions.

The second aniline studied **120** is less deactivated with only one methyl ether at the *para* position (Scheme 30). As for the previous case (**116**), three separate experiments were carried out, each run with the following conditions: number of equivalents of aniline **120** *versus* that of phenol **97** ([aniline] / [phenol]) set at 2 / 1, 1 / 1 and 2 / 3. This time, the first condition (2 / 1 ratio) largely favors the appearance of the *bis*-azobenzene adduct **123**, as much as 62% of product being cropped. This is strikingly different from the previous case (**116**), where nearly twice as less *bis*-azobenzene **119** had been collected (38%). The two other conditions (1 / 1 and 2 / 3 molar ratios) increasingly favor the formation of *mono*-azobenzenes **121** and **122**, which are formed in increasing amounts. As before, the quantity of *para*-*mono*-azobenzene amounts to around 75% of the mixtures of *mono*-azobenzenes. All these experiments demonstrate that only one methyl ether is really much less deactivating than two. Nevertheless, it has to be observed that the detrimental effect of electron-donating groups is still clearly at work in the *mono*-substituted case, when compared to the reference (Scheme 26). Indeed, upon going from no substituent, to one methoxy and two methoxy groups (Scheme 29), the conditions favoring the formation of *bis*-azobenzenes lead to 85%, 62% then 38% of these products respectively.

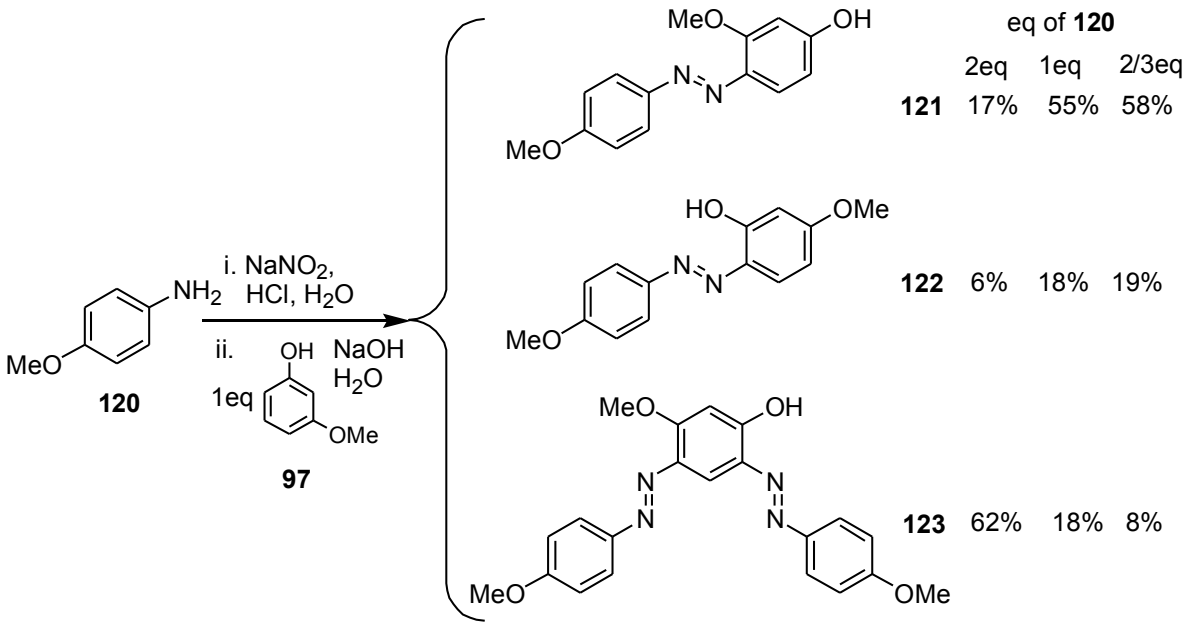

Scheme 30. Synthesis of azobenzene derivatives from aniline **120** with one methyl ether

In terms of yields, there is also much to learn. For example, the total yields of formed products (*mono*-azobenzenes + *bis*-azobenzene) are usually greater when the aniline, hence its diazonium salt, is in excess (Table 1). When there is no deactivation of the diazonium salt reactant (reference), as much as 96% of products was observed ([aniline] / [phenol] = 2), this same figure went down to 82% when the diazonium salt suffered maximal deactivation. This deactivating effect is even more obvious when inverse ratios of reactant are used ([aniline] / [phenol] = 3 / 2). For the reference case, 89% of final products could still be obtained. However, the total yield became very low at 64% when deactivation was the strongest.

Table 1. Effect of substituents on aniline and [aniline] / [phenol] on the total yield

	Total yield / %		
aniline	[aniline] / [phenol] = 2	[aniline] / [phenol] = 1	[aniline] / [phenol] = 2 / 3
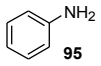 **95**	96	90	89
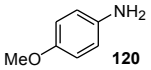 **120**	85	86	85
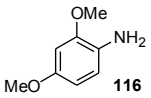 **116**	82	78	64

Two other deactivated anilines **124** and **128** were studied (Schemes 31 and 32). Since these two compounds look very much like the *para*-methoxy aniline **120** (Scheme 30), the results were also very similar and added grounds to the previous observations concerning electron donating groups.

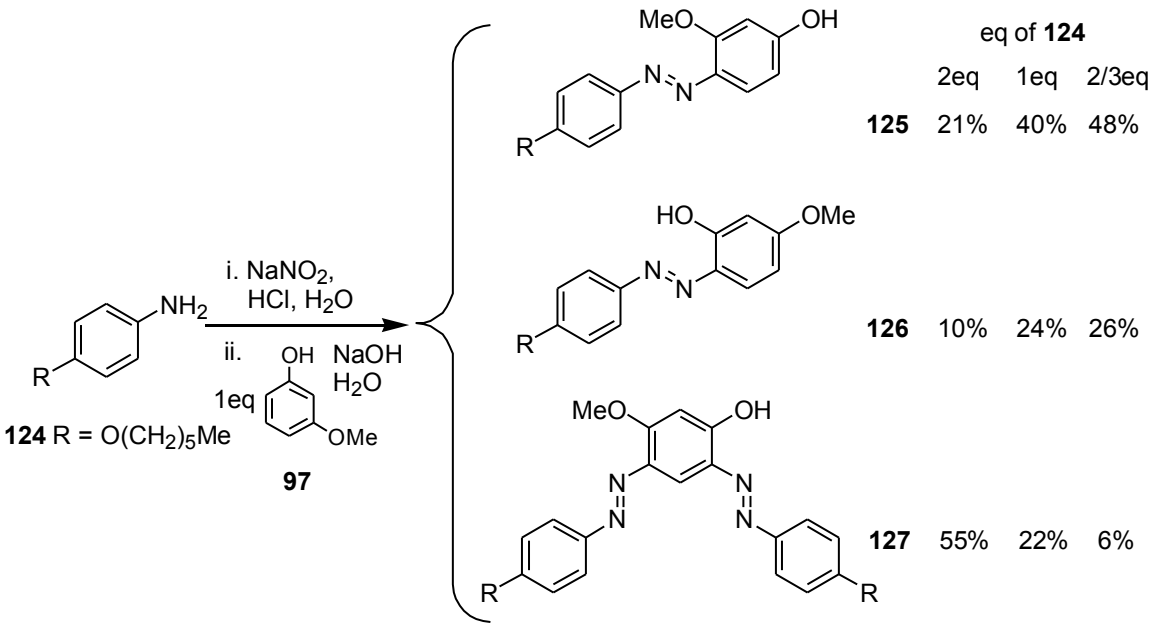

Scheme 31. Synthesis of azobenzene derivatives from aniline **124** with -$O(CH_2)_5Me$

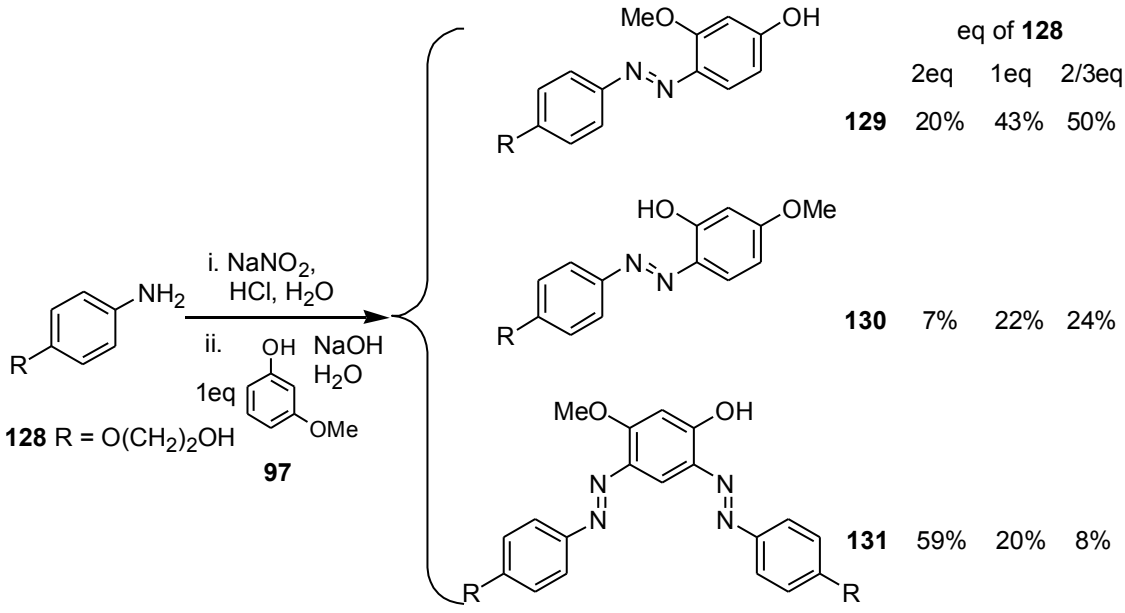

Scheme 32. Synthesis of azobenzene derivatives from aniline **128** with -$O(CH_2)_2OH$

1.2.2.2 Electron deficient anilines

As previously discussed, the anilines with electron-donating group are deactivated during the coupling reactions leading to azobenzenes and more particularly to *bis*-azobenzenes. Let us think about the anilines with the electron-withdrawing groups (EWG) -F and -CO_2*t*-Bu. The *t*-Bu ester group was added to the simple aniline in *para*-position in order to reduce the electron density of the diazonium group. The expected effect would be to render the diazonium salt more reactive. However, at first sight (Scheme 33), this does not seem to be absolutely true, since less *bis*-azobenzene **135** (66%) was formed, by comparison with the reference (**120**) for which 85% of equivalent *bis*-azobenzene had been obtained, following the optimal conditions for generating *bis*-azobenzenes ([aniline] / [phenol] = 2). However, the overall yield is still very good, being 96%, like the reference. On the other hand, there is now much more *mono*-azobenzenes (**133** and **134**) formed, 30% versus only 11% for the reference.

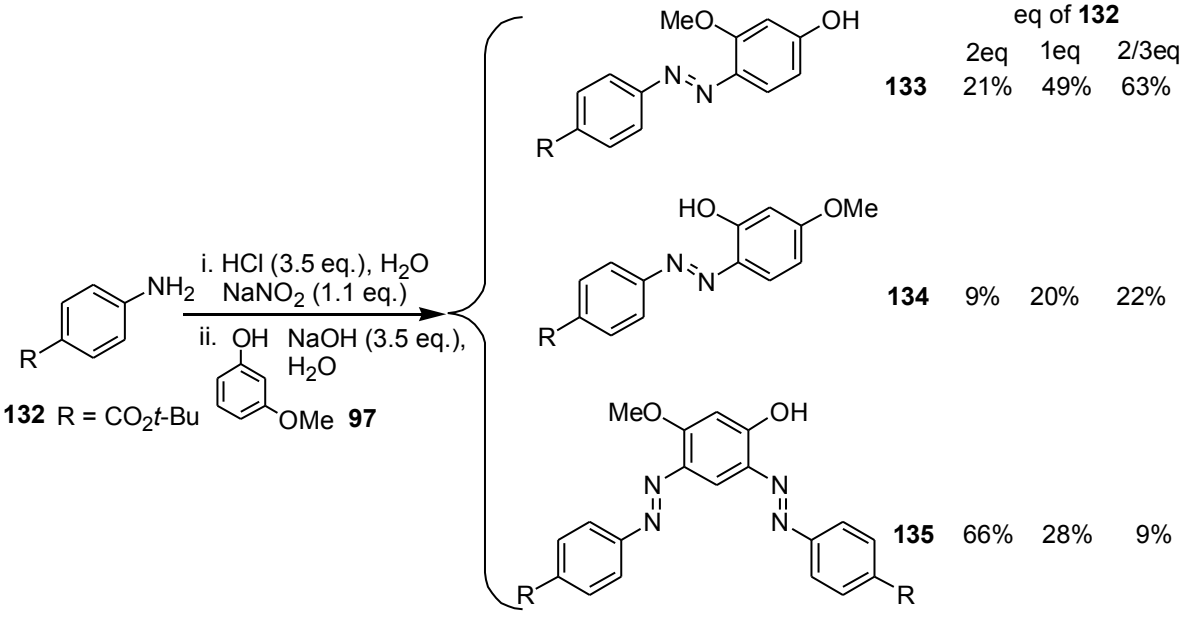

Scheme 33. Synthesis of azobenzene derivatives from aniline **132** with -CO_2*t*-Bu group

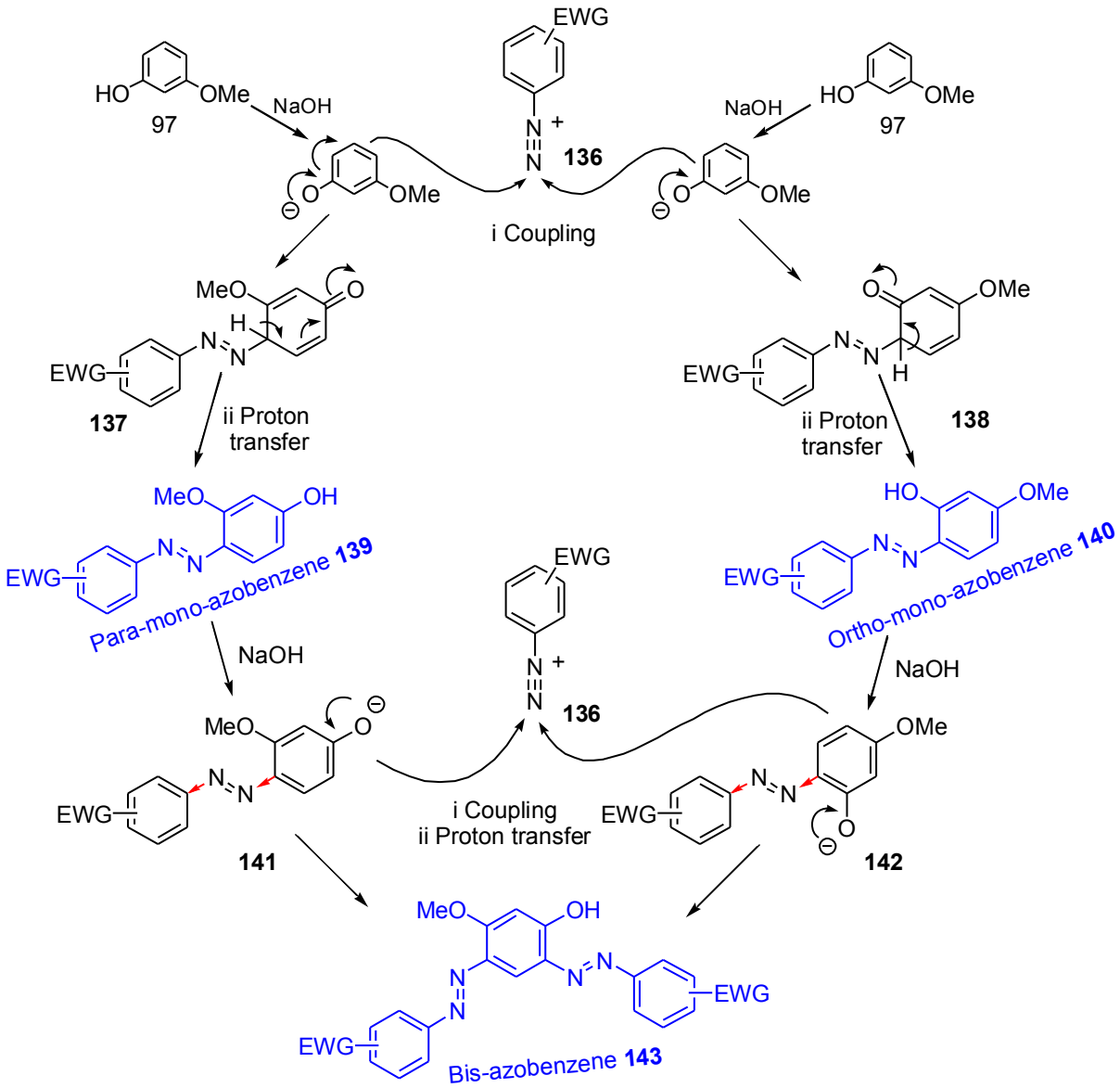

Scheme 34. Proposed mechanistic pathways

Consequently, one may argue that the second step is not as favored as the first. This absolutely makes sense, when we compare the nucleophilicities of **113** and **114** with electron-donation group (Scheme 28) and of the products obtained after the first coupling (Scheme 34). These latter *para*- and *ortho-mono*-azobenzenes **141** and **142** are much less reactive because the *t*-Bu ester group is now able to exert its electron-withdrawing

influence by resonance, through the azo bridge, into the phenol ring. Consequently, the second coupling is not as efficient as the first. Therefore, there is accumulation of *mono*-azobenzenes in the reaction medium that do not react further.

When we deprive the mixture of reactive aniline ([aniline] / [phenol] = 1), it is expected that less *bis*-azobenzene will be formed, and even more so with less aniline ([aniline] / [phenol] = 2 / 3). Such is indeed the case, as the isolated yields demonstrate, with 28% and 9% of *bis*-azobenzene being created during these two last experiments respectively.

The formation of *bis*-azobenzene seems to be in a "catch 22" situation because there are two consecutive steps involved.

a) If the first step is disfavored, it is not as easy to obtain the *mono*-azobenzene adducts. But it will generate the *bis*-azobenzene. This case, which corresponds to anilines substituted (*ortho* and / or *para*) with electron-donating groups, led to lower yields similar to those observed for the methoxy anilines (and other ethers).

b) If the first step is favored but the second step is not, then it is not as easy to generate the *bis*-azobenzene molecules. But, there is accumulation of the less reactive *mono*-azobenzenes. This case, that corresponds to anilines substituted (*ortho* and / or *para*) with electron-withdrawing groups like *t*Bu esters, produced higher yields (total yields equal or over 90%).

The consequence of all these contributing and sometimes conflicting parameters, is that the various ratios observed for anilines *mono*-substituted with a *para*-methoxy or a *para*-*t*Bu ester lead to very similar ratios of products (*mono*-*para*, *mono*-*ortho* and *bis*-azobenzene) but for different reasons (Table 2). The obvious difference between the two cases remains the total yields, high for electron-withdrawing groups and substantially lower for electron

donating groups.

Table 2. Effect of substituents on aniline and [aniline] / [phenol] on the yield

	Yield / %								
	[aniline] / [phenol] = 2 / 1			[aniline] / [phenol] = 1 / 1			[aniline] / [phenol] = 2 / 3		
anilines	Mono	Bis	*Tot*	Mono	Bis	*Tot*	Mono	Bis	*Tot*
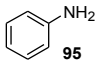 **95**	11	85	*96*	68	22	*90*	81	8	*89*
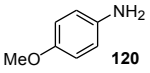 **120**	23	62	*85*	68	18	*86*	77	8	*85*
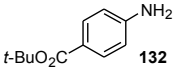 **132**	30	66	*96*	69	28	*97*	85	9	*94*

Tot: total yield

1.2.2.3 Fluorinated anilines

Fluorine substituents (*para* and *ortho* positions) are electron-withdrawing by induction and electron-donating by resonance. The inductive effect is highly dependent on the distance, contrarily to the resonance, for which distance does not seem to be an issue.

Two anilines **144** and **148**, bearing one *para*-fluorine atom and two fluorine atoms at *para*- and *ortho*-positions, respectively, have been studied (Schemes 35 and 36). Careful analysis (Table 3) of the results suggests that **144** behaves more like an electron-donating group due to the resonance effect of its F atom, its inductive electron-withdrawing effect being very weak because of its *para*-position.

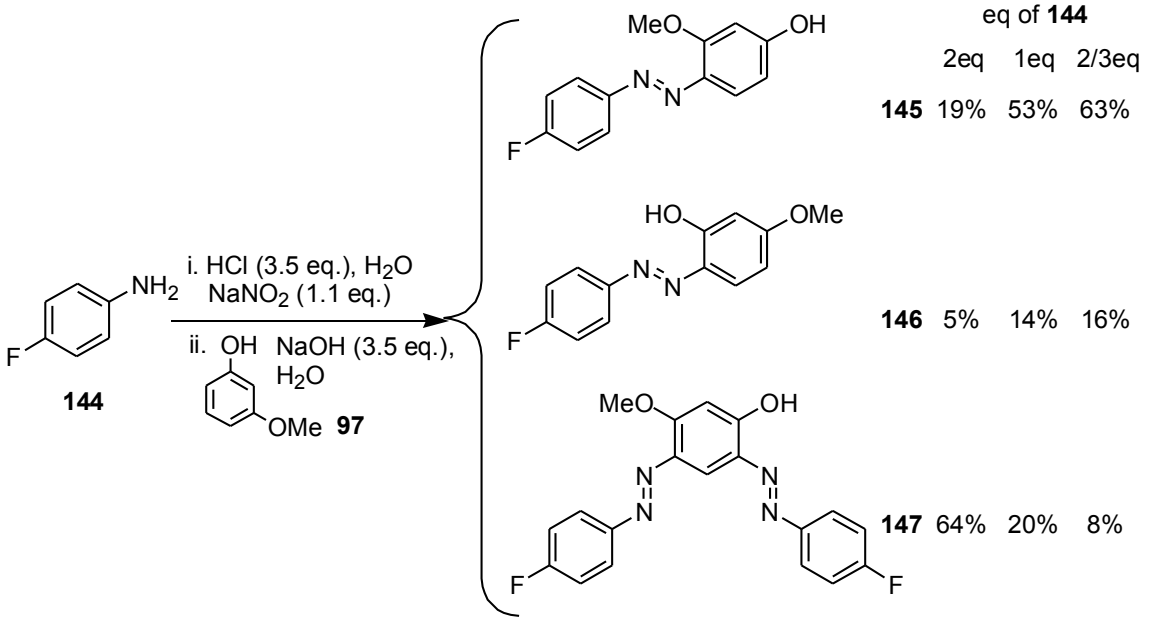

Scheme 35. Synthesis of azobenzene derivatives from aniline **144** with *para*-fluorine atom

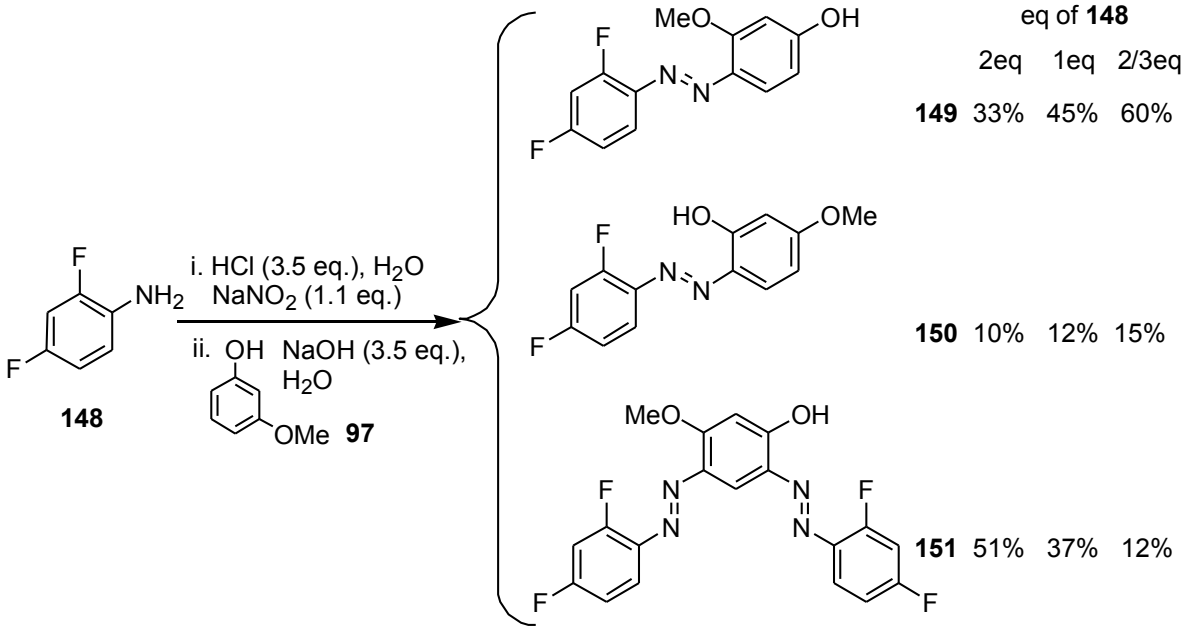

Scheme 36. Synthesis of azobenzene derivatives from aniline **148** with *para*- and *ortho*-fluorine atoms

Meanwhile, **148** exhibits an electron-withdrawing behavior. Indeed, both fluorine atoms are electron donating by resonance, but the *ortho* fluorine atom exerts a strong electron-withdrawing influence on the diazonium salt. This leads to good overall yields and the resulting *mono*-azobenzenes **149** and **150** are favored products. However, these two new compounds may become not so good substrates for the second step leading to the *bis*-azobenzene **151**. This may be explained by the electron-withdrawing influence exerted by the two F atoms on the phenol ring. With diminished electron density, the second coupling is not as favored as the first. Thus, there is accumulation of *mono*-azobenzenes by comparison with the *mono*-fluoro case (Table 3). When the [aniline] / [phenol] molar ratio is 4 / 1, the *bis*-azobenzenes only are obtained with excellent yields of 93%, 87%, 90% and 97% for **95**, **120**, **144** and **132**, respectively.

Table 3. Effect of substituents on aniline and [aniline] / [phenol] on the yield

	Yield / %								
	[aniline] / [phenol] = 2 / 1			[aniline] / [phenol] = 1 / 1			[aniline] / [phenol] = 2 / 3		
anilines	Mono	Bis	*Tot*	Mono	Bis	*Tot*	Mono	Bis	*Tot*
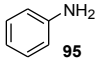 **95**	11	85	*96*	68	22	*90*	81	8	*89*
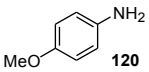 **120**	23	62	*85*	68	18	*86*	77	8	*85*
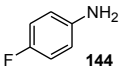 **144**	24	64	*88*	67	20	*87*	79	8	*87*
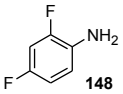 **148**	43	51	*94*	57	37	*94*	75	12	*87*
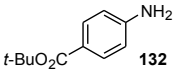 **132**	30	66	*96*	69	28	*97*	85	9	*94*

1.2.2.4 Improving the yield of *tris*-azobenzene

We have shown that electron-deficient anilines lead to diazonium salts which are particularly reactive during the coupling reactions with phenolates and leading to azobenzenes.

As previously described, aniline **95** reacted with triphenol **105** (Scheme 27), leading mostly to *bis*-azobenzenes with less *tris*-azobenzenes, even when the conditions should normally favor the formation of the latter. We demonstrate here that this trend can be overcome completely when the diazonium salt, prepared from an electron deficient aniline, reacts with triphenol **105**. Therefore, we employed aniline **132** and triphenol **105** to conduct the corresponding diazonium salts coupling reaction (Scheme 37). Using a 3:1 molar ratio of aniline **132** to triphenol **105**, only the desired *tris*-azobenzenes **152** was obtained in 68% yield, with no traces of competing *bis*-azobenzene.

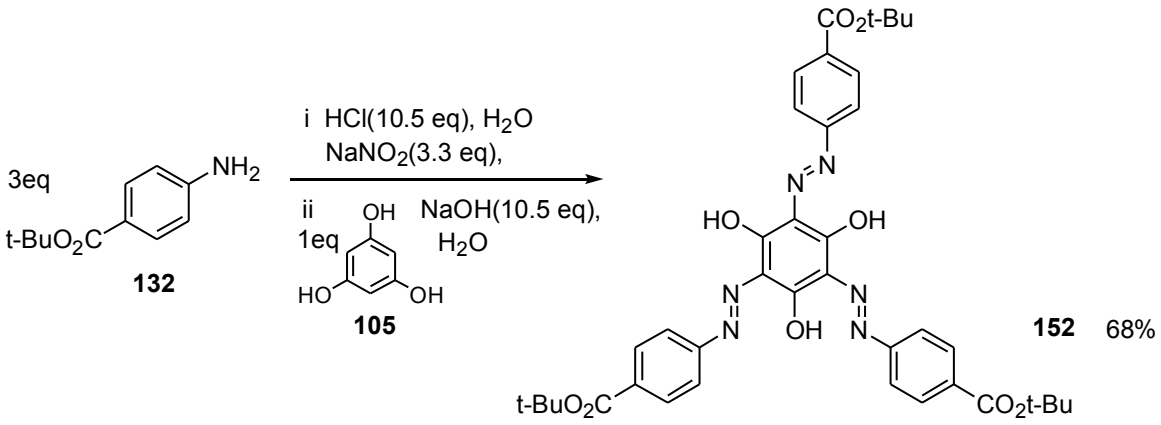

Scheme 37. Synthesis of *tris*-azobenzene from aniline with more electron-withdrawing group (-CO_2*t*-Bu)

According to these results, the yields of azobenzene compounds are dependent on the substituent groups on the phenols and diazonium salt rings, the molar ratio of starting

materials. The more electron-rich is the phenol ring, the more reactive it becomes. For the diazonium salt, it is exactly the opposite, the more electron-poor the aniline the more reactive the diazonium salt. This rule applies to the formation of the *mono*-azobenzene.

The second and third couplings may be affected in a different way, because the *mono*-azobenzene products of the first coupling reactions are the starting materials of the subsequent reaction leading to *bis*-azobenzenes. Each *mono*-azobenzene product reacts as a phenol reactant in the subsequent coupling reaction. The reactivity of the diazonium salt is obviously unchanged because it is in fact the same molecule as during the first coupling. Therefore, it is always a better choice to use electron deficient anilines.

1.2.2.5 Single crystal of azobenzenes

Some crystals of *mono*- and *bis*-azobenzene compounds were obtained by slow evaporation of EtOAc / n-Hexane solutions at room temperature in the dark. Their crystal structures could then be determined by X-ray crystallography (Table 4).

The structures demonstrate that the stable azobenzenes are always *trans*, as expected, and that molecules are fully conjugated. The geometries are also governed by hydrogen bonds involving phenols and the azo-groups, in relative *ortho* positions, to form six-membered rings. In the case of methoxy groups *ortho* to the azo-groups, the preferred geometry is always the one where steric interactions are minimized. The structures of the *mono*-azobenzenes also show that there is no steric clash that could prevent the second coupling leading to the *bis*-azobenzene products.

Table 4. Crystal structures of *mono*- and *bis*-azobenzenes

Mono-azobenzenes	*Bis*-azobenzenes
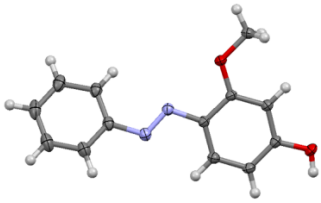	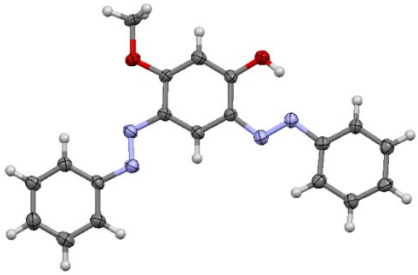
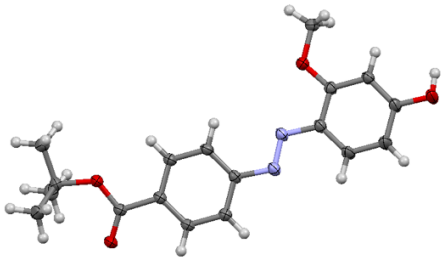	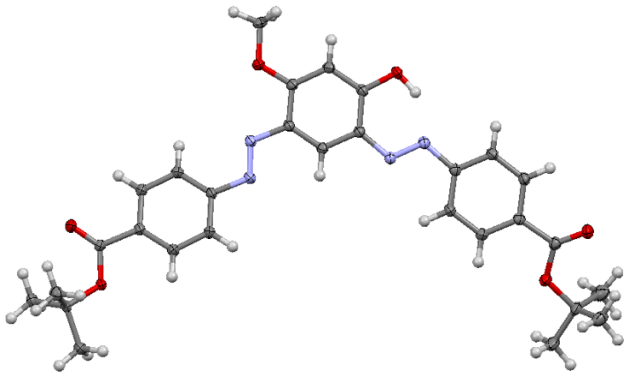
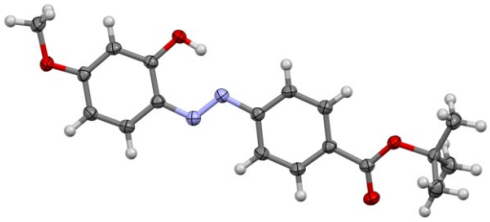	

1.3 Conclusions

In summary, we have established a novel and facile one-pot synthetic route for the preparation of *bis*-azobenzene and *tris*-azobenzene derivatives. The formation of *bis*-azobenzene compounds was mainly dependent on the groups on the phenol and the diazonium salt reactants. Compared to the simple aniline set as a reference (no substituent), electron-withdrawing substituted anilines, leading to electron-deficient diazonium salts, are

favorable for the formation of *mono*-azobenzene, and less favorable for the appearance of *bis*-azobenzenes. This is contrary to anilines substituted with electron-donating functional groups, which are not as efficient during the first step leading to the formation of *mono*-azobenzene and later favor the generation of *bis*-azobenzenes. As a rule, electron deficient anilines in over two-fold and three-fold excesses are the best choice for the preparation of *bis*- and *tris*-azobenzenes respectively in good yields.

CHAPTER 2 UNEXPECTED LIGHT INDUCED CYCLIZATION OF 2-(PHENYLAZO)PHENOL AND RELATED FRAMEWORKS WITH *ORTHO*-FLUORO GROUPS

2.1 Introduction

2.1.1 Motivation

In the first chapter, we had introduced the synthesis of *bis*-azobenzenes. Without surprise, the structures from X-ray crystallography demonstrate that the stable azobenzenes are always *trans*, and that the pi systems are fully conjugated. As the hydroxyl group is at the *ortho*-position of the azo-group, the geometries are also governed by hydrogen bonds involving six-membered rings (Table 4 in the Chapter 1). In the case of methoxy groups *ortho* to the azo-groups, the preferred geometry is rather the one where steric interactions are minimized. It is well known that a kind of reversible geometric changes of the azobenzenes would be occurred upon the light; in particular, the metastable *cis*-isomer can return to the more stable *trans*-state either through absorption of visible light or thermal relaxation.[120] Therefore, we became interested in stabilizing the *cis*-form of our *bis*-azobenzene systems. This was sought as a way to get different behaviors and some interesting photomechanical properties of these molecules.

2.1.2 The use of fluorine atom to favor the *cis*-form of azobenzenes

In order to favor the *cis*-form of azobenzene, we considered adding fluorine atoms in the *para*- or *ortho*-positions of their frameworks. Indeed, such fluoro substituents are known to increase the population of the *cis*-azobenzene form, because *ortho*-fluoro substituent can

decrease the n orbital energy of the *cis*-isomer. For instance, Blege*r et al.*[288-290] reported that *ortho*-fluoro azobenzenes can isomerize with visible light. Meanwhile, F atoms *ortho* to the azo-group lead to an effective separation of the n-π* bands of the *trans*- and *cis*-isomers. They also showed that *o*-fluorinated azobenzenes can greatly enhance thermal stability of the *cis*-isomers.

Therefore, using our procedure developed in Chapter 1, we wanted to prepare the following *bis*-azobenzene **151** (Figure 23):

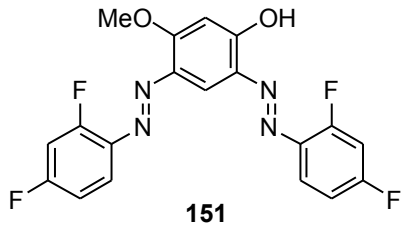

151

Figure 23. Chemical structure of fluoro *bis*-azobenzene, **151**

The corresponding *mono*-azobenzenes, **149** and **150**, are also expected to be easily obtained following the procedure described in Chapter 1 (Figure 24):

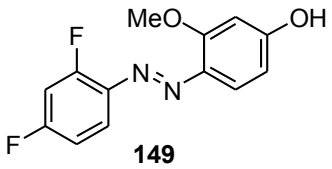

149

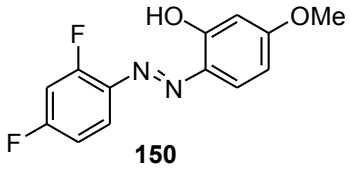

150

Figure 24. Chemical structures of fluoro *mono*-azobenzenes, **149** and **150**

Having these two *mono*-azobenzenes **149** and **150** in hands, we decided to study these model molecules to see whether the *cis*-form was somehow more stable than the same molecules without fluoro substituents, as was expected from literature precedents.[291,292]

2.2 Quest for the unidentified product

2.2.1 Effect of environment

2.2.1.1 In daylight

When **149** and **150** were dissolved in various solvents, from non-polar to polar, and also with solvents capable of intervening as hydrogen bond partners, some unexpected results appeared during the optical analyses over time. The recorded UV-vis absorption spectra of both *mono*-azobenzenes **149** and **150** did not change over time in EtOAc (Figure 25).

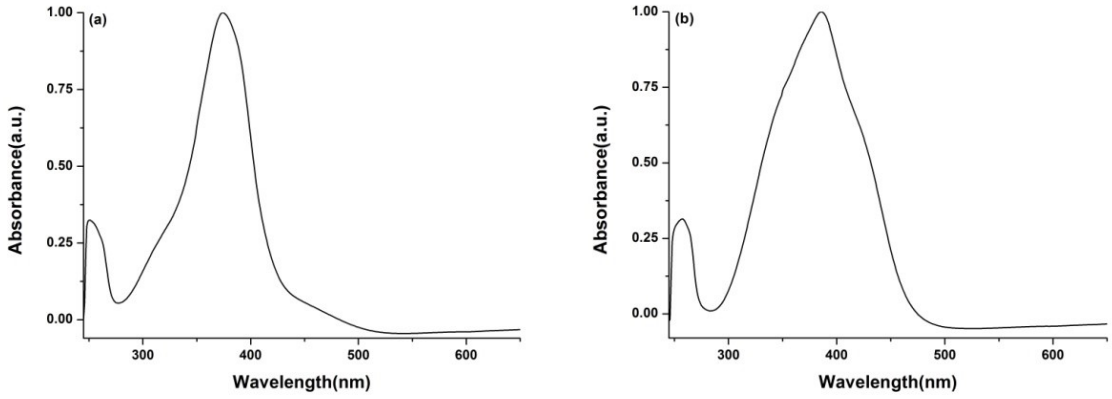

Figure 25. UV-vis absorption spectra of *mono*-azobenzenes over 96 hours in EtOAc at room temperature (a) **149** and (b) **150**

Conversely, the outcome is different in DMSO. The *mono*-azobenzene **149** displays clear isosbestic points (at 270 nm, 310 nm and 417 nm). The *mono*-azobenzene **150** does not show the same spectral pattern (Figure 26). From these preliminary results, we can understand that **149** is involved in a chemical equilibrium. Such equilibrium does not exist in the case of the molecule **150**, which is involved in some more complex phenomenon.

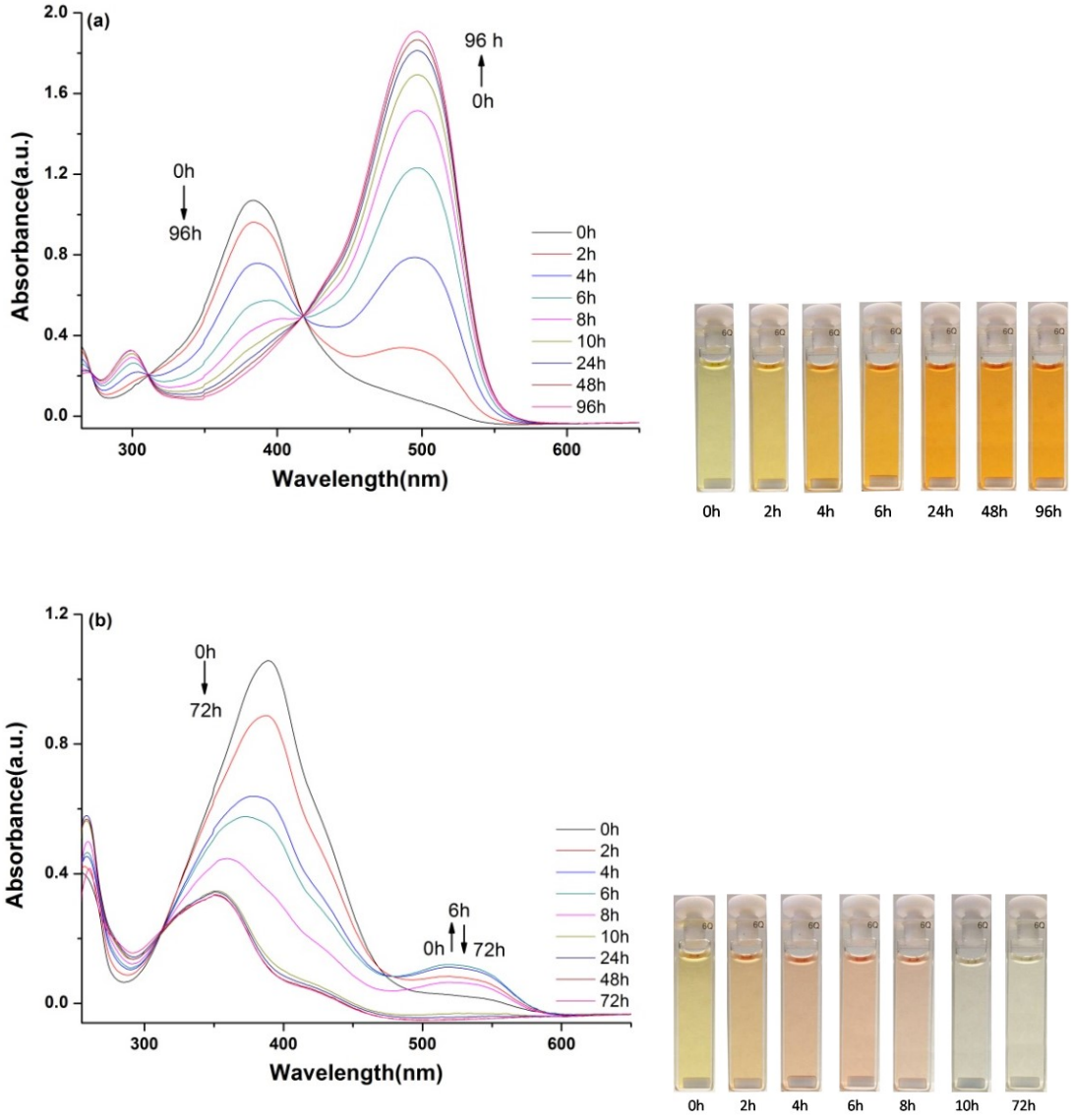

Figure 26. UV-vis absorption spectra of *mono*-azobenzenes over time in DMSO at room temperature and the corresponding photographs of solution, (a) **149** and (b) **150**

In order to get a deeper understanding of what was going on, we studied the evolution of ^{1}H NMR spectra over time in DMSO-d_6 at room temperature. The spectra recorded from *mono*-azobenzene **149** in DMSO-d_6 demonstrated that the molecule was remaining the same from the beginning until the end (Figure 27). The same series of NMR spectra,

recorded under the same conditions of concentration for *mono*-azobenzene **150**, indicated that this compound was slowly irreversibly transformed into something else (Figure 28).

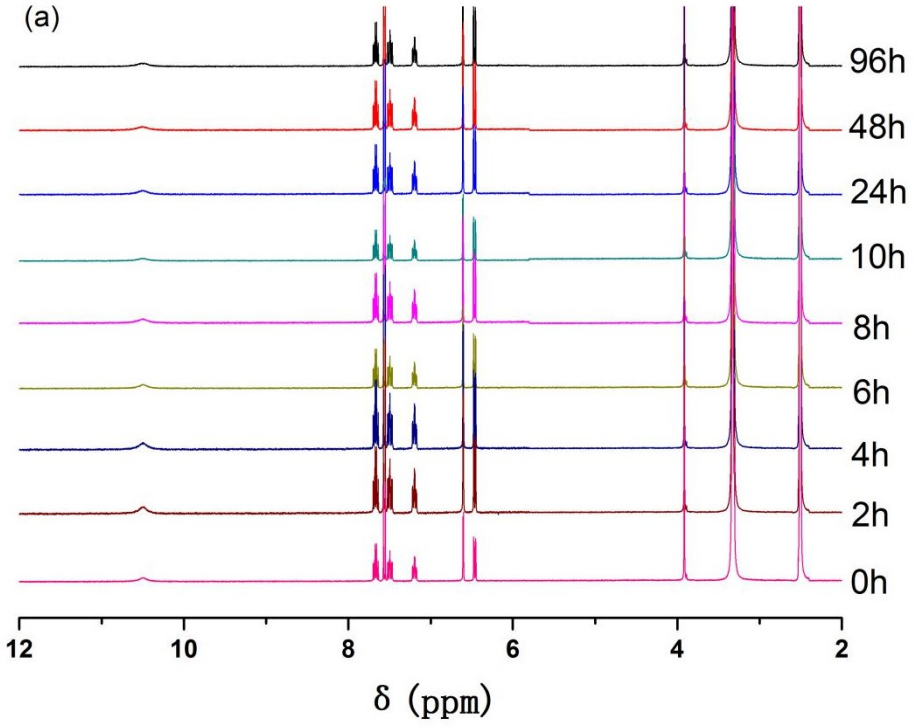

Figure 27. Time-dependent ^{1}H NMR of **149** over time in DMSO-d_6

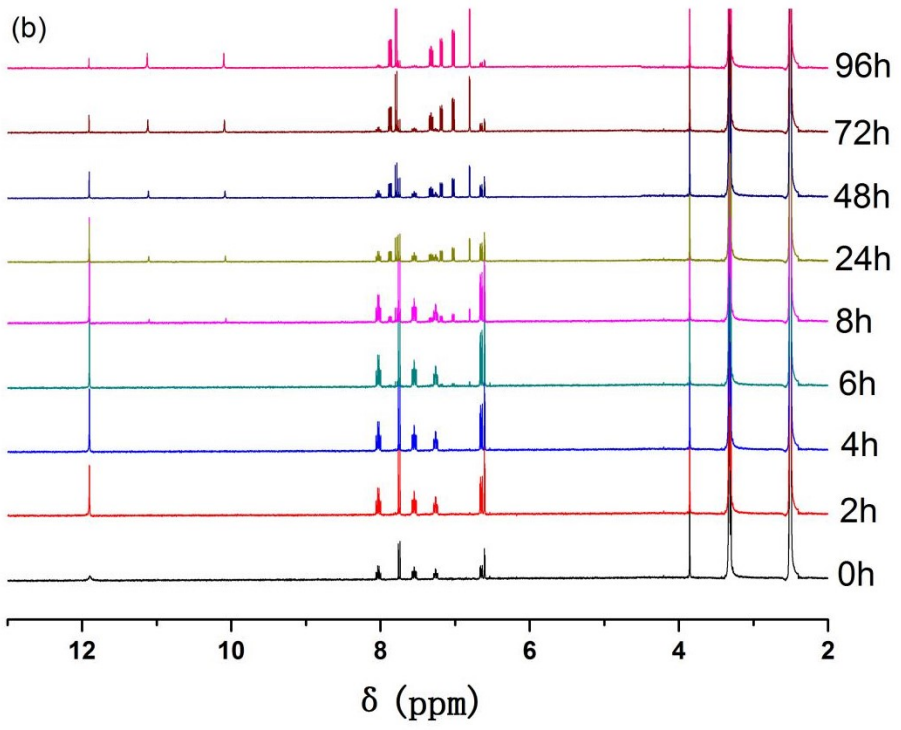

Figure 28. Time-dependent ^{1}H NMR of **150** over time in DMSO-d_6

The new compound was therefore isolated and its mass spectrum was recorded (Figure 29). The mass of **149** did not change from beginning to end (Figure 29a). However, it revealed a loss of 20 g.mol^{-1} in Figure 29b and it also showed that the new unknown compound is more polar. From these experiments, we could figure out that a molecule of HF had been formed during the reaction. Since the ^{1}H NMR signal (11.88 ppm) from the phenol group had also disappeared, it was a clear indication that the phenol had certainly been transformed into an ether **153** with extrusion of HF (Scheme 38). In addition, the peak of **149** at -107.6 ppm and -121.30 ppm do not change after 96 hours in the ^{19}F NMR spectroscopy. This is contrary to **150**, for which the peak at -120.87 ppm disappears whereas the other one at -106.39 ppm is retained (new close value of -106.58 ppm) after 96 hours. Noteworthy, the two peaks at 11.18 ppm and 10.10 ppm are attributed to impurities

that appear with the new product **153** after 96h (Figure 28b). They disappeared in the NMR spectrum of pure **153** after extraction (The identity of these impurities remains unknown). Obviously, this reaction can only take place when the azobenzene moiety adopts a *cis*-conformation, bringing the fluorine atom and the phenol groups close to each other. This proximity effect must be the reason why these two rather stable groups are able to react with each other in what looks like a nucleophilic aromatic substitution (S_NAr) process (Scheme 39). It is also an indication that the fluorine atom may indeed provide increased stability to the *cis*-azobenzene form, as was originally expected.

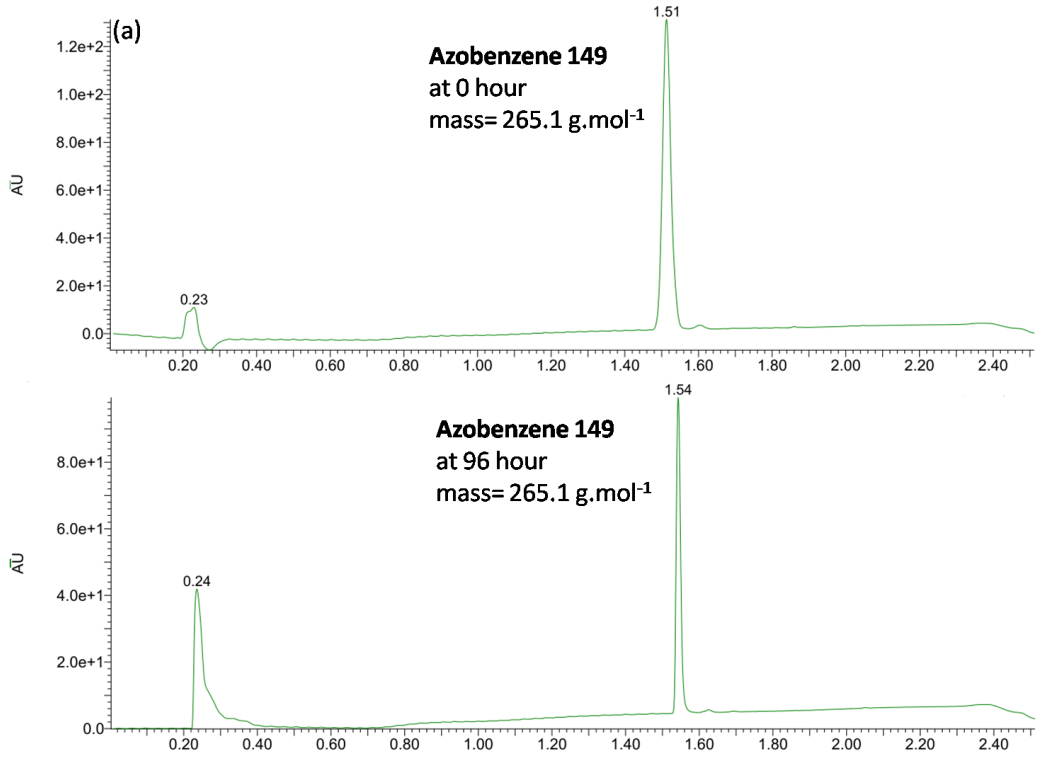

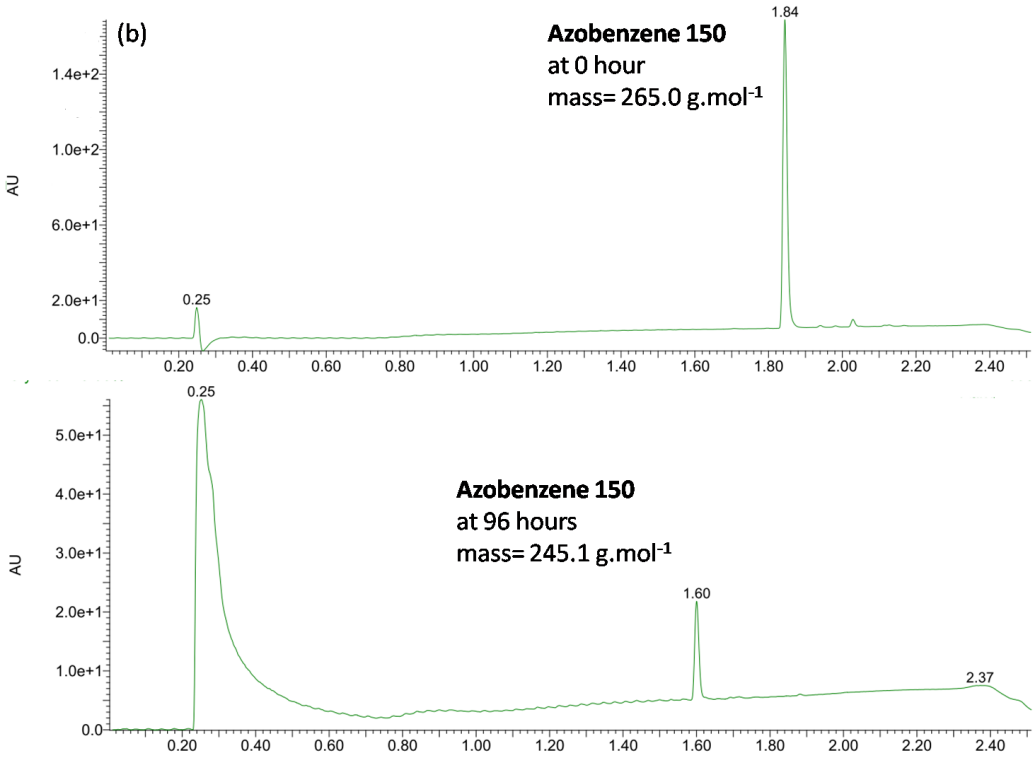

Figure 29. Mass spectroscopy of **149** (a) and **150** (b) at 0h and 96h respectively. Compounds measurement was carried out on a Waters (Canada) Acquity H-Class UPLC-MS system having PDA UV and SQD2 Mass detectors, equipped with a BEH C_{18} column (50 × 2.1 mm, 1.7 µm spherical particle size column) with a 0.8 mL / min flow rate using a gradient of 5-95 % (acetonitrile + 0.1 % HCO_2H) in (water + 0.1 % HCO_2H) over 2.5 min.

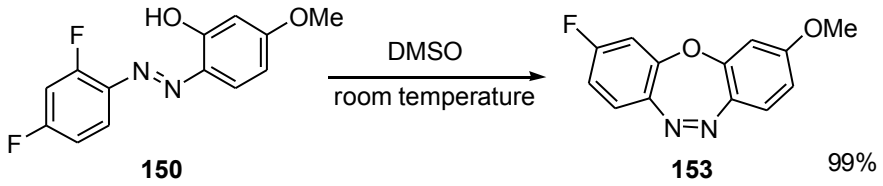

Scheme 38. Synthesis of cyclic *cis*-azobenzene **153**

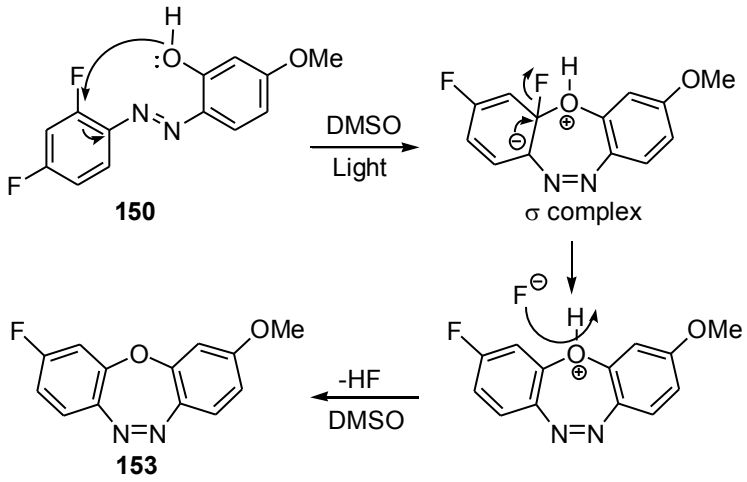

Scheme 39. Mechanism for the nucleophilic aromatic substitution (S_NAr) process from **150** to **153**

In another experiment, the NMR tube containing the azobenzene **150** in DMSO-d_6 was irradiated with UV light at 365 nm. Under these conditions the cyclization reaction of azobenzene **150** was completed in 20 seconds.

2.2.1.2 In the dark

Since the *cis*-azobenzene geometry is induced by light, another series of ^{1}H NMR spectra were recorded from samples that had been kept in the dark. The successive ^{1}H NMR spectra showed that no reaction was occurring over time, proving that the *cis*-azo conformer is the active species during the S_NAr reaction.

Moreover, the UV-vis spectra of azobenzene **149** in the dark (Figure 30b) behaved like that in the daylight (Figure 26a or Figure 30a), showing that tautomerization was proceeding over time. The peak centered at 495 nm belongs to the hydrazone tautomer.[134] The proposed mechanism is shown in Scheme 40.

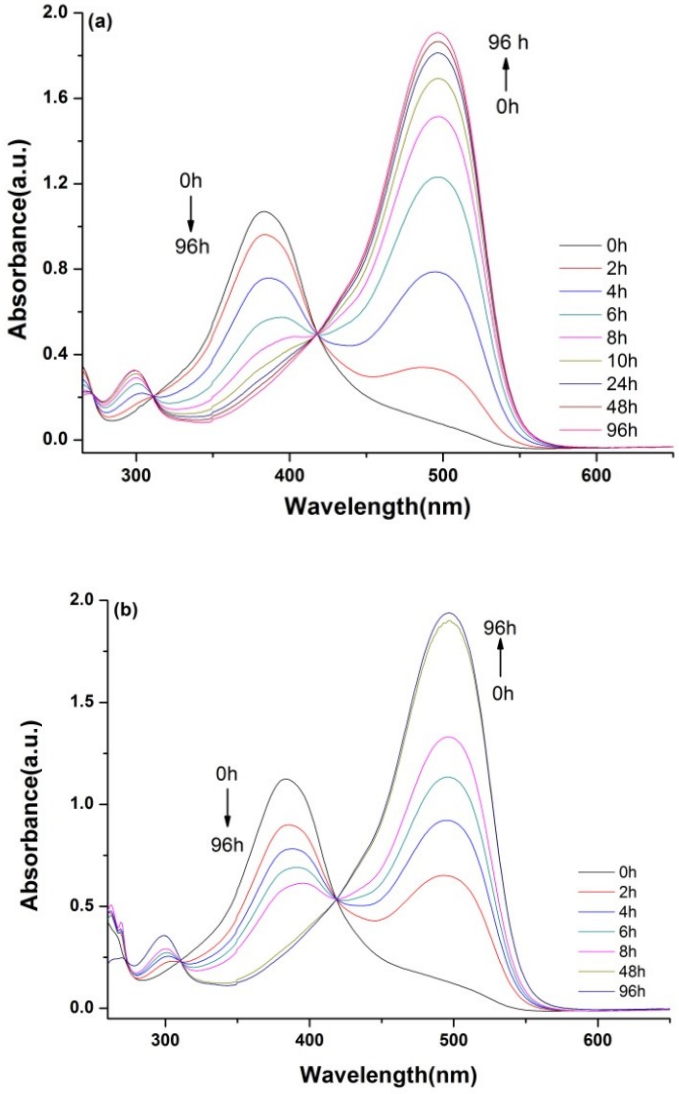

Figure 30. UV-vis spectra of *mono*-azobenzene **149** over time in DMSO in the daylight (a) and in the dark (b)

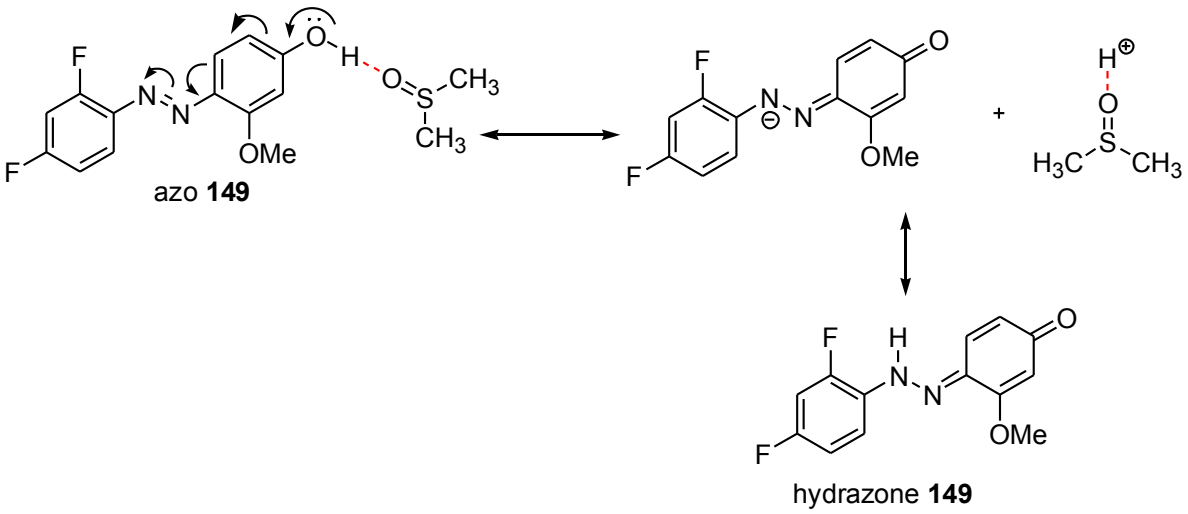

Scheme 40. Mechanism for the tautomerization between azo and hydrazone species

From Figure 31b, in the light, the absorption peak of the *mono*-azobenzene **150** at 520nm increased at first 6 hours and then decreased gradually. When it was left in the dark, its UV-vis absorption spectra became stable after 24 hours, showing the azo species and hydrazone species at 390 nm and 520 nm respectively (Figure 31a), proving once more that the daylight is very important for the cyclization to occur.

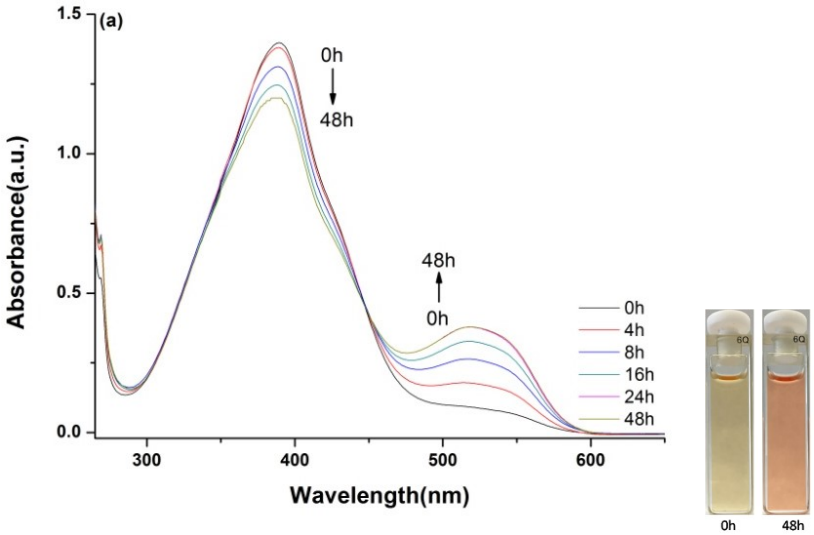

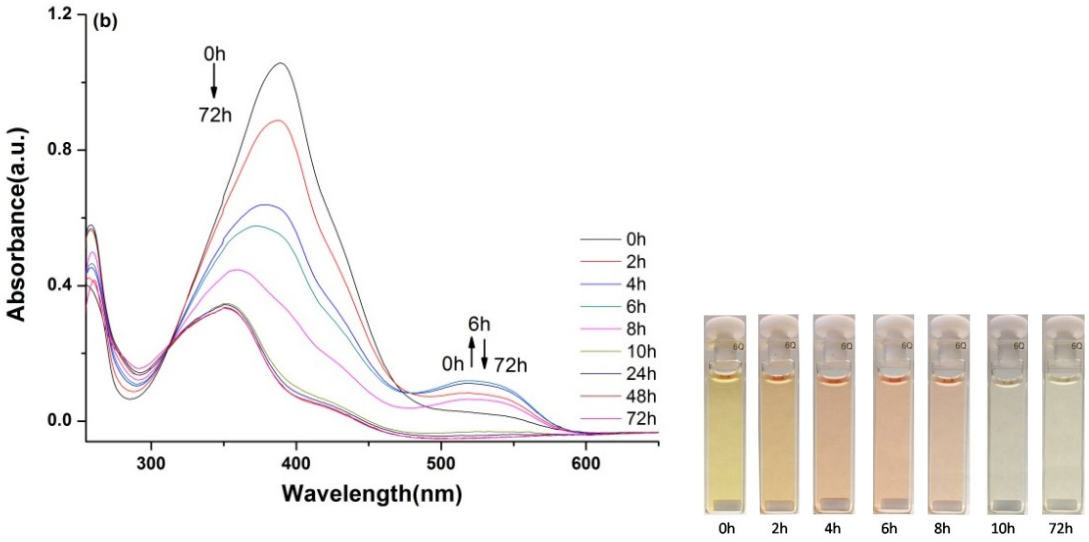

Figure 31. UV-vis absorption spectra of *mono*-azobenzenes **150** over time in DMSO at room temperature, (a) in the dark and (b) in the light

2.2.2 Effect of solvent

During our various experiments, we had noticed that **149** is invariably stable in various solvents, like EtOAc, $CHCl_3$, DMSO, DMF, etc. Things become a little more complicated in the case of **150**. Indeed **150** can produce the new ring system **153**, but this does not happen in all solvents. For example, DMSO appears to be ideal, contrarily to other solvent like EtOAc in which **150** does not react. This important aspect will be discussed more thoroughly, when the limitation of the reaction are studied.

2.3 The appeal of the new reaction and a new scaffold

This reaction could find applications in stimuli responsive materials, pretty much like other light sensitive groups, among others like the well-known spiro-pyran and diarylethene (Figure 32). The only limitation of this new reaction is its single time usage.

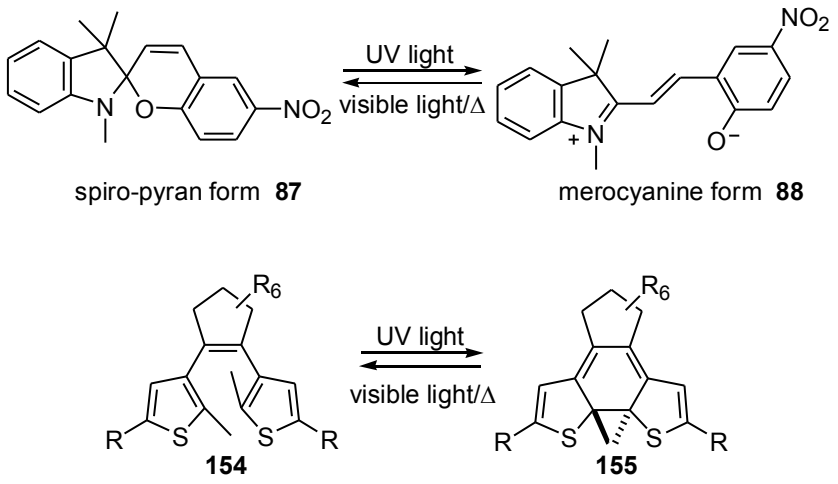

Figure 32. Chemical equilibrium of spiro-pyran and diarylethene

Compound **153** is also a very interesting molecule. The middle ring, which contains 8 pi electrons, is not stabilizing, on the contrary, since it violates the 4n+2 electrons aromaticity Hückel rule.[293] However, the molecule is capable of avoiding this detrimental condition, by adopting a geometry in which the central is bent (shown in Figure 33). Instead of being anti-aromatic (as would be the case if the whole molecule was flat) the compound is simply non-aromatic. This curved shape is found in many biologically active molecules like agents acting on the central nervous system (CNS) to treat many ailments like depression, schizophrenia, etc.[294]

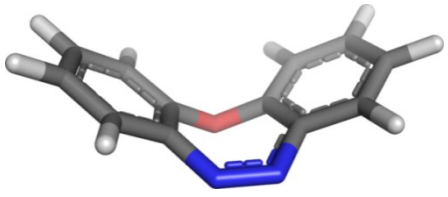

Figure 33. Bent structure of dibenzoxadiazepine as in **153**

In addition, the benzoannelated nitrogen and oxygen heterocycles are pivotal elements in

modern drug discovery programs.[17] They are druglike molecules due to the fact that they mimic related compounds having a bent structure. For instance, **22** and **23** are both inhibitors of 17a-hydroxylase-$C_{17,20}$-lyase and testosterone-5a-reductase (Figure 7 in the introduction), they can constitute prototypes for drugs used for the treatment of prostate cancer.[23]

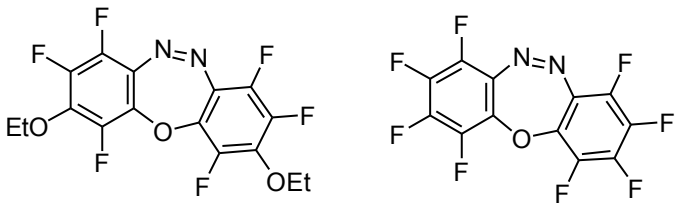

22 **23**

Figure 7. Biologically active dibenzoxadiazepines

2.3.1 Comparison between known syntheses of dibenzoxadiazepines with ours

Noteworthy, this type of dibenzoxadiazepines has already been prepared in the past following other methods, which can be divided into two branches according to their modes of cyclization. The first possible method is to sequentially form the ether then to cyclise by making the azobenzene *via* the formation of Ph-N=N-Ph bond as showed in Scheme 41.[7,17,111-117,295,296] As mentioned, the formation of ether bridge was performed at first, then a nitro group was reduced to the free amine and diazotized to the corresponding diazonium salt, that finally provided the desired dibenzoxadiazepine **160**.

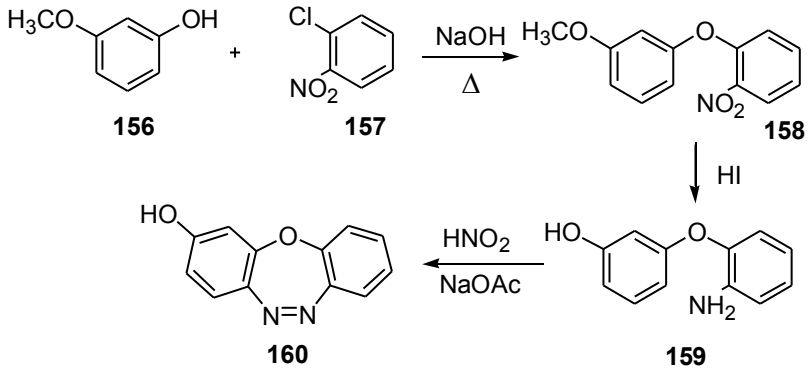

Scheme 41. Synthesis of cyclic azobenzene *via* the formation of *cis*-azo-group

Another similar strategy was used to synthesize **162** (Scheme 42) on solid support. The heterocycle **162** was obtained by cleavage with TFA from the resin at room temperature with an excellent yield of 80%.[17,118]

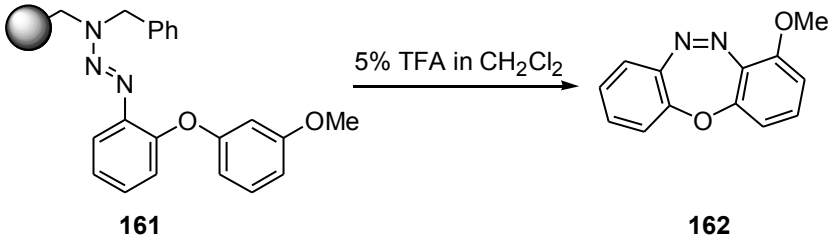

Scheme 42. Synthesis of cyclic azobenzene *via* the formation of *cis*-azo-group

There still exists another method that would require primarily the formation of the azobenzene followed by the cyclization leading to the ether bond. There are no examples of this approach in the literature, but this is precisely what happened during the synthesis of the dibenzoxadiazepine core. This is therefore a novel and original route.

2.4 Factors controlling the cyclization reaction of *mono*-azobenzenes

2.4.1 Effect of solvent on the cyclization reaction of *mono*-azobenzenes

It appears that our method (Scheme 38) is significantly simpler and also more efficient than the ones previously discussed (Schemes 41 and 42). Regarding the reaction medium, we studied the effect of solvents on the cyclization reaction. The reactions were carried out in various solvents at room temperature by taking the mixture of fluoro-azobenzene (**150**) and solvents. As shown in Table 5, significant amounts of cyclic products were collected in polar solvents. With DMSO, DMF and DMAc as solvents, the reactions were completed in 10h, 12h and 72h, respectively. In acetone and pyridine, the reactions proceeded slowly and were completed in three months. In EtOH, the reaction finished in nine months. No product was ever observed in less polar solvents, such as, EtOAc, $CHCl_3$, THF and Toluene. A systematic scan of solvents showed that solvents of lower polarity were not suitable, this might be the result of their inability to stabilize the σ complex. DMSO proved to be the most efficient solvent, both in terms of yield and kinetics.

Table 5. Effect of solvents on the cyclization of **150** to **153**.[a]

Solvent	Polarity (D)[297]	Time	Yield (%)
DMSO	7.2	10h	99
DMAc	6.5	72h	99
DMF	6.4	12h	99
pyridine	5.3	Three months	98
acetone	5.1	Three months	98
EtOH	5.2	Nine months	98.
EtOAc	4.4	Three months	N.R.
$CHCl_3$	4.1	Three months	N.R.
THF	4.0	Three months	N.R.
Toluene	2.4	Three months	N.R.

[a] Reaction conditions: organic solvents, room temperature, concentration of **150** (2.5×10^{-5}mol·L^{-1}), N.R.: No Reaction.

2.4.2 Effect of the substituents on the cyclization reaction of *mono*-azobenzenes

We then studied the scope and limitations (if any) of the reaction (Schemes 38). According to the mechanism of the S_NAr reaction, electron-withdrawing groups will stabilize the σ complex. Sure enough, when the withdrawing extra fluoro substituent at the *para*-position was removed, the process was much slower, requiring reaction times as long as 14 days for the *mono*-azobenzene **163** leading to the dibenzoxadiazepine **164** with nearly quantitative yields (Scheme 43).

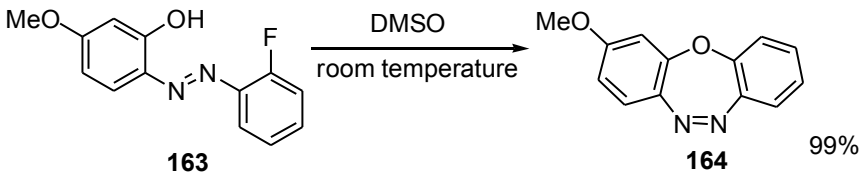

Scheme 43. Synthesis of dibenzoxadiazepine **164**

During this reaction, the UV-vis absorption spectra were recorded over time (Figure 34). The tautomerization was dominant at the beginning, meaning for the first 24 hours, being indicated by the isosbestic point at 453 nm. Then, after that time, the typical peaks corresponding to the azo (390 nm) and the hydrazone (520 nm) are slowly replaced by new peaks corresponding to the product **164**. Since the new peaks (from **164**) are not aligned with the old ones (from **163**), the spectra are not straightforward for the sixteen following days (convolution of spectra of **163** and **164**). After fourteen days, nothing changes, because there is now only the product **164** present in the cells. From its UV-vis spectrum, it can be seen that the new peaks are located at 345 nm and 425 nm, these are indicative of the cyclization.

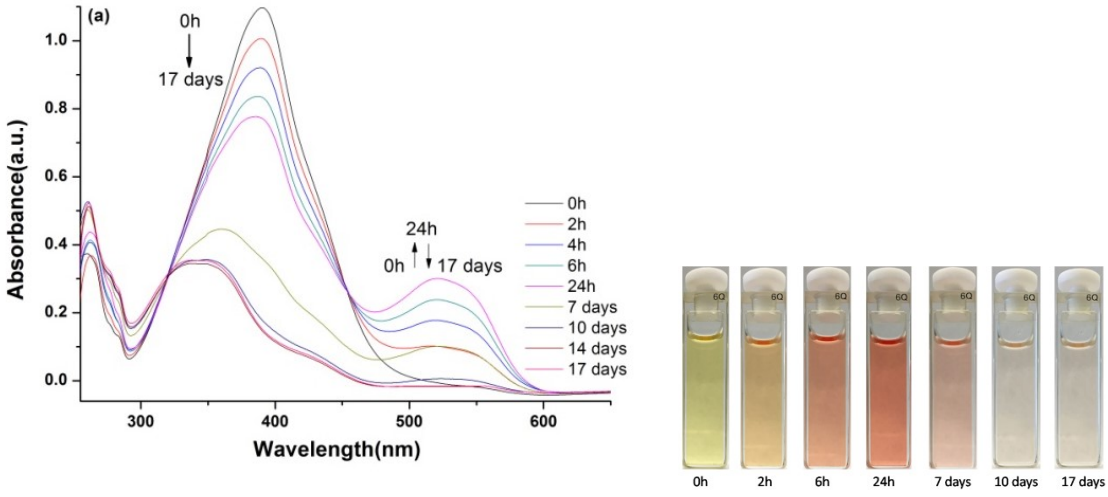

Figure 34. UV-vis absorption spectra of *mono*-azobenzene **163** recorded over time in

DMSO solution at room temperature and the photos of solution corresponding to 0 h, 2 h, 6 h, 24 h, 7 days, 10 days, 17 days, respectively.

The replacement of the *ortho*-fluoro leaving group by other halides (bromo-azobenzene **165** and chloro-azobenzene **166**, in Figure 35) produced no adduct, showing the optimal activation property of the *ortho*-fluorine atom.

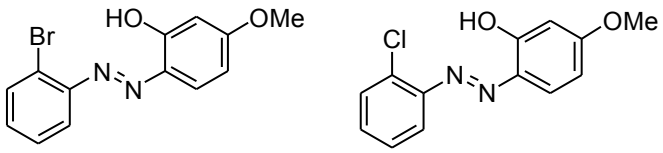

165 **166**

Figure 35. Chemical structures of bromo-azobenzene **165** and chloro-azobenzene **166**

2.4.3 The proposed mechanism for cyclization of *mono*-azobenzenes, 150 and 163

As described above, for azobenzenes with -F and -OH both *ortho* to -N=N- group, cylcization reactions occurred under the daylight or UV light and tautomerization happened in the dark. As shown in the proposed mechanism in Scheme 44, in the dark, the molecules in the polar solvents only undergo the *enol-keto* tautomerization (a), under the daylight or UV light, they go with *trans*-to-*cis* isomerization (b) and cyclization reaction (c). We can see that once the *cis*-isomers were formed under the light, the molecule undergoes the cyclization *via* the elimination of HF (c) to obtain the final compounds.

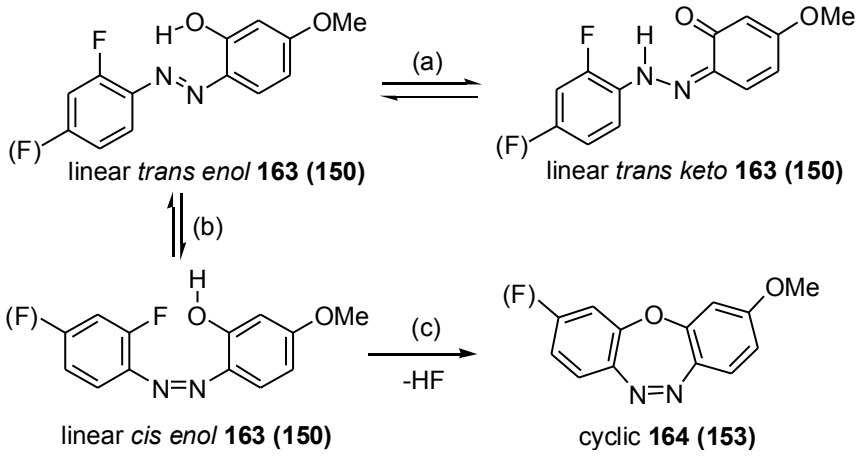

Scheme 44. The proposed mechanism for cyclization of *mono*-azobenzenes **150** and **163** (a) *enol-keto* tautomerization; (b) *trans-cis* isomerization; (c) cyclization *via* elimination of HF.

2.5 Preparation of fused dibenzoxadiazepine from *bis*-azobenzenes

These interesting results urged us to investigate other variations from *bis*-azobenzenes as starting materials in the daylight. From the chemical structure of *bis*-azobenzene **151**, the methoxy and hydroxy groups are at the *ortho*-position of the azo-group respectively. After cyclization reaction, one seven-membered ring was obtained between the *ortho*-fluorine atom and the *ortho*-hydroxyl group in 8 hours, showing the crucial role of hydroxyl group (Scheme 45). Unless stated otherwise, the concentration of the solution is 2.5×10^{-5} mol·L $^{-1}$.

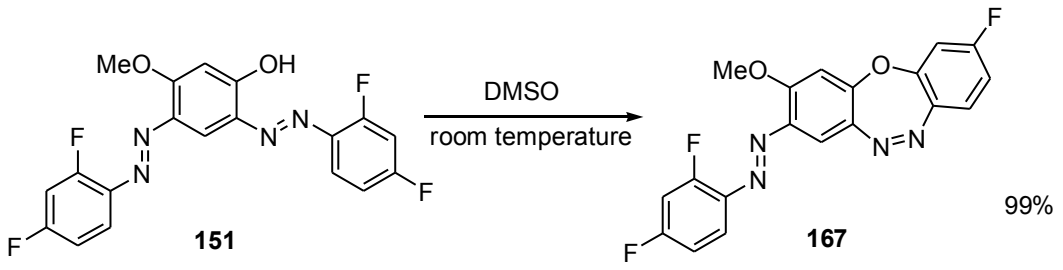

Scheme 45. Synthesis of dibenzoxadiazepine **167**

When the withdrawing extra fluoro substituent at the *para*-position was removed, the process was much slower, requiring reaction times as long as 4 days for the *bis*-azobenzene **168** leading to the dibenzoxadiazepine **169** in 98% yields (Scheme 46).

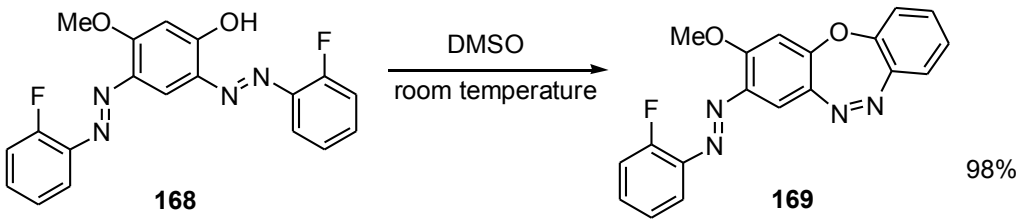

Scheme 46. Synthesis of dibenzoxadiazepine **169**

Moreover, the suitable *bis*-azobenzene **170** was also cyclized twice to form the pentacyclic system **171** very cleanly and with very high yields in DMSO (98%).

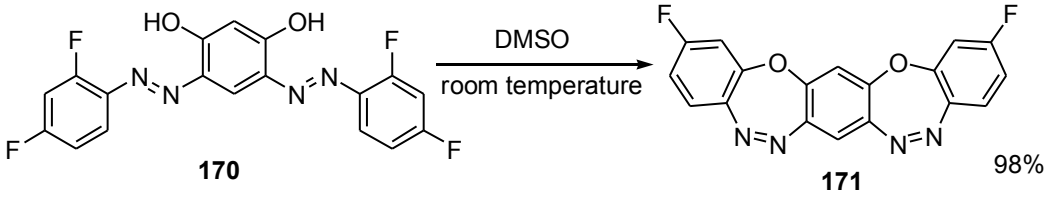

Scheme 47. Synthesis of cyclic *cis*-azobenzene **171**

However, instead of the fluoro leaving group by other halides (bromo-*bis*-azobenzene **172** and chloro-*bis*-azobenzene **173**, in Figure 36) produced no adduct, also showing the optimal activation property of the *ortho*-fluorine atom.

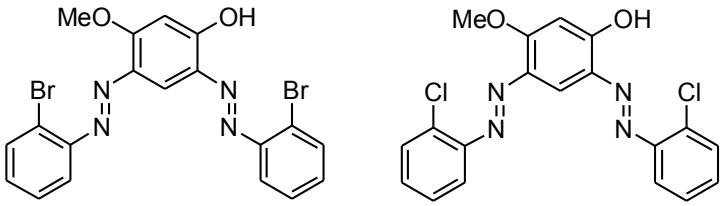

172 **173**

Figure 36. Chemical structures of bromo-*bis*-azobenzene **172** and chloro-*bis*-azobenzene **173**

2.5.1 Evolution of UV-vis spectra during the cyclization reactions of *bis*-azobenzenes

When these reactions (Scheme 45-47) were carried out (all are in DMSO), the corresponding UV-vis absorption spectra were also recorded, these are shown in Figures 35-37 respectively. By comparison with the simpler systems involving *mono*-azobenzenes (see parts **2.2.1**), the *bis*-azobenzenes cases constitute a whole different story. Everything becomes more complex. The time-dependent UV-vis absorption spectra of the reaction *bis*-azobenzene **151→ 167** (Figure 37a) shows the evolution of the various peaks in the spectra as the reaction proceeds. The following phenomena were observed: 1) the intensity of the left-most peak decreased gradually, 2) the middle and right-most peaks underwent a hyperchromic shift during the first 2 hours, and then decreased until total disappearance after 72 h. Meanwhile, the color of the solution changed significantly passing through the following colors: light green, peacock green, peacock blue and finally light yellow at the corresponding times: 0 h, 2 h (and 4 h), 6 h and 8 h (and until 72 h).

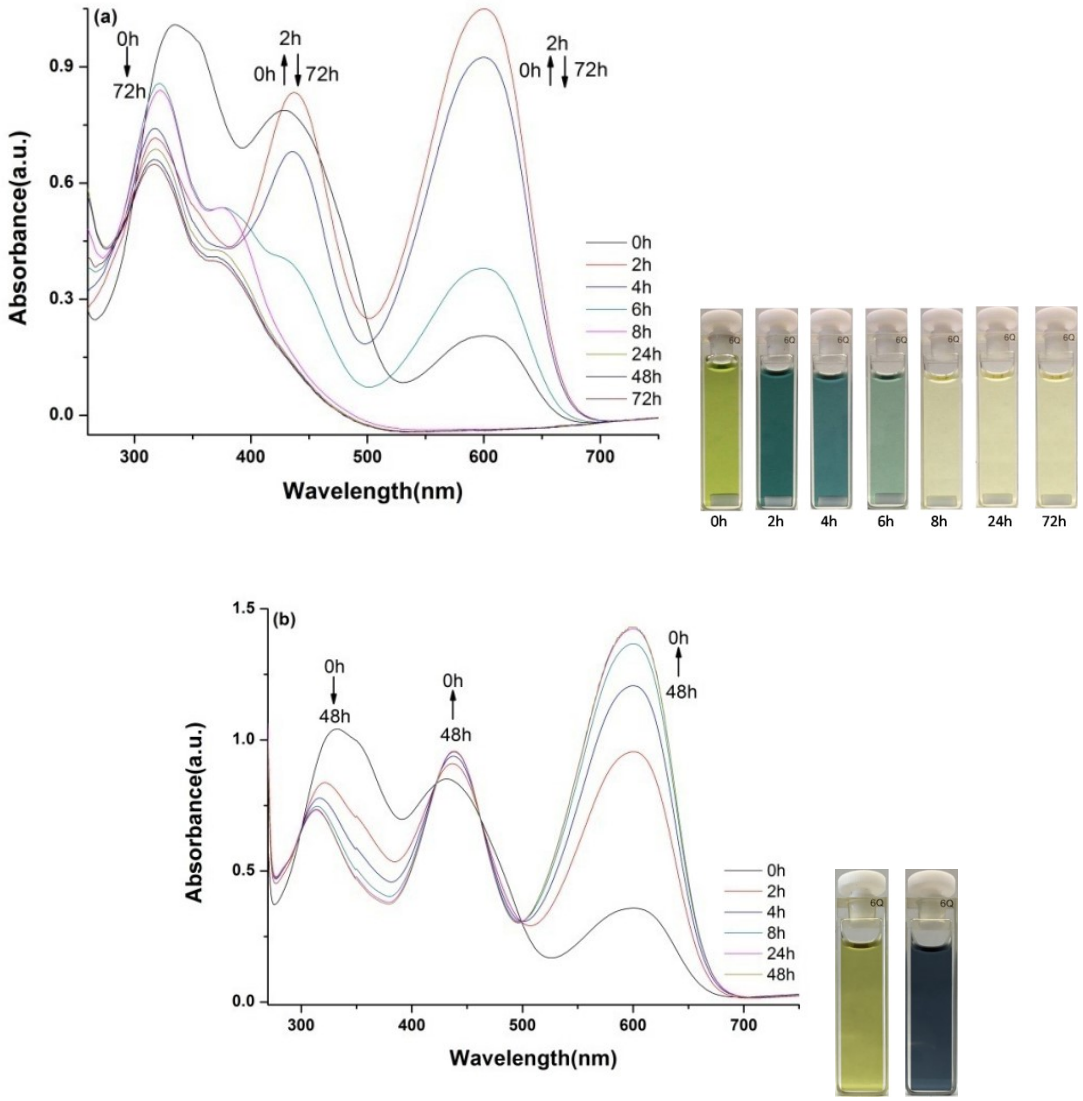

Figure 37. UV-vis absorption spectra of the reaction *bis*-azobenzene **151→ 167** over time in DMSO at room temperature with the corresponding photographs of the solution (a) in the daylight and (b) in the dark.

For the interpretation, the UV-vis absorption spectra were monitored over time in the dark. The UV-vis absorption spectra displayed clear isosbestic points at 300 nm, 423 nm, 462 nm and 499 nm (Figure 37b). From these preliminary results, we concluded that **151** is involved in an equilibrium in the dark. Such simple equilibrium does not occur in daylight

because the molecule was involved in some more complex competing phenomenon. We propose that in the dark, **151** is only able to tautomerize (Scheme 48, process a); whereas in light, this tautomerization equilibrium is in competition with its light induced isomerization (Scheme 48, process b) leading to the cyclization of its *cis*-form (Scheme 48, process c) to produce **167** irreversibly with departure of HF.

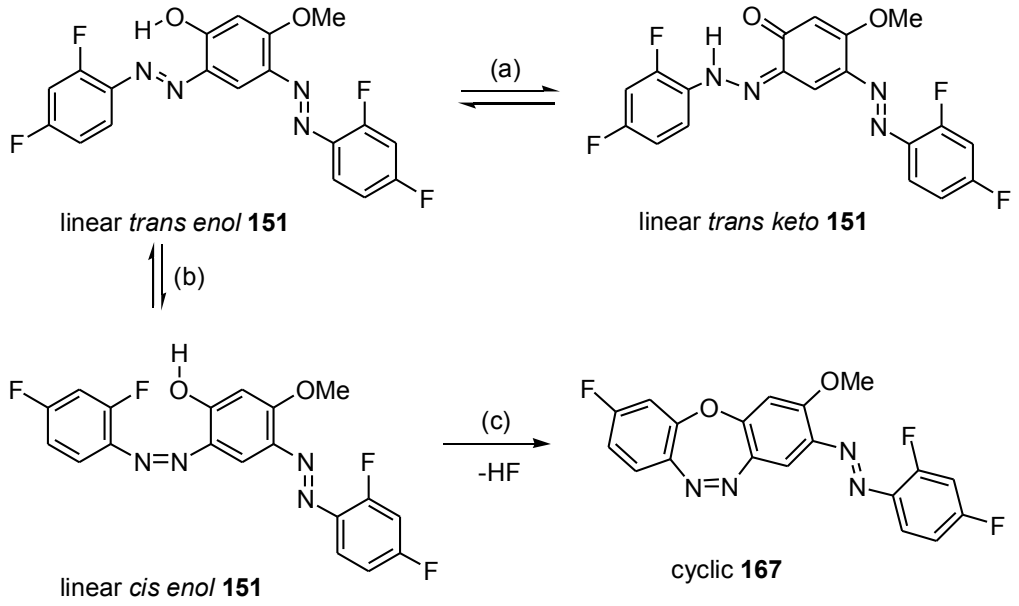

Scheme 48. The proposed mechanism for cyclization of *bis*-azobenzenes **151**, (a) *enol-keto* tautomerization; (b) *trans-cis* isomerization; (c) cyclization *via* elimination of HF.

From the UV-vis spectra in Figure 38, the *bis*-azobenzene **168** shows a similar behaviour as **151**, during its transformation into the dibenzoxadiazepine **169**. In the light, the colors of the solution change from light green to dark green, finally to pale yellow with time, almost like during the **151** → **167** transform. With only two fluorine atoms difference between **168** and its parent molecule **151**, the whole story is indeed much the same. The UV-vis absorption spectra in the obscurity and in the light look the same (compare Figures 37 and 38). The only difference in fact, as already mentionned, is the speed of the reaction **168** →

169, being slower than the reaction **151** → **167**. Presumably, the species that intervene amount also to four, involved in (a) *enol-keto* tautomerization, (b) *trans-cis* isomerization and (c) cyclization (Scheme 49).

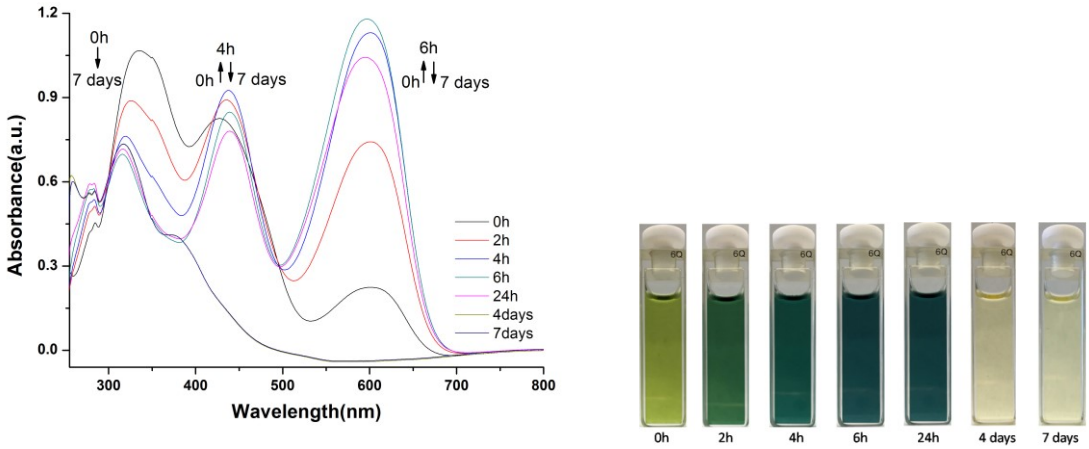

Figure 38. UV-vis absorption spectra of *bis*-azobenzene **168** over time in DMSO at room temperature, and the corresponding photos taken at 0 h, 2 h, 4 h, 6 h, 24 h, 4 days, 7 days.

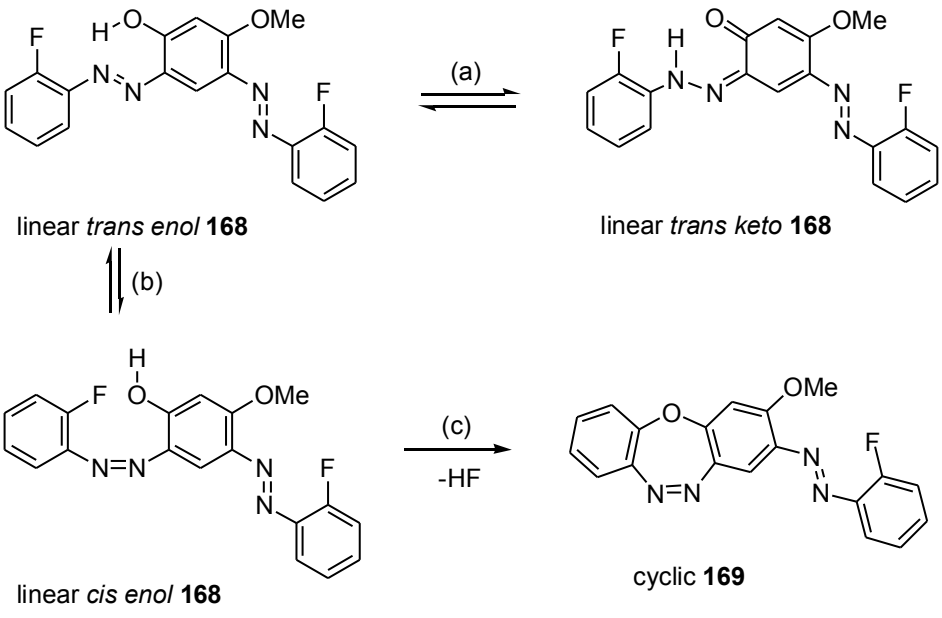

Scheme 49. The proposed mechanism for cyclization of *bis*-azobenzenes **168** (a) *enol-keto*

tautomerization; (b) *trans*-*cis* isomerization; (c) cyclization *via* elimination of HF.

The case of **170** → **171** (with light) is expected to be more complex. Indeed, as many as seven species are anticipated (Scheme 50). The *trans* / *trans enol* **170**, is likely the most stable form of the starting material, being in equilibrium in the dark (and in the light as well) with its *trans* / *trans keto* form. With light the *trans* / *trans enol* can first lead to its *cis* / *trans enol* conformer, then to its *cis* / *cis* conformer. The two latter enols having at least one *cis* azobenzene moiety can lead irreversibly to the corresponding dibenzoxadiazepines, the *cyclic* / *trans* enol and the *cyclic* / *cis* enol respectively, which are rapidly interconverting with light. The *cyclic* / *cis* enol is still able to form the bicyclic molecule **171**, driving the whole system to formation of this sole original fused-dibenzoxadiazepine. In terms of color change, one can observe the samples going through orange, dark pink then pale yellow for pure **171** (Figure 39a). In the dark the colors observed are dark pink. In the dark again, the UV-vis spectra recorded over time display three isosbestic points at 273 nm, 390 nm and 442 nm (Figure 39b), adding credit to the equilibrium between the *enol* and the *keto* forms of *trans* / *trans* **170**. In the light, despite the large number of possible equilibrating structures, the spectra do not appear unduly more complicated than in the previous cases. In fact, the same general trend is observed. However, under the same concentration, the highest intensity of *keto* species of **170** is much higher than that of *bis*-azobenzenes **151** and **168** (compare Figures 37, and 38).

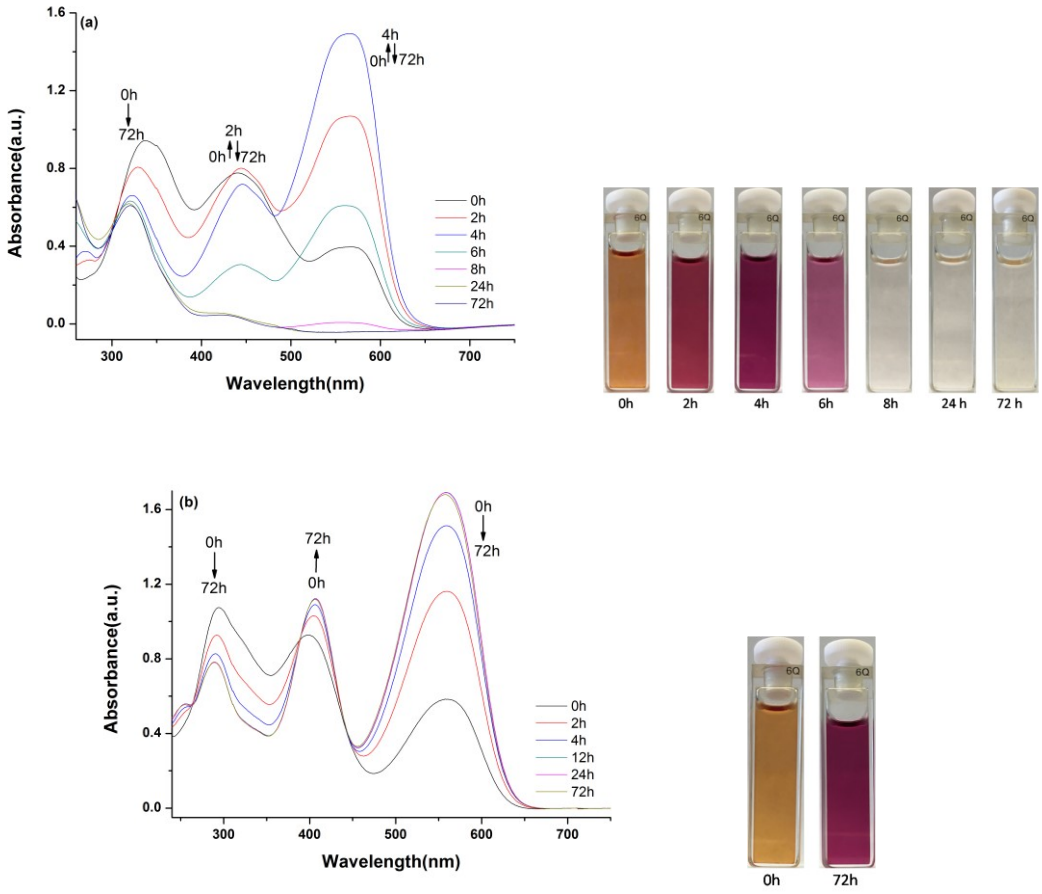

Figure 39. UV-vis absorption spectra of *bis*-azobenzene **170 → 171** over time in DMSO at room temperature, (a) in daylight, the photos taken at 0 h, 2 h, 4 h, 6 h, 8 h, 24 h, 72 h, respectively, (b) in the dark.

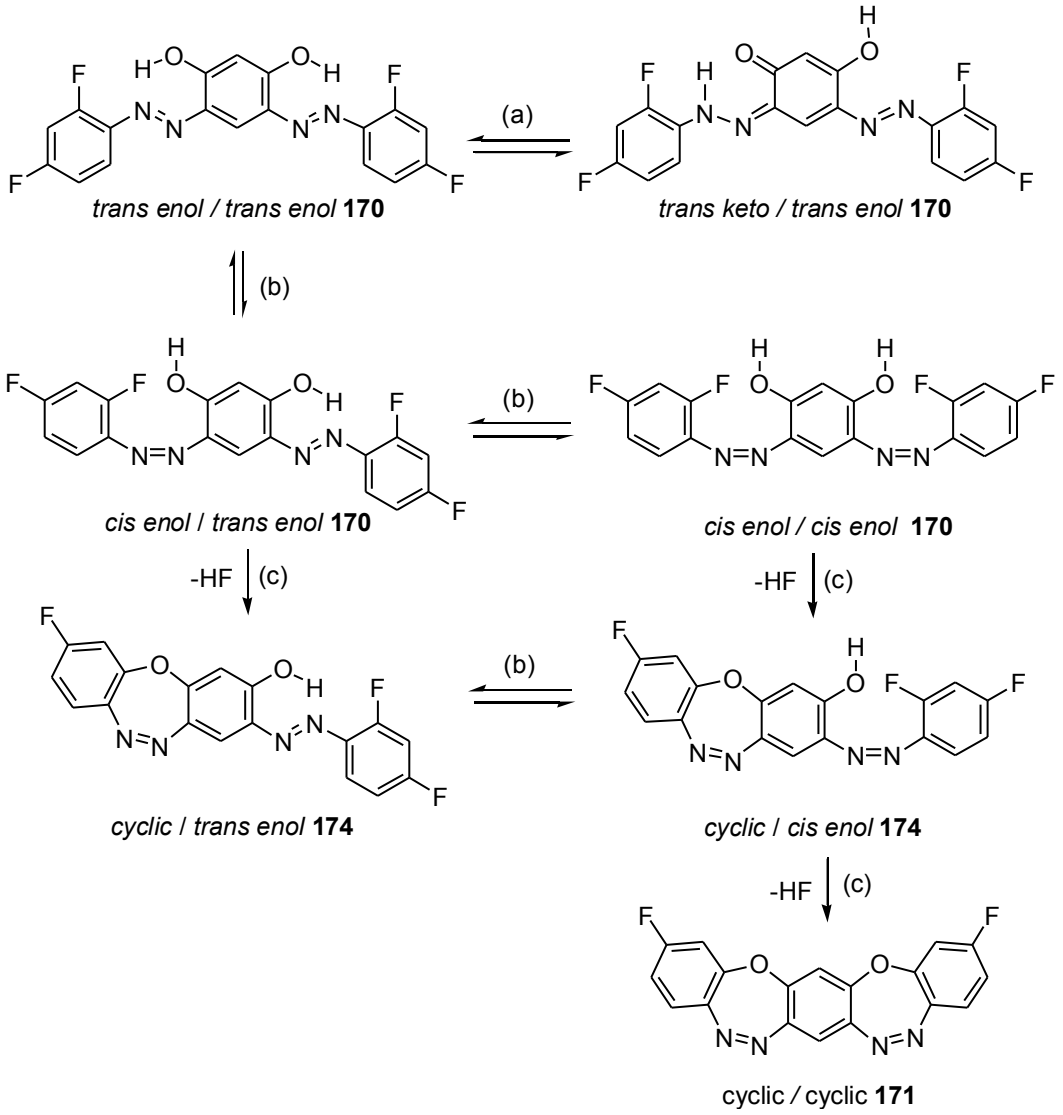

Scheme 50. The proposed mechanism for cyclization of *bis*-azobenzenes **170** (a) *enol-keto* tautomerization; (b) *trans-cis* isomerization; (c) cyclization *via* elimination of HF.

2.6 Conclusions

In summary, we discovered and studied a novel method for preparation of dibenzoxadiazepine (that are formally cyclic stable *cis*-azobenzenes) from *mono*- and *bis*-azobenzenes with daylight or ultraviolet light. The *ortho*-OH and *ortho*-F had a decisive

role in the cyclization reactions. Indeed, the fluorine atom provides increased stability to the *cis*-azobenzene form, which is the reactive species. The polar solvents also stabilize the σ intermediate complex. These azobenzenes cyclization reactions provide additional tools for the synthesis of druglike dibenzoxadiazepine derivatives, without the need of tedious and time-consuming purifications. When azobenzenes contain -OH and –F, both *ortho* to the azo-bond, the light is efficient to control this type of reactions: 1) in the light, goes with cyclization; 2) in the dark, proceed with tautomerization.

The compounds prepared in chapter are summarized in Table 6 with their corresponding reaction times and yields. Nothworthy, although the reaction times may appear very long, they can become as short as a few seconds by applying UV light irradiation. In the latter case, the reaction is very powerful.

Table 6. Cyclization of the hydroxyl fluoro-azobenzene derivatives[a]

Fluoro-azobenzenes	Cyclic azobenzenes	Time	Yield (%)
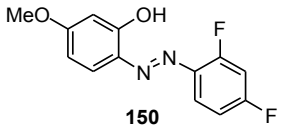 **150**	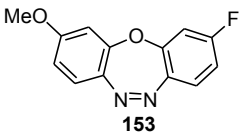 **153**	10 hours	99%
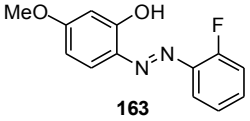 **163**	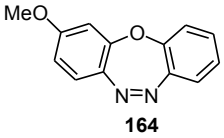 **164**	14 days	99%
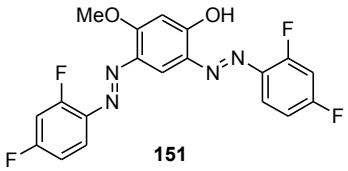 **151**	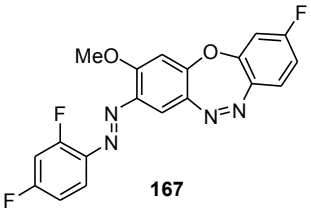 **167**	8 hours	99%
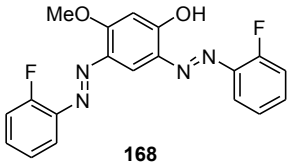 **168**	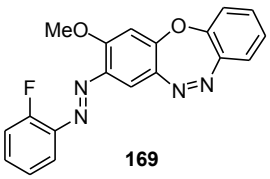 **169**	4 days	98%
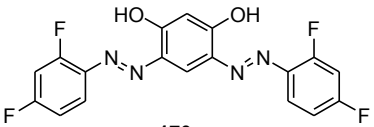 **170**	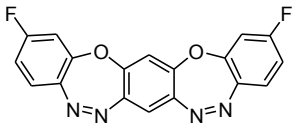 **171**	8 hours	98%

[a] Reaction conditions: DMSO, fluoro azobenzene compounds, concentration of starting material (2.5×10^{-5}mol·L^{-1}), room temperature, in daylight.

CHAPTER 3 SYNTHESIS AND STUDY OF PHOTO- AND THERMO-RESPONSIVE COPOLYMERS BASED ON *BIS*-AZOBENZENE DERIVATIVES

3.1 Introduction

Poly(*N*-isopropylacrylamide) (PNIPAM) is a typical thermo-responsive polymer which exhibits a lowest critical solution temperature (LCST) in aqueous solution due to its structure containing both hydrophobic and hydrophilic parts. The LCST behavior of PNIPAM is attributed to a reversible shift in the distribution of the hydrophobic and hydrogen-bonding interactions. Below the LCST, hydrogen bonds between the hydrophilic groups in polymer chains and water molecules are dominant, which leads to good solubility of the polymer chains in water. As the temperature increased, these hydrogen bonds become weaker and the hydrophobic interactions among hydrophobic side groups in the polymer chains become increasingly strong. When the temperature is above the LCST, the hydrophobic interactions become dominant resulting in a phase separation and collapse of polymer chains. In practice, the LCST is measured by monitoring the polymer solution transmittance as a function of temperature. On heating, the initially transparent solution becomes turbid at the LCST as a result of the phase transition. Approximately, the temperature at which the transmittance drops, denoted as the cloud point, is considered to be the LCST. The LCST of PNIPAM is about 32 ºC, i.e., close to the body temperature (37 °C), which makes it a potentially useful polymer for biomedical applications.[298,299]

On the other hand, azobenzene, as a reversible photo switch, was widely studied in combination with thermosensitive polymers. It was reported that the *trans*-*cis* isomerization of azobenzene can affect the LCST of thermosensitive polymers due to a change in

hydrophilicity or hydrophobicity resulting from the isomerization.[300-303] If the reversible photoisomerization can reversibly shift the LCST, it will be possible to switch the polymer between water-soluble and insoluble state by light at a constant solution temperature, which is of much interest for applications.

There are a few examples reported in the literature about the preparation of photo-and thermo-responsive copolymers including PNIPAM bearing azobenzene comonomer units.[261,262] However, a remaining major issue still needs to be addressed through further studies. That is, how to minimize the amount of stimuli-responsive comonomer, such as azobenzene, required to induce a significant change in LCST, or how to increase the magnitude of the cloud point shift at a given comonomer content. This question is important, because a very small amount of comonomer does not alter too much the thermo-responsive polymer, which is desirable in applications. In the case of using azobenzene comonomer, the literature shows that the *trans*-*cis* isomerization induced LCST shift is very small. Generally, a large amount of azobenzene comonomer (~ 5-10 mol%) is necessary to observe a LCST shift of a few degrees. To study this question, we synthesized random copolymers of PNIPAM with our novel *bis*-azobenzene derivatives. The basic idea is as follows. Since each *bis*-azobenzene molecule may undergo two *trans*-*cis* isomerizations, the possible effect on the LCST shift may be more important than one *mono*-azobenzene molecule. This means that it will be possible to use fewer *bis*-azobenzene comonomer units in PNIPAM to produce a similar effect on the LCST compared to using *mono*-azobenzene comonomer. In the present study, the phase transition behavior of PNIPAM has been investigated from the cloud point measurements. To the best of our knowledge, this work is the first observation about the effect of the photoisomerization of *bis*-azobenzene on the thermal phase transition behavior of PNIPAM.

3.2 Experimental Section

3.2.1 Preparation of *bis*-azobenzene monomer

All reagents, unless stated otherwise, were purchased from Sigma-Aldrich and used without further purification. Anhydrous dioxane was obtained in organic synthesis grade; all others were of special grade (> 99.5%).

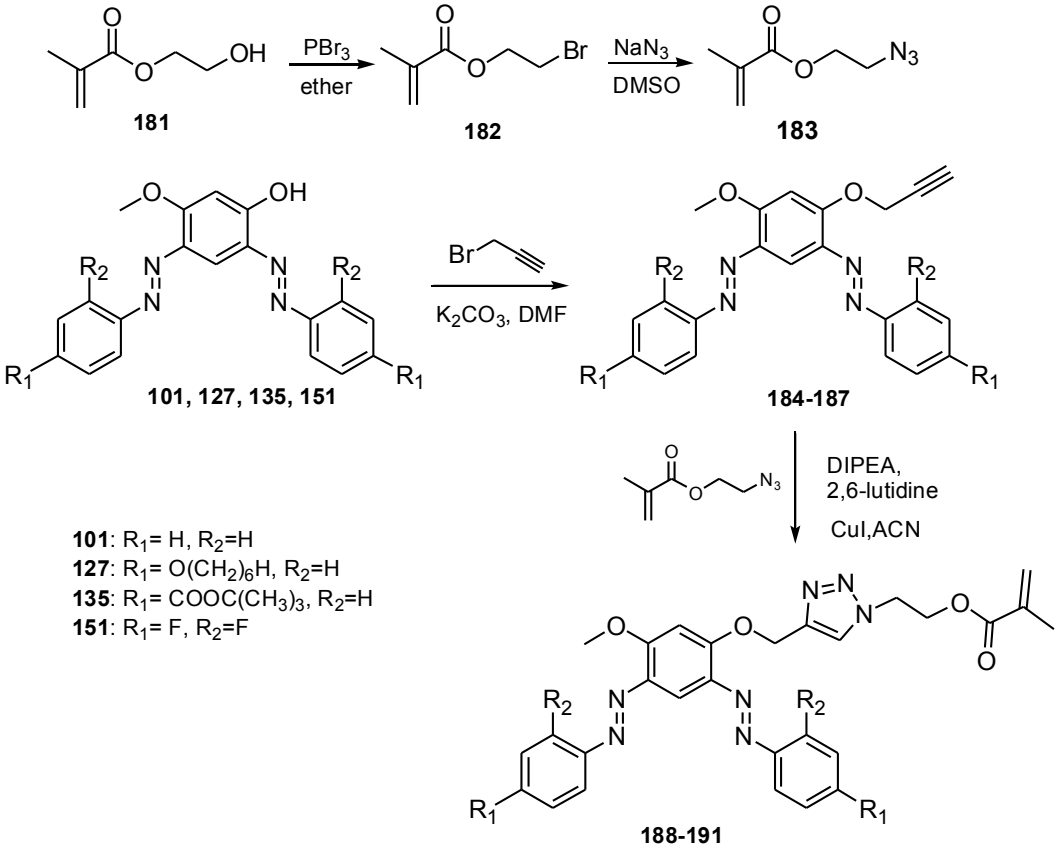

Scheme 51. Synthetic route for *bis*-azobenzene monomers **188-191**

The compound **183** was obtained by two steps (Scheme 51). In the first step, compound **182** was prepared by using PBr_3 (80%) under -20 ^oC.[304] In the second step, **182** was transformed into its corresponding azide **183** by means of NaN_3 in DMSO at room

temperature (94%).[305] The *bis*-azobenzene (Bisazo) derivatives **188-191** were prepared by treatment of **183** with alkyne **184-187** in DIPEA and 2,6-lutidine solution.[306]

3.2.2 Preparation of *mono*-azobenzene monomer

In order to assess the effect of *bis*-azobenzene, a *mono*-azobenzene (Monoazo) monomer was also synthesized for the polymer used for comparison. The monomer **196** was prepared by three steps (Scheme 52). The allylic alcohol **194** was synthesized by following a Baylis-Hillman procedure from t-butyl acrylate, giving 79% yield.[307] Compound **194** was then transformed into its corresponding allylic bromide **195** using PBr_3 (80%) at -20 ^oC in ether.[304] The **196** was obtained by reaction of the previously prepared azo phenol **125** with potassium carbonate, followed by addition of **195** (as an alkylating agent) in acetone under reflux overnight.

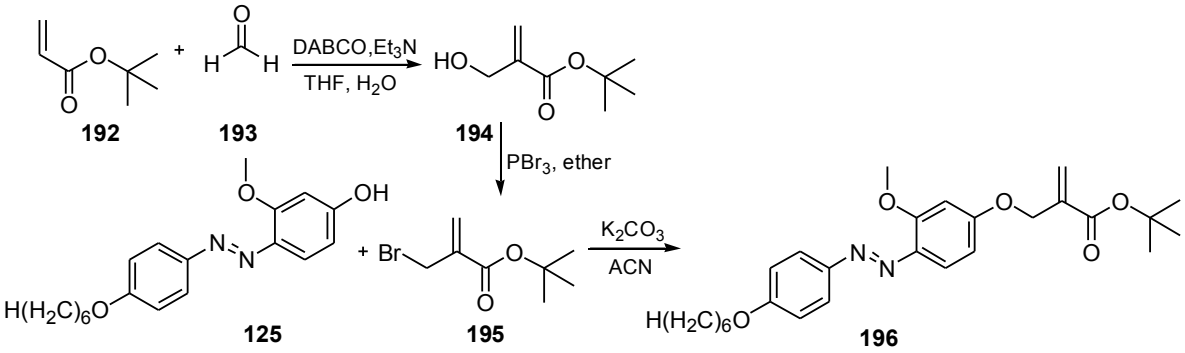

Scheme 52. Synthetic route for *mono*-azobenzene monomers, **196**

3.2.3 Preparation of P(NIPAM-co-Bisazo)copolymers

The *N*-isopropylacrylamide (NIPAM) monomer was recrystallized in hexane at 50 ^oC and dried under vacuum before use. The P(NIPAM-*co*-Bisazo) copolymers were synthesized according to the following procedure (see Scheme 53). *Bis*-azobenzene **188** (13.1 mg, 0.025 mmol) and NIPAM (0.110 g, 0.975 mmol) were mixed in dioxane (1.10 mL) under

an argon atmosphere and stirred at room temperature, followed by the addition of 1.23 mg of AIBN (1 mol% with respect to the monomer content). The reaction was allowed to proceed for 5 h at 85 °C under argon atmosphere. The products were reprecipitated 3 times from THF as a good solvent and cold diethyl ether as a poor solvent, and dried in a vacuum at 50 °C. Scheme 53 shows the structures of the *bis*-azobenzene based copolymers as well as their acronyms used in this chapter. Other P(NIPAM-*co*-Bisazo) copolymers (P_2, P_3 and P_4) were synthesized using the same procedure.

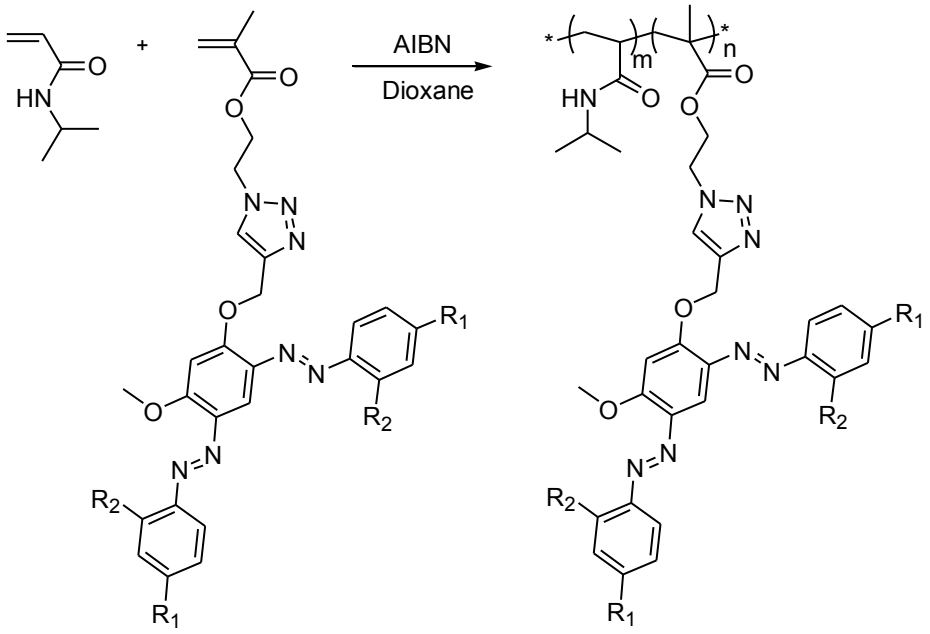

P_1 : P(NIPAM-*co*-Bisazo**188**): R_1= H, R_2 = H
P_2 : P(NIPAM-*co*-Bisazo**189**): R_1= $O(CH_2)_6H$, R_2 = H
P_3 : P(NIPAM-*co*-Bisazo**190**): R1= $COOC(CH_3)_3$, R_2 = H
P_4 : P(NIPAM-*co*-Bisazo**191**): R_1= F, R_2 = F

Scheme 53. Synthesis of copolymers containing NIPAM and *bis*-azobenzenes **188-191**

The polymerization procedure for P(NIPAM-*co*-Monoazo) P_5 is the same as above (Scheme 54). The molar ratio of [*mono*-azobenzene] / [NIPAM] in the polymer is 3.9 / 96.1 in 58% yield.

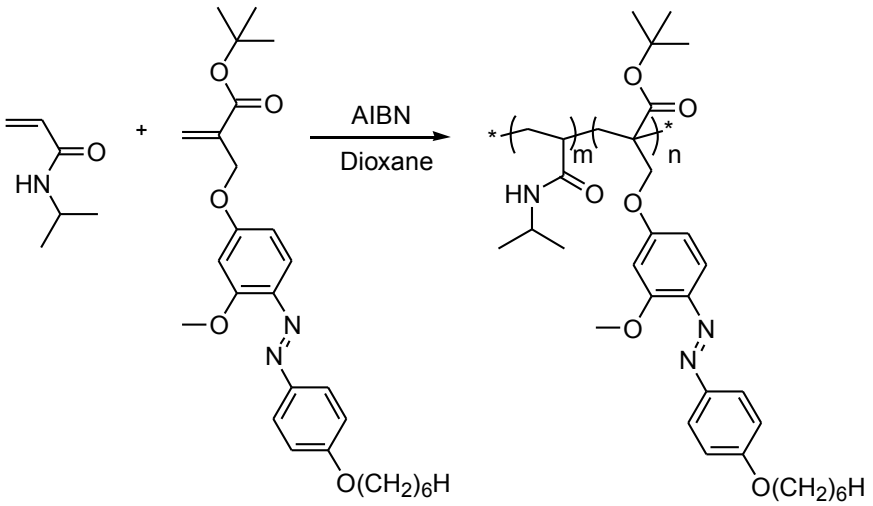

P_5 : P(NIPAM-*co*-Monoazo**196**): R_1= $O(CH_2)_6H$, R_2 = H

Scheme 54. Synthesis of copolymer P_5 containing NIPAM and *mono*-azobenzenes, **196**

3.2.4 Characterizations

The solution transmittance was measured using on an UV-Vis-NIR spectrophotometer (Agilent Carry Series 6000i) with a temperature controller. A 1 cm^2 sample cell, containing approximately 3 mL polymer solution, was used against distilled water as reference. Unless stated otherwise, the optical transmittance was measured by heating (1 °C min^{-1}) the copolymer solution (4 mg / mL) from 10 to 70 °C in the dark surrounding. The measurement wavelength was set at 700 nm that is sufficiently apart from the absorption of the chromophores. The cloud point of a given polymer solution was taken as the peak maximum of the first derivative of the transmittance (%T) *vs* temperature curves. Note that the copolymer solution was prepared by dissolving appropriate amounts of copolymers into distilled water in an ice-water bath, while being stirred continuously for at least 1 h until a transparent solution was obtained. The polymer solution was kept at 4 °C in a refrigerator before use.

^{1}H NMR spectra were recorded on an Ascend^{TM} 400 spectrometer, using $CDCl_3$ or D_2O as the solvent. The compositions of the various copolymer samples were determined from the ^{1}H NMR spectra by comparing the integrals of the peaks (3.8 ppm, from the tertiary carbons of NIPAM side groups and 7.0-8.0 ppm from the benzene ring). Variable-temperature ^{1}H NMR spectra were recorded in D_2O (deuterium oxide) over a temperature range between 10 and 70 °C at an interval of 3 ºC and a thermal equilibrium time of 5 min at each temperature before taking the spectrum. Gel Permeation Chromatography (GPC) measurements were performed on a Waters system equipped with a photodiode array detector (PDA 996) and a refractive index detector (RI 410). THF was used as the eluent at an elution rate of 1 mL min^{-1}, and polystyrene standards were used for calibration. The sample solution (0.1 mg / mL) was placed in a quartz cell having an optical length of 1 cm. UV irradiation was conducted using 365 nm light from the UV-Vis-NIR spectrophotometer. The UV-vis spectra of diluted polymer solutions (0.1 mg / mL) were recorded to monitor the progress of photoisomerization of azobenzene.

3.3 Results and discussion

Note that all chemical structures are drawn to show the polymer units. Table 7 summarizes the characterization data of the copolymers.

Table 7. Characteristics of the synthesized copolymers

Sample	Copolymer	Azo in polymer(mol%)[a]	*Mn*[b]	*Mw*/*Mn*[b]
P_1	P(NIPAM-*co*-Bisazo**188**)	1.7	6200	1.45
P_2	P(NIPAM-*co*-Bisazo**189**)	1.9	5800	1.53
P_3	P(NIPAM-*co*-Bisazo**190**)	1.8	6000	1.26
P_4	P(NIPAM-*co*-Bisazo**191**)	2.0	7200	1.37
P_5	P(NIPAM-*co*-Monoazo**196**)	3.9	7000	1.42

a: Calculated from ^{1}H NMR spectra in $CDCl_3$.

b: Measured by GPC in THF using polystyrene standards.

Mn: number-average molecular weight; *Mw*: weight-average molecular weight

3.3.1 Effects of azobenzene content and UV light irradiation on the cloud point

Comparing the cloud point of P(NIPAM-*co*-Bisazo**188**) with different contents of *bis*-azobenzene **188**, the curves of transmittance *vs* temperature of P(NIPAM-*co*-Bisazo**188**) are shown in Figure 40. The results show that the three polymers display the LCST-type phase transition. Their cloud points are at 23, 25 and 26 ºC with *bis*-azobenzene **188** 2.4 mol% (black line), 1.7 mol% (blue line), 1.2 mol% (purple line), respectively. Because of the higher hydrophobicity of *bis*-azobenzene moieties in comparison with terminal amino groups, an increase of the *bis*-azobenzene proportion decreases the overall hydrophilicity of thepolymer, resulting in a lower cloud point. Thus, the introduction of a hydrophobic monomer and the increase of its content result in lowering of the phase transition temperature, which is consistent with the previous results.[308]

The effect of UV light irradiation (365 nm UV irradiation, 10 min) on the cloud points of the various P(NIPAM-*co*-Bisazo**188**) aqueous solutions are also shown in Figure 40. After UV light irradiation, the cloud point of the polymer solutions increases to 25 (red line), 26 (green line), and 27 ^{o}C (yellow line), respectively.

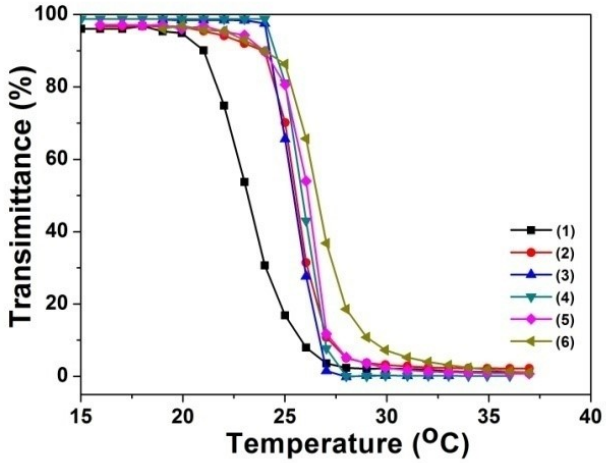

Figure 40. Transmittance *vs* temperature for aqueous solutions of three random copolymers: (1) and (2): P(NIPAM-*co*-Bisazo**188**)-2.4% (2.4 mol% of bisazo) before and after UV; (3) and (4): P(NIPAM-*co*-Bisazo**188**)-1.7% (1.7 mol% of bisazo) before and after UV; and (5) and (6): P(NIPAM-*co*-Bisazo**188**)-1.2% (1.2 mol% of bisazo) before and after UV, respectively.

To further confirm the change in phase transition temperature of the copolymers, the variable-temperature ^{1}H NMR spectra in D_2O of P(NIPAM-*co*-Bisazo**188**) (P_1 with 1.7 mol% of *bis*-azobenzene) were recorded and shown in Figure 41. Upon heating, the gradual decreasing resonance signal in the range of 7.0-8.0 ppm (aromatic protons) is ascribed to the soluble-to-insoluble phase transition of the azobenzene moieties, while the decreasing signals at 3.91 ppm and 0.5-2.5 ppm are attributed to the soluble-to-insoluble phase transition of PNIPAM at elevated temperature. From Figure 41, the LCST-type phase

transition of the random copolymer is evidenced. This can also be seen in Figure 42, where the plot of peak integral *vs* temperature is shown.

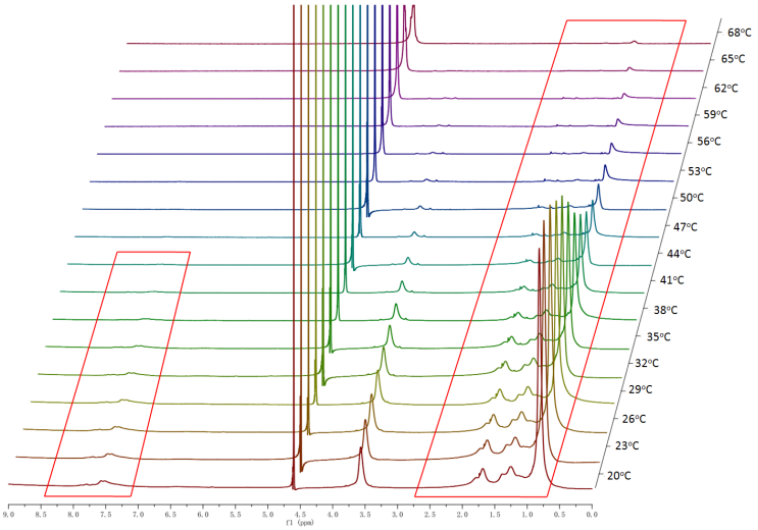

Figure 41. Variable-temperature ^{1}H NMR spectra of P_1 in D_2O recorded from 20 ^{o}C to 70 ^{o}C with an interval of 3 ^{o}C.

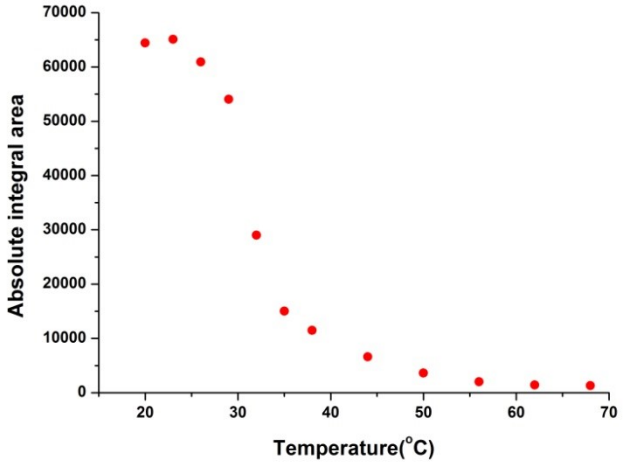

Figure 42. Change in the integral of the resonance peaks from 0.5 to 2.5 ppm as a function of temperature (from Figure 41), showing the LCST-type phase transition.

3.3.2 Effect of substituents of *bis*-azobenzene derivatives on the cloud point

By varying the substituents on *bis*-azobenzenes, more analyses of photo sensitive properties of the polymers can be performed. In this part, P_1-P_4 were investigated to compare the effect of different chemical structures of *bis*-azobenzenes on their cloud points, with P_1 and P_2 having donor on the *bis*-azobenzene moieties, and P_3 and P_4 containing donor-acceptor on the *bis*-azobenzene moieties, respectively. Figure 43 shows the results obtained with the random copolymers P_2.

From Figure 43(a), the cloud point is at 28 ^{o}C upon heating before irradiation (black line). After 10 minutes of irradiation with 365 nm UV light, the occurrence of the photo-isomerization reaction from *trans*-states to *cis*-states could be seen from the UV-vis spectra in Figure 43(b). Apparently, only about 26% *trans*-isomers were converted to *cis*-isomers. Meanwhile, From Figure 43(a), it can be seen that the cloud point of the polymer solution increases from 28 to at 30 ^{o}C after UV irradiation, while the content of *cis*-isomers remains quite stable over the range of temperatures. At the end of the heating process (40 ^{o}C), there are still 16% of *cis*-isomers remained in the solution. Part of the *cis*-to-*trans* isomerization occurs thermally. In addition, under the visible light irradiation, the cloud point can be recovered to its original temperature.

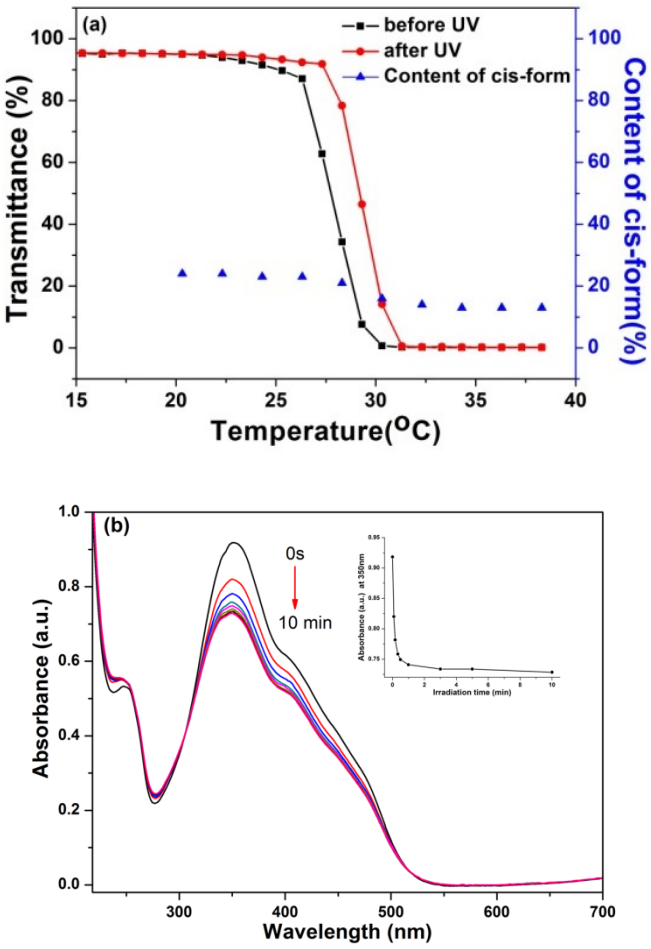

Figure 43. (a) Transmittance *vs* temperature for P_2 aqueous solutions before (black line) and after (red line) UV light irradiation. The blue points show the *cis*-isomer content during the heating process. (b) Change in absorption spectra upon sequential irradiation of UV light inducing the photoisomerization. The inset indicates the absorbance change at 350 nm as the irradiation time increases.

It is well known that under the UV irradiation, azobenzene moieties can undergo the *trans*-to-*cis* photo isomerization. The *cis*-form of azobenzene can be more hydrophilic than the *trans*-form in solution, which results in an increase of its cloud point after UV irradiation. However, the effect of photoisomerization appears to depend on the substitution

pattern on azobenzene. The curves of transmittance *vs* temperature for the representative polymers, P_3 and P_4 containing donor-acceptor *bis*-azobenzene moieties are shown in Figure 44. In contrast to P_1, after 365 nm UV irradiation, the apparent cloud points of the two polymer solutions shifted to a lower temperature and decreased by 1 ^oC and 2 ^oC respectively. These results are not really surprising because this kind of behavior has already been reported in the literature.[309] From the blue points in Figure 44(a) and (b), we can see that the content of *cis*-isomers decreased rapidly. Moreover, the thermal relaxation mainly took place at around the cloud point. At the end of the heating process (50 ^oC), most of the *cis*-isomers were relaxed back to *trans*-isomers.

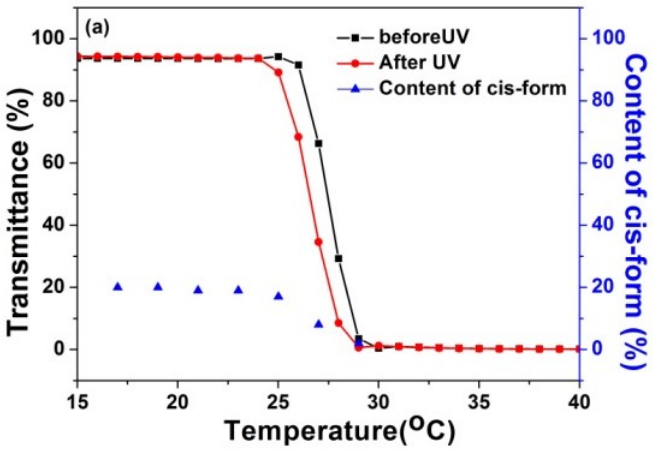

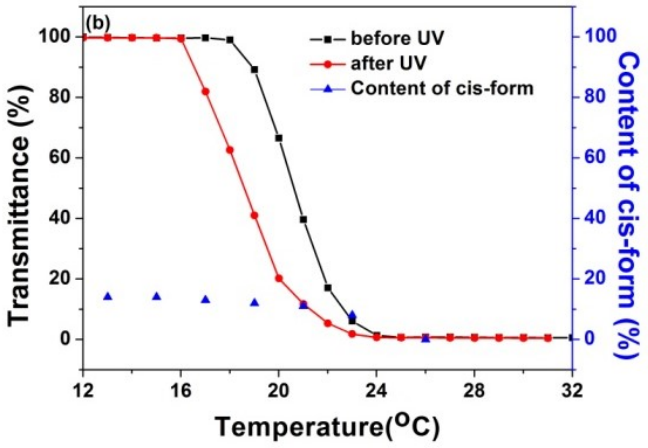

Figure 44. Transmittance *vs* temperature for aqueous solutions of two random copolymers: (a) P_3 and (b) P_4. Black line shows the phase transition before UV irradiation, red line the phase transition after UV, and blue points are the *cis*-isomer content during the heating process.

Generally speaking, the photo-induced shifting of the cloud point was mainly due to the difference of the hydrophobic / hydrophilic balance of the chromophores. The *cis*-isomer of azobenzene can be either more hydrophilic or more hydrophobic than its *trans*-isomer counterpart. In the case of P_3 and P_4, because of the substitution of donor-acceptor groups on the *bis*-azobenzene moiety, it is likely that the *trans*-isomer has a larger dipole moment than the *cis*-isomer. In other words, after UV light irradiation induced *trans-cis* isomerization, these two polymers may become less hydrophilic due to decreased polarity, which explains the decreased cloud point. The hypothesis of decreased water solubility of P_4 after UV light irradiation is also consistent with the result of another experiment. Indeed, the size distribution of P_4 before and after UV irradiation was measured by dynamic light scattering (DLS) and the results are shown in Figure 45. It appears that the average hydrodynamic diameter of P_4 in water increased from 9.36 nm to 17.72 nm after UV irradiation at room temperature, which suggests some agglomeration of P_4 chains due to

decreased water solubility.

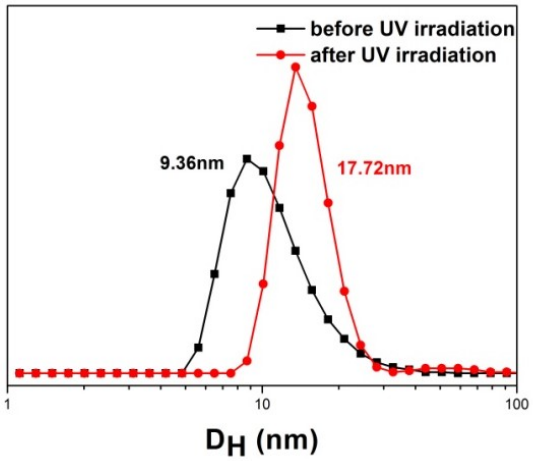

Figure 45. Size distribution of polymer aqueous solution of P_4 before (black line) and after UV irradiation for 30 min (red line) at 5 ^oC

3.3.3 Comparison of the effect of *mono*-azobenzene and *bis*-azobenzene moieties on the cloud point

The plots of transmittance *vs* temperature for P_5 are shown in Figure 46. A sharp transition curve was found for the polymer solution displaying LCST-type phase transition behavior. Firstly, the cloud point of P_5 bearing *mono*-azobenzene groups with electron-donating group (-OCH_3 and -$O(CH_2)_6H$) was at about 28 ^oC in Figure 46(a). After re-solubilization at low temperature (0 ^oC), the solution was exposed to UV light to undergo the *trans*-to-*cis* photoisomerization. As can be seen from the UV-vis spectra of the solution of P_5 recorded upon 365 nm UV light irradiation, shown in Figure 46(b), with increasing their radiation time, the decreased absorbance (*trans*-azobenzene) at around 375 nm and enhanced absorbance (*cis*-azobenzene) centered at 450 nm are an indication of efficient *trans*-to-*cis* photoisomerization. After UV irradiation for 5 min, the polymer solution reached the photostationary state with 78% of *trans*-isomers converted to *cis*-isomers. After turning off

the UV light, the solution subjected to heating shows a cloud point shifted to a higher temperature by almost 3 ^{o}C.

Comparing the UV light induced cloud point shifts of the PNIPAM copolymers with *mono*-azobenzene (P_5) and *bis*-azobenzene comonomer units (P_1-P_4), the observed largest shift is similar, being about 3 K. This shift is significant and can be explored for light-tunable polymer solubility in water in certain applications. However, the amount of *mono*-azobenzene comonomer required to achieve the 3 K cloud point shift is basically twice that of *bis*-azobenzene comonomer, and with a much higher *cis*-isomer concentration of *mono*-azobenzene (near 80%, Fig.46) than *bis*-azobenzene (about 20%, Fig.44). These results, although limited in the amount of data, support the working hypothesis that *bis*-azobenzene comonomers may be more efficient than *mono*-azobenzene comonomers for light-tunable phase transition temperatures of thermosensitive polymers like PNIPAM. This higher efficiency will allow the use of a minimal amount of comonomer units in preparying thermo-sensitive polymers, which is desired for applications.

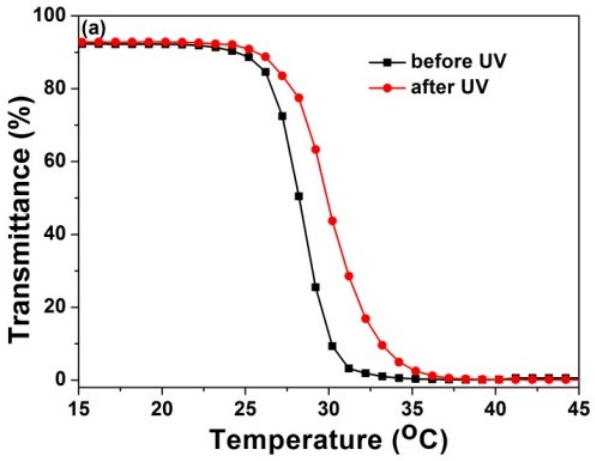

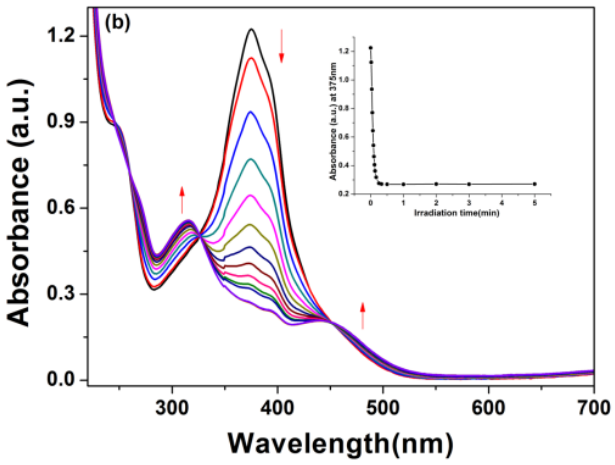

Figure 46. (a) Plots of transmittance vs. temperature for P_5 aqueous solution before and after UV light irradiation inducing the photoisomerization of *mono*-azobenzene groups.(b) Change in absorption spectra upon UV light irradiation of various times.

3.4 Conclusions

We have successfully synthesized a class of novel dual-responsive (photo- and thermo-) copolymers by modifying PNIPAM with *bis*-azobenzene moieties, and investigated the effect of photoisomerization of *bis*-azobenzenes on the LCST-type phase transition temperature of the aqueous copolymer solution by monitoring the change in cloud point. It was found that *bis*-azobenzene moieties could influence the cloud point of the polymers with a very small amount of comonomer units (about 2 mol%). Depending on the substituents on *bis*-azobenzene moieties, the copolymer solution can display either an increase or decrease of the cloud point shift after UV light irradiation inducing the *trans*-to-*cis* photoisomerization of azobenzene. When the substituents on azobenzene have pull-push feature, after UV irradiation, the polymer becomes less soluble in water and tend to aggregate on heating, as a result of decreased. By contrast, with donors on azobenzenes, the cloud point shifts to higher temperature upon UV light irradiation, which is caused by a more polar *cis*-isomer than the *trans*-state. The whole of the results show that the effect of

photoisomerization of *bis*-azobenzenes on the cloud point shift appears to be greater than the effect with *mono*-azobenzene comonomer.

CONCLUSION AND PERSPECTIVES

4.1 What we achieved in this work

During this work, we tackled several challenges, concerning the efficient synthesis of new azobenzene scaffolds, and some new derivatives from them and their incorporation into polymers.

These are precisely what we had achieved:

1) We selected and fine-tuned a new fast and easy route to *bis*- and *tris*-azobenzenes (Scheme 55).

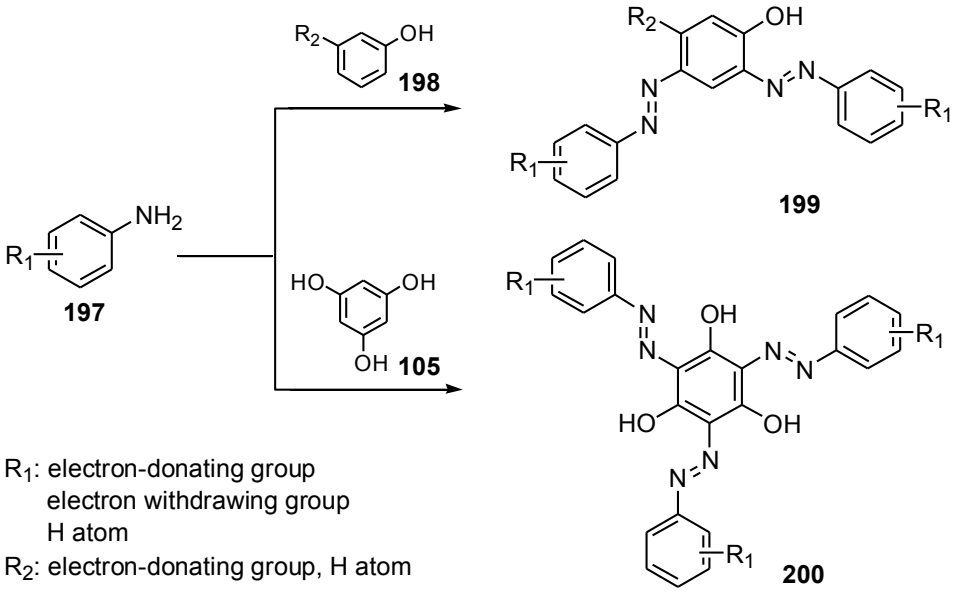

Scheme 55. Synthesis of *bis*- and *tris*-azobenzene derivatives

This work (Chapter 1) not only extended the diversity of azobenzenes, but also, more importantly, addressed some unresolved fundamental issue that the *bis*-azobenzenes cannot be obtained in a one-step procedure by *mono*-amino via diazonium salts coupling reaction.

2) We discovered and studied a new method to cyclize the *ortho*-fluoro-azobenzenes with *ortho*-hydroxyl group into dibenzoxadiazepine (Table 8).

Table 8. Cyclization of the fluoro-azobenzenes into dibenzoxadiazepines

Fluoro-azobenzenes	Dibenzoxadiazepines
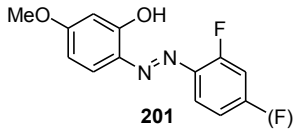 **201**	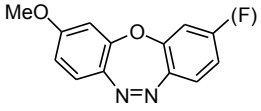 **202**
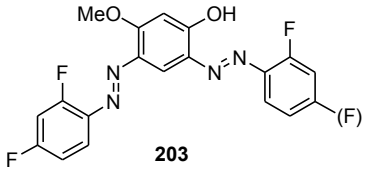 **203**	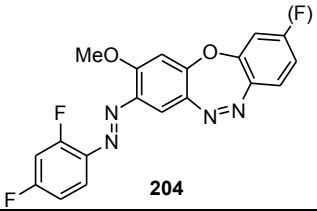 **204**
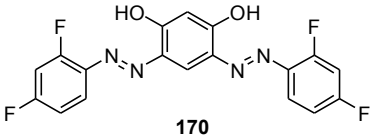 **170**	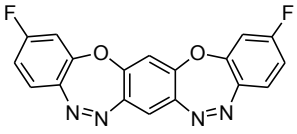 **171**

We made the first demonstration of the effect of solvents and light that can induce the cyclization of azobenzene derivatives, meanwhile, exhibited gradual changes in UV-vis absorption spectra and various color features with time evolution.

3) We introduced the new *bis*-azobenzenes structures into NIPAM (*N*-isopropylacrylamide) polymers to study their thermal- and photo-responsive behaviors. We discovered that the properties of the PNIPAM (poly(*N*-isopropylacrylamide)) can be modulated with the *bis*-azobenzene moieties in

Figure 47. It was found that the copolymer solutions displayed an opposite LCST shift after the photo-reactions of the chromophores due to the different substituents on the azobenzene moieties. As the substituents on azobenzenes has pull-push feature, after ultraviolet light irradiation, the cloud point decreased, while donors on azobenzenes, the cloud point shifted to higher temperature.

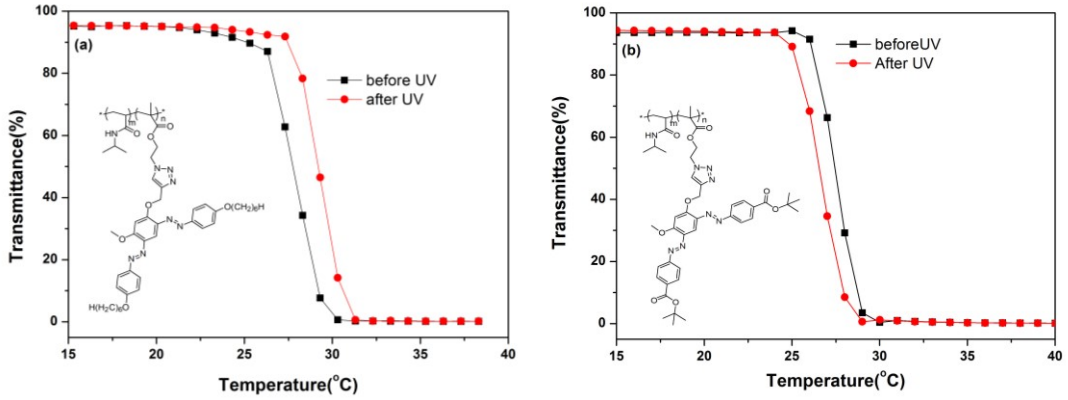

Figure 47. Plots of transmittance vs. temperature in aqueous solution before and after UV light irradiation, (a) *bis*-azobenzene bearing electron-donating group; (b) *bis*-azobenzene containing electron-donating group and electron-withdrawing group.

4.2 Perspectives

Now that we have developed efficient methods to prepare *bis*- and *tris*-azobenzenes and that we have learnt to cyclize some of them. Also, we have studied their properties of corresponding polymers. The fields of azobenzenes as stimulus responsive materials are ever-growing. There is still a great deal of room for expansion beyond this work. More time and patience are indeed required to pursue the project. Two ideas are described below that are worth being investigated.

4.2.1 The effect of light irradiation, gas and solvents on the polymers containing azobenzenes

Although the thermo- and light-responsive polymers had been studied, the design of polymer structure is necessary to achieve multi-functions. As mentioned above, one big drawback that the efficiency of transformation from *trans*-state to *cis*-state is very low in aqueous solutions (Figure 48a). However, the degree of isomerization increases in organic solvents, for example, THF (Figure 48b). Therefore, in this perspective part, we would like to briefly introduce the polymers based on azobenzenes in organic solvents which is very interesting.

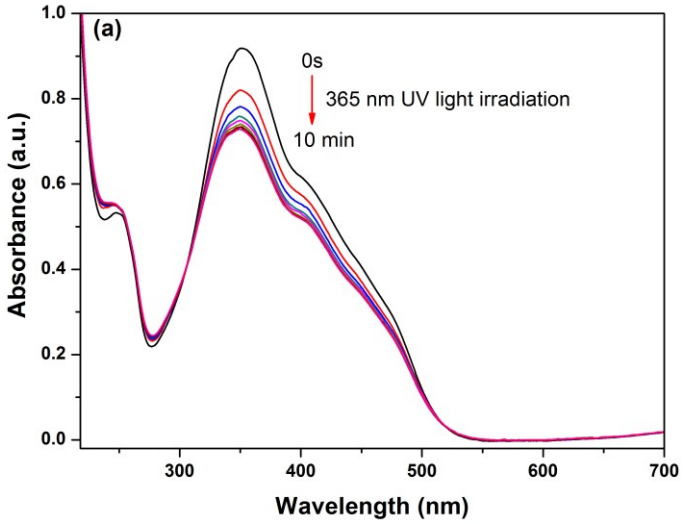

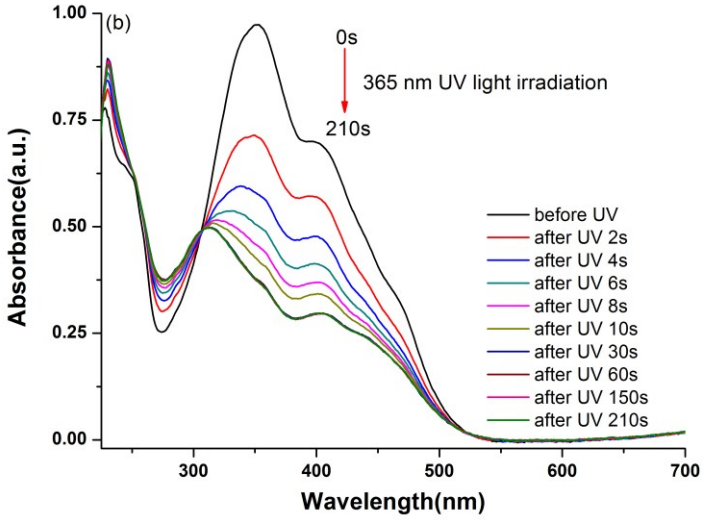

Figure 48. UV-vis absorption spectra upon irradiation of 365 nm UV light over time (a) in aqueous solution and (b) in THF (the concentration of solution is 0.1 mg / mL).

The azobenzenes bearing hydroxyl group and F atom are good choice to provide a possibility for multi-responsive polymers. The hydroxyl group at the *para*- and *ortho*-position of azo-bond plays a crucial role in inducing the *keto-enol* tautomerization (reversible part) over time in polar solvents, while *plus ortho*-fluoro atom, the cyclization happens under light and is irreversible. Those two reactions are affected by the solvents, pH of medium as well as the UV / visible light irradiation over time. During these two reactions, the UV-vis absorption of compounds will be varied, leading to the change in the color of polymer solutions. The corresponding chemical structures of monomers are designed in Scheme 56.

Interestingly, the color of corresponding polymers was proposed that not only changed over time, and also can be tailed by solvents and light irradiation, etc. As shown in Scheme 57, the stimuli-responsive polymers are developed to further expand the scope of multi-functional polymers based on azobenzenes, meanwhile, combine the photo-activity,

thermo-sensitivity and pH sensitivity together.

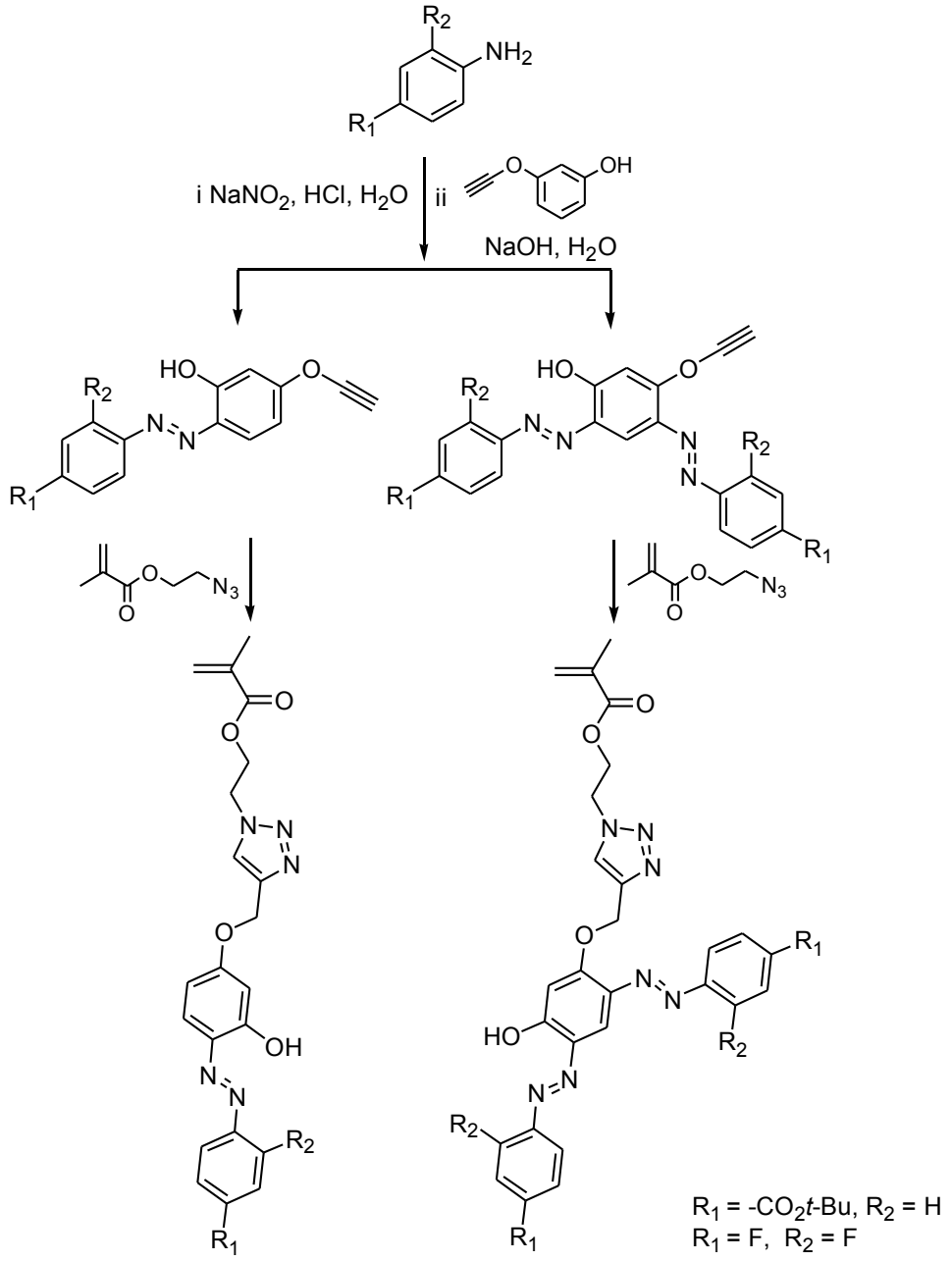

Scheme 56. Synthesis of *ortho*-hydroxyl *mono*-azobenzenes and *bis*-azobenzenes

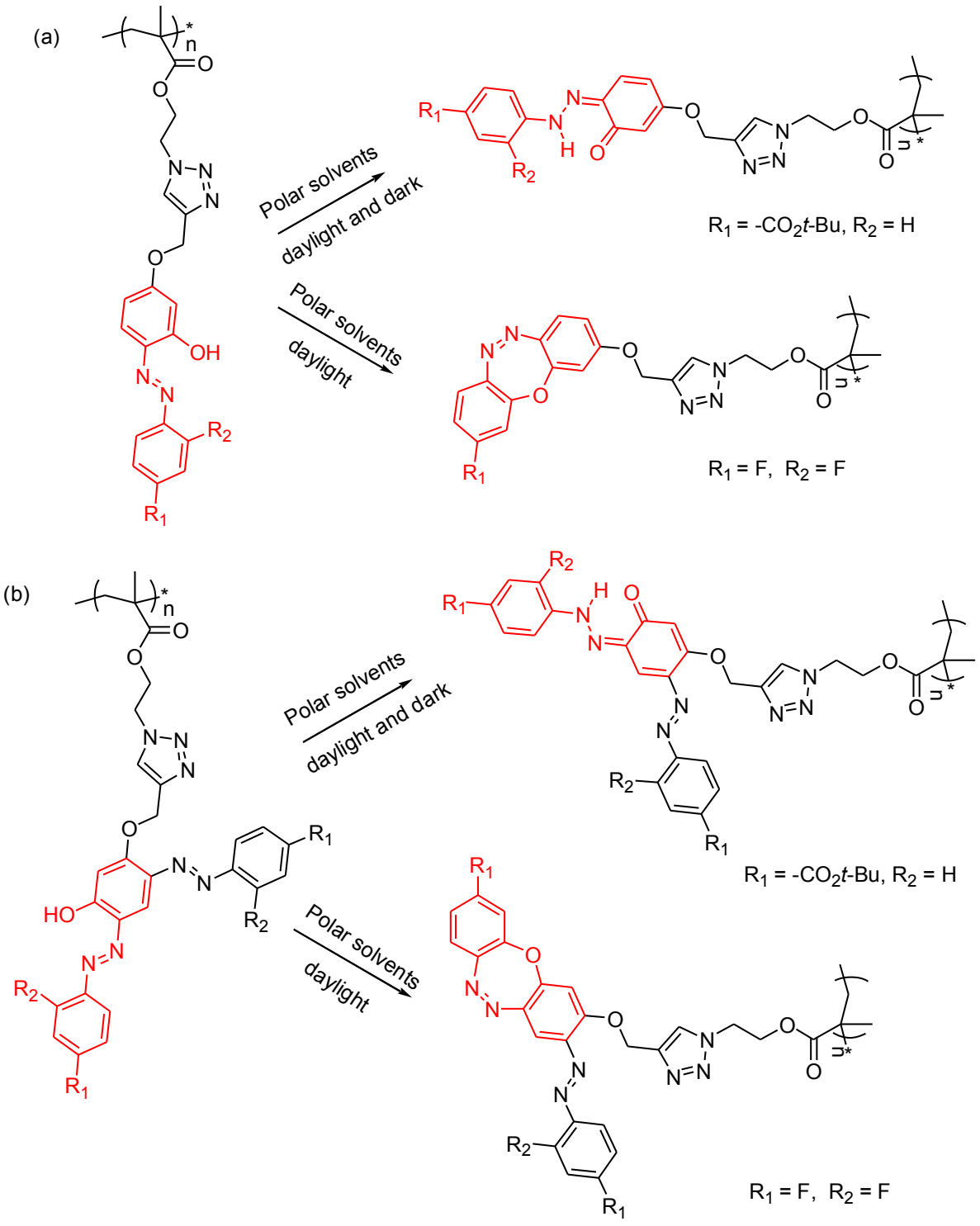

Scheme 57. Changes in chemical structures of polymers based on *ortho*-hydroxyl (a) *mono*-azobenzenes and (b) *bis*-azobenzenes under different conditions

4.2.2 Photo-responsive liquid crystalline polymers (LCP) based on the *bis*-azobenzenes

For *mono*-azobenzene, there are two isomers either *trans*-state or *cis*-state. Usually, *trans*-azobenzene is highly symmetric and less polar, which presents a rod-like shape. It favors the formation of liquid crystalline phases. In contrast, the *cis*-azobenzene owns a higher polarity and bent shape, which is unfavorable for liquid crystal formation. Upon irradiation with visible light or through thermal relaxation, it can be reversible between liquid crystalline phases and non-liquid crystalline phases. However, the *trans*-*cis* isomerizations of *bis*-azobenzenes are much richer than that of single azobenzenes. Liquid crystalline polymers based on the *bis*-azobenzenes are still interesting. Figure 49 shows a chemical structures of liquid crystalline polymers based on the *bis*-azobenzenes. Under the light irradiation, the liquid crystalline polymer could be polarized *via* photo-isomerization reaction of *bis*-azobenzenes.

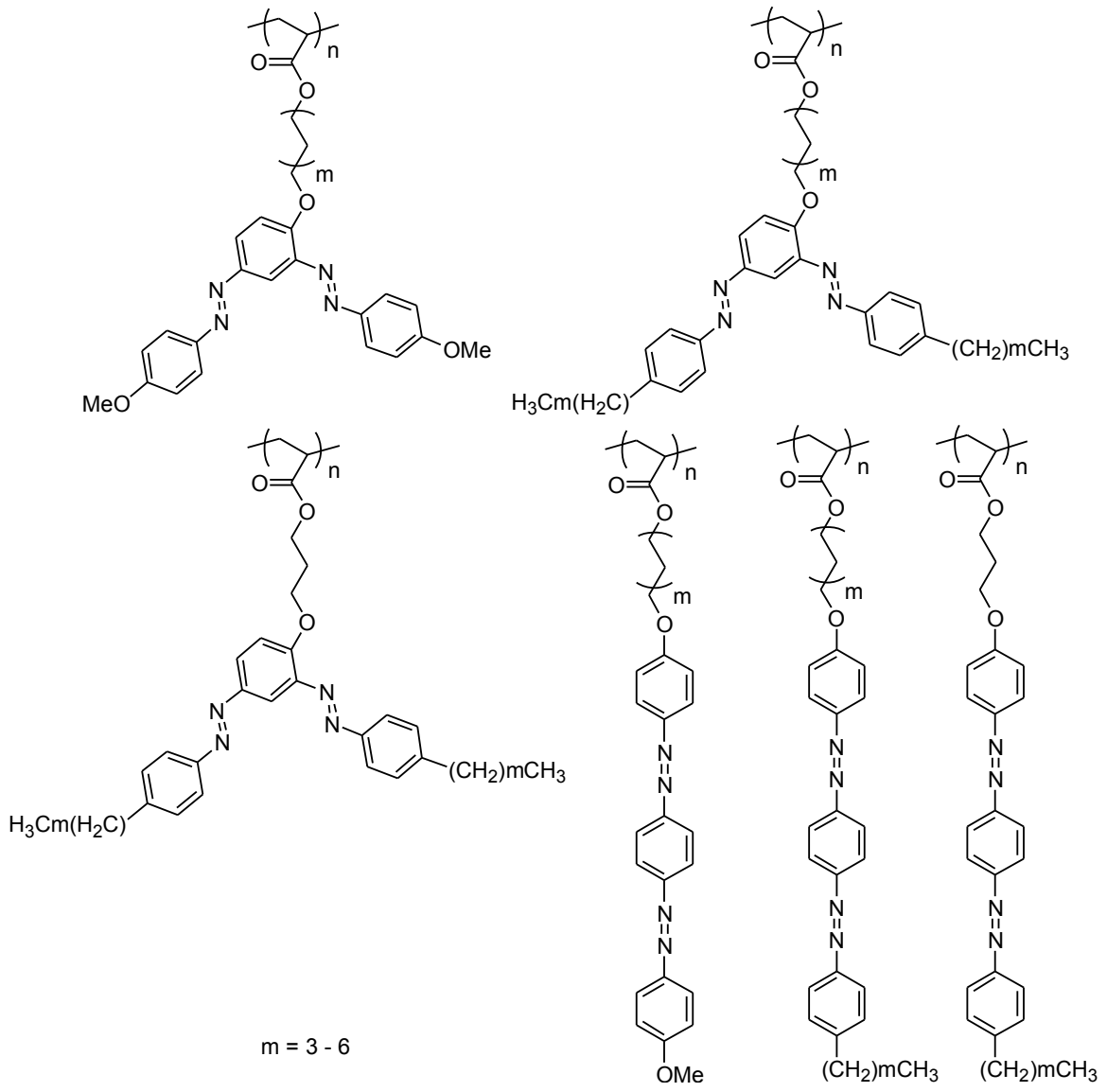

Figure 49. Schematically illustration of liquid crystalline polymers based on the *bis*-azobenzenes

4.3 Conclusions

In this thesis, we have developed novel methodologies for the preparation of *bis*-azobenzene, *tris*-azobenzene and the cyclization of azobenzene derivatives, at the same time, have found special stimuli-responsive polymers based on the *bis*-azobenzene

moieties.

In Chapter 1, we achieved a novel method for synthesis of *bis*- and *tris*-azobenzenes. Through rational designs of chemical structures, our studies demonstrated one new approach that furnish *bis*-azobenzene and *tris*-azobenzene derivatives from *mono*-amino in one-pot procedure *via* diazonium salts coupling reaction. For phenols, the more electron-rich the phenol ring, the more reactive it becomes. Compared with the simplest aniline, electron-withdrawing substituted anilines, corresponding to electron-deficient diazonium salts, are favorable for the formation of *mono*-azobenzene, and less favorable for the appearance of *bis*-azobenzenes. On the contrary, anilines substituted with electron-donating functional groups are not efficient during the first step leading to the formation of *mono*-azobenzene, however, favor the generation of *bis*-azobenzenes in the second step. As a rule, electron deficient anilines in over two-fold and three-fold excess are the best choice for the preparation of *bis*- and *tris*-azobenzenes respectively in good yields.

In Chapter 2, a novel method for cyclization of *mono*- and *bis*-azobenzenes has been discovered. The *ortho*-OH and *ortho*-F had a decisive role in the cyclization reaction. Indeed, the fluorine atom provided increased stability to the *cis*-azobenzene form. The polar solvents played a crucial role in stabilizing the σ intermediate complex. These azobenzenes cyclization reactions offered a supplement for the synthesis of druglike dibenzoxadiazepine derivatives, without the need of tedious and time-consuming purifications. Noteworthy, the cyclization reaction can become as short as a few seconds by applying ultraviolet light. Meanwhile, it is the first observation that the color changed over time induced by spontaneous *keto-enol* tautomerization, *trans*-to-*cis* isomerization and cyclization of azobenzene derivatives. In polar solvents, such as, DMSO, DMF and DMAc, the hydroxyl azobenzene compounds can undergo *keto-enol* tautomerization under the daylight and dark. However, for azobenzenes with F and -OH both *ortho* to -N=N- group, it happened

keto-enol taumorization in the dark, *trans*-to-*cis* isomerization and cyclization reaction occurred in the daylight or ultraviolet light.

In Chapter 3, we have synthesized novel dual-responsive copolymers by modifying PNIPAM with *mono*-azobenzene and *bis*-azobenzene moieties, and have investigated the effects of light irradiation on the phase transition of the aqueous copolymer solution. It was found that the copolymer solutions displayed an opposite LCST shift after the photo-reactions of the chromophores. As the substituents on azobenzenes has pull-push feature, after ultraviolet light irradiation, the polymer chain favored aggregation on heating resulting in the decrease of cloud point, while donors on azobenzenes, the cloud point shifted to higher temperature due to *cis*-state is more hydrophilic than *trans*-state. This change of phase transition behavior was not only dependent on the hydrophilicity of the *trans* and *cis* state of azobenzenes, and also on the conformation of the polymer chain in solution. However, the effect of photoisomerization of *bis*-azobenzenes on the cloud point shift appears to be greater for PNIPAM containing mono-azobenzene pendent groups.

BIBLIOGRAPHY

1. Mahimwalla, Z.; Yager, K. G.; Mamiya, J.-i.; Shishido, A.; Priimagi, A.; Barrett, C. *J. Polym. Bull*. **2012**, 69, 967-1006.

2. Rivera, E.; Carreon-Castro, M.; Buendıa, I.; Cedillo, G. *Dyes Pigm*. **2006**, 68, 217-226.

3. Cardona, M. A.; Magri, D. C. *Tet. Lett.* **2014**, 55, 4559-4563.

4. Cheung, W.; Shadi, I.T.; Xu, Y.; Goodacre, R. *J. Phys. Chem. C.* **2010**, 114, 7285-7290.

5. Pharr S, Wood Da, Traut, H. *Am. J. Clin. Pathol*. **1954**, 24, 239-242.

6. Lachheb, H.; Puzenat, E.; Houas, A.; Ksibi, M.; Elaloui, E.; Guillard, C.; Herrmann, J.-M. *Appl. Catal. B*. **2002**, 39, 75-90.

7. Allinger N.L.; Youngdale, G.A. *J. Am. Chem. Soc*. **1962**, 84, 1020-1026.

8. Karwa, A. S.; Poreddy, A. R.; Asmelash, B.; Lin, T.-S.; Dorshow, R. B.; Rajagopalan. *R. ACS Med. Chem. Lett*. **2011**, 2, 828-833.

9. Bandara, H. M. D.; Burdette, S. C. *J. Chem. Soc. Rev*. **2012**, 41, 1809-1825.

10. Griffiths, *J. Chem. Rev. Soc*. **1972**, 1, 481-493.

11. Hartley, G. S. *Nature*. **1937**, 140, 281-282.

12. Pandey, A.; Singh, P.; Iyengar, L. *Int. Biodeterior. Biodegradation*. **2007**, 59, 73-84.

13. Vandenabeele, P.; Moens, L.; Edwards, H. G. M.; Dams, R. *J. Raman Spectrosc*. **2000**, 31, 509-517.

14. Department of Chemistry, University of York, UK. Colorants. *The Essential Chemical Industry - online*, 2017-10-23.

15. Fouts, J.R.; Kamm, J.J.; Brodie, B.B. *J. Pharmacol. Exp. Ther.* **1957**,120, 291-300.

16. Ehrlich, P.; Shiga, K. *Wien. Klin. Wochenschr*. **1904**, 41, 329-332.

17. Knepper, K.; Themann, A.; Brase, S. *J. Comb. Chem*. **2005**, 7, 799-801.

18. Kittakoop, P.; Nopichai, S.; Thongon, N.; Charoenchai, P.; Thebtaranonth, Y. *Helv. Chim. Acta*. **2004**, 87, 175-179.

19. Stopka, T.; Marzo, L.; Zurro, M.; Janich, S.; Wurthwein, E.-U.; Daniliuc, C. G.; Aleman, J.; Mancheno, O. G. *Angew. Chem. Int. Ed*. **2015**, 54, 5049-5053.

20. Yadav, N.; Khanam, T.; Shukla, A.; Rai, N.; Hajela, K.; Ramachandran, R. *Org. Biomol. Chem*. **2015**, 13, 5475-5487.

21. Novak, I.; Klasinc, L.; McGlynn, S. P. *J. Electron. Spectrosc. Relat. Phenom.* **2016**, 212, 56-61.

22. Moreno, D. R. R. Giorgi, G.; Salas, C. O.; Tapia, R. A.. *Molecules*. **2013**, 18, 14797-14806.

23. Jarman, M.; Barrie, S. E.; Deadman, J. J.; Houghton, J.; McCague, R.; Rowlands, M. G. *J. Med. Chem*. **1990**, 33, 2452-2455.

24. Yager, K.G.; Barrett, C. J. *J. Photochem. Photobiol. A*. **2006**,182, 250-261.

25. Mendes, P. M. *Chem. Soc. Rev*. **2013**, 42, 9207-9218.

26. Wang, G.; Zhu, X.; Zhenping, C. Zhu, J. *J. Polym. Sci. A*. **2005**, 43, 2358-2367.

27. Gumireddy, K.; Young, D. D.; Xiong, X.; Hogenesch, J.B.; Huang, Q.; Deiters, A. *Angew. Chem. Int. Ed*. **2008**, 47, 7482-7484.

28. Sadovski, O.; Beharry, A. A.; Zhang, F.; Woolley, G. A. *Angew. Chem. Int. Ed*. **2009**, 48, 1484-1486.

29. Banghart, M.; Borges, K.; Isacoff, E.; Trauner, D.; Kramer, R.H. *Nat. Neurosci*. **2004**, 7,

1381-1386.

30. Kramer, R.H.; Chambers, J.J.; Trauner, D. *Nat. Chem. Biol*. **2005**, 1, 360-365.

31. Volgraf, M.; Gorostiza, P.; Numano, R.; Kramer, R.H.; Isacoff, E.Y.; Trauner, D. *Nat. Chem. Biol*. **2006**, 2, 47-52.

32. Bose, M.; Groff, D.; Xie, J.; Brustad, E.; Schultz, P. G. *J. Am. Chem. Soc*. **2006**, 128, 388-389.

33. Peng, S.; Guo, Q.; Hartley, P. G.; Hughes, T. C. *J. Mater. Chem. C*. **2014**, 2, 8303-8312.

34. Tao, N. J. *Nat. Nanotechnol*. **2006**, 1, 173-181.

35. Nakano, H.; Takahashi, T.; Kadota, T.; Shirota, Y. *Adv. Mater*. **2002**, 14, 1157-1160.

36. Koskela, J. E.; Vapaavuori, J.; Hautala, J.; Priimagi, A.; Faul, C. F. J.; Kaivola, M.; Ras, R. H. A. *J. Phys. Chem. C*. **2012**, 116, 2363-2370.

37. Commins, P.; Garcia-Garibay, M. A. *J. Org. Chem*. **2014**, 79, 1611-1619.

38. Hansen, M.J.; Lerch, M.M.; Szymanski, W.; Feringa. B.L. *Angew. Chem*. **2016**, 128, 13712-13716.

39. Konrad, D.B.; Frank, J.A.; Trauner, D. *Chem. Eur. J*. **2016**, 22, 4364-4368.

40. Hegde, G.; Rajkumar, Y.A.; Mei, G.S.; Mahmood, S.; Mandal, U. K.; Sudhakar, A.A. *Korean J. Chem. Eng*. **2016**, 33, 1480-1488.

41. Zhao, C.W.; Wang, T.Y.; Li, D.M.; Lu, T.; Liu, D.Z.; Meng, Q.B.; Zhang, Q.Q.; Li, F.Q.; Li, W.; Hu, W.P.; Wang, L.C.; Zhou. X.Q. *Dyes Pigm*. **2017**, 137, 256-264.

42. Chi, Z.; Ran, X.; Shi, L.L.; Lou, J.; Kuang, Y.M.; Guo, L.J. *Spectrochim. Acta A*. **2017**, 171, 25-30.

43. Xu,D.; Geng, J.; Dai, Y.; Peng, Y.X.; Qian, H.F.; Huang, W. *Dyes Pigm*. **2017**, 136, 398-403.

44. Hamon, F.; Djedaini-Pilard, F.; Barbot, F.; Len, C. *Tetrahedron*. **2009**, 65, 10105-10123.

45. Lee, S. J.; Jung, J. H.; Seo, J.; Yoon, I.; Park, K. M.; Lindoy, L. F.; Lee, S. S. *Org. Lett*. **2006**, 8, 1641-1643.

46. Tomasulo, M.; Raymo, F. M. *Org. Lett*. **2005**, 7, 4633-4636.

47. Lee, S. J.; Lee, S.S.; Jeong, I. Y.; Lee, J. Y.; Jung, J. H. *Tet. Lett*. **2007**, 48, 393-396.

48. Campbell, V. E.; In, I.; McGee, D.J.; Woodward, N.; Caruso, A.; Gopalan, P. *Macromolecules*. **2006**, 39, 957-961.

49. Lee, M.H.; Cho, B.-K.; Yoon, J.; Kim, J. S. *Org. Lett*. **2007**, 9, 4515-4518.

50. Gopalan, P.; Katz, H. E.; McGee, D. J.; Erben, C.; Zielinski, T.; Bousquet, D.; Muller, D.; Grazul, J.; Olsson, Y. *J. Am. Chem. Soc*. **2004**, 126, 1741-1747.

51. Lee, S. J.; Lee, S. S.; Lee, J. Y.; Jung, J. H. *Chem. Mater*. **2006**, 18, 4713-4715.

52. Haghbeen, K.; Tan, E. W. *J. Org. Chem*. **1998**, 63, 4503-4505.

53. Lin, S.-J.; Shiao, Y.-J.; Chi, C.-W.; Yang, L.-M. *Bioorg. Med. Chem. Lett*. **2004**, 14, 1173-1176.

54. Zarwell, S.; Ruck-Braun, K. *Tet. Lett*. **2008**, 49, 4020-4025.

55. Roth, I.; Simon, F.; Bellmann, C.; Seifert, A.; Spange, S. *Chem. Mater*. **2006**, 18, 4730-4739.

56. Dong, S. -L.; Loweneck, M.; Schrader, T. E.; Schreier, W. J.; Zinth, W.; Moroder, L.; Renner, C. *Chem. Eur. J*. **2006**, 12, 1114-1120.

57. Davey, M. H.; Lee, V. Y.; Miller, R. D.; Marks, T. J. *J. Org. Chem*. **1999**, 64, 4976-4979.

58. Nihei, M.; Kurihara, M.; Mizutani, J.; Nishihara, H. *J. Am. Chem. Soc*. **2003**, 125, 2964-2973.

59. Kamei, T.; Kudo, M.; Akiyama, H.; Wada, M.; Nagasawa, J.; Funahashi, M.; Tamaoki, N.; Uyeda, T. Q. P. *Eur. J. Org. Chem*. **2007**, 1846-1853.

60. Wang, S.; Wang, X.; Li, L.; Advincula, R. C. *J. Org. Chem*. **2004**, 69, 9073-9084.

61. Tie, C.; Gallucci, J. C.; Parquette, J. R. *J. Am. Chem. Soc*. **2006**, 128, 1162-1171.

62. Priewisch, B.; Ruck-Braun, K. *J. Org. Chem*. **2005**, 70, 2350-2352.

63. Park, S. B.; Standaert, R. F. *Tet. Lett*. **1999**, 40, 6557-6560.

64. Peters, M. V.; Stoll, R. S.; Goddard, R.; Buth, G.; Hecht, S. *J. Org. Chem*. **2006**, 71,7840-7845.

65. Shee, B.; Pratihar, J. L.; Chattopahyay, S. *Polyhedron*. **2006**, 25, 2513-2518.

66. Priewisch, B.; Ruck-Braun, K. *J. Org. Chem*. **2005**, 70, 2350-2352.

67. Drug, E.; Gozin, M. *J. Am. Chem. Soc*. **2007**, 129, 13784-13785.

68. Gilbert, A. M.; Failli, A.; Shumsky, J.; Yang, Y.; Severin, A.; Singh, G.; Hu, W.; Keeney, D.; Petersen, P. J.; Katz, A. H. *J. Med. Chem*. **2006**, 49, 6027-6036.

69.Ortiz, B.; Villanueva, P.; Walls, F. *J. Org. Chem*. **1972**, 37, 2748-2750.

70.Fetizon, M.; Golfier, M.; Milcent, R.; Papadakis, I. *Tetrahedron*. **1975**, 31, 165-170.

71. Mehta, S. M.; Vakilwala, M. V. *J. Am. Chem. Soc*. **1952**, 74, 563-564.

72. Pausaker, K. H.; Scroggie, J. G. *J. Chem. Soc*. **1954**, 4003-4006.

73. Baer, E.;Tosoni, A. L. *J. Am. Chem. Soc*. **1956**, 78, 2857-2858.

74. Firouzabadi, H. Mostafavipoor, Z. *Bull. Chem. Soc. Jpn*. **1983**, 56, 914-917.

75. Firouzabadi, H.; Vessal, B.; Naderi, M. *Tet. Lett*. **1982**, 23, 1847-1850.

76. Firouzabadi, H.; Sardarian, A. R.; Naderi, M.; Vessal, B. *Tetrahedron*. **1984**, 40, 5001-5004.

77. Nakagawa, K.; Tsuji, *T. Chem. Pharm. Bull*. **1963**, 11, 296-301.

78. Pausaker, K. H. *J. Chem. Soc*. **1953**, 107, 1989-1990.

79. Wang, X. -Y.; Wang, Y. -L. J. Li, P. Duan, Z. -F. Zhang, Z. -Y. *Synth. Commun*. **1999**, 29, 2271-2276.

80. Habibi, M. H.; Tangestaninejad, S.; Mirkhani, V. *J. Chem. Res. (S)* **1998**, 648-649.

81. Horner, L.; Dehnert, *J. Chem. Ber*. **1963**, 96, 786-797.

82. Farhadi, S.; Zaringhadama, P.; Sahamiehb, R. Z. *Acta Chim. Slov*. **2007**, 54, 647-653.

83. Kinoshita, K. *Bull. Chem. Soc. Jpn*. **1959**, 32, 777-780.

84. Orito, K.; Hatakeyama, T.; Takeo, M.; Uchiito, S.; Tokuda, M.; Suginome, H. *Tetrahedron*. **1998**, 54, 8403-8410.

85. Srinivasa, G. R.; Abiraj, K.; Gowda, D. C. *Tet. Lett*. **2003**, 44, 5835-5837.

86. Barth, M.; Shah, S. T. A.; Rademann, J. *Tetrahedron*. **2004**, 60, 8703-8709.

87. Mihara, M.; Nakai, T.; Iwai, T.; Ito, T.; Mizuno, T. *Synlett*. **2007**, 13, 2124-2126.

88. Corral, C.; Lissavetzky, J.; Quintanilla, G. *J. Org. Chem*. **1982**, 47, 2214-2215.

89. Lefevre, G. N.; Crawford, R. J. *J. Am. Chem. Soc*. **1986**, 108, 1019-1027.

90. Cohen, S. G.; Zand, R. *J. Am. Chem. Soc*. **1962**, 84, 586-591.

91. Billera, C. F.; Dunn, T. B.; Barry, D. A.; Engel, P. S. *J. Org. Chem*. **1998**, 63, 9763-9768.

92. Wang, C. -L.; Wang, X. -X.; Wang, X. -Y.; Xiao, J. -P.; Wang, Y. -L. *Synth. Commun*. **1999**, 29, 3435-3438.

93. Whalley, B. J. P.; Evans, H. G. V.; Winkler, C. A. *Can. J. Chem*. **1956**, 34, 1154-1162.

94. Barth, M.; Tasadaque, S.; Shah, A.; Rademann, J. *Tetrahedron*. **2004**, 60, 8703-8709.

95. Qiao, R. -Z.; Zhang, Y.; Hui, X. -P.; Xu, P. -F.; Zhang, Z. -Y.; Wang, X. -Y.; Wang, Y. -L. *Green Chem*. **2001**, 3, 186-188.

96. Hoffman, R. V.; Kumar, A. *J. Org. Chem*. **1984**, 49, 4014-4017.

97. Kim, K.-Y.; Shin, J.-T.; Lee, K.-S.; Cho, C.-G. *Tet. Lett*. **2004**, 45, 117-120.

98. Patel, D. R.; Patel, B. M.; Patel, N. B. Patel, K. C. *J. Saudi. Chem. Soc*. **2014**, 18, 245-254.

99. Patel, D. M.; Patel, T. S.; Dixit, B. C. *J. Saudi. Chem. Soc*. **2013**, 17, 203-209.

100. Samanta, S.; Qureshi, H. I.; Woolley, G. A. *Beilstein J. Org. Chem*. **2012**, 8, 2184–2190.

101. Fatas, P.; Longo, E.; Rastrelli, F.; Crisma, M.; Toniolo, C.; Jimenez, A. I.; Cativiela, C.; Moretto, A. *Chem. Eur. J*. **2011**, 17, 12606-12611.

102. Homocianu, M.; Serbezeanu, D.; Carja, I.-D.; Macsim, A. M.; Vlad-Bubulac, T.;

Airinei, A. *RSC Adv*. **2016**, 6, 49980-49987.

103. Reuter, Raphael.; Wegner, H. A. *Beilstein J. Org. Chem*. **2012**, 8, 877-883.

104. Balamurugan, S.; Yeap, G.-Y.; Mahmood, W. A. K.; Tan, P.-L.; Cheong, K.-Y. *J. Photochem. Photobiol. A*. **2014**, 278, 19-24.

105. Feng, W.; Li, S.; Li, M.; Qin, C.; Feng, Y. *J. Mater. Chem. A*, **2016**, 4, 8020-8028.

106. Rijeesh, K.; Hashim, P. K.; Noro, S.; Tamaoki, N. *Chem. Sci.*, **2015**, 6 , 973-980.

107. Blackburn, O. A. Coe, B. J.; Helliwell, M. *Organometallics*. **2011**, 30, 4910-4923.

108. Bellotto, S.; Reuter, R.; Heinis, C.; Wegner, H. A. *J. Org. Chem.* **2011**, 76, 9826-9834.

109. Slavov, C.; Yang, C.; Schweighauser, L.; Boumrifak, C.; Dreuw, A.; Wegner, H. A.; Wachtveitl, J. *Phys. Chem. Chem. Phys*., **2016**, 18, 14795-14804.

110. Jin, M.; Yang, Q.X.; Lu, R.; Xu, T.H.; Zhao, Y.Y. *J. Polym. Sci. A*. **2004**, 42, 4237-4247.

111. Thomas, R.; Yoshida, Y.; Akasaka, T.; Tamaoki, N. *Chem. Eur. J*. **2012**, 18, 12337-12348.

112. Norikane, Y.; Hirai, Y.; Yoshida, M. *Chem. Commun*. **2011**, 47, 1770-1772.

113. Reuter, R.; Wegner, H. A. *Chem. Commun*. **2013**, 49, 146-148.

114. Luboch, E.; Wagner-Wysiecka, E.; Poleska-Muchlado, Z.; Kravtsov, V. C. *Tetrahedron*. **2005**, 61, 10738-10747.

115. Luboch, E.; Wagner-Wysiecka, E.; Biernat, J. F. *J. Supramol. Chem.* **2002**, 2, 279-291.

116. Wagner-Wysiecka, E.; Luboch, E.; Kowalczyk, M.; Biernat, J.F. *Tetrahedron*. **2003**, 59, 4415-4420.

117. Joshi, D. K.; Mitchell, M. J. Bruce, D.; Lough, A. J.; Yan, H. *Tetrahedron*. **2012**, 68, 8670-8676.

118. Brase, S. *Acc. Chem. Res*. **2004**, 37, 805-816.

119. Li, J.; Zhou, N.; Zhang, Z.; Xu, Y.; Chen, X.; Tu, Y.; Hu, Z.; Zhu, X. *Chem. Asian J*. **2013**, 8, 1095-1100.

120. Moustafa, M. E.; Boyle, P. D.; Puddephatt, R. *J. Can. J. Chem*, **2014**, 92, 706-715.

121. Rau, H.; Luddecke, E. *J. Am. Chem. Soc*. **1982**, 104, 1616-1620.

122. Crecca, C. R.; Roitberg, A. E. *J. Phys. Chem. A*. **2006**, 110, 8188-8203.

123. Magee, J. L.; Jr, W. S.; Eyring, H. *J. Am. Chem. Soc*., **1941**, 63, 677-688.

124. Curtin, D. Y.; Grubbs E. J.; McCarty, C. G. *J. Am. Chem. Soc*., **1966**, 88, 2775-2786.

125. Fujino, T.; Arzhantsev, S. Y.; Tahara,T. *J. Phys. Chem. A*, **2001**, 105, 8123-8129.

126. Fischer, E.; Frankel, M.; Wolovsky, R. *J. Chem. Phys*., **1955**, 23, 1367-1368.

127. Bortolus, P.; Monti, S. *J. Phys. Chem*., **1979**, 83, 648-652.

128. Malkin, S.; Fischer, E. *J. Phys. Chem*., **1962**, 66, 2482-2486.

129. Asano,T.; Yano, T.; Okada,T. *J. Am. Chem. Soc*., **1982**, 104, 4900-4904.

130. Rauf, M. A.; Hisaindee, S.; Saleh, N. *RSC Adv.*, **2015**, 5, 18097-18110.

131. Babür, B.; Seferoglu, N.; Aktan, E.; Hökelek, T.; Sahin, E.; Seferoglu, Z. *J. Mol. Struct*. **2015**, 1081, 175-181.

132. Adegoke, O.A.; Idowu, O. S.*Spectrochim. Acta. A*. **2010**, 75, 719-727.

133. Duarte, L.; Giuliano, B. M.; Reva, I.; Fausto, R. *J. Phys. Chem. A*. **2013**, 117, 10671-10680.

134. Steinwand, S.; Halbritter, T.; Rastadter, D.; OrtizSanchez, J.M.; Burghardt, I.; Heckel, A.; Wachtveitl, J. *Chem. Eur. J*. **2015**, 21, 15720-15731.

135. Rageh, N. M. *Spectrochim. Acta. A*. **2004**, 60, 103-109.

136. Ferreira, G. R.; Garcia, H. C.; Couri, M. R. C.; DosSantos, H. F.; Oliveira, L. F. C. *J. Phys. Chem. A*. **2013**, 117, 642-649.

137. Ozen, A. S.; Doruker, P.; Aviyente, V. *J. Phys. Chem. A*. **2007**, 111, 13506-13514.

138. Ozen, A. S.; Aviyente, V. *J. Phys. Chem. A*. **2005**, 109, 3506-3516.

139 Satheshkumar, A.; El-Mossalamy, E.H.; Manivannan, R.; Parthiban, C.; Al-Harbi, L.M.; Kosa, S.; Elango, K. P. *Spectrochim. Acta. A*. **2014**, 128, 798-805.

140. Unal, A.; Eren, B.; Eren, E. *J. Mol. Struct*. **2013**, 1049, 303-309.

141. Racane, L.; Mihalic, Z.; Ceric, H.; Popovic, J.; Kulenovic, V. T. *Dyes Pigm*. **2013**, 96, 672-678.

142. Nedeltcheva, D.; Kurteva, V.; Topalova, I. *Rapid Commun. Mass Spectrom*. **2010**, 24, 714-720.

143. Zhu, Y.; Yang, B.; Chen, S.; Du, J. *Prog. Polym. Sci*. **2017**, 64, 1-22.

144. Wu, D.; Abezgauz, L.; Danino, D.; Ho, C.-C.; Co, C. C. *Soft Matter*, **2008**, 4, 1066-1071.

145. Yang, X.; Grailer, J. J.; Rowland, I. J.; Javadi, A.; Hurley, S. A.; Matson, V. Z.; Steeber, D. A.; Gong, S. *Acs, Nano*.**2010**, 4, 6805-6817.

146. Bellomo, E. G.; Wyrsta, M. D.; Pakstis, L.; Pochan, D.; Deming, T. *Nat. Mater*. **2004**, 3, 244-248.

147. Li, M. -H.; Keller, P. *Soft Matter*. **2009**, 5, 927-937.

148. Cho, J. H.; Kim, S.-H.; Park, K. D.; Jung, M. C.; Yang, W. I.; Han, S. W.; Noh, J.Y.; Lee, J. W. *Biomaterials*. **2004**, 25, 5743-5751.

149. Zhao, B.; Li, D.; Hua, F.; Green, D. R. *Macromolecules*. **2005**, 38, 9509-9517.

150. Dimitrov, I.; Trzebick, B.; Mu¨ ller, A. H. E.; Dworak, A.; Tsvetanov, C. B. *Prog. Polym. Sci*. **2007**, 32, 1275-1343.

151. Nonaka, T.; Hanada, Y.; Watanabe, T.; Ogata, T.; Kurihara, S. *J. Appl. Polym. Sci*. **2004**, 92, 116-125.

152. Das, S.; Samanta, S.; Chatterjee, D. P. Nandi, A. K. *J. Polym. Sci. A*. **2013**, 51, 1417-1427.

153. Mora-Huertas, C.E.; Fessi, H.; Elaissari, A. *Int. J. Pharm*. **2010**, 385, 113-142.

154. Marturano, V.; Cerruti, P.; Giamberini, M.; Tylkowski, B.; Ambrogi, V. *Polymers*. **2017**, 9, 1-19.

155. Hu, J. M.; Liu, T.; Zhang, G. Y.; Jin, F.; Liu, S. Y. *Macromol. Rapid Commun*. **2013**, 34, 749-758.

156. Xu, P.; Li, S. -Y.; Li, Q.; van Kirk, E. A.; Ren, J.; Murdoch, W. J.; Zhang, Z.; Radosz, M.; Shen, Y. Q. *Angew. Chem., Int. Ed*. **2008**, 47, 1260-1264.

157. Ge, Z.; Liu, S. *Macromol. Rapid Commun*. **2013**, 34, 922-930.

158. Zhang, Q.; Ko, N. R.; Oh, J. K. *Chem. Commun*. **2012**, 48, 7542-7552.

159. Du, J.; Willcock, H.; Patterson, J. P.; Portman, I.; O' Reilly, R. K. *Small*. **2011**, 7, 2070-2080.

160. Stile, R.A.; Healy, K.E. *Biomacromolecules.* **2001**, 2, 185-194.

161. Vihola, H.; Laukkanen, A.; Tenhu, H.; Hirvonen, *J. Pharm. Sci*. **2008**, 97, 4783-4793.

162. Twaites, B.R.; Alarcon, C.D.H.; Lavigne, M.; Saulnier, A.; Pennadam, S.S.; Cunliffe, D.; Gorecki, D.C.; Alexander, C. *J. Control. Release*. **2005**, 108, 472-483.

163. Pasparakis, G.; Vamvakaki, M. *Polym. Chem*. **2011**, 2, 1234-1248.

164. Doorty, K.B.; Golubeva, T.A.; Gorelov, A.V.; Rochev, Y.A.; Allen, L.T.; Dawson, K.A.; Gallagher, W.M.; Keenan, A.K. *Cardiovasc. Pathol*. **2003**, 12, 105-110.

165. Hacker, M.C.; Klouda, L.; Ma, B.B.; Kretlow, J.D.; Mikos, A.G. *Biomacromolecules.* **2008**, 9, 1558-1570.

166. Vihola, H.; Laukkanen, A.; Tenhu, H.; Hirvonen, J. *J. Pharm. Sci*. **2008**, 97, 4783-4793.

167. Aw, M. S.; Addai-Mensah, J.; Losic, D. *J. Mater. Chem*. **2012**, 22, 6561-6563.

168. Liu, F.; Urban, M.W. *Prog. Polym. Sci*. **2010**, 35, 3-23.

169. Shimizu, K.; Fujita, H.; Nagamori, E. *Biotechnol. Bioeng*. **2010**, 106, 303-310.

170. Seuring, J.; Agarwal, S. *ACS Macro Lett*. 2013, 2, 597-600.

171. Schild, H. G.; Tirrel, D. A. *J. Phys. Chem*. **1990**, 94, 4352-4356.

172. Jain, K.; Vedarajan, R.; Watanabe, M.; Ishikiriyama, M.; Matsumi, Noriyoshi. *Polym. Chem*. **2015**, 6, 6819-6825.

173. Gandhi, A.; Paul, A.; Sen, S. O.; Sen, K. K. *Asian J. Pharm. Sci*. **2015**, 10, 99-107.

174. Verdonck, B.; Gohy, J. F.; Khousakoun, E.; Jérôme, R.; Prez, F. D. *Polymer*. **2005**, 46, 9899-9907.

175. Liu, J.; Debuigne, A.; Detrembleur, C.; Jérôme, C. *Adv. Healthcare Mater*. **2014**, 3, 1941-1968.

176. Hoogenboom, R. *Angew. Chem. Int. Ed*. **2009**, 48, 7978-7994.

177. Sedlacek, O.; Monnery, B. D.; Filippov, S. K.; Hoogenboom, R.; Hruby, M. *Macromol.*

Rapid Commun. **2012**, 33, 1648-1662.

178. Sosnik, A.; Cohn, D. *Biomaterials*. **2004**, 25, 2851-2858.

179. Berthier, D.L.; Schmidt, I.; Fieber, W.; Schatz, C.; Furrer, A.; Wong, K.; Lecommandoux, S. *Langmuir*. **2010**, 26, 7953-7961.

180. Louguet, S.; Rousseau, B.; Epherre, Guidolin, R.; Goglio, N. G. ; Mornet, S. ; Duguet, E.; Lecommandoux, S.; Schatz, C. *Polym.Chem*. **2012**, 3, 1408-1417.

181. Miguel, V. S.; Limer, A.J.; Haddleton, D.M.; Catalina, F.; Peinado, C. *Eur. Polym. J*. **2008**, 44, 3853-3863.

182. Han, D.; Tong, X.; Boissière, O.; Zhao, Y. *ACS Macro Lett*. **2012**, 1, 57-61.

183. Wang, B.; Xub, X.-D.; Wang, Z.-C.; Chengb, S.-X.; Zhang, X.-Z.; Zhuo, R.-X. *Colloids and Surfaces B: Biointerfaces*. **2008**, 64, 34-41.

184. Kim, E.J.; Cho, S. H.; Yuk, S. H.; *Biomaterials*. **2001**, 22, 2495-2499.

185. Meléndez-Ortiz, H. I.; Bucio, E. *Polym. Bull*. **2008**, 61, 619-629.

186. Zhang, Y.; Furyk, S.; Sagle, L.B.; Cho, Y.; Bergbreiter, D.E.; Cremer, P. S. *J. Phys. Chem. C*. **2007**, 111, 8916-8924.

187. Lessard, D. G.; Ousalem, M.; Zhu, X. X. *Can. J. Chem*. **2001**, 79, 1870-1874.

188. Hoogenboom, R.; Thijs, H. M. L.; Jochems, M.J. H. C.; van Lankvelt, B.M.; Fijten, M.W. M.; Schubert, U.S. *Chem. Commun*. **2008**, 5758-5760.

189. Furyk, S.; Zhang, Y.; Ortiz-Acosta, D.; Cremer, P. S.; Bergbreiter, D.E. *J. Polym. Sci. A*. **2006**, 44, 1492-1501.

190. Xia, Y.; Burke, N. A. D.; Stover, H. D. H. *Macromolecules*. **2006**, 39, 2275-2283.

191. Kujawa, P.; Segui, F.; Shaban, S.; Diab, C.; Okada, Y.; Tanaka, F.; Winnik, F. M. *Macromolecules*. **2006**, 39, 341-348.

192. Rzaev, Z. M. O.; Dincer, S.; Piskin, E. *Prog. Polym. Sci*. **2007**, 32, 534-595.

193. Aoshima, S.; Kanaoka, S. *Adv. Polym. Sci*. **2008**, 210, 169-208.

194. Plummer, R.; Hill, D. J. T.; Whittaker, A. K. *Macromolecules*. **2006**, 39, 8379-8388.

195. Carter, S.; Rimmer, S.; Rutkaite, R.; Swanson, L.; Fairclough, J. P. A.; Sturdy, A.; Webb, M. *Biomacromolecules*. **2006**, 7, 1124-1130.

196. Rimmer, S.; Carter, S.; Rutkaite, R.; Haycock, J. W.; Swanson, L. *Soft Matter*. **2007**, 3, 971-973.

197. Xia, Y.; Yin, X.; Burke, N. A. D.; Stover, H. D. H. *Macromolecules*. **2005**, 38, 5937-5943.

198. Liu, X.-M.; Wang, L.-S.; Wang, L.; Huang, J.; He, C. *Biomaterials*. **2004**, 25, 5659-5666.

199. Pei, Y.; Chen, J.; Yang, L.; Shi, L.; Tao, Q.; Hui, B.; Li, J. *J. Biomater. Sci. Polymer Edn*. **2004**, 15, 585-594.

200. Yin, X.; Hoffman, A. S.; Stayton, P. S. *Biomacromolecules*. **2006**, 7, 1382-1385.

201. Jones, M.S . *Eur. Polym. J*. **1999**, 35, 795-801.

202. Orzechowski, K. *Chem. Phys. Lett*.. **1999**, 240, 275-281.

203. Yoo, M.K.; Sung, Y.K.; Lee, Y.M.; Cho, C.S. *Polymer*. **2000**, 41, 5713-5719.

204. Durme, K. V.; Rahier, H.; Mele, B. V. *Macromolecules*. **2005**, 38, 10155-10163.

205. McPhee, W.; Tam, K. C.; Pelton, R. *J. Colloid Interface Sci*. **1993**, 156, 24-30.

206. Katsumoto, Y.; Tanaka, T.; Sato, H.; Ozaki, Y. *J. Phys. Chem. A*. **2002**, 106, 3429-3435.

207. Yim, H.; Kent, M. S. *Macromolecules*. **2004**, 37, 1994-1997.

208. Yim, H.; Kent, M. S. *Macromolecules*. **2006**, 39, 3420-3426.

209. Kim, J.-H.; Lee, T. R. *Drug Dev. Res*. **2006**, 67, 61-69.

210. Zhang, J. L.; Srivastava, R. S.; Misra, R. D. K. *Langmuir*. **2007**, 23, 6342-6351.

211. Kanazawa, H.; Yamamoto, K.; Matsushima, Y. *Anal. Chem*. **1996**, 68, 100-105.

212. Liu, G.; Liu, W.; Dong, C.-M. *Polym. Chem*. **2013**, 4, 3431-3443.

213. Fomina, N.; McFearin, C.; Sermsakdi, M.; Edigin, O.; Almutairi, A. *J. Am. Chem. Soc*. **2010**, 132, 9540-9542.

214. Mahimwalla, Z.; Yager, K. G.; Mamiya, J.; Shishido, A.; Priimagi, A.; Barrett, C. J.; *Polym. Bull.* **2012**, *69*, 967-1006.

215. Huang, Y.; Liang, W.; Poon, J. K. S.; Xu, Y.; Lee, R. K.; Yariv, A.; *Appl. Phys. Lett.* **2006**, *88*, 181102.

216. Hirakura, T.; Nomura, Y.; Aoyama, Y.; Akiyoshi, K.; *Biomacromolecules.* **2004**, *5*, 1804-1809.

217. Maddipatla, M. V. S. N.; Wehrung, D.; Tang, C.; Fan, W.; Oyewumi, M. O.; Miyoshi, T.; Joy, A.; *Macromolecules.* **2013**, *46*, 5133-5140.

218. Liu, F.; Eisenberg, A. *J. Am. Chem. Soc*. **2003**, 125, 15059-15064.

210. Zhang, Y.; Jiang, M.; Zhao, J.; Wang, Z.; Dou, H.; Chen, D. *Langmuir*. **2005**, 21, 1531-1538.

220. Du, J.; Armes, S. P. *J. Am. Chem. Soc*. **2005**, 127, 12800-12801.

221. Du, J.; Tang, Y.; Lewis, A. L.; Armes, S. P. *J. Am. Chem. Soc*. **2005**, 127, 17982-17983.

222. Shen, H.; Zhang, L.; Eisenberg, A. *J. Am. Chem. Soc*. **1999**, 121, 2728-2740.

223. Che´cot, F.; Lecommandoux, S.; Gnanou, Y.; Klok, H. -A. *Angew. Chem., Int. Ed*. **2002**, 41, 1339-1343.

224. Rodríguez-Herna´ndez, J.; Lecommandoux, S. *J. Am. Chem. Soc*. **2005**, 127, 2026-2027.

225. Klaikherd, A.; Nagamani, C.; Thayumanavan, S. *J. Am. Chem. Soc*. **2009**, 131, 4830-4838.

226. Du, J. Z.; Tang, Y. Q.; Lewis, A. L.; Armes, S. P. *J. Am. Chem. Soc*. **2005**, 127, 17982-17983.

227. Smith, A. E.; Xu, X. W.; McCormick, C. L. *Prog. Polym. Sci*. **2010**, 35, 45-93.

228. Rodrguez-Hernndez, J.; Lecommandoux, S. *J. Am. Chem. Soc*. **2005**, 127, 2026-2027.

229. Klaikherd, A.; Nagamani, C.; Thayumanavan, S. *J. Am. Chem. Soc*. **2009**, 131, 4830-4838.

230. Liu, F. T.; Eisenberg, A. *J. Am. Chem. Soc*. **2003**, 125, 15059-15064.

231. Du, J. Z.; Armes, S. P. *J. Am. Chem. Soc*. **2005**, 127, 12800-12801.

232. Zhang, Y. W.; Jiang, M. J.; Zhao, X.; Wang, Z. X.; Dou, H. J.; Chen, D. Y. *Langmuir*. **2005**, 21, 1531-1538.

233. Chcot, F.; Lecommandoux, S.; Gnanou, Y.; Klok, H. -A. *Angew. Chem*. **2002**, 114, 1395-1399.

234. Yan, Q.; Zhou, R.; Fu, C.; Zhang, H.; Yin, Y.; Yuan, J. *Angew. Chem., Int. Ed*. **2011**, 50, 4923-4927.

235. Yan, Q.; Wang, J.; Yin, Y.; Yuan, J. *Angew. Chem., Int. Ed*. **2013**, 52, 5070-5073.

236. Yan, Q.; Zhao, Y. *J. Am. Chem. Soc*. **2013**, 135, 16300-16303.

237. Yan, Q.; Zhao, Y. *Angew. Chem., Int. Ed*. **2013**, 52, 9948-9951.

238. Brown, P.; Butts, C. P.; Eastoe, J. *Soft Matter*. **2013**, 9, 2365-2374.

239. Liu, F.; Urban, M. W. *Prog. Polym. Sci*. **2010**, 35, 3-23.

240. Chu, Z. L.; Dreiss, C. A.; Feng, Y. J. *Chem. Soc. Rev*. **2013**, 42, 7174-7203.

241. Liu, H.; Lin, S.; Feng, Y.; Theato, P. *Polym. Chem*. **2017**, 8, 12-23.

242. Chen, W.; Du, J. *Sci. Rep*. **2013**, 3, 2162-2170.

243. Napoli, A.; Valentini, M.; Tirelli, N.; Mu¨ ller, M.; Hubbell, J. A. *Nat. Mater*. **2004**, 3, 183-189.

244. Ma, N.; Li, Y.; Xu, H.; Wang, Z.; Zhang, X. *J. Am. Chem. Soc*. **2010**, 132, 442-443.

245. Ryu, J. -H.; Roy, R.; Ventura, J.; Thayumanavan, S. *Langmuir*. *2010*, 26, 7086-7092.

246. Ma, N.; Li, Y.; Xu, H. P.; Wang, Z. Q.; Zhang, X. *J. Am. Chem. Soc*. **2010**, 132, 442-443.

247. Napoli, A.; Valentini, M.; Tirelli, N.; Mller, M.; Hubbell, J. A. *Nat. Mater*. **2004**, 3, 183-189.

248. Ryu, J.-H.; Roy, R.; Ventura, J.; Thayumanavan, S. *Langmuir*. **2010**, 26, 7086-7092.

249.Power-Billard, K. N.; Spontak, R. J.; Manners, I. *Angew. Chem*. **2004**, 116, 1280-1284.

250. Ulijn, R. V. *J. Mater. Chem*. **2006**, 16, 2217-2225.

251. Park, C.; Kim, H.; Kim, S.; Kim, C. *J. Am. Chem. Soc*. **2009**, 131, 16614-16615.

252. Rao, J.; Khan, A. *J. Am. Chem. Soc*. **2013**, 135, 14056-14059.

253. Yan, Q.; Yuan, J. Y.; Cai, Z. N.; Xin, Y.; Kang, Y.; Yin, Y. W. *J. Am. Chem. Soc*. **2010**, 132, 9268-9270.

254. Peng, L.; Feng, A.; Zhang, H.; Wang, H.; Jian, C.; Liu, B.; Gao, W.; Yuan, J. *Polym. Chem*. **2014**, 5, 1751-1759.

255. Sumalekshmy, S.; Fahrni, C. J. *Chem. Mater*. **2011**, 23, 483-500.

256. Liu, X.; Jiang, M. *Angew. Chem., Int. Ed*. **2006**, 45, 3846-3850.

257. Ueki, T.; Nakamura, Y.; Lodge, T. P.; Watanabe, M. *Macromolecules*. **2012**, 45, 7566-7573.

258. Jochum, F. D.; Theato, P. *Polymer*. **2009**, 50, 3079-3085.

259. H. S. Blair, H. I. Pogue, J. E. Riordan, *Polymer*. **1980**, 21, 1195-1198.

260. H. S. Blair, C. B. McArdle, *Polymer*. **1984**, 25, 1347-1352.

261. Gindre, D.; Boeglin, A.; Fort, A.; Mager, L.; Dorkenoo, K. D. *Opt. Express*. **2006**, 14, 9896-9901.

262. Yager, K. G.; Barrett, C. J. *J Photochem Photobio A: Chem*. **2006**, 182, 250-261.

263. Serak, S. V.; Tabiryan, N. V.; White, T. J.; Bunning, T. J. *Opt. Express*. **2009**, 17, 15736-15746.

264. Yamada, M.; Kondo, M.; Mamiya, J.-i.; Yu, Y.; Kinoshita, M.; Barrett, C. J.; Ikeda, T. *Angew. Chem. Int. Ed*. **2008**, 47, 4986-4988.

265. Yamada, M.; Kondo, M.; Miyasato, R.; Naka, Y.; Mamiya, J.-i.; Kinoshita, M.;

Shishido, A.; Yu, Y.; Barrett, C. J. Ikeda, T. *J. Mater. Chem*. **2009**, 19, 60-62.

266. White, T. J.; Tabiryan, N. V.; Serak, S. V.; Hrozhyk, U. A.; Tondiglia, V. P.; Koerner, H.; Vaia, R.A.; Bunning, T.J. *Soft Matter*. **2008**, 4, 1796-1798.

267. Serak, S.; Tabiryan, N.; Vergara, R.; White, T. J.; Vaia, R. A.; Bunning, T. J. *Soft Matter*. **2010**, 6, 779-783.

268. Yager, K. G.; Barrett, C. J. *Macromolecules*. **2006**, 39, 9320-9326.

269. Barrett, C. J.; Mamiya, J.-I.; Yager, K. G.; Ikeda, T. *Soft Matter*. **2007**, 3, 1249-1261.

270. Yager, K. G.; Barrentt, C. J. *Curr. Opin. Solid State Mater. Sci*. **2001**, 5, 487-494.

271. Yin, R.; Xu, W.; Kondo, M.; Yen, C.-C.; Mamiya, J.-i.; Ikeda, T.; Yu, Y. *J. Mater. Chem*. **2009**, 19, 3141-3143.

272. Finkelmann, H.; Nishikawa, E. Pereira, G. G.; Warner, M. *Phys. Rev. Lett*. **2001**, 87, 015501-1-4.

273. Li, Y.; He, Y.; Tong, X.; Wang, X. *J. Am. Chem. Soc*. **2005**, 127, 2402-2403.

274. Natansohn, A.; Rochon, P. *Chem. Rev*. **2002**, 102, 4139-4175.

275. Bogdanov, A. V.; Vorobiev, A.K. *J. Phys. Chem. B*. **2013**, 117, 13936-13945.

276. Kadota, S.; Aoki, K.; Nagano, S.; Seki, T. *J. Am. Chem. Soc*. **2005**, 127, 8266-8267.

277. Vollmer, M. S.; Clark, T. D; Steinem, C.; Ghadiri, M. R. *Angew. Chem. Int. Ed*. **1999**, 38, 1598-1601.

278. Alvarez-Lorenzo, C.; Bromberg, L.; Concheiro, A. *J. Photochem. Photobiol*. 2009, 85, 848-860.

279. Zhao, Y. *Macromolecules* **2012**, 45, 3647-3657.

280. Ueki, T.; Yamaguchi, A.; Ito, N.; Kodama, K.; Sakamoto, J.; Ueno, K.; Kokubo, H.; Watanabe, M. *Langmuir*. **2009**, 25, 8845-8848.

281. Zhao, Y.; Tremblay, L.; Zhao, Y. *J. Polym. Sci. A*. **2010**, 48, 4055-4066.

282. Ueki, T.; Nakamura, Y.; Yamaguchi, A.; Niitsuma, K.; Lodge, T. P.; Watanabe, M. *Macromolecules.* **2011**, 44, 6908-6914.

283. Rao, J.; Khan, A. *J. Am. Chem. Soc*. **2013**, 135, 14056-14059.

284. Bauman, D.; Mykowska, E.; Zieba, A. *Mol. Cryst. Liq. Cryst*. **2008**, 494, 79-92.

285. Floß, G.; Saalfrank, P. *J. Phys. Chem. A*. **2015**, 119, 5026-5037.

286. Ito, Y.; Ito, H.; Matsuura, T. *Tet. Lett.* **1988**, 29, 563-566.

287. Merino, E. *Chem. Soc. Rev*. **2011**, 40, 3835-3853.

288. Knie, C.; Utecht, M.; Zhao, F.; Kulla, H.; Kovalenko, S.; Brouwer, A. M.; Saalfrank, P.; Hecht, S.; Bleger, D. *Chem. Eur. J*. **2014**, 20, 16492-16501.

289. Bléger, D.; Schwarz, J.; Brouwer, A.M.; Hecht, S. *J. Am. Chem. Soc*. **2012**, 134, 20597-20600.

290. Bushuyev, O.S.; Tomberg, A.; Friščić, T.; Barrett, C.J. *J. Am. Chem. Soc*. **2013**, 135, 12556-12559.

291. Garcia-Amoros, J.; Diaz-Lobo, M.; Nonell, S.; Velasco, D. *Angew. Chem. Int. Ed*. **2012**, 51, 12820-12823.

292. Garcia-Amoro´s, J.; Sanchez-Ferrer, A.; Massad, W.A.; Nonell, S.; Velasco, D. *Phys. Chem. Chem. Phys*. **2010**, 12, 13238-13242.

293. Kikuchi, S. *J. Chem. Educ*. **1997**, 74, 194-201.

294. Kulkarni, S. K.; Dhir. A.; *Phytother. Res*. **2010**, 24: 317-324.

295. Grundon, M. F.; Wasfi, A. S. *J. Chem. Soc*. **1963**, 1982-1986.

296. Grundon, M. F.; Johnston, B. T.; Wasfi, A. S. *J. Chem. Soc*. **1963**, 1436-1440.

297. Rusu, E.; Dorohoi, D.-O.; Airinei, A.; *J. Mol. Struct.***2008**, 887, 216–219.

298. Zhang, X.-Z. Zhuo, R.-X. *Langmuir*. **2001**, 17, 12-16.

299. Katsumoto, Y.; Tanaka, T.; Sato, H.; Ozaki, Y. *J. Phys. Chem. A*. **2002**, 106, 3429-3435.

300. Ravi, P.; Sin, S. L.; Gan, L. H.; Gan, Y. Y.; Tam, K. C.; Xia, X. L.; Hu, X. *Polymer*. **2005**, 46, 137-146.

301. Desponds, A., Freitag, R. *Langmuir*. **2003**, 19, 6261-6270.

302. Zhao, Y.; Tremblay, L.; Zhao, Y. *J. Polym. Sci. A*. **2010**, 48, 4055-4066.

303. Desponds, A.; Freitag, R. *Langmuir*. **2003**, 19, 6261-6270.

304. Udayakumar,V.; Pandurangan, A. *RSC Adv*., **2015**, 5, 78719-78727.

305. Annedi, S.C.; Li, W.; Samson, S.; Kotra, L.P. *J. Org. Chem*. **2003**, 68, 1043-1049.

306. Li, Y.; Yang, J.; Benicewicz, B. C. *J. Polym. Sci. A*. **2007**, 45, 4300-4308.

307. Grenning, A. J.; Van Allen, C. K. Maji, T.; Lang, S. B.; Tunge, J. A. *J. Org. Chem.* **2013**, 78, 7281-7287.

308. He, J.; Tremblay, L.; Lacelle, S.; Zhao, Y. *Polym. Chem*. **2014**, 5, 5403-5411

309. Yu, B.; Jiang, X.; Wang, R.; Yin, J. *Macromolecules*. **2010**, 43, 10457-10465.

APPENDIX I: EXPERIMENTAL PART

General remarks

All reagents and solvents were purchased from commercial sources and used without further purification unless stated otherwise, Tetrahydrofuran (THF), Chloroform ($CHCl_3$), Dimethyl Sulphoxide (DMSO), *N,N*-Dimethylformamide (DMF), Dimethylacetamide (DMAc), Ethyl Acetate (EtOAc), Ethanol (EtOH), Dichloromethane (DCM). ^1H (400Hz) and ^{13}C NMR (100 Hz) spectra were recorded in DMSO-d_6, $CDCl_3$ or DMF-d_7 using an Ascend^{TM} 400 spectrometer, with tetramethylsilane as the internal standard. The chemical shifts are reported in ppm, using the solvent signal as an internal reference, in $CDCl_3$ (δH = 7.26 ppm, δC = 77.2 ppm), DMSO-d_6 (δH = 2.50 ppm, δC = 39.5 ppm) or DMF-d_7 (δH = 8.03 ppm, 2.92 and 2.75 ppm, δC = 163.15 ppm, 34.89 ppm and 29.76 ppm). High-resolution mass spectra were obtained via ESI / EI mode with a TOF mass analyzer. Column chromatography was performed on silica gel (40 - 63 μm) using EtOAc, Hexane, DCM, etc. The X-ray intensity data were measured on a Bruker Apex DUO system equipped with a Cu Kα ImuS micro-focus source with MX optics (λ = 1.54178 Å). Compounds on TLC (Thin Layer Chromatography) were revealed by ultraviolet lamp (254 nm) or by dipping in aqueous $KMnO_4$ followed by heating. UV-vis (Ultraviolet-visible) absorption measurements were performed with an Agilent 8453 spectrophotometer equipped with thermostated cell compartments at ± 0.1 °C, using 1cm square quartz cuvettes.

Chapter 1

4-phenylazo-phenol (81)

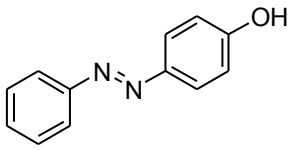

To a 100 ml flask, anilines (1.86 g, 0.02 mol), HCl (6.03 ml, 0.07 mol) were mixed in deionized water (2 M). The mixture was cooled to 0 ^{o}C over an ice bath. Then, $NaNO_2$ (1.518 g, 0.022 mol) in 1.1 M deionized water was added. Another mixture composed of 3-methoxyphenol (2.48 g, 0.02 mol), NaOH (2.8 g, 0.07 mol) and deionized water (1 M) was prepared and cooled in an ice bath to 0 ^{o}C. The diazonium salt solution was subsequently slowly added to the formed phenolate solution over a period of half of hour. Brownish-orange slurry mixture was formed for additional 2-3 h. As the reaction finished, the slurry was then neutralized by diluted HCl solution. The red-orange product was precipitated and washed with water for several times. The crude product was purified by flash column chromatography on silica gel with 9:1 Hexane / EtOAc as the eluent to aff ord the brown solid (1.426 g, 72%). **^{1}H NMR (400 MHz, $CDCl_3$) δ(ppm):** 7.94 (t, *J* = 9.8 Hz, 4H), 7.58 – 7.44 (m, 3H), 7.00 (d, *J* = 11.7 Hz, 2H). **^{13}C NMR (100 MHz, $CDCl_3$) δ(ppm):** 159.5, 152.5, 145.1, 130.7, 128.8, 124.1, 122.7, 116.0. Hexane : EtOAc (v:v) = 8:2, R_f = 0.10; **HRMS** (ESI-Q-TOF), m/z: calculated for $C_{12}H_{10}N_2O$: 199.1040 $[M+H]^+$, found: 199.1053.

2, 4-bis((E)-phenyldiazenyl)phenol (96)

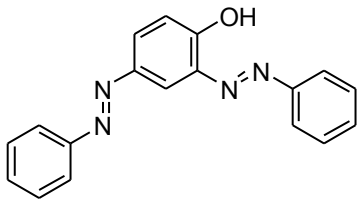

A brown solid (0.302 g, 10%) was obtained using the same procedure with aniline (1.82 ml, 20 mmol) and phenol (0.94 g, 10 mmol) as starting material. **^{1}H NMR (400 MHz, $CDCl_3$) δ(ppm):** 8.63 (d, *J* = 3.1 Hz, 1H), 7.97 (d, *J* = 9.5 Hz, 4H), 7.57 (m, 7H), 7.19 (d, *J* = 11.8 Hz, 1H). **^{13}C NMR (100 MHz, $CDCl_3$) δ(ppm):** 155.54 , 152.62 , 150.29 , 146.33 , 136.78 , 131.69 , 130.74 , 129.50 , 129.12 , 128.91 , 127.06 , 122.75 , 122.46 , 118.91. Hexane : EtOAc (v:v) = 8:2, R_f = 0.36; **HRMS** (ESI-Q-TOF), m/z: calculated for $C_{18}H_{14}N_4O$: 303.1240 $[M+H]^+$, found: 303.1253.

(E)-3-methoxy-4-(phenyldiazenyl)phenol (99)

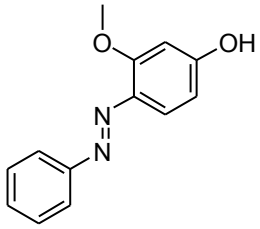

A red solid (0.741 g, 65%) was obtained using the same procedure with aniline (0.465 g, 5 mmol) and 3-methoxyphenol (0.93 g, 7.5 mmol) as starting material. **^{1}H NMR (400 MHz, $CDCl_3$) δ(ppm):** 7.89 (d, *J* = 10.4 Hz, 2H), 7.74 (d, *J* = 11.7 Hz, 1H), 7.47 (m, 3H), 6.63 (d, *J* = 3.1 Hz, 1H), 6.52 (dd, *J* = 11.7, 3.3 Hz, 1H), 4.05 (s, 3H). **^{13}C NMR (100 MHz, $CDCl_3$) δ(ppm):** 160.08, 148.25, 133.05, 131.06, 129.29, 128.47, 123.15, 120.04, 118.00, 113.09, 105.82, 101.69, 56.39. Hexane : EtOAc (v:v) = 8:2, R_f = 0.16; **HRMS** (ESI-Q-TOF) m/z: calculated for $C_{13}H_{12}N_2O_2$: 229.0972 $[M + H]^+$, found: 229.0982.

(E)-5-methoxy-2-(phenyldiazenyl)phenol (100)

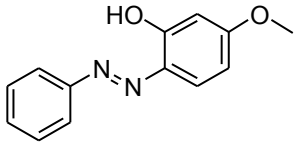

A red-orange solid (0.137 g, 12%) was obtained using the same procedure with aniline (0.465 g, 5 mmol) and 3-methoxyphenol (0.62 g, 5 mmol) as starting material. **^{1}H NMR (400 MHz, $CDCl_3$) δ(ppm)**: 13.91 (s, 1H), 7.84 (t, *J* =22.8 Hz, 3H), 7.54 (m, 2H), 7.49 – 7.44 (m, 1H), 6.66 (dd, *J* = 11.9, 3.5 Hz, 1H), 6.51 (d, *J* = 3.5 Hz, 1H), 3.92(s, 3H). **^{13}C NMR (100 MHz, $CDCl_3$) δ(ppm)**: 164.41, 157.13, 149.61, 134.86, 132.83, 130.11, 129.35, 121.48, 108,71, 101.37, 55.79. Hexane : EtOAc (v:v) = 8:2, R_f = 0.68; **HRMS** (ESI-Q-TOF) m/z: calculated for $C_{13}H_{12}N_2O_2$: 251.0791 $[M + Na]^+$, found: 251.0811.

2, 4-bis((E)-phenyldiazenyl)-5-methoxyphenol (101)

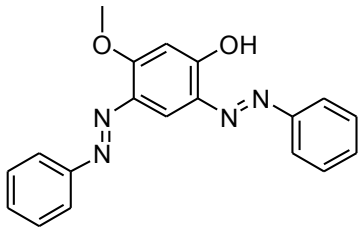

A brown solid (1.411 g, 85%) was obtained using the same procedure with aniline(0.93 g, 10 mmol) and 3-methoxyphenol (0.62 g, 5 mmol) as starting material. **^{1}H NMR (400 MHz, $CDCl_3$) δ(ppm)**: 14.11 (s, 1H), 8.38 (s, 1H), 7.96 (d, *J* = 10.7 Hz, 2H), 7.90 (d, *J* = 10.7 Hz, 2H), 7.61 – 7.44 (m, 6H), 6.69 (s, 1H), 4.16 (s, 3H). **^{13}C NMR (100 MHz, $CDCl_3$) δ(ppm)**: 161.59, 154.49, 152.73, 149.76, 136.44, 131.81, 130.86, 130.69, 129.44, 129.12, 122.84, 121.89, 100.76, 56.74. Hexane : EtOAc (v:v) = 8:2, R_f = 0.44; **HRMS** (ESI-Q-TOF) m/z: calculated for $C_{19}H_{16}N_4O_2$: 333.1346 $[M + H]^+$, found: 333.1360.

2-phenylazo-3-prop-2-ynyloxy-phenol (102)

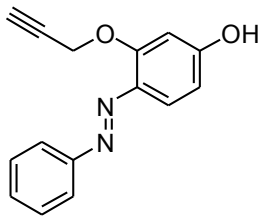

A brown solid (0.454 g, 18%) was obtained using the same procedure with aniline (1.82 ml, 20 mmol) and phenol (0.94 g, 10 mmol) as starting material. **^{1}H NMR (400 MHz, $CDCl_3$) δ(ppm)**: 7.89 (d, *J* = 9.5 Hz, 2H), 7.74 (d, *J* = 11.7 Hz, 1H), 7.47 (dt, *J* = 20.7, 10.1 Hz, 3H), 6.63 (d, *J* = 3.1 Hz, 1H), 6.53 (d, *J* = 3.1 Hz, 1H), 5.03 (d, *J* = 2.5 Hz, 2H), 2.66 (t, *J* = 2.4 Hz, 1H). **^{13}C NMR (100 MHz, $CDCl_3$) δ(ppm)**: 160.41, 155.13, 148.61, 130.86, 131.83, 127.35, 120.48, 106,71, 104.37, 77.96, 77.53, 57.39. Hexane : EtOAc (v:v) = 8:2, R_f = 0.63; **HRMS** (ESI-Q-TOF), m/z: calculated for $C_{18}H_{12}N_2O_2$: 253.1150 $[M+H]^+$, found: 253.1175.

2-phenylazo-5-prop-2-ynyloxy-phenol (**103**)

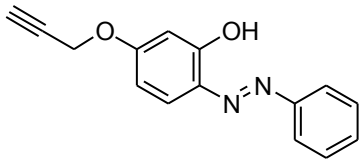

A brown solid (0.227 g, 9%) was obtained using the same procedure with aniline (1.82 ml, 20 mmol) and phenol (0.94 g, 10 mmol) as starting material. **^{1}H NMR (400 MHz, $CDCl_3$) δ(ppm)**: 13.93 (s, 1H), 7.83 (t, *J* = 11.2 Hz, 3H), 7.59 – 7.50 (m, 2H), 7.47 (d, *J* = 9.6 Hz, 1H), 6.71 (d, *J* = 3.5 Hz, 1H), 6.51 (d, *J* = 3.5 Hz, 1H), 5.02 (d, *J* = 2.5 Hz, 2H), 2.64 (t, *J* = 2.4 Hz, 1H). **^{13}C NMR (100 MHz, $CDCl_3$) δ(ppm)**: 164.41, 157.13, 149.61, 134.86, 132.83, 129.35, 121.48, 108,71, 101.37, 77.46, 77.23, 57.29. Hexane : EtOAc (v:v) = 8:2, R_f = 0.10; **HRMS** (ESI-Q-TOF), m/z: calculated for $C_{18}H_{12}N_2O_2$: 253.1040 $[M+H]^+$, found:

253.1053.

2,4-bis-phenylazo-5-prop-2-ynyloxy-phenol (104)

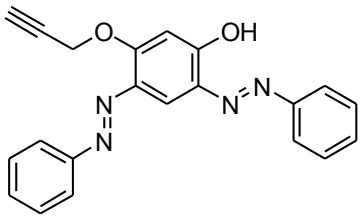

A brown solid (2.065 g, 58%) was obtained using the same procedure with aniline (1.82 ml, 20 mmol) and phenol (0.94 g, 10 mmol) as starting material. **^{1}H NMR (400 MHz, $CDCl_3$) δ(ppm)**:13.96 (s, 1H), 8.40 (s, 1H), 7.95 (d, *J* = 8.2 Hz, 2H), 7.89 (d, *J* = 7.1 Hz, 2H), 7.53 (ddd, *J* = 17.4, 10.6, 5.2 Hz, 6H), 6.84 (s, 1H), 5.03 (d, *J* = 2.4 Hz, 2H), 2.66 (t, *J* = 2.4 Hz, 1H). **^{13}C NMR (100 MHz, $CDCl_3$) δ(ppm)**: 159.16, 158.44, 153.01, 149.99, 136.83, 132.33, 131.01, 130.71, 129.45, 129.11, 122.94, 122.02, 121.67, 102.66, 77.46, 77.23, 57.29. Hexane : EtOAc (v:v) = 8:2, R_f = 0.55; **HRMS** (ESI-Q-TOF), m/z: calculated for $C_{21}H_{16}N_4O_2$: 357.1240 [M+H]+, found: 357.1253.

2, 4-bis((E)-phenyldiazenyl)benzene-1, 3, 5-triol (106)

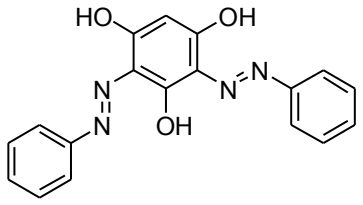

A red solid (0.190 g, 57%) was obtained using the same procedure with aniline (0.273 ml, 3 mmol) and Phloroglucinol (0.126 g, 1 mmol) as starting material. **^{1}H NMR (400 MHz, $CDCl_3$) δ(ppm)**: 15.37 (s, 1H), 7.62 (d, *J* = 7.6 Hz, 2H), 7.52 – 7.40 (m, 7H), 7.32 – 7.24 (m, 1H), 5.96 (s, 1H). **^{13}C NMR (100 MHz, $CDCl_3$) δ(ppm)**: 184.67, 177.80, 161.60,

141.31, 140.88, 129.91, 129.70, 129.17, 127.12, 126.26, 123.95, 117.48, 116.20, 102.70. Hexane : EtOAc (v:v) = 7:3, R_f = 0.08; **HRMS** (ESI-Q-TOF), m/z: calculated for $C_{18}H_{14}N_4O_3$: 335.1139 $[M+H]^+$, found: 335.1154.

2, 4, 6-Tris-phenylazo-benzene-1, 3, 5-triol (107)

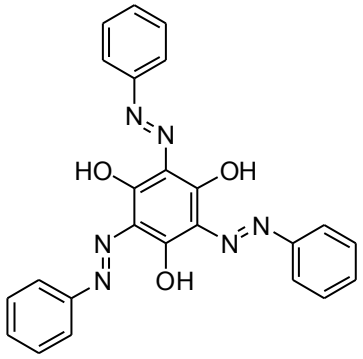

A red solid (0.145 g, 33%) was obtained using the same procedure with aniline (0.279 g, 3 mmol) and 1,3,5-Trihydroxybenzene (0.126 g, 1 mmol) as starting material. **^{1}H NMR (400 MHz, $CDCl_3$) δ(ppm)**: 7.67 (d, *J* = 8.7 Hz, 5H), 7.50 (m, 6H), 7.33 (m, 4H), 5.33 (s, 2H). **^{13}C NMR (100 MHz, $CDCl_3$) δ(ppm)**: 178.70, 141.26, 129.86, 128.83, 127.57, 117.65. Hexane : EtOAc (v:v) = 7:3, R_f = 0.36; **HRMS** (ESI-Q-TOF) m/z: calculated for $C_{24}H_{18}N_6O_3$: 439.1513 $[M + H]^+$, found: 439.1531.

(E)-4-((2,4-dimethoxyphenyl)diazenyl)-3-methoxyphenol (117)

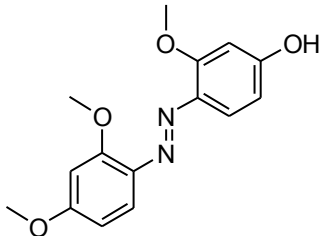

A orange-yellow solid (0.576 g, 40%) was obtained using the same procedure with 2,4-dimethoxyaniline (0.765 g, 5 mmol) and 3-methoxyphenol (0.93 g, 7.5 mmol) as

starting material. **^{1}H NMR (400 MHz, $CDCl_3$) δ(ppm)**: 7.68 (d, *J* = 11.5 Hz, 1H), 7.46 (d, *J* = 12.3 Hz, 1H), 6.62 – 6.47 (m, 4H), 4.00 (s, 3H), 3.98 (s, 3H), 3.87 (s, 3H). **^{13}C NMR (100 MHz, $CDCl_3$) δ(ppm)**: 163.76, 160.91, 159.53, 158.74, 157.09, 137.47, 118.61, 117.32, 113.07, 106.09, 102.29, 98.91, 56.48, 56.39, 55.75. Hexane : EtOAc (v:v) = 6:4, R_f = 0.12; **HRMS** (ESI-Q-TOF) m/z: calculated for $C_{15}H_{16}N_2O_4$: 289.1183 $[M + H]^+$, found: 289.1196.

(E)-2-((2,4-dimethoxyphenyl)diazenyl)-5-methoxyphenol (118)

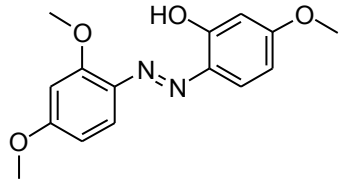

A red solid (0.173 g, 12%) was obtained using the same procedure with 2,4-dimethoxyaniline (0.765 g, 5 mmol) and 3-methoxyphenol (0.62 g, 5 mmol) as starting material. **^{1}H NMR (400 MHz, $CDCl_3$) δ(ppm)**: 14.57 (s, 1H), 7.87 (d, *J* = 13.1 Hz, 1H), 7.75 (d, *J* = 11.8 Hz, 1H), 6.61 (ddd, *J* = 10.2, 6.1, 3.4 Hz, 3H), 6.50 (d, *J* = 3.5 Hz, 1H), 4.01 (s, 3H), 3.92 (s, 3H), 3.89 (s, 3H). **^{13}C NMR (100 MHz, $CDCl_3$) δ(ppm)**: 164.39, 163.17, 157.67, 156.19, 134.01, 132.96, 131.25, 117.53, 108.74, 106.24, 101.55, 98.59, 56.13, 55.86, 55.73. Hexane : EtOAc (v:v) = 6:4, R_f = 0.56; **HRMS** (ESI-Q-TOF) m/z: calculated for $C_{15}H_{16}N_2O_4$: 289.1183 $[M + H]^+$, found: 289.1196.

2, 4-bis((E)-(2,4-dimethoxyphenyl)diazenyl)-5-methoxyphenol (119)

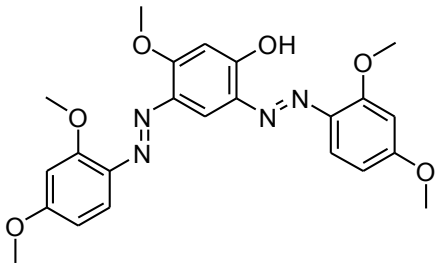

A dark-brown solid (0.859 g, 38%) was obtained using the same procedure with 2,4-dimethoxyaniline (1.578 g, 1 mmol) and 3-methoxyphenol (0.62 g, 5 mmol) as starting material. **^{1}H NMR (400 MHz, $CDCl_3$) δ(ppm)**: 14.90 (s, 1H), 8.24 (s, 1H), 7.89 (d, *J* = 12.2 Hz, 1H), 7.76 (d, *J* = 11.8 Hz, 1H), 6.74 – 6.49 (m, 5H), 4.09 (s, 3H), 4.07 (s, 3H), 4.03 (s, 3H), 3.93 (d, *J* = 2.4 Hz, 6H). **^{13}C NMR (100 MHz, $CDCl_3$) δ(ppm)**: 163.32, 163.16, 160.20, 159.30, 158.33, 156.85, 137.64, 137.11, 132.75, 132.61, 120.55, 118.54, 117.34, 106.02, 105.53, 100.74, 99.08, 98.65, 56.49, 56.40, 56.02, 55.69, 55.61. Hexane : EtOAc (v:v) = 6:4, R_f = 0.25; **HRMS** (ESI-Q-TOF) m/z: calculated for $C_{23}H_{24}N_4O_6$: 453.1768 $[M + H]^+$, found: 453.1792.

(E)-3-methoxy-4-((4-methoxyphenyl)diazenyl)phenol (121)

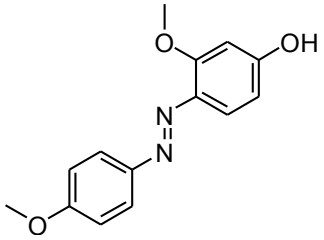

A red-orange solid (0.774 g, 60%) was obtained using the same procedure with p-Anisidine (0.615 g, 5 mmol) and 3-methoxyphenol (0.93 g, 7.5 mmol) as starting material. **^{1}H NMR (400 MHz, $CDCl_3$) δ(ppm)**: 7.90 (d, *J* = 11.6Hz, 1H), 7.71 (d, *J* = 11.7 Hz, 1H), 7.02 (d, *J* = 12Hz, 1H), 6.61 (d, *J* = 3.2 Hz, 0H), 6.49 (dd, *J* = 11.7, 2.9 Hz, 1H), 5.36 (s, 1H), 4.03 (s, 3H), 3.92 (s, 3H). **^{13}C NMR (100 MHz, $CDCl_3$) δ(ppm)**: 160.83, 158.83, 145.26, 134.86, 125.02, 123.26, 114.29, 113.13, 110.60, 100.66, 56.21, 55.58. Hexane : EtOAc (v:v) = 8:2,

R_f = 0.09; **HRMS** (ESI-Q-TOF) m/z: calculated for $C_{14}H_{14}N_2O_3$: 259.1077 $[M + H]^+$, found: 259.1091.

(E)-5-methoxy-2-((4-methoxyphenyl)diazenyl)phenol (122)

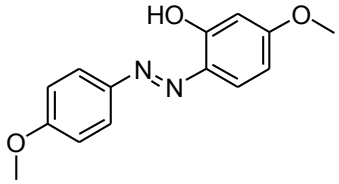

A red solid (0.258 g, 20%) was obtained using the same procedure with p-Anisidine (0.615 g, 5 mmol) and 3-methoxyphenol (0.62 g, 5 mmol) as starting material. **^{1}H NMR (400 MHz, $CDCl_3$) δ(ppm)**: 13.70 (s, 1H), 7.83 (d, *J* = 12.4 Hz,2H), 7.79 (d, *J* = 11.6 Hz,1H), 7.04 (d, *J* = 12.4 Hz,2H), 6.64 (dd, *J* = 11.8, 3.6 Hz, 1H), 6.51 (d, *J* = 3.5 Hz, 1H), 3.93 (s, 3H), 3.90 (s, 3H). **^{13}C NMR (100 MHz, $CDCl_3$) δ(ppm)**: 164.24, 161.57, 156.44, 143.13, 134.46, 132.36, 123.18, 114.67, 108.61, 101.37, 55.89, 55.68. Hexane : EtOAc (v:v) = 8:2, R_f = 0.56; **HRMS** (ESI-Q-TOF) m/z: calculated for $C_{14}H_{14}N_2O_3$: 259.1077 $[M + H]^+$, found: 259.1089.

2, 4-bis((E)-(4-methoxyphenyl)diazenyl)-5-methoxyphenol (123)

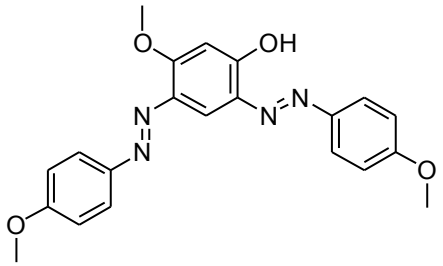

A drak-brown solid (0.607 g, 62%) was obtained using the same procedure with P-Anisidine (0.615 g, 5 mmol) and 3-methoxyphenol (0.31 g, 2.5 mmol) as starting material. **^{1}H NMR(400 MHz, $CDCl_3$) δ(ppm)**: 13.94 (s, 1H), 8.32 (s, 1H), 7.96 (d, *J* =

11.8 Hz, 2H), 7.87 (d, *J* = 11.9 Hz, 2H), 7.02 (d, *J* = 24.0 Hz, 4H), 6.67 (s, 1H), 4.12 (s, 3H), 3.93 (s, 6H). **^{13}C NMR (100 MHz, $CDCl_3$) δ(ppm)**: 161.92, 161.78, 160.48, 158.23, 147.10, 144.19, 136.23, 131.71, 124.69, 123.68, 121.06, 114.60, 114.24, 100.61, 56.63, 55.67, 55.60. Hexane : EtOAc (v:v) = 8:2, R_f = 0.21; **HRMS** (ESI-Q-TOF) m/z: calculated for $C_{21}H_{20}N_4O_4$: 393.1557 $[M + H]^+$, found: 333.1574.

(E)-4-((4-(hexyloxy)phenyl)diazenyl)-3-methoxyphenol (125)

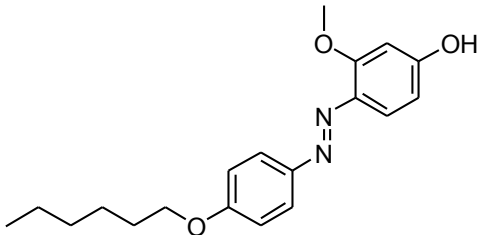

A orange-brown solid (0.787 g, 48%) was obtained using the same procedure with 4-(hexyloxy)benzenamine (0.965 g, 5 mmol) and 3-methoxyphenol (0.93 g, 7.5 mmol) as starting material. **^{1}H NMR (400 MHz, $CDCl_3$) δ(ppm)**: 7.89 (d, *J* = 11.9 Hz, 2H), 7.70 (d, *J* = 11.7 Hz, 1H), 7.00 (d, *J* = 11.9 Hz, 2H), 6.60 (d, *J* = 3.0 Hz, 1H), 6.49 (dd, *J* = 11.7, 3.2 Hz, 1H), 5.35 (s, 1H), 4.07 (d, *J* = 8.5 Hz, 2H), 4.03 (s, 3H), 1.91 – 1.78 (m, 2H), 1.54 (d, *J* = 18.7 Hz, 2H), 1.46 – 1.34 (m, 4H), 0.95 (t, *J* = 8.5 Hz, 3H). **^{13}C NMR (100 MHz, $CDCl_3$) δ(ppm)**: 161.00, 160.38, 158.25, 147.25, 136.35, 124.38, 118.33, 114.67, 108.20, 100.00, 68.36, 56.15, 31.59, 29.19, 25.70, 22.61, 14.05. Hexane : EtOAc (v:v) = 8:2, R_f = 0.16; **HRMS** (ESI-Q-TOF) m/z: calculated for $C_{19}H_{24}N_2O_3$: 351.1366 $[M + Na]^+$, found: 351.1693.

(E)-2-((4-(hexyloxy)phenyl)diazenyl)-5-methoxyphenol (126)

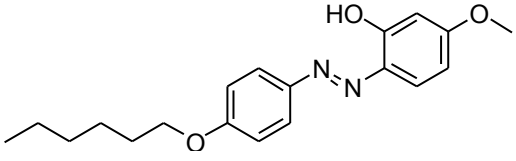

A bright-yellow solid (0.394 g, 24%) was obtained using the same procedure with 4-(hexyloxy)benzenamine (0.965 g, 5 mmol) and 3-methoxyphenol (0.62 g, 5 mmol) as starting material. **^{1}H NMR (400 MHz, $CDCl_3$) δ(ppm)**: 13.72 (s, 1H), 7.82 (d, *J* = 12 Hz, 2H), 7.77 (s, 1H), 7.02(d, *J* = 12 Hz,2H), 6.64 (dd, *J* = 11.8, 3.6 Hz, 1H), 6.51 (d, *J* = 3.5 Hz, 1H), 4.07 (t, *J* = 8.8 Hz, 2H), 3.90 (s, 3H), 1.91 – 1.80 (m, 2H), 1.51 (dd, *J* = 20.2, 9.5 Hz, 2H), 1.40 (td, *J* = 9.4, 4.8 Hz, 4H), 0.96 (t, *J* = 9.4 Hz, 3H). **^{13}C NMR (100 MHz, $CDCl_3$) δ(ppm)**: 163.77, 161.20, 156.09, 143.38, 134.26, 132.45, 123.20, 115.09, 108.30, 101.37, 68.45, 55.77, 31.57, 29.15, 25.69, 22.60, 14.05. Hexane : EtOAc (v:v) = 8:2, R_f = 0.74; **HRMS** (ESI-Q-TOF) m/z: calculated for $C_{19}H_{24}N_2O_3$: 351.1366 $[M + Na]^+$, found: 351.1690.

2, 4-bis((E)-(4-(hexyloxy)phenyl)diazenyl)-5-methoxyphenol (127)

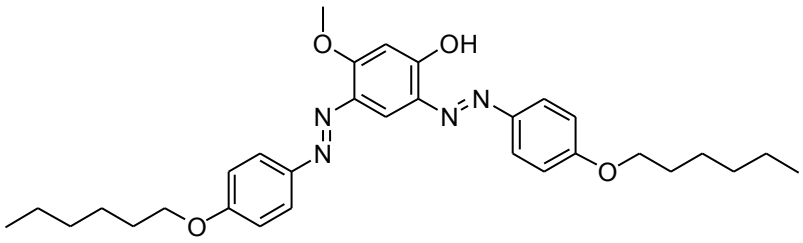

A brown solid (0.732 g, 55%) was obtained using the same procedure with 4-(hexyloxy)benzenamine (0.965 g, 5 mmol) and 3-methoxyphenol (0.31 g, 2.5 mmol) as starting material. **^{1}H NMR (400 MHz, $CDCl_3$) δ(ppm)**: 13.96 (s, 1H), 8.31 (s, 1H), 7.94 (d, *J* = 11.7 Hz, 2H), 7.85 (d, *J* = 11.8 Hz, 2H), 7.04 (d, *J* = 11.9 Hz, 4H), 6.66 (s, 1H), 4.11 (s, 3H), 4.07 (d, *J* = 8.6 Hz, 4H), 1.93 – 1.80 (m, 4H), 1.57 – 1.48 (m, 4H), 1.45 – 1.35 (m, 8H), 0.97 (t, 6H). **^{13}C NMR (100 MHz, $CDCl_3$) δ(ppm)**: 161.53, 161.36, 160.23, 157.79, 147.36, 144.11, 136.49, 131.74, 124.67, 123.63, 120.64, 115.05, 114.68, 100.57, 68.40, 56.57, 31.60, 29.18, 25.72, 22.62, 14.06. Hexane : EtOAc (v:v) = 8:2, R_f = 0.46; **HRMS** (ESI-Q-TOF) m/z: calculated for $C_{31}H_{40}N_4O_4$: 555.2942 $[M + Na]^+$, found: 555.2959.

(E)-4-((4-(2-hydroxyethoxy)phenyl)diazenyl)-3-methoxyphenol (129)

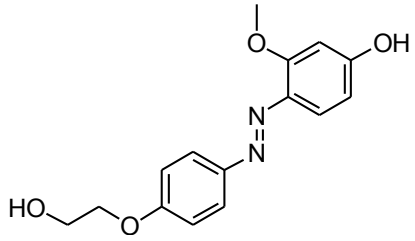

A yellow-brown solid (0.720 g, 50%) was obtained using the same procedure with 2-(4-aminophenyl)ethanol (0.765 g, 5 mmol) and 3-methoxyphenol (0.93 g, 7.5 mmol) as starting material. **^{1}H NMR (400 MHz, DMSO-d$_6$) δ(ppm)**: 10.21 (s, 1H), 7.74 (d, *J* = 8.9 Hz, 2H), 7.52 (d, *J* = 8.8 Hz, 1H), 7.08 (d, *J* = 8.1 Hz, 2H), 6.58 (s, 1H), 6.34 (d, *J* = 65.8 Hz, 1H), 6.26 (d, *J* = 65.8 Hz, 1H), 4.08 (t, 2H), 3.90 (s, 3H), 3.74 (m, 2H). **^{13}C NMR (100 MHz, CDCl$_3$) δ(ppm)**: 162.43, 160.77, 158.94, 147.22, 135.27, 124.30, 117.76, 115.33, 108.31, 104.32, 100.39, 70.33, 59.97, 56.44, 56.24. MS (EI), m/z (% relative intensity): 289.98 (M+2). DCM : EtOAc (v:v) = 7:3 R_f = 0.30; **HRMS** (ESI-Q-TOF) m/z: calculated for $C_{15}H_{16}N_2O_4$: 289.1183 $[M + H]^+$, found: 289.1198.

(E)-2-((4-(2-hydroxyethoxy)phenyl)diazenyl)-5-methoxyphenol (130)

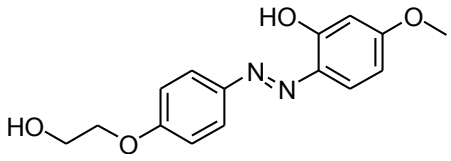

A red-brown solid (0.409 g, 22%) was obtained using the same procedure with 2-(4-aminophenyl)ethanol (0.765 g, 5 mmol) and 3-methoxyphenol (0.62 g, 5 mmol) as starting material. **^{1}H NMR (400 MHz, DMSO-d$_6$) δ(ppm)**: 12.16 (s, 1H), 7.89(d, *J* = 9.2 Hz, 2H), 7.73 (d, *J* = 8.9 Hz, 1H), 7.11 (d, *J* = 9.2 Hz, 2H), 6.63 (dd, *J* = 8.9, 2.7 Hz, 1H), 6.56 (d, *J* = 2.7 Hz, 1H), 4.92 (t, *J* = 5.5 Hz, 1H), 4.09 (t, *J* = 10 Hz, 2H), 3.83 (s, 3H), 3.75 (dd, J = 9.9, 5.5 Hz, 2H). **^{13}C NMR (100 MHz, CDCl$_3$) δ(ppm)**: 163.53, 161.23, 156.07, 145.24, 133.14, 128.74, 124.20, 115.57, 108.06, 101.98, 70.46, 59.96, 56.15. DCM : EtOAc

(v:v) = 7:3 R_f = 0.6; **HRMS** (ESI-Q-TOF) m/z: calculated for $C_{15}H_{16}N_2O_4$: 289.1183 $[M + H]^+$, found: 289.1196.

2, 4-bis((E)-(4-(2-hydroxyethoxy)phenyl)diazenyl)-5-methoxyphenol (131)

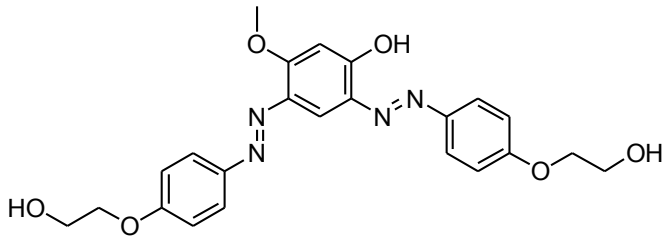

A brown solid (0.667 g, 59%) was obtained using the same procedure with 2-(4-aminophenyl)ethanol (0.765 g, 5 mmol) and 3-methoxyphenol (0.31 g, 2.5 mmol) as starting material. **^{1}H NMR (400 MHz, $CDCl_3$) δ(ppm)**: 13.92 (s, 1H), 8.32 (s, 1H), 7.96 (d, *J* = 12.0 Hz, 2H), 7.88 (d, *J* = 12.1 Hz, 2H), 7.08 (dd, *J* = 12.0, 2.0 Hz, 4H), 6.67 (s, 1H), 4.22 (m, 4H), 4.12 (s, 3H), 4.06 (dd, *J* = 12.5, 6.3 Hz, 4H). **^{13}C NMR (100 MHz, $CDCl_3$) δ(ppm)**: 161.56, 161.41, 160.89, 159.16, 147.15, 145.79, 135.75, 132.59, 124.76, 115.49, 110.64, 101.66, 70.47, 59.96, 56.92. DCM : EtOAc (v:v) = 7:3, R_f = 0.44; **HRMS** (ESI-Q-TOF) m/z: calculated for $C_{23}H_{24}N_4O_6$: 453.1769 $[M + H]^+$, found: 453.1786.

(E)-tert-butyl 4-((4-hydroxy-2-methoxyphenyl)diazenyl)benzoate (133)

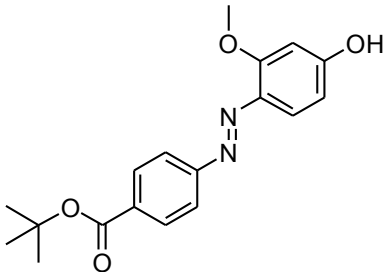

A red-orange solid (0.103 g, 63%) was obtained using the same procedure with tert-butyl 4-aminobenzoate (0.765 g, 5 mmol) and 3-methoxyphenol (0.93 g, 7.5 mmol) as starting material. **^{1}H NMR (400 MHz, DMSO-d_6) δ(ppm)**: 8.03(d, *J* = 12 Hz , 2H), 7.80 (d, *J* =

11.6 Hz, 2H), 7.61 (d, *J* = 11.9 Hz, 1H), 6.60 (d, *J* = 3.2 Hz, 1H), 6.45 (dd, *J* = 11.9, 3.2 Hz, 1H), 3.91 (s, 3H), 1.56 (s, 9H). **^{13}C NMR (100 MHz, $CDCl_3$) δ(ppm)**: 165.10, 158.58, 152.07, 151.98, 135.14, 133.33, 132.58, 130.66, 120.86, 109.50, 101.38, 81.42, 55.82, 28.22. Hexane : EtOAc (v:v) = 8:2, R_f = 0.12; **HRMS** (ESI-Q-TOF) m/z: calculated for $C_{19}H_{20}N_2O_4$: 329.1496 $[M + H]^+$, found: 329.1507.

(E)-tert-butyl 4-((2-hydroxy-4-methoxyphenyl)diazenyl)benzoate (134)

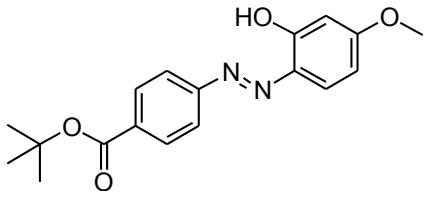

A orange solid (0.328 g, 20%) was obtained using the same procedure with tert-butyl 4-aminobenzoate (0.765 g, 5 mmol) and 3-methoxyphenol (0.62 g, 5 mmol) as starting material. **^{1}H NMR(400 MHz, $CDCl_3$) δ(ppm)**: 8.12 (d, *J* = 11.6 Hz, 2H), 7.83 (d, *J* = 11.6 Hz, 2H), 7.78 (d, *J* = 12.0 Hz, 1H), 6.64 (dd, *J* = 12.0, 3.5 Hz, 1H), 6.47 (d, *J* = 3.5 Hz, 1H), 3.91 (s, 3H), 1.65 (s, 9H). **^{13}C NMR (100 MHz, $CDCl_3$) δ(ppm)**: 165.25, 160.85, 132.64, 130.84, 130.42, 122.65, 118.50, 117.98, 113.11, 105.58, 102.60, 81.35, 54.49, 28.22. Hexane : EtOAc (v:v) = 8:2, R_f = 0.64; **HRMS** (ESI-Q-TOF) m/z: calculated for $C_{19}H_{20}N_2O_4$: 329.1496 $[M + H]^+$, found: 329.1512.

2, 4-bis((E)-(4-tert-butyl)diazenyl)-5-methoxyphenol (135)

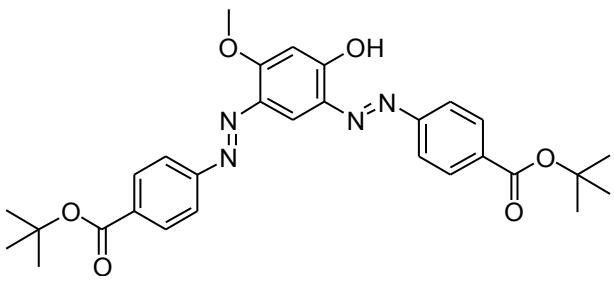

A dark-brown solid (1.29 g, 66%) was obtained using the same procedure with tert-butyl 4-aminobenzoate (1.4 g, 7.25 mmol) and 3-methoxyphenol (0.45 g, 3.62 mmol)as starting material. **^{1}H NMR (400 MHz, CDCl$_3$) δ(ppm)**: 8.38 (s, 1H), 8.15 (d, *J* = 10.9 Hz, 4H), 7.95 (d, *J* = 11.6 Hz, 2H), 7.89 (d, *J* = 11.6 Hz, 2H), 6.67 (s, 1H), 4.14 (s, 3H), 1.65 (s, 18H). **^{13}C NMR (100 MHz, CDCl$_3$) δ(ppm)**: 28.22, 56.82, 81.42, 81.63, 100.86, 121.43, 122.02, 122.52, 130.45, 130.72, 132.13, 133.42, 133.53, 136.85, 152.06, 155.10, 160.36, 162.43, 164.94, 165.23. Hexane : EtOAc (v:v) = 8:2, R_f = 0.40; **HRMS** (ESI-Q-TOF) m/z: calculated for $C_{29}H_{32}N_4O_5$: 555.2218 $[M + Na]^+$, found: 555.2229.

(E)-fluoro-4-((4-hydroxy-2-methoxyphenyl)diazenyl)benzoate (145)

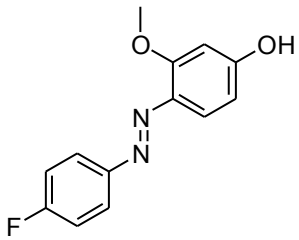

A red-orange solid (0.77 g, 63%) was obtained using the same procedure with 4-fluoroalinine (0.833 g, 7.5 mmol) and 3-methoxyphenol (0.62 g, 5 mmol) as starting material. **^{1}H NMR (400 MHz, DMSO-d$_6$) δ(ppm)**: 10.37 (s, 1H), 7.81 (dd, *J* = 9.0, 5.4 Hz, 1H), 7.56 (d, *J* = 8.9 Hz, 1H), 7.35 (t, *J* = 8.8 Hz, 1H), 6.60 (d, *J* = 2.3 Hz, 2H), 6.45 (dd, *J* = 8.9, 2.4 Hz, 2H), 3.91 (s, 3H). **^{13}C NMR (100 MHz, CDCl$_3$) δ(ppm)**: 164.19, 162.92, 161.72, 159.15, 149.48, 134.79, 124.26, 117.57, 116.29, 116.06, 108.18, 100.00, 55.87. **^{19}F NMR (400 MHz, CDCl$_3$) δ(ppm):** -111.53. Hexane : EtOAc (v:v) = 8:2, R_f = 0.24; **HRMS** (ESI-Q-TOF) m/z: calculated for $C_{13}H_{11}FN_2O_2$: 269.0697 $[M + Na]^+$, found: 269.0695.

(E)-fluoro- 4-((2-hydroxy-4-methoxyphenyl)diazenyl)benzoate (146)

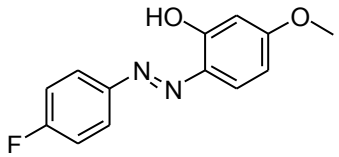

A orange-brown solid (0.17 g, 14%) was obtained using the same procedure with 4-fluoroalinine (0.555 g, 5 mmol) and 3-methoxyphenol (0.62 g, 5 mmol) as starting material. **^{1}H NMR(400 MHz, CDCl$_3$) δ(ppm)**:13.52 (s, 1H), 7.82 (dd, *J* = 9.1, 5.1 Hz, 2H), 7.77 (d, *J* = 8.9 Hz, 1H), 7.18 (dd, *J* = 9.1, 8.2 Hz, 2H), 6.62 (dd, *J* = 8.9, 2.7 Hz, 1H), 6.48 (d, *J* = 2.6 Hz, 1H), 3.87 (s, 3H). **^{13}C NMR (100 MHz, CDCl$_3$) δ(ppm)**: 165.11, 164.05, 162.62, 156.11, 146.97, 134.80, 132.91, 123.69, 116.54, 116.31, 108.41, 101.49, 55.85. **^{19}F NMR (400 MHz, CDCl$_3$) δ(ppm):** -110.11. Hexane : EtOAc (v:v) = 8:2, R_f = 0.73; **HRMS** (ESI-Q-TOF) m/z: calculated for $C_{13}H_{11}FN_2O_2$: 269.0697 $[M + Na]^+$, found: 269.0697.

2, 4-bis((E)-(4-fluoro)diazenyl)-5-methoxyphenol (147)

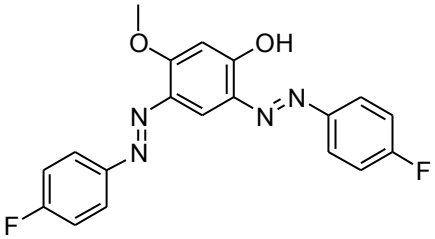

A light-brown solid (0.58 g, 64%) was obtained using the same procedure with 4-fluoroaniline (0.555 g, 5 mmol) and 3-methoxyphenol (0.31 g, 2.5 mmol) as starting material. **^{1}H NMR (400 MHz, CDCl$_3$) δ(ppm)**: 13.71 (s, 1H), 8.31 (s, 1H), 7.93 (dd, *J* = 9.0, 5.3 Hz, 2H), 7.87 (dd, *J* = 9.1, 5.1 Hz, 2H), 7.24 – 7.16 (m, 4H), 6.65 (s, 1H), 4.09 (s, 1H). **^{13}C NMR (100 MHz, CDCl$_3$) δ(ppm)**: 165.55, 163.05, 161.35, 158.55, 149.78, 146.84, 136.56, 131.81, 124.89, 123.94, 121.47, 116.72, 116.49, 116.29, 116.06, 100.83,

56.81. Hexane : EtOAc (v:v) = 8:2, **^{19}F NMR (400 MHz, $CDCl_3$) δ(ppm):** -108.97, -109.94. R_f = 0.58; **HRMS** (ESI-Q-TOF) m/z: calculated for $C_{19}H_{14}F_2N_4O_2$: 391.0977 $[M + Na]^+$, found: 391.0973.

(E)-4-((2,4-difluorophenyl)diazenyl)-3-methoxyphenol (149)

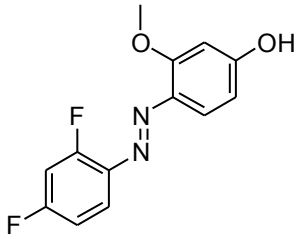

A red-brown solid (0.792 g, 60%) was obtained using the same procedure with 2,4-difluorineaniline (0.65 g, 5 mmol) and 3-methoxyphenol (0.93 g, 7.5 mmol) as starting material. **^{1}H NMR (400 MHz, DMSO-d_6) δ(ppm)**: 7.67 (m, 1H), 7.56 (d, *J* = 11.9 Hz, 1H), 7.54 – 7.44 (m, 1H), 7.24 – 7.15 (m, 1H), 6.61 (d, *J* = 3.0 Hz, 1H), 6.47 (dd, *J* = 11.9, 3.1 Hz, 1H), 3.90 (s, 3H). **^{13}C NMR (100 MHz, $CDCl_3$) δ(ppm)**:164.02, 159.96, 135.60, 119.50, 118.17, 112.82, 112.52, 108.77, 106.03, 105.70, 105.36, 100.40, 56.33. **^{19}F NMR (400 MHz, $CDCl_3$) δ(ppm):** -107.80, -121.52. Hexane : EtOAc (v:v) = 8:2, R_f = 0.15; **HRMS** (ESI-Q-TOF) m/z: calculated for $C_{13}H_{10}F_2N_2O_2$: 265.0783 $[M + H]^+$, found: 265.0794.

(E)-2-((2,4-difluorophenyl)diazenyl)-5-methoxyphenol (150)

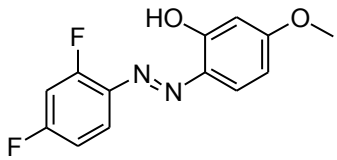

A orange-brown solid (0.158 g, 12%) was obtained using the same procedure with 2,4-difluorineaniline (0.65 g, 5 mmol) and 3-methoxyphenol (0.62 g, 5 mmol) as starting material. **^{1}H NMR (400 MHz, $CDCl_3$) δ(ppm)**: 7.97 – 7.87 (m, 1H), 7.81 (d, *J* = 11.9 Hz,

1H), 7.07 – 6.96 (m, 2H), 6.65 (dd, *J* = 11.9, 3.5 Hz, 1H), 6.51 (d, *J* = 3.5 Hz, 1H), 3.91 (s, 3H). **^{13}C NMR (100 MHz, $CDCl_3$) δ(ppm)**: 164.43, 156.23, 134.88 , 133.48, 118.40, 112.18, 108.66, 105.27, 104.95, 104.62, 101.35, 55.78, 30.94. **^{19}F NMR (400 MHz, $CDCl_3$) δ(ppm):** -106.61, -121.08. Hexane : EtOAc (v:v) = 8:2, R_f = 0.70; **HRMS** (ESI-Q-TOF) m/z: calculated for $C_{13}H_{10}F_2N_2O_2$: 265.0783 $[M + H]^+$, found: 265.0792.

2, 4-bis((E)-(2,4-difluorophenyl)diazenyl)-5-methoxyphenol (151)

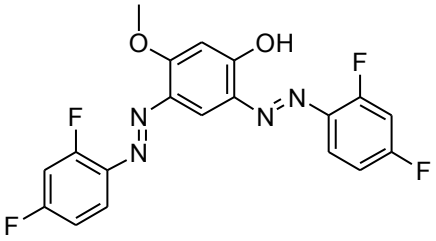

A red-brown solid (0.515 g, 51%) was obtained using the same procedure with 2,4-difluorineaniline (0.65 g, 5 mmol) and 3-methoxyphenol (0.31 g, 2.5 mmol) as starting material. **^{1}H NMR (400 MHz, DMSO-d_6) δ(ppm)**: 8.11 (m, 1H), 7.97 (s, 1H), 7.72 (dd, *J* = 20.2, 11.5 Hz, 1H), 7.57 (m. 2H), 7.26 (m, 2H), 6.92 (s, 1H), 4.06 (s, 3H). **^{13}C NMR (100 MHz, DMF-d_7) δ(ppm)**: 162.81, 161.15, 136.47, 133.31, 119.60, 112.98, 112.72, 112.42, 105.89, 105.65, 105.25, 101.71, 56.84. **^{19}F NMR (400 MHz, $CDCl_3$) δ(ppm):** -106.01, -106.41, -120.74. Hexane : EtOAc (v:v) = 8:2, R_f = 0.48; **HRMS** (ESI-Q-TOF) m/z: calculated for $C_{19}H_{12}F_4N_4O_2$: 405.0969 $[M + H]^+$, found: 405.0983.

2, 4, 6-Tris-tert-butyl-phenylazo-benzene-1, 3, 5-triol (152)

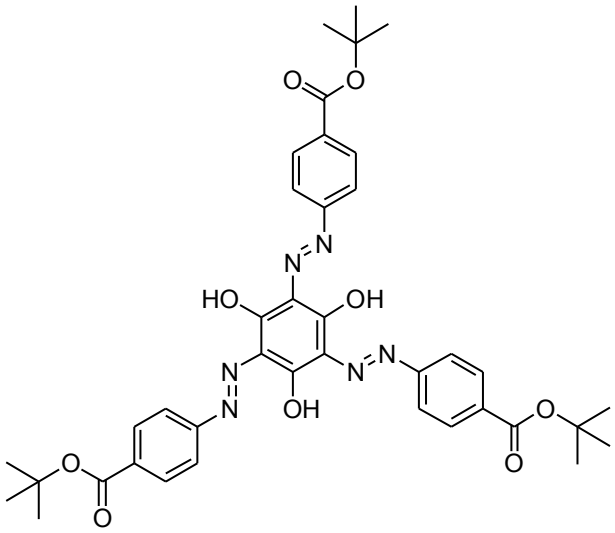

A red solid (0.251 g, 68%) was obtained using the same procedure with tert-butyl 4-aminobenzoate (0.289 g, 1.5 mmol) and 1, 3, 5-Trihydroxybenzene (0.063 g, 0.5 mmol) as starting material. **^{1}H NMR (400 MHz, $CDCl_3$) δ(ppm)**: 8.00 (d, J = 8.7 Hz, 6H), 7.57 (d, J = 8.7 Hz, 6H), 1.58 (s, 27H). **^{13}C NMR (100 MHz, $CDCl_3$) δ(ppm)**: 178.66, 164.87, 144.18, 131.42, 130.88, 129.63, 117.20, 81.65, 28.32. Hexane : EtOAc (v:v) = 8:2, R_f = 0.86; **HRMS** (ESI-Q-TOF) m/z: calculated for $C_{39}H_{42}N_6O_9$: 739.3018 $[M + H]^+$, found: 739.3032.

Chapter 2

Dibenzoxadiazepine (153)

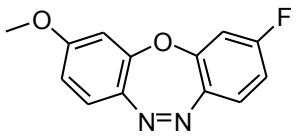

A red-orange solid (0.10 g) was dissolved into the DMSO, the product, dibenzoxadiazepines (**153**), were obtained in 99% yield. **^{1}H NMR (400 MHz, CDCl3)**

δ(ppm): 7.72 (dd, *J* = 8.4, 5.8 Hz, 1H), 7.69 (d, *J* = 8.8 Hz, 1H), 6.96 (td, *J* = 8.2, 2.6 Hz, 1H), 6.79 (dd, *J* = 8.8, 2.6 Hz, 1H), 6.70 (dd, *J* = 8.8, 2.6 Hz, 1H), 6.47 (d, *J* = 2.6 Hz, 1H), 3.80 (s, 3H). **^{19}F NMR (400 MHz, $CDCl_3$) δ(ppm)**: -106.58. Hexane : EtOAc (v:v) = 8:2, R_f = 0.54; **HRMS** (ESI-Q-TOF) m/z: calculated for $C_{13}H_9FN_2O_2$: 245.1877 $[M + H]^+$, found: 245.0895.

2-(2-Fluoro-phenylazo)-5-methoxy-phenol (163)

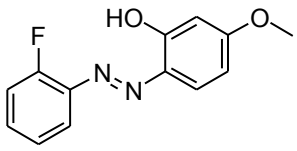

A red-orange solid (0.10 g, 8%) was obtained using the same procedure with 2-fluorineaniline (0.555 g, 5 mmol) and 3-methoxyphenol (0.62 g, 5 mmol) as starting material. **^{1}H NMR (400 MHz, $CDCl_3$) δ(ppm):** 13.82 (s, 1H), 7.87 (td, *J* = 7.7, 1.7 Hz, 1H), 7.78 (d, *J* = 8.9 Hz, 1H), 7.39 (m, 1H), 7.23 (t, *J* = 7.6 Hz, 2H), 6.62 (dd, *J* = 8.9, 2.7 Hz, 1H), 6.48 (d, *J* = 2.6 Hz, 1H), 3.88 (s, 3H). **^{13}C NMR (100 MHz, $CDCl_3$) δ(ppm):** 164.95, 157.65, 157.18, 157.01, 141.95, 137.43, 131.82, 126.48, 122.65, 116.83, 109.54, 101.56, 57.02. **^{19}F NMR (400 MHz, $CDCl_3$) δ(ppm):** -125.51. Hexane : EtOAc (v:v) = 8:2, R_f = 0.64; **HRMS** (ESI-Q-TOF) m/z: calculated for $C_{13}H_{11}FN_2O_2$: 247.0877 $[M + H]^+$, found: 247.0885.

Dibenzoxadiazepine (164)

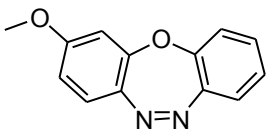

A red-orange solid (0.10 g) was dissolved into the DMSO, the product, dibenzoxadiazepines (**164**) were obtained in 98% yield. **^{1}H NMR (400 MHz, $CDCl_3$)**

δ(ppm): 7.76 (d, *J* = 2.6 Hz, 1H), 7.59 – 7.49 (m, 1H), 7.44 (td, *J* = 3.9, 1.3 Hz, 2H), 7.21 (dd, *J* = 8.1, 1.2 Hz, 1H), 6.99 (dd, *J* = 8.8, 2.7 Hz, 1H), 6.81 (d, *J* = 2.6 Hz, 1H), 3.84 (s, 3H). **HRMS** (ESI-Q-TOF) m/z: calculated for $C_{13}H_{10}N_2O_2$: 227.2877 $[M + H]^+$, found: 227.1895.

2-(2- Bromo-phenylazo)-5-methoxy-phenol (165)

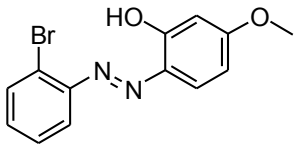

A red-orange solid (0.10 g, 6%) was obtained using the same procedure with 2-bromoaniline (0.86 g, 5 mmol) and 3-methoxyphenol (0.62 g, 5 mmol) as starting material. **^{1}H NMR (400 MHz, $CDCl_3$) δ(ppm):** 13.87 (s, 1H), 7.89 (dd, *J* = 8.1, 1.6 Hz, 1H), 7.79 (d, *J* = 8.9 Hz, 1H), 7.73 (dd, *J* = 8.0, 1.3 Hz, 1H), 7.44 – 7.38 (m, 1H), 7.27 (ddd, *J* = 8.0, 7.3, 1.6 Hz, 1H), 6.63 (dd, *J* = 8.9, 2.7 Hz, 1H), 6.49 (d, *J* = 2.6 Hz, 1H), 3.89 (s, 3H). **^{13}C NMR (100 MHz, $CDCl_3$) δ(ppm):** 165.18, 157.45, 147.62, 135.62, 133.97, 133.93, 131.37, 128.67, 123.48, 118.07, 109.46, 101.87, 56.24. Hexane : EtOAc (v:v) = 8:2, R_f = 0.81; **HRMS** (APCI-Q-TOF) m/z: calculated for $C_{13}H_{11}BrN_2O_2$: 305.9998 $[M]^+$, found:. 306.0004.

2-(2-Chloro-phenylazo)-5-methoxy-phenol (166)

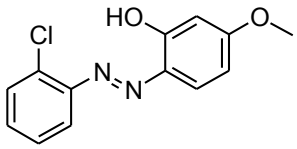

A red-orange solid (0.12 g, 9%) was obtained using the same procedure with 2-bromoaniline (0.635 g, 5 mmol) and 3-methoxyphenol (0.62 g, 5 mmol) as starting material. **^{1}H NMR (400 MHz, $CDCl_3$) δ(ppm):** 14.06 (s, 1H), 7.91 (dd, *J* = 7.3, 2.5 Hz,

1H), 7.78 (d, *J* = 9.0 Hz, 1H), 7.54 (dd, *J* = 7.0, 2.3 Hz, 1H), 7.43 – 7.31 (m, 2H), 6.63 (dd, *J* = 9.0, 2.7 Hz, 1H), 6.48 (d, *J* = 2.6 Hz, 1H), 3.89 (s, 3H). **^{13}C NMR (100 MHz, $CDCl_3$) δ(ppm):** 164.91, 157.76, 146.00, 135.18, 133.85, 132.52, 130.70, 130.51, 127.70, 117.38, 109.25, 101.56, 55.92. Hexane : EtOAc (v:v) = 8:2, R_f = 0.72; **HRMS** (ESI-Q-TOF) m/z: calculated for $C_{13}H_{11}ClN_2O_2$: 285.0401 $[M+Na]^+$, found:. 285.0400.

Dibenzoxadiazepine (167)

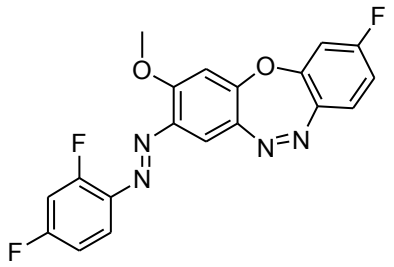

A red-orange solid (0.10 g) was dissolved into the DMSO, the product, dibenzoxadiazepines (**167**), were obtained in 98% yield. **^{1}H NMR (400 MHz, $CDCl_3$) δ(ppm):** 7.92 (s, 1H), 7.96 – 7.84 (m, 1H), 7.80 – 7.69 (m, 1H), 7.40 – 7.30 (m, 2H), 7.24 (dd, *J* = 9.0, 2.7 Hz, 1H), 7.12 (dd, *J* = 9.1, 2.7 Hz, 1H), 7.02 (dd, *J* = 8.0, 2.3 Hz, 1H), 4.06 (s, 3H). **^{19}F NMR (400 MHz, $CDCl_3$) δ(ppm)**: -118.55, -109.22, -104.52. HRMS (ESI-Q-TOF) m/z: calculated for C19H11F3N4O2: 385.1077 $[M + H]^+$, found: 385.0895.

2,4-Bis-(2-Fluoro-phenylazo)-5-methoxy-phenol (168)

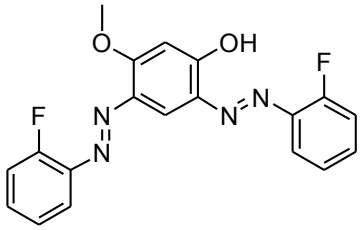

A brown solid (0.25 g, 27%) was obtained using the same procedure with 2-fluorineaniline (0.555 g, 5 mmol) and 3-methoxyphenol (0.62 g, 5 mmol) as starting material. **^{1}H NMR**

(400 MHz, $CDCl_3$) δ(ppm): 13.97 (s, 1H), 8.39 (s, 1H), 7.91 (td, *J* = 7.8, 1.4 Hz, 1H), 7.76 (td, *J* = 7.8, 1.7 Hz, 1H), 7.51 – 7.39 (m, 2H), 7.35 – 7.15 (m, 4H), 6.66 (s, 1H), 4.11 (s, 3H). **^{13}C NMR (100 MHz, $CDCl_3$) δ(ppm):** 162.00, 159.55, 137.14, 132.66, 132.34, 132.12, 124.94, 124.51, 122.09, 118.43, 117.44, 117.14, 116.94, 100.98, 56.88. **^{19}F NMR (400 MHz, $CDCl_3$) δ(ppm):** -124.78, -124.99. **HRMS** (ESI-Q-TOF) m/z: calculated for $C_{19}H_{14}F_2N_4O_2$: 369.1158 $[M + H]^+$, found: 369.1161.

Dibenzoxadiazepine (169)

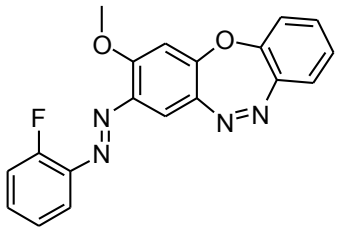

A red-orange solid (0.10 g) was dissolved into the DMSO, the product, dibenzoxadiazepines (**158**) were obtained in 98% yield. **^{1}H NMR (400 MHz, $CDCl_3$) δ(ppm):** 7.95 (s, 1H), 7.91 – 7.80 (m, 1H), 7.65 – 7.54 (m, 1H), 7.55 – 7.35 (m, 4H), 7.36 – 7.21 (m, 2H), 6.64 (s, 1H), 3.98 (s, 3H). **^{19}F NMR (400 MHz, $CDCl_3$) δ(ppm)**: -125.71. **HRMS** (ESI-Q-TOF) m/z: calculated for $C_{19}H_{13}FN_4O_2$: 349.1077 $[M + H]^+$, found: 349.0895.

4,6-Bis-(2,4-difluoro-phenylazo)-benzene-1,3-diol (170)

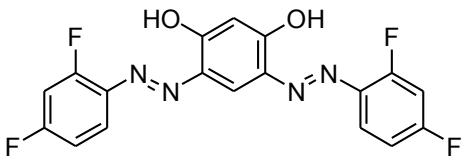

A brown-yellow solid (0.439 g, 45%) was obtained using the same procedure with 2,4-difluorineaniline (0.65 g, 5 mmol) and Resorcinol (0.275 g, 2.5 mmol) as starting material. **^{1}H NMR (400 MHz, $CDCl_3$) δ(ppm):** 13.59 (s, 2H), 8.53 (s, 1H), 8.07 – 7.86 (m,

2H), 7.06 (m, 4H), 6.59 (s, 1H). **^{13}C NMR (100 MHz, $CDCl_3$) δ(ppm):** 159.15, 139.80, 133.19, 118.61, 118.53, 112.60, 112.40, 105.49, 105.25, 105.00. **^{19}F NMR (400 MHz, $CDCl_3$) δ(ppm):** -104.40, -119.97. Hexane : EtOAc (v:v) = 8:2, R_f = 0.75; **HRMS** (APCI-Q-TOF) m/z: calculated for $C_{18}H_{10}F_4N_4O_2$: 390.0734 $[M]^+$, found: 390.0742.

Dibenzoxadiazepine (171)

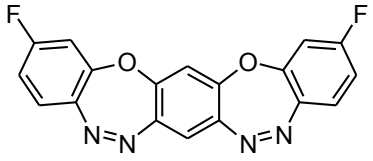

A red-orange solid (**170**, 0.10 g) was dissolved into the DMSO, the product, dibenzoxadiazepines (**171**) were obtained in 98% yield. **^{1}H NMR (400 MHz, $CDCl_3$) δ(ppm):** 8.06 (s, 1H), 8.10 – 7.98 (m, 1H), 7.61 – 7.50 (m, 2H), 7.33 – 7.18 (m, 2H), 6.76 (dd, *J* = 7.8, 1.6 Hz, 1H), 6.68 (s, 1H). **^{19}F NMR (400 MHz, $CDCl_3$) δ(ppm)**: -127.24, -130.85. **HRMS** (ESI-Q-TOF) m/z: calculated for $C_{18}H_8F_2N_4O_2$: 350.1077 $[M + H]^+$, found: 350.0542.

2,4-Bis-(2-Bromo-phenylazo)-5-methoxy-phenol (172)

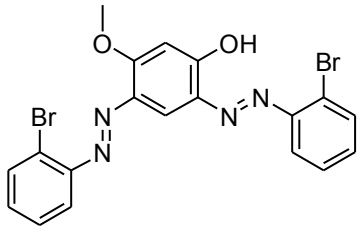

A brown solid (0.21 g, 17%) was obtained using the same procedure with 2-bromoaniline (0.86 g, 5 mmol) and 3-methoxyphenol (0.62 g, 5 mmol) as starting material. **^{1}H NMR (400 MHz, $CDCl_3$) δ(ppm):** 14.01 (s, 1H), 8.41 (s, 1H), 7.97 (dd, *J* = 8.1, 1.6 Hz, 1H), 7.75 (ddd, *J* = 8.0, 3.3, 1.3 Hz, 2H), 7.67 (dd, *J* = 8.0, 1.6 Hz, 1H), 7.48 – 7.36 (m, 2H),

7.36 – 7.28 (m, 2H), 6.67 (s, 1H), 4.11 (s, 3H). **^{13}C NMR (100 MHz, $CDCl_3$) δ(ppm):** 162.26, 159.42, 150.43, 147.25, 136.99, 133.77, 133.71, 132.49, 131.97, 131.58, 128.51, 128.20, 125.28, 123.93, 122.65, 118.44, 118.05 , 100.99 , 56.90. Hexane : EtOAc (v:v) = 8:2, Rf=0.65; **HRMS** (APCI-Q-TOF) m/z: calculated for $C_{19}H_{14}Br_2N_4O2$: 489.9459 $[M]^+$, found: 489.9467.

2,4-Bis-(2-chloro-phenylazo)-5-methoxy-phenol (173)

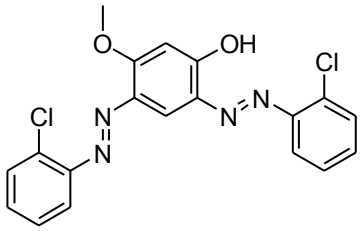

A red-orange solid (0.36 g, 18%) was obtained using the same procedure with 2-bromoaniline (0.635 g, 5 mmol) and 3-methoxyphenol (0.62 g, 5 mmol) as starting material. **^{1}H NMR (400 MHz, $CDCl_3$) δ(ppm):** 14.17 (s, 1H), 8.40 (s, 1H), 7.98 (dd, *J* = 6.3, 3.5 Hz, 1H), 7.72 – 7.66 (m, 1H), 7.60 – 7.52 (m, 2H), 7.43 – 7.31 (m, 4H), 6.67 (s, 1H), 4.11 (s, 4H). **^{13}C NMR (100 MHz, $CDCl_3$) δ(ppm):** 162.27, 159.83, 149.48, 146.01, 137.17, 134.91, 133.34, 132.68, 131.68, 131.36, 130.72, 130.62, 127.88, 127.51, 122.44, 118.24, 117.66, 101.01, 56.89. Hexane : EtOAc (v:v) = 8:2, R_f = 0.51; **HRMS** (ESI-Q-TOF) m/z: calculated for $C_{19}H_{14}Cl_2N_4O_2$: 423.0386 $[M+Na]^+$, found:. 423.0386.

4-(2-Fluoro-phenylazo)-3-methoxy-phenol (175)

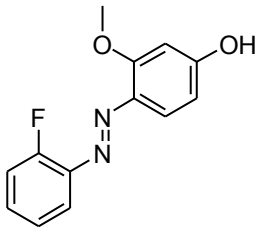

A red-orange solid (0.65 g, 53%) was obtained using the same procedure with 2-fluorineaniline (0.555 g, 5 mmol) and 3-methoxyphenol (0.62 g, 5 mmol) as starting material. **^{1}H NMR (400 MHz, $CDCl_3$) δ(ppm):** 10.46 (s, 1H), 7.58 (td, *J* = 8.0, 1.7 Hz, 1H), 7.56 (d, *J* = 8.9 Hz, 1H), 7.50 (dd, *J* = 12.9, 6.0 Hz, 1H), 7.45 – 7.39 (m, 1H), 7.32 – 7.25 (m, 1H), 6.60 (d, *J* = 2.2 Hz, 1H), 6.46 (dd, *J* = 8.9, 2.3 Hz, 1H), 3.91 (s, 3H). **^{13}C NMR (100 MHz, $CDCl_3$) δ(ppm):** 163.53, 159.97, 159.53, 157.45, 140.56, 135.29, 131.59, 124.84, 117.69, 116.97, 108.28 , 99.93, 55.86. **^{19}F NMR (400 MHz, $CDCl_3$) δ(ppm):** -125.96. Hexane : EtOAc (v:v) = 8:2, R_f = 0.10; **HRMS** (ESI-Q-TOF) m/z: calculated for $C_{13}H_{11}FN_2O_2$: 247.0877 $[M + H]^+$, found: 247.0833.

4-(2- Bromo-phenylazo)-3-methoxy-phenol (176)

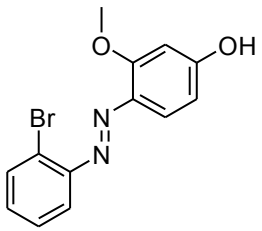

A red-orange solid (0.58 g, 40%) was obtained using the same procedure with 2-bromoaniline (0.86 g, 5 mmol) and 3-methoxyphenol (0.62 g, 5 mmol) as starting material. **1H NMR (400 MHz, CDCl3) δ(ppm):** 10.52 (s, 1H), 7.80 (dd, *J* = 8.0, 1.1 Hz, 1H), 7.60 (d, *J* = 8.9 Hz, 1H), 7.49 (dtd, *J* = 9.3, 8.0, 1.6 Hz, 2H), 7.42 – 7.32 (m, 1H), 6.61 (d, *J* = 2.3 Hz, 1H), 6.49 (dd, *J* = 8.9, 2.4 Hz, 1H), 3.92 (s, 3H). **13C NMR (100 MHz, CDCl3) δ(ppm):** 163.68, 159.64, 149.54, 135.15, 133.47, 131.27, 128.54, 123.57, 117.99, 117.94, 108.37, 99.94, 55.87. Hexane : EtOAc (v:v) = 8:2, R_f = 0.23; **HRMS** (ESI-Q-TOF) m/z: calculated for $C_{13}H_{11}BrN_2O_2$: 307.0077 $[M+H]^+$, found:. 307.0076.

4-(2-Chloro-phenylazo)-3-methoxy-phenol (177)

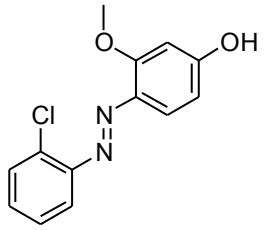

A red-orange solid (0.64 g, 49%) was obtained using the same procedure with 2-bromoaniline (0.635 g, 5 mmol) and 3-methoxyphenol (0.62 g, 5 mmol) as starting material. **^{1}H NMR (400 MHz, $CDCl_3$) δ(ppm):** 10.51 (s, 1H), 7.66 – 7.62 (m, 1H), 7.59 (d, *J* = 8.9 Hz, 1H), 7.56 – 7.52 (m, 1H), 7.49 – 7.40 (m, 2H), 6.61 (d, *J* = 2.4 Hz, 1H), 6.48 (dd, *J* = 8.9, 2.4 Hz, 1H), 3.92 (s, 3H). **^{13}C NMR (100 MHz, $CDCl_3$) δ(ppm):** 163.69, 159.67, 148.62, 135.32, 132.80, 131.04, 130.49, 127.95, 117.96, 117.78, 108.38, 99.95, 55.89. Hexane : EtOAc (v:v) = 8:2, R_f = 0.11; **HRMS** (ESI-Q-TOF) m/z: calculated for $C_{13}H_{11}ClN_2O_2$: 263.0582$[M + H]^+$, found: 263.0583.

4-(2,4-Difluoro-phenylazo)-benzene-1,3-diol(178)

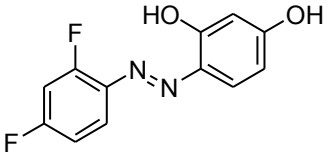

A brown-orange solid (0.25 g, 40%) was obtained using the same procedure with 2,4-difluorineaniline (0.65 g, 5 mmol) and Resorcinol (0.275 g, 2.5 mmol) as starting material. **^{1}H NMR (400 MHz, $CDCl_3$) δ(ppm):** 13.33 (s, 1H), 7.93 – 7.84 (m, 1H), 7.78 (d, *J* = 8.7 Hz, 1H), 7.04 – 6.94 (m, 2H), 6.56 (dd, *J* = 8.7, 2.6 Hz, 1H), 6.44 (d, *J* = 2.6 Hz, 1H). **^{13}C NMR (100 MHz, $CDCl_3$) δ(ppm)**: 160.77, 156.06, 135.64 , 133.88, 118.54, 112.44, 112.21, 108.98, 105.37, 105.13, 104.88, 103.96. **^{19}F NMR (400 MHz, $CDCl_3$) δ(ppm):** -105.98 (d, *J* = 7.9 Hz, 1F), -120.69 (d, *J* = 7.9 Hz, 1F). Hexane : EtOAc (v:v) =

8:2, R_f = 0.45; **HRMS** (APCI-Q-TOF) m/z: calculated for $C_{12}H_8F_2N_2O_2$: 250.0548 $[M]^+$, found: 250.0556.

Chapter 3

2-Methyl-acrylic acid 2-bromo-ethyl ester (182)

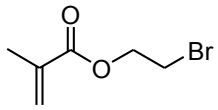

To a round-bottomed flask containing HEMA (20 mmol, 2.43 ml) in dry diethyl ether (20 mL) under an atmosphere of nitrogen, was added phosphorus tribromide (2.09 ml, 22 mmol) at -10 ºC. The mixture was stirred for 3 h at -10 ºC, and then removed to room temperature still react for 2 hours. When the reaction finished, the reaction mixture was quenched by addition of ice-water (5 mL). The organic layer was extracted with hexane (3X10 mL). The combined organic layer was washed by brine and was dried over anhydrous MgSO4, filtered and the filtrate was evaporated. Chromatography of the residue on silica gel with hexane: ethyl acetate 9:1 gave 3.536 g (the yield is 80%) as a colourless oil. 2-bromoethyl methacrylate **182** (3.127 g, 81%) was obtained. **^{1}H NMR (400 MHz, $CDCl_3$) δ(ppm)**: 6.21 (s, 1H), 5.66 (s, 1H), 4.50 (t, *J* = 8.2 Hz, 2H), 3.60 (t, *J* = 8.2 Hz, 2H), 2.01 (s, 3H). Hexane : EtOAc (v:v) =6:4, R_f = 0.79; **HRMS** (ESI-Q-TOF), m/z calculated for $C_6H_9BrO_2$: 216.1108 $[M+ Na]^+$, found: 216.1121.

2-Methyl-acrylic acid 2-azido-ethyl ester (183)

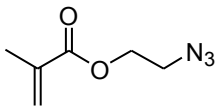

Sodium azide (1.474 g, 22 mmol) was added to 15 ml of DMSO, and the mixture was stirred at ambient temperature overnight. To the heterogeneous mixture was then added 2-bromoethyl methacrylate ((1.93 g, 10 mmol)) along with 2 ml of DMSO. After being stirred for 12 h at ambient temperature, the mixture was partitioned between H_2O (50ml) and ether (50 ml). After the layers were separated, the aqueous layer was extracted with ether (2×50 ml), and the combined organic layers were washed with water (2×100 ml) and brine (100 ml) and then dried over $MgSO_4$ and concentrated in vacuo, affording 2-azidoethyl methacrylate as **183** a yellow oil (1.457 g, 94%). **^{1}H NMR (400 MHz, $CDCl_3$) δ(ppm)**: 5.98 (s, 1H), 5.46 (s, 1H), 4.19 (t, 2H), 3.38 (t, 2H), 1.88 (s, 3H). Hexane : EtOAc (v:v) = 9:1, R_f = 0.57; **HRMS** (ESI-Q-TOF), m/z calculated for $C_6H_9N_3O_2$: 178.2576 $[M+Na]^+$, found: 178.2588.

Compound 184

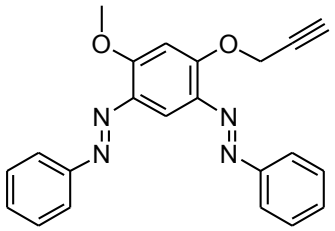

A solution of compound **101** (0.332 g, 1 mmol), propargyl choride (0.2 ml, 2 mmol) (80% in Toluene)and potassium carbonate (0.345 g, 2.5 mmol) in DMF (10 ml) was stirred 16 h at 50 ºC. The reaction was cooled to RT and poured into HCl 1N (50 ml) and extracted with EtOAc. The organic phase was washed with HCl 1 N, then brine, dried over MgSO4 and the volatiles removed under reduced pressure. Flash chromatography on silica gel (benzene: hexanes 48:2) afforded the product **184** as colorless oil (0.33 g, 89 % yield). **^{1}H NMR(400 MHz, $CDCl_3$) δ(ppm)**: 8.20 (s, 1H), 7.97 (d, *J* = 2.1 Hz, 2H), 7.94 (d, *J* = 1.5 Hz, 2H), 7.62-7.41 (m, 6H), 7.02 (s, 1H), 5.12 (d, *J* = 3.2 Hz, 2H), 4.16 (s, 3H), 2.69 (t, *J* = 3.2 Hz,

1H). **^{13}C NMR (100 MHz, $CDCl_3$) δ(ppm)**: 160.51, 158.99, 153.19, 137.27, 136.88, 130.74, 129.14, 123.02, 105.37, 100.12, 78.14, 76.9, 58.39, 56.84. Hexane : EtOAc (v:v) = 9:1, R_f = 0.30; **HRMS** (ESI-Q-TOF), m/z calculated for $C_{23}H_{22}N_4O_2$: 393.1322 $[M + Na]^+$, found: 393.1330.

Compound 185

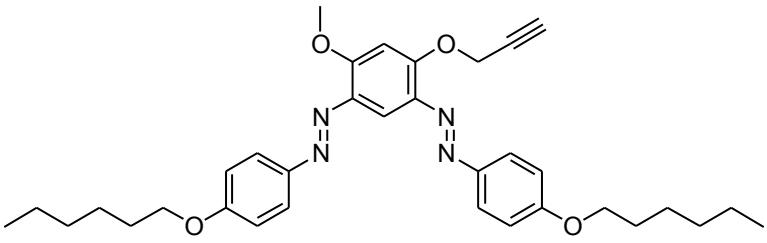

A red-orange solid **185** (0.242 g, 85%) was obtained using the same procedure with compound **127** (0.266 g, 0.5 mmol) as starting material. **^{1}H NMR (400 MHz, $CDCl_3$) δ(ppm)**: 8.14 (s, 1H), 7.96 (d, *J* = 2.5 Hz, 2H), 7.93 (d, *J* = 2.5 Hz, 2H), 7.02 (d, *J* = 12.0 Hz, 4H), 6.98 (s, 1H), 5.09 (d, *J* = 3.2 Hz, 2H), 4.15 (s, 3H), 4.07 (t, *J* = 8.7 Hz, 4H), 2.66 (t, *J* = 3.2 Hz, 1H), 1.92 – 1.80 (m, 4H), 1.59 – 1.47 (m, 4H), 1.45 – 1.37 (m, 8H), 0.96 (t, *J* = 9.3 Hz, 6H). **^{13}C NMR (100 MHz, $CDCl_3$) δ(ppm)**: 161.60, 159.53, 158.06, 147.52, 137.56, 137.16, 124.90, 114.76, 105.30, 100.49, 78.40, 76.74, 68.45, 58.62, 56.82, 31.70, 31.05, 29.30, 25.82, 22.72, 14.16. Hexane : EtOAc (v:v) = 7:3, R_f = 0.62; **HRMS** (ESI-Q-TOF), m/z calculated for $C_{34}H_{44}N_4O_4$: 593.3098 $[M+ Na]^+$, found: 593.3107.

Compound 186

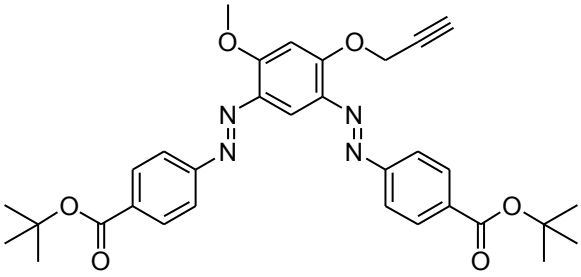

A red-orange solid **186** (0.520 g, 91%) was obtained using the same procedure with compound **135** (0.532 g, 1 mmol) as starting material. **^{1}H NMR (400 MHz, $CDCl_3$) δ(ppm)**: 8.38 (s, 1H), 8.15 (d, *J* = 10.9 Hz, 4H), 7.95 (d, *J* = 11.6 Hz, 2H), 7.89 (d, *J* = 11.6 Hz, 2H), 6.67 (s, 2H), 5.08 (d, *J* = 3.2 Hz, 2H), 4.14 (s, 3H), 2.68 (t, *J* = 3.2 Hz, 1H), 1.65 (s, 18H). **^{13}C NMR (100 MHz, $CDCl_3$) δ(ppm)**: 165.70, 161.76, 160.20, 155.78, 137.47, 137.13, 133.84, 130.85, 123.02, 105.57, 100.09, 81.84, 78.20, 58.57, 57.26, 31.39, 28.66. Hexane : EtOAc (v:v) = 7:3, R_f = 0.51; **HRMS** (ESI-Q-TOF), m/z calculated for $C_{32}H_{34}N_4O_6$: 593.2371 $[M + Na]^+$, found: 593.2375.

Compound 187

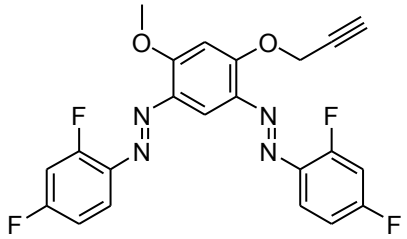

A red-orange solid **187** (0. 218 g, 98%) was obtained using the same procedure with compound **151** (0.202 g, 0.5 mmol) as starting material. **^{1}H NMR (400 MHz, $CDCl_3$) δ(ppm)**: 8.13 (s, 1H), 7.78 (m, 2H), 7.10 - 6.90 (m, 5H), 5.08 (d, *J* = 3.2 Hz, 2H), 4.15 (s, 3H), 2.68 (t, *J* = 3.2 Hz, 1H). **^{13}C NMR (100 MHz, $CDCl_3$) δ(ppm)**: 165.68, 160.19,

155.87, 141.89, 134.95, 133.44, 123.99, 117.91, 106.42, 105.37, 105.14, 104.94, 99.29 , 63.95, 62.58, 56.96. Hexane : EtOAc (v:v) = 8:2, R_f = 0.10; **HRMS** (ESI-Q-TOF), m/z calculated for $C_{22}H_{14}F_4N_4O_2$: 465.1190 $[M + Na]^+$, found: 465.1199.

***Bis*-azobenzene monomer 188**

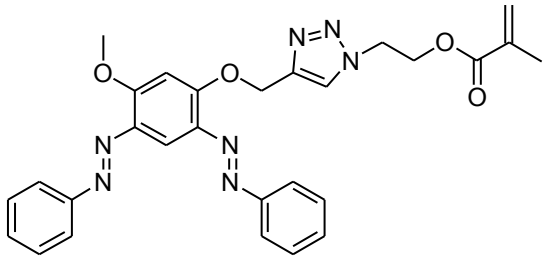

Azide (77.5 mg, 0.5 mmol) and compound **183** (0.185 g, 0.5 mmol) were dissolved in MeCN (10m) under an argon atmosphere. Diisopropylethylamine (0.18 ml, 1 mmol) and 2,6-lutidine (0.12 ml, 1 mmol) were added to the mixture. Copper Iodide (16 mg, 0.28 mmol), previously dried in the oven at 60 ºC, was added and the reaction was stirred at room temperature under an atmosphere for 16 h. The mixture was concentrated under vacuum and the crude mixture was dissolved in EtOAc (50 ml). The organic phase was washed with 1N HCl (3 x 30ml), dried ($MgSO_4$) and concentrated under vacuum. The crude oil was purified by flash chromatography on silica gel eluting with EtOAc and hexanes (8:2) to afford the total compound **188** as a white solid (0.231g, 88%). **^{1}H NMR (400 MHz, $CDCl_3$) δ(ppm)**: 8.16 (s, 1H), 7.99 – 7.90 (m, 4H), 7.80 (s, 1H), 7.60 – 7.43 (m, 6H), 7.10 (s, 1H), 6.03 (s, 1H), 5.68 (s, 2H), 5.53 (s, 1H), 4.76 – 4.70 (t, 2H), 4.61 – 4.56 (t, 2H), 4.15 (s, 3H), 1.87 (s, 3H). **^{13}C NMR (100Hz, $CDCl_3$) δ(ppm)**: 18.15, 49.34, 56.86, 62.49, 64.15, 99.69, 105.32, 122.82, 122.87, 123.79, 126,75, 129.02, 130.55, 135.20, 136.68, 144.05, 153.12, 159.50, 160.62, 166.55. Hexane : EtOAc (v:v) = 5:5, R_f = 0.21; **HRMS** (ESI-Q-TOF), m/z calculated for $C_{28}H_{27}N_7O_4$: 548.2017 $[M+Na]^+$, found: 548.2028.

***Bis*-azobenzene monomer 189**

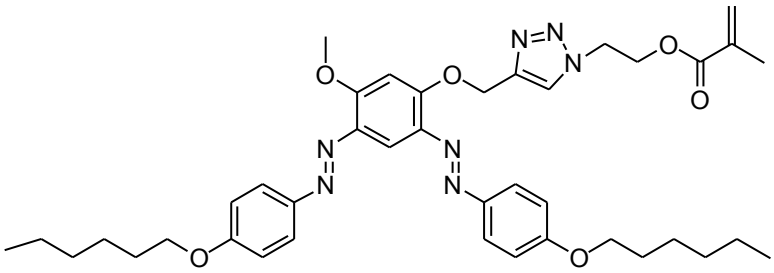

A red-orange solid **189** (0.323 g, 89%) was obtained using the same procedure with compound **184** (0.285 g, 0.5 mmol) as starting material. **^{1}H NMR (400 MHz, $CDCl_3$) δ(ppm)**: 8.12 (s, 1H), 7.94 (d, *J* = 3.8 Hz, 2H), 7.92 (d, *J* = 3.7 Hz, 2H), 7.79 (s, 1H), 7.02 (d, *J* = 6.4 Hz, 3H), 7.00 (s, 1H), 6.03 (s, 1H), 5.66 (s, 2H), 5.54 (s, 1H), 4.72 (t, *J* = 12.0 Hz, 2H), 4.58 (t, *J* = 12.0 Hz, 2H), 4.12 (s, 3H), 4.07 (t, *J* = 9.0 Hz, 4H), 1.91 – 1.80 (m, 4H), 1.72 (s, 3H), 1.56 -1.48 (m, 4H), 1.39 (m, 8H), 0.96 (t, *J* = 8.2 Hz, 6H). **^{13}C NMR (100Hz, $CDCl_3$) δ(ppm)**:166.53, 161.53, 159.74, 158.49, 147.37, 144.20, 137.24, 135.27, 126.70, 124.75, 124.66, 123.64, 114.71, 114.67, 105.44, 68.39, 64.36, 62.39, 56.86, 49.36, 31.57, 29.18, 25.69, 22.58, 18.10, 13.99. Hexane : EtOAc (v:v) = 5:5, R_f = 0.33; **HRMS** (ESI-Q-TOF), m/z calculated for $C_{40}H_{51}N_7O_6$: 748.3793 $[M + Na]^+$, found: 748.3821.

***Bis*-azobenzene monomer 190**

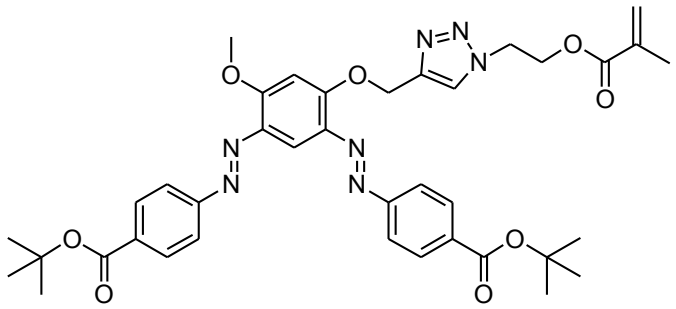

A red-orange solid **190** (0.653 g, 90%) was obtained using the same procedure with compound **185** (0.570 g, 1 mmol) as starting material. **^{1}H NMR (400 MHz, $CDCl_3$)**

δ(ppm): 8.20 (s, 1H), 8.17 (d, *J* = 2.6 Hz, 2H), 8.14 (d, *J* = 2.6 Hz, 2H), 7.96 (d, *J* = 4.4 Hz, 2H), 7.93 (d, *J* = 4.4 Hz, 2H), 7.82 (s, 1H), 7.15 (s, 1H), 6.03 (s, 1H), 5.68 (s, 2H), 5.54 (s, 1H), 4.78 – 4.67 (m, 3H), 4.64 – 4.56 (m, 3H), 4.18 (s, 3H), 1.88 (s, 4H), 1.67 (s, 6H), 1.66 (s, 9H). **^{13}C NMR (100Hz, $CDCl_3$) δ(ppm)**: 166.55, 165.25, 161.65, 160.44, 155.34, 143.76, 136.62, 135.33, 133.42, 130.39, 126.74, 123.92, 122.53, 122.47, 105.10, 99.43, 81.40, 63.90, 62.45, 56.95, 49.42, 26.22, 18.15. Hexane : EtOAc (v:v) = 7:3, R_f = 0.44; **HRMS** (ESI-Q-TOF), m/z calculated for $C_{38}H_{43}N_7O_8$: 748.3065 $[M + Na]^+$, found: 748.3029.

***Bis*-azobenzene monomer 191**

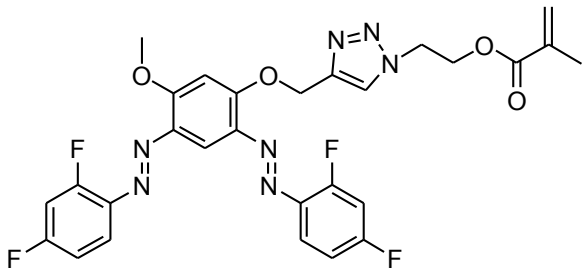

A red-orange solid **191** (0.233 g, 78%) was obtained using the same procedure with compound **186** (0.221 g, 0.5 mmol) as starting material. **^{1}H NMR (400 MHz, $CDCl_3$) δ(ppm)**: 8.10 (s, 1H), 7.80 (s, 1H), 7.78 – 7.66 (m, 2H), 7.09 (s, 1H), 7.07 – 6.86 (m, 4H), 6.02 (s, 1H), 5.64 (s, 2H), 5.54 (s, 1H), 4.80 – 4.66 (m, *J*=12Hz, 2H), 4.64 – 4.52 (m, *J*= 12Hz, 2H), 4.13 (s, 3H), 1.86 (s, 3H). **^{13}C NMR (100Hz, $CDCl_3$) δ(ppm)**: 166.68, 161.19, 159.87, 143.89, 136.95, 136.84, 135.44 , 126.86, 123.99, 120.01, 119.82, 111.93, 111.71, 106.42, 105.37, 105.14, 104.94, 99.29, 63.95, 62.58, 56.96, 49.45, 30.43, 18.24. Hexane : EtOAc (v:v) = 6:4, R_f = 0.09; **HRMS** (ESI-Q-TOF), m/z calculated for $C_{28}H_{23}F_4N_7O_4$: 620.1640 $[M + Na]^+$, found: 620.1616.

2-Hydroxymethyl-acrylic acid *tert*-butyl ester (194)

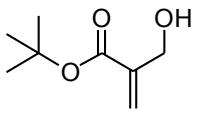

Preparation of *tert*-Butyl (2-Hydroxymethyl)acrylate was indicated according to the procedure. tButyl-acrylate (12 mL, 82.5 mmol), formaldehyde (10 g, 0.125 mol) (or paraformaldehyde, 0.125 mL, 3.75 g), Triethylamine (1.148 mL, 8.25 mmol), THF (12.5 ml) and water (8 ml) were added to a 25 ml flask over an ice bath. The mixture of DABCO, 1mL THF and 1mL H_2O was added dropwise. The solution was stirred at room temperature for 3 h, followed by stirring at 55 ^oC for overnight under Argon. As the reaction finished, the reaction mixture was extracted with ethyl ether for three times and all organic layers were merged and washed by brine, followed by drying over $MgSO_4$. After doing flash chromatography with eluent of Hexane : EtOAc 7:3, it obtained 10.3 g of colorless liquid (compound **194**)with a yield of 79%. **^{1}H NMR (400 MHz, $CDCl_3$) δ(ppm)**: 6.26-6.02 (m, 1H), 5.81-5.62 (m, 1H), 4.27 (d, *J* = 1.0 Hz, 2H), 2.36 (s, 1H), 1.49 (s, 9H). **^{13}C NMR (100 MHz, $CDCl_3$) δ(ppm)**: 164.80, 138.31, 124.68, 80.70, 60.20, 27.71. Hexane : EtOAc (v:v) = 7:3, R_f = 0.62; **HRMS** (ESI-Q-TOF), m/z calculated for $C_8H_{14}O_2$: 143.2190 $[M+H]^+$, found: 143.2199.

2-Bromomethyl-acrylic acid tert-butyl ester (195)

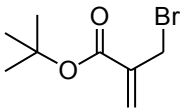

Tert-Butyl (2-bromomethyl)acrylate was prepared by a modification of the method of Mehrnoosh Ostovar and Charles M. Marson. To a round-bottomed flask containing tert-Butyl (2-Hydroxymethyl)acrylate (3.1 mL, 20 mmol) in dry diethyl ether (20 mL)

under an atmosphere of argon, was added phosphorus tribromide (2.09 ml, 22 mmol) at -10 ^{o}C. The mixture was stirred for 3 h at -10 ^{o}C, then removed to room temperature still reacting for 2 hours. After completing the reaction, the reaction mixture was quenched by addition of ice-water (5 mL). The organic layer was extracted with hexane (3×10 mL). The combined organic layer was washed by brine and was dried over anhydrous $MgSO_4$, filtered and the filtrate was evaporated. Chromatography of the residue on silica gel with hexane: ethyl acetate 9:1 gave 3.536 g (the yield is 80%) as a colourless oil (compound **195**). **^{1}H NMR (400 MHz, $CDCl_3$) δ(ppm)**: 6.22 (dd, *J* = 2.1 and 1.3 Hz, 1H), 5.85 (dd, *J* = 2.1 and 1.1 Hz, 1H), 4.14 (dd, *J* = 2.0 and 1.1 Hz, 2H), 1.51 (s, 9H). **^{13}C NMR (100 MHz, $CDCl_3$) δ(ppm)**: 163.59, 138.80, 127.73, 81.23, 30.91, 27.80. Hexane : EtOAc (v:v) = 7:3, R_f = 0.95; **HRMS** (ESI-Q-TOF), m/z calculated for $C_8H_{12}BrO_2$: 242.9991 $[M+Na]^+$, found: 243.0002.

2-[4-(4-Hexyloxy-phenylazo)-3-methoxy-phenoxymethyl]-acrylic acid tert-butyl ester (196)

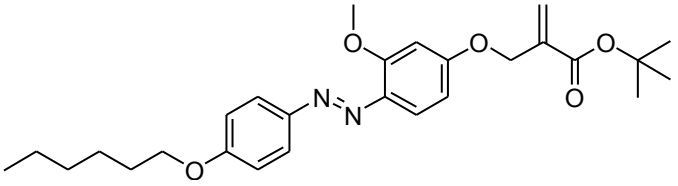

To a solution of (E)-4-((4-(hexyloxy)phenyl)diazenyl)-3-methoxyphenol (0.328 g, 1 mmol) and 10 mL acetonitrile was added K_2CO_3 (0.276 g, 2 mmol) portionwise and tert-Butyl (2-bromomethyl)acrylate (0.258 mL, 1.5 mmol) dropwise on the ice-water bath under argon, and the resulting solution was heated at 55 ^{o}C reflux overnight. The reaction mixture was cooled and concentrated in vacuo. The residue was partitioned between EtOAc (20 mL) and H_2O (5 mL). The aqueous phase was extracted with EtOAc and the combined organic extracts were sequentially washed with H_2O and brine, dried by $MgSO_4$, filtered and concentrated in vacuo. The residue was purified by flash chromatography eluting with

hexane and EtOAc. The product **196** was obtained as a red-orange solid (0.449 g, 96%). **^{1}H NMR (400 MHz, $CDCl_3$) δ(ppm)**: 7.89 (d, *J* = 11.9 Hz, 2H), 7.74 (d, *J* = 11.9 Hz, 1H), 7.01 (d, *J* = 11.9 Hz, 2H), 6.68 (d, *J* = 3.0 Hz, 1H), 6.61 (dd, *J* = 11.9, 3.1 Hz, 1H), 6.37 (s, 1H), 5.99 (s, 1H), 4.82 (s, 2H), 4.29 – 3.89 (m, 5H), 1.91 – 1.78 (m, 2H), 1.57 (s, 9H), 1.54 – 1.45 (s, 2H), 1.43 – 1.32 (m, 4H), 0.96 (t, *J* = 8.3 Hz, 3H). **^{13}C NMR (100 MHz, $CDCl_3$) δ(ppm)**: 164.79, 161.91 , 161.23, 158.30, 147.56, 137.29, 137.14, 125.79, 124.61, 118.05, 114.73, 106.45, 100.02, 81.61, 68.42, 66.57, 56.52, 31.71, 29.32, 28.22, 25.83, 22.73, 14.17. Hexane : EtOAc (v:v) = 9:1, R_f = 0.48; **HRMS** (ESI-Q-TOF), m/z calculated for $C_{27}H_{36}N_2O_5$: 491.2516 $[M+ Na]^+$, found: 491.2533.

APPENDIX II: NUCLEAR MAGNETIC RESONANCE SPECTRA OF PROTONS

4-phenylazo-phenol (81)

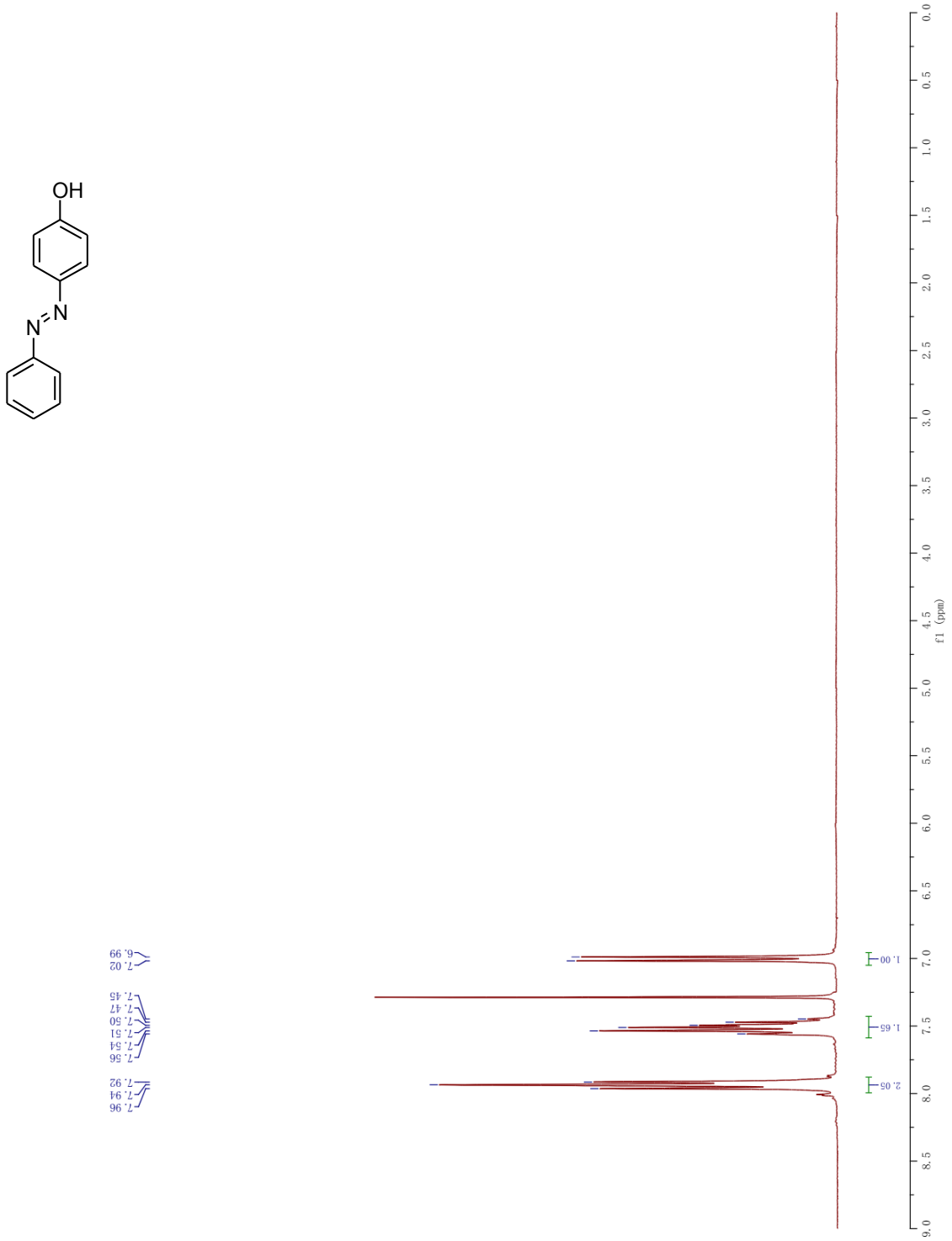

2,4-bis((E)-phenyldiazenyl)phenol (96)

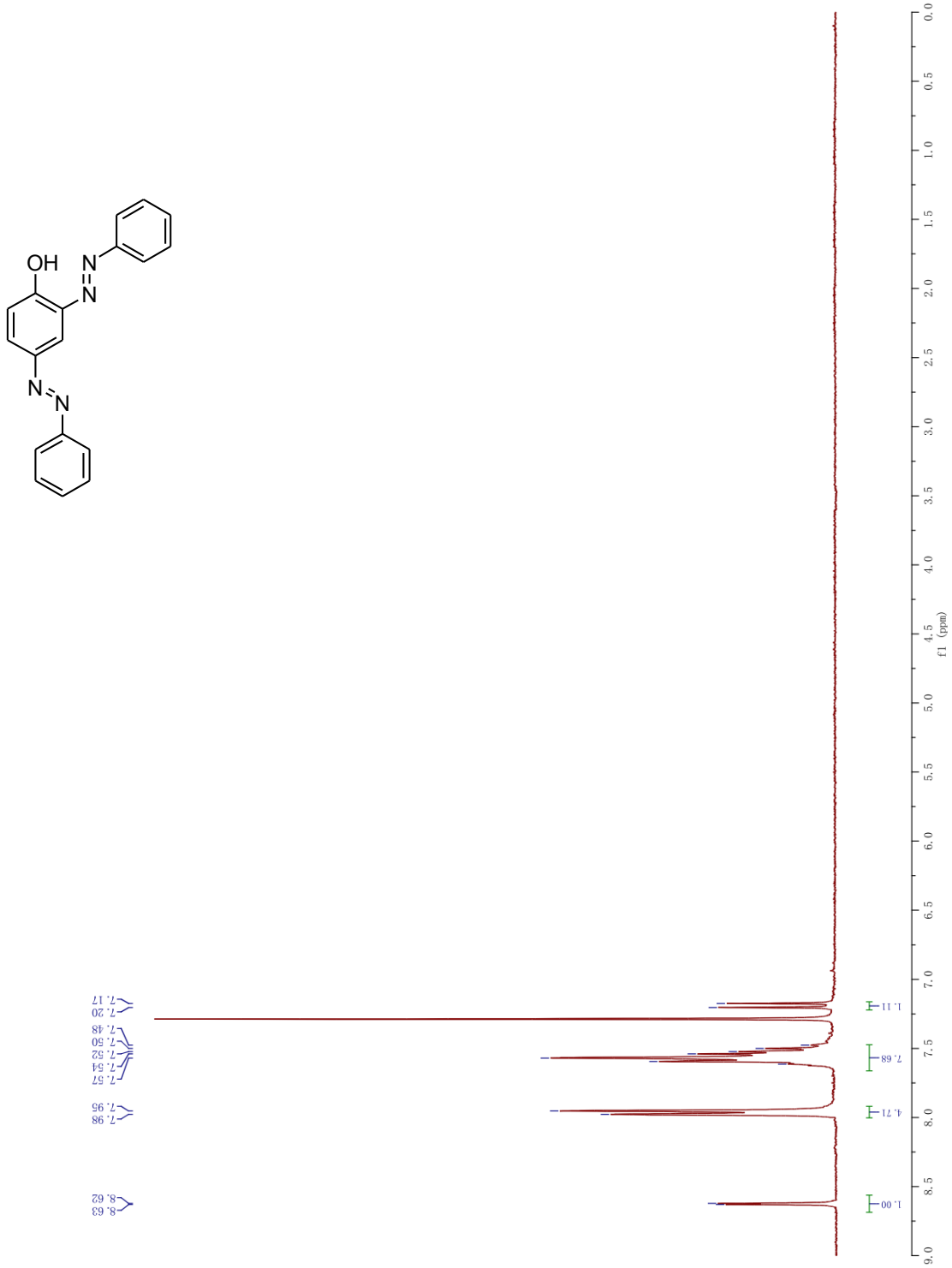

(E)-3-methoxy-4-(phenyldiazenyl)phenol (99)

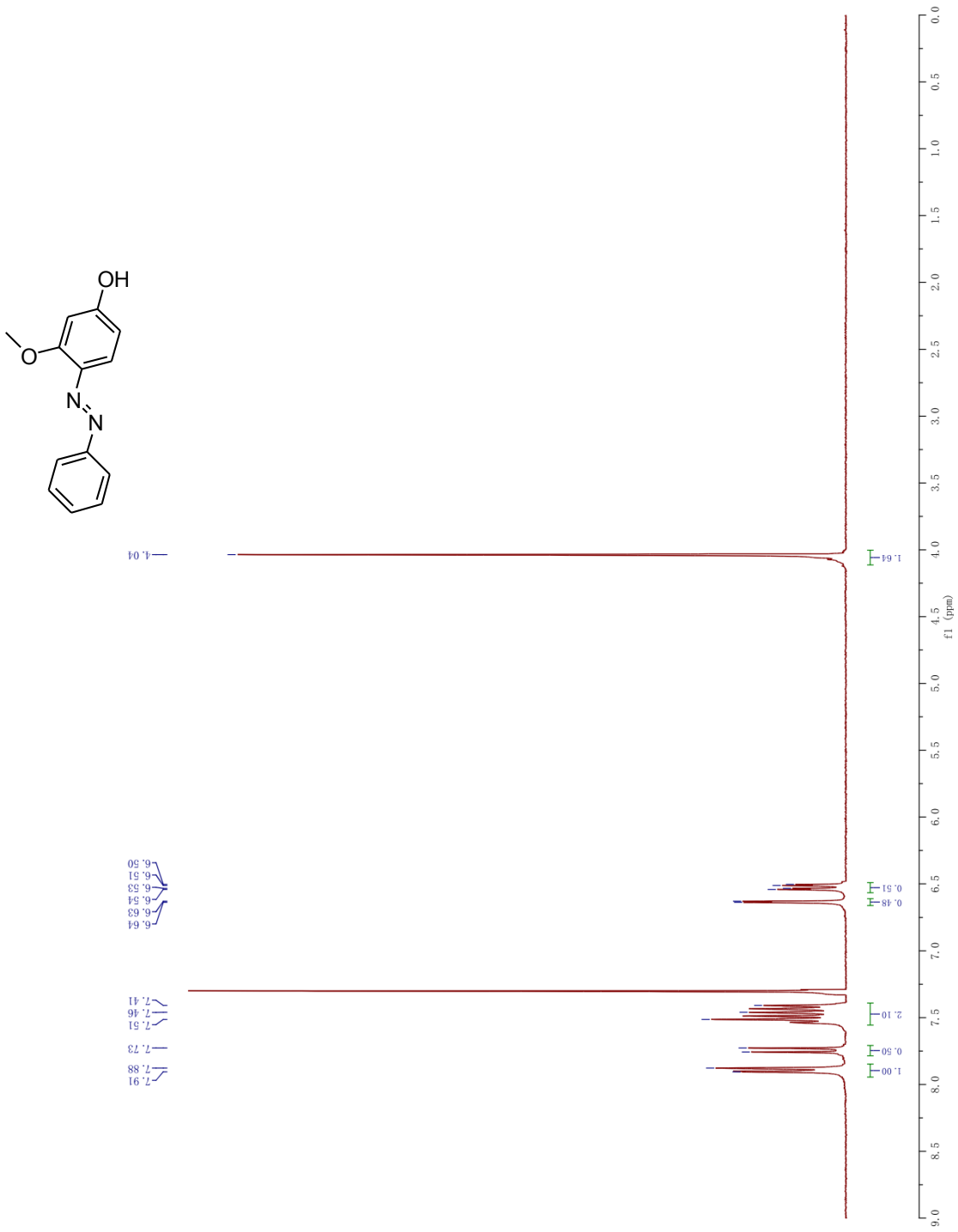

(E)-5-methoxy-2-(phenyldiazenyl)phenol (100)

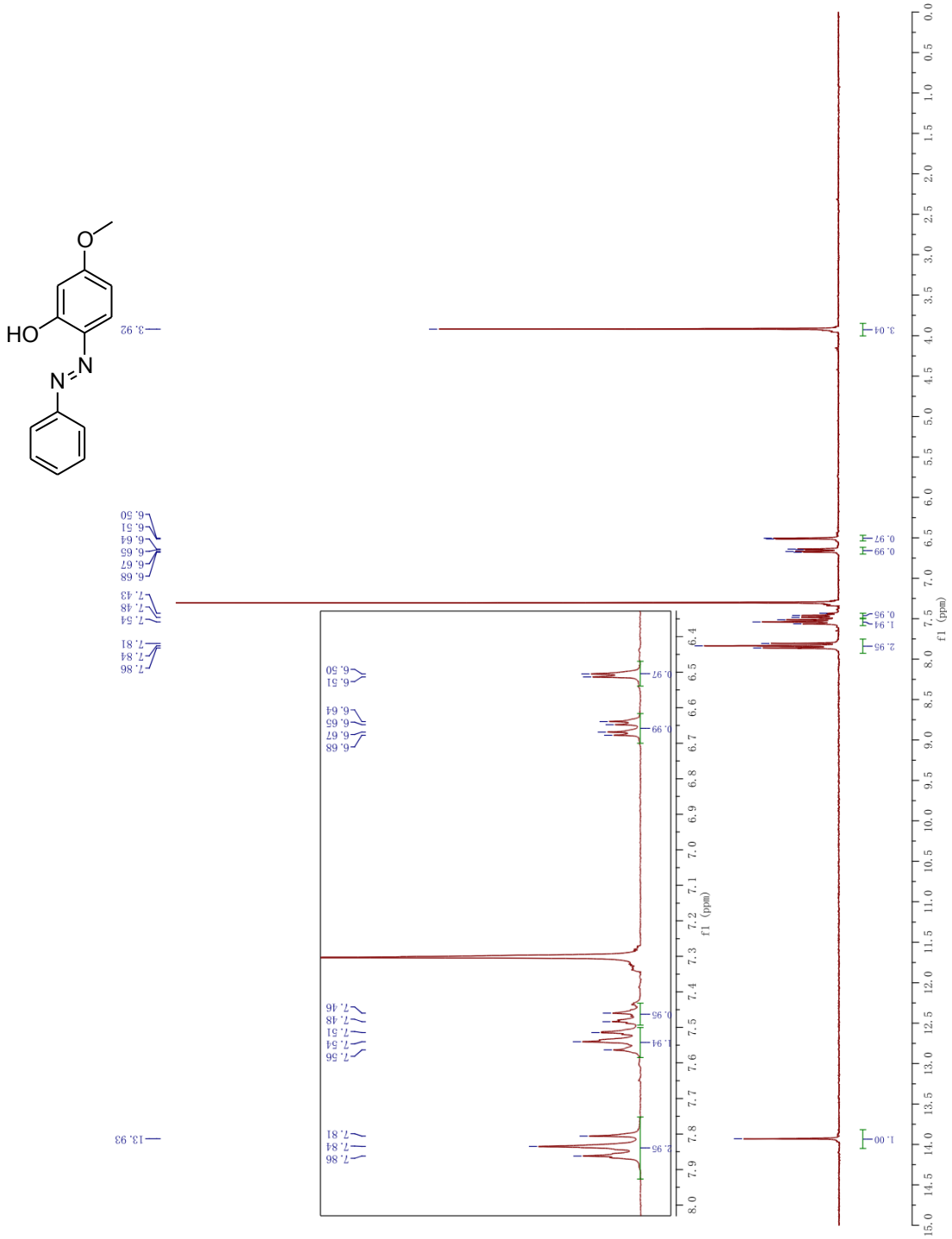

2, 4-bis((E)-phenyldiazenyl)-5-methoxyphenol (101)

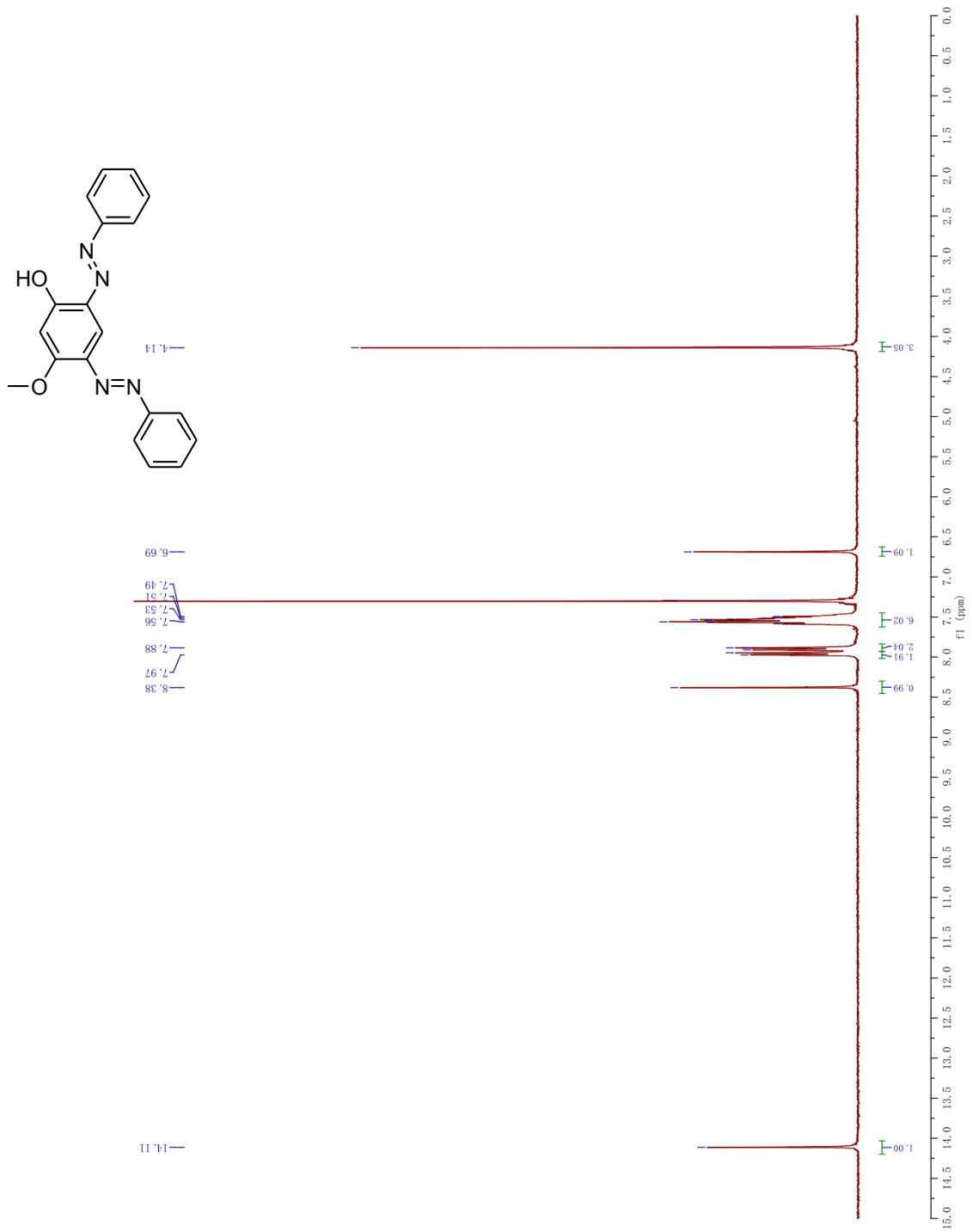

2-phenylazo-3-prop-2-ynyloxy-phenol (102)

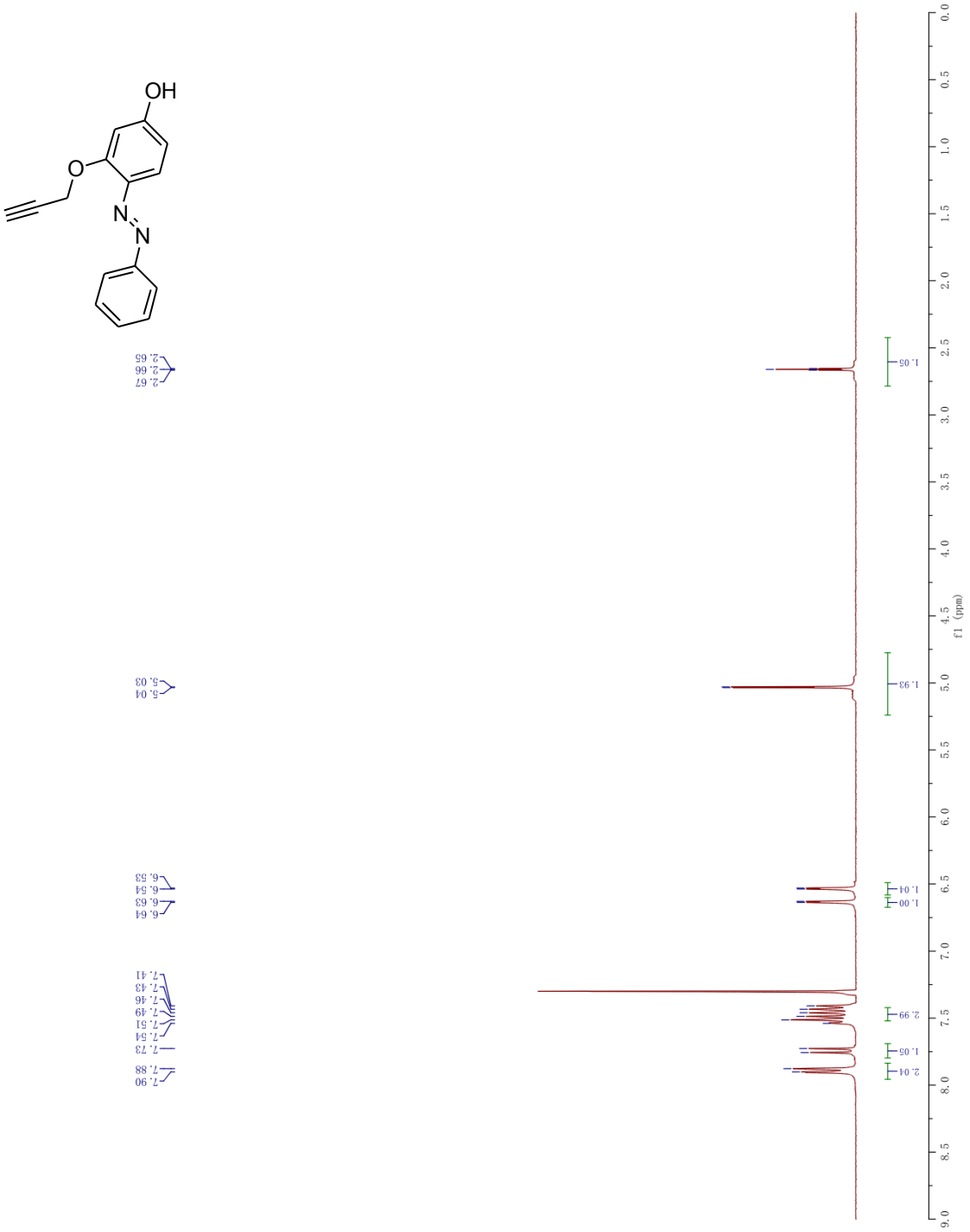

2-phenylazo-5-prop-2-ynyloxy-phenol (103)

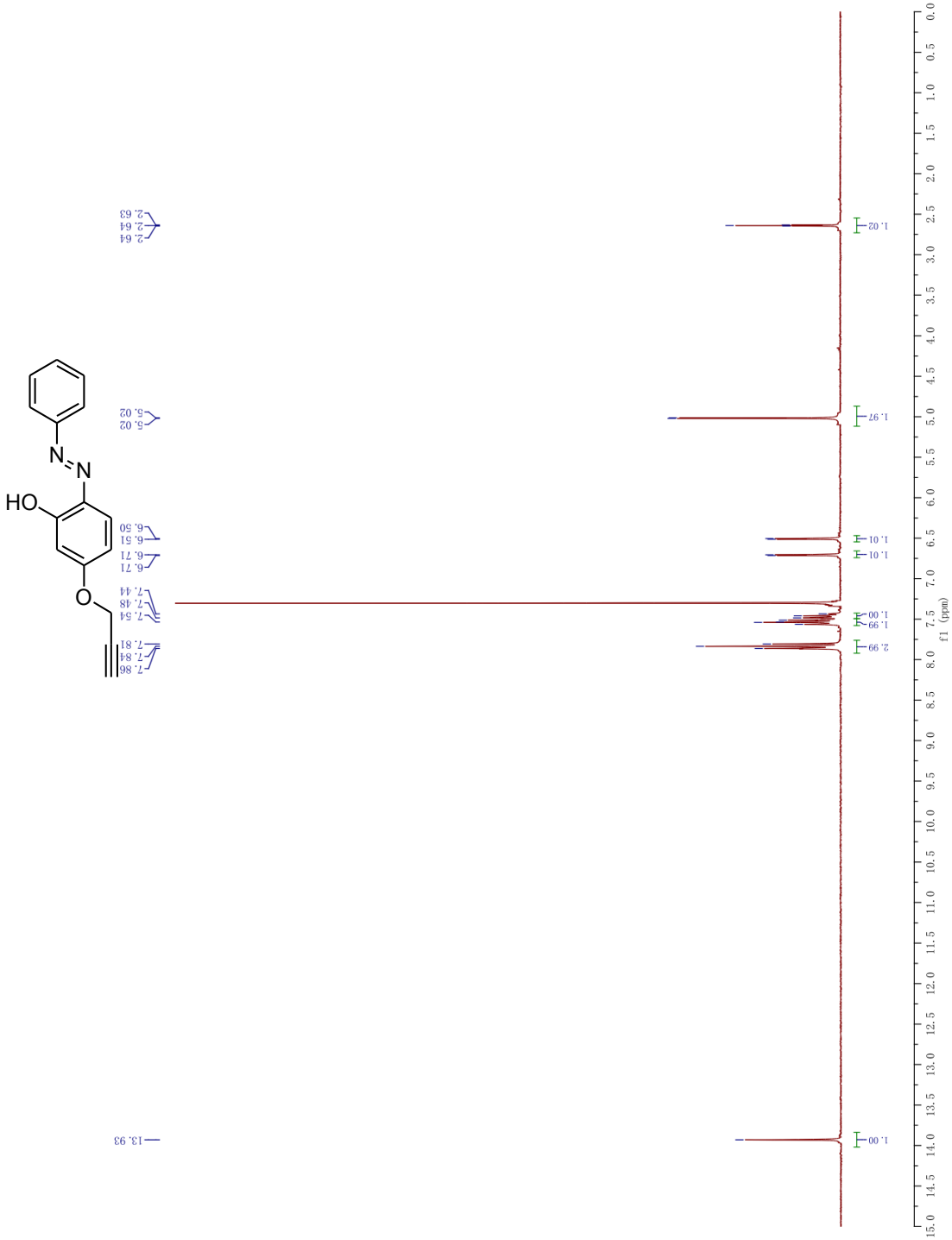

2,4-bis-phenylazo-5-prop-2-ynyloxy-phenol (104)

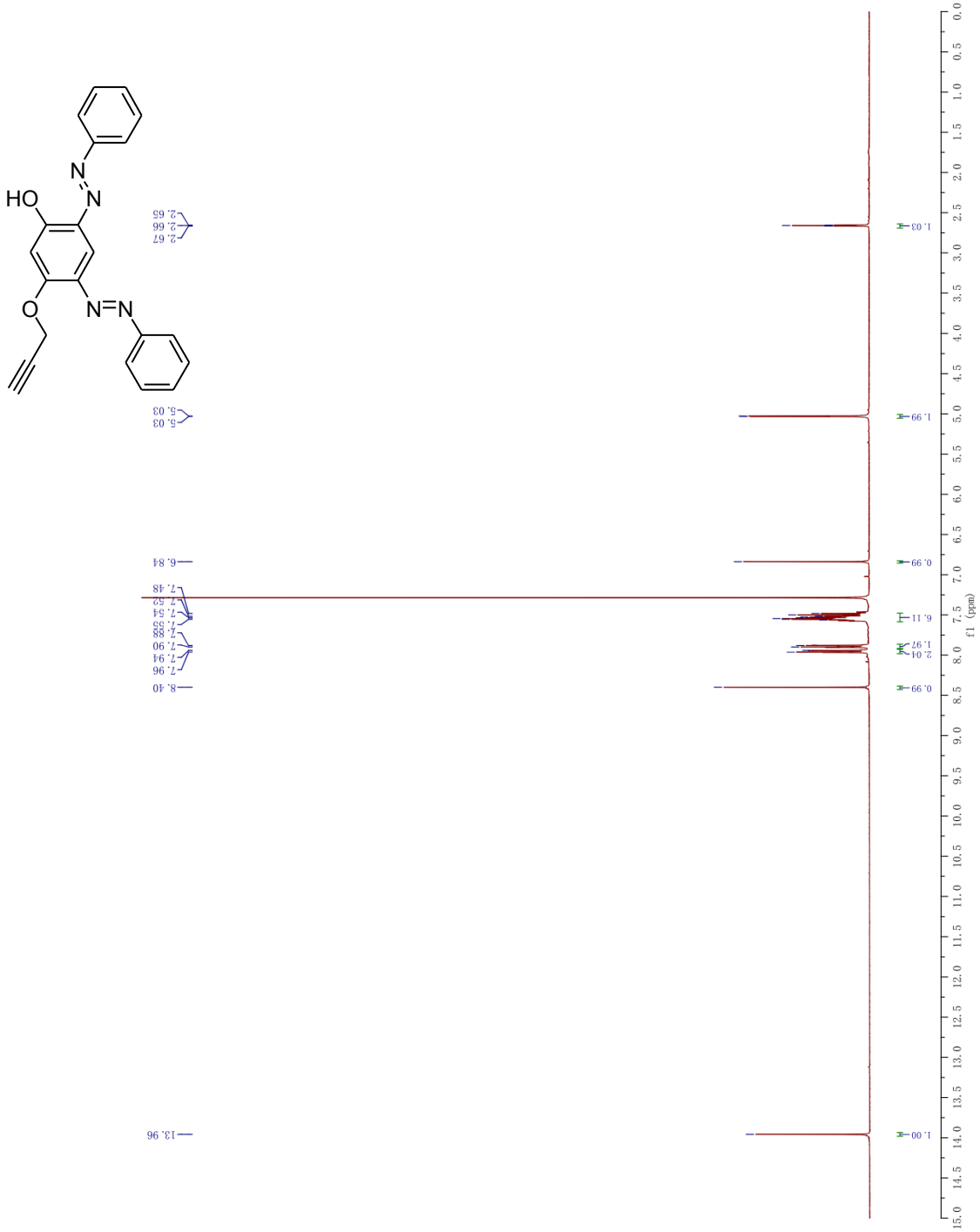

2,4-bis((E)-phenyldiazenyl)benzene-1,3,5-triol (106)

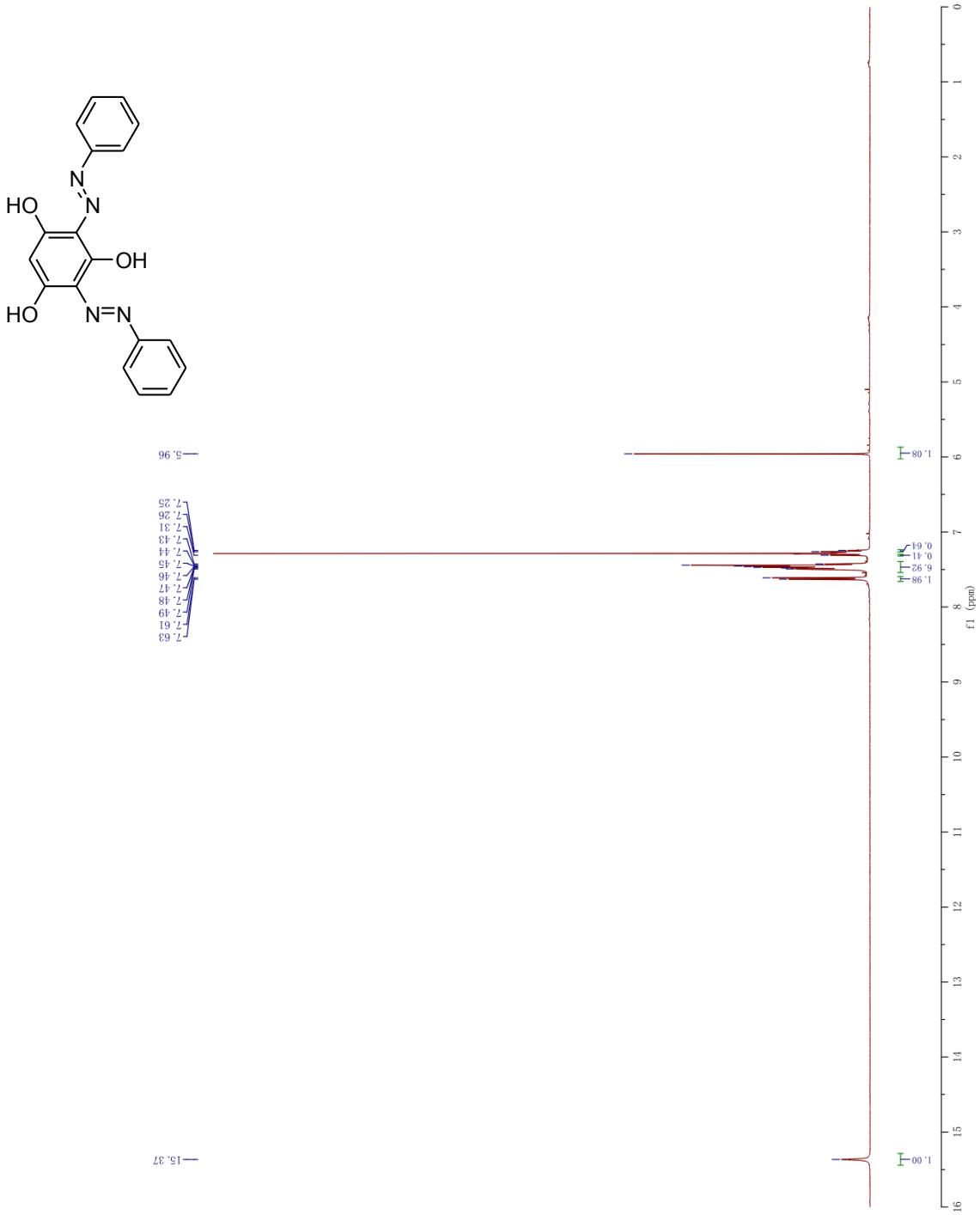

2, 4, 6-Tris-phenylazo-benzene-1, 3, 5-triol (107)

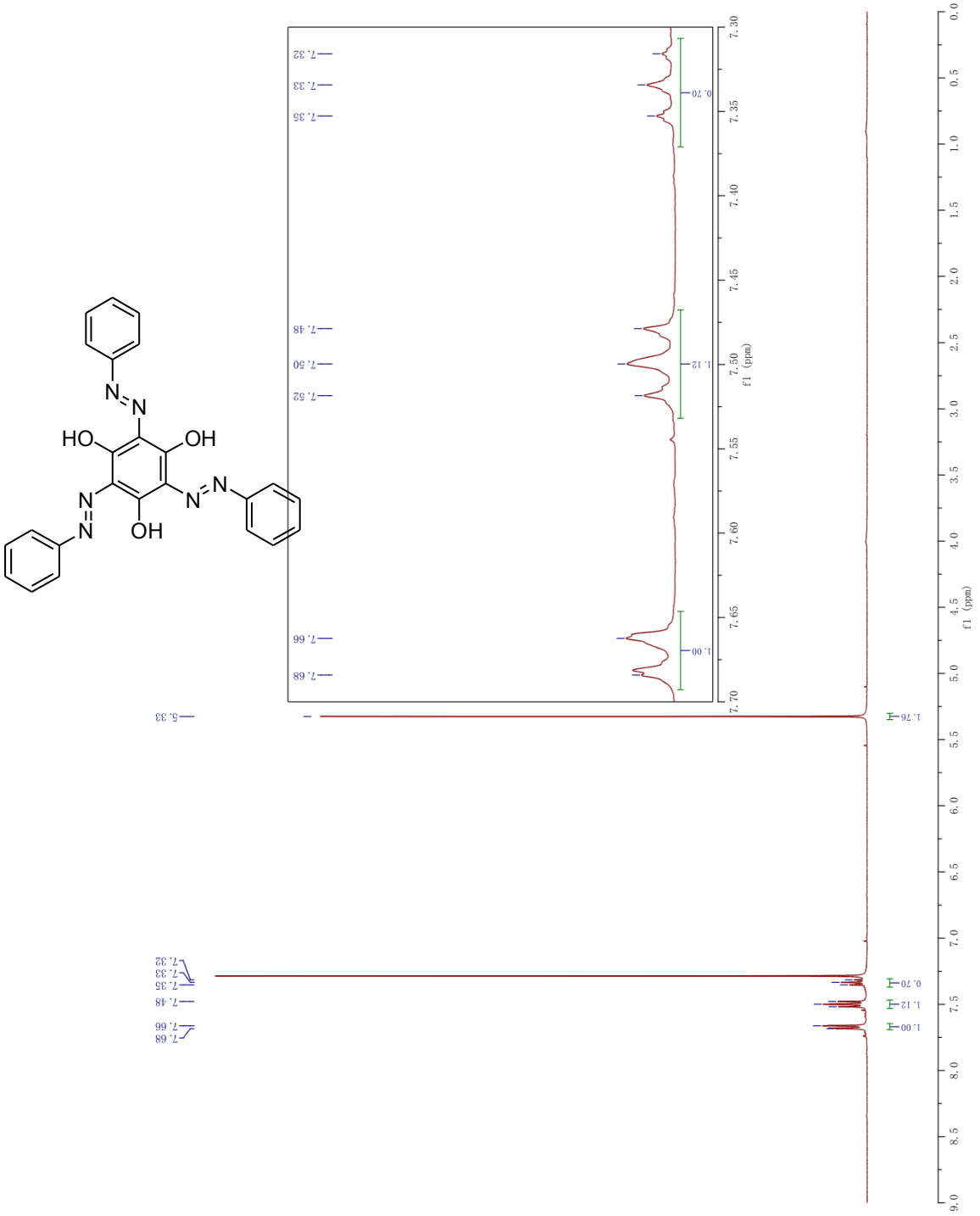

(E)-4-((2,4-dimethoxyphenyl)diazenyl)-3-methoxyphenol (117)

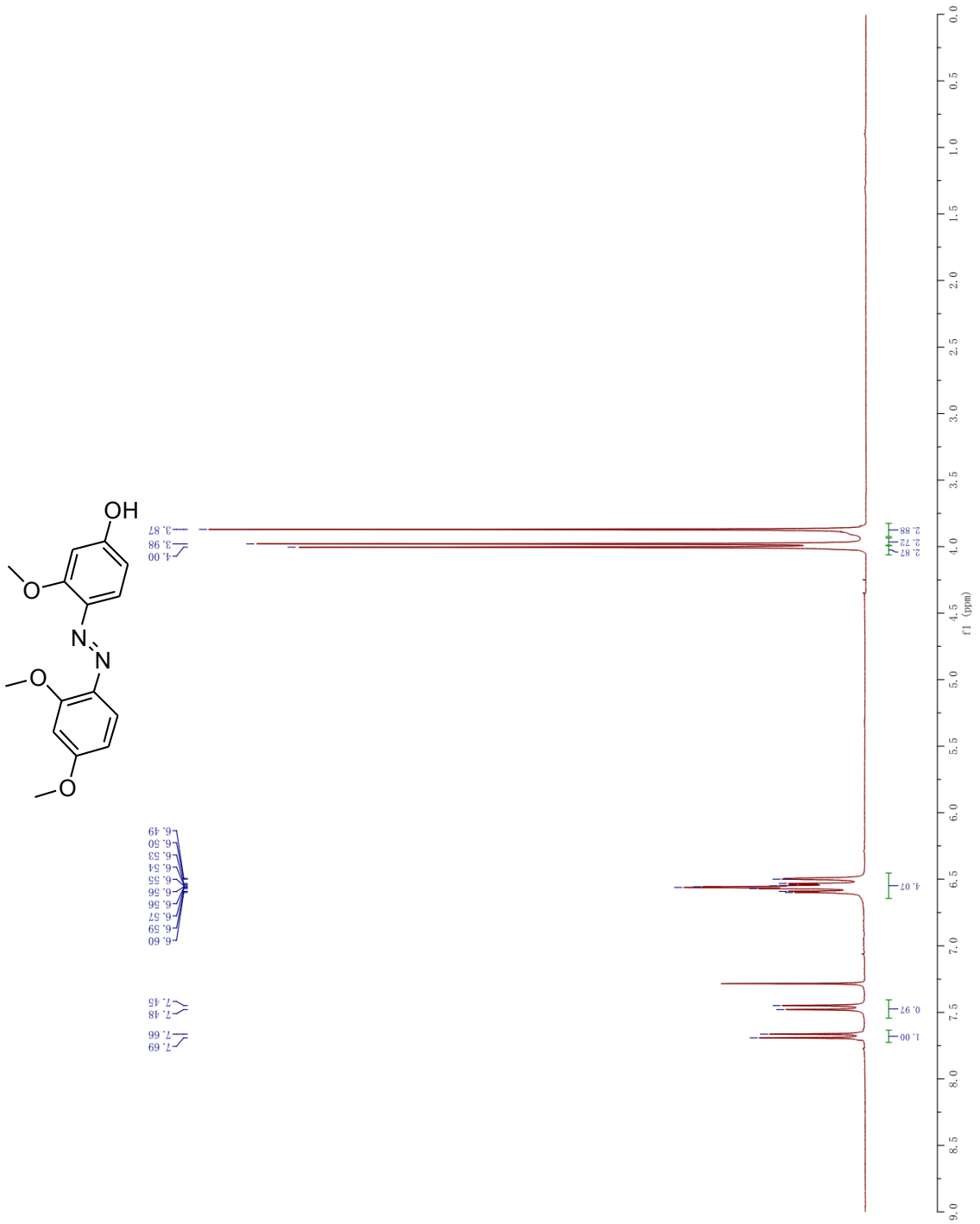

(E)-2-((2,4-dimethoxyphenyl)diazenyl)-5-methoxyphenol (118)

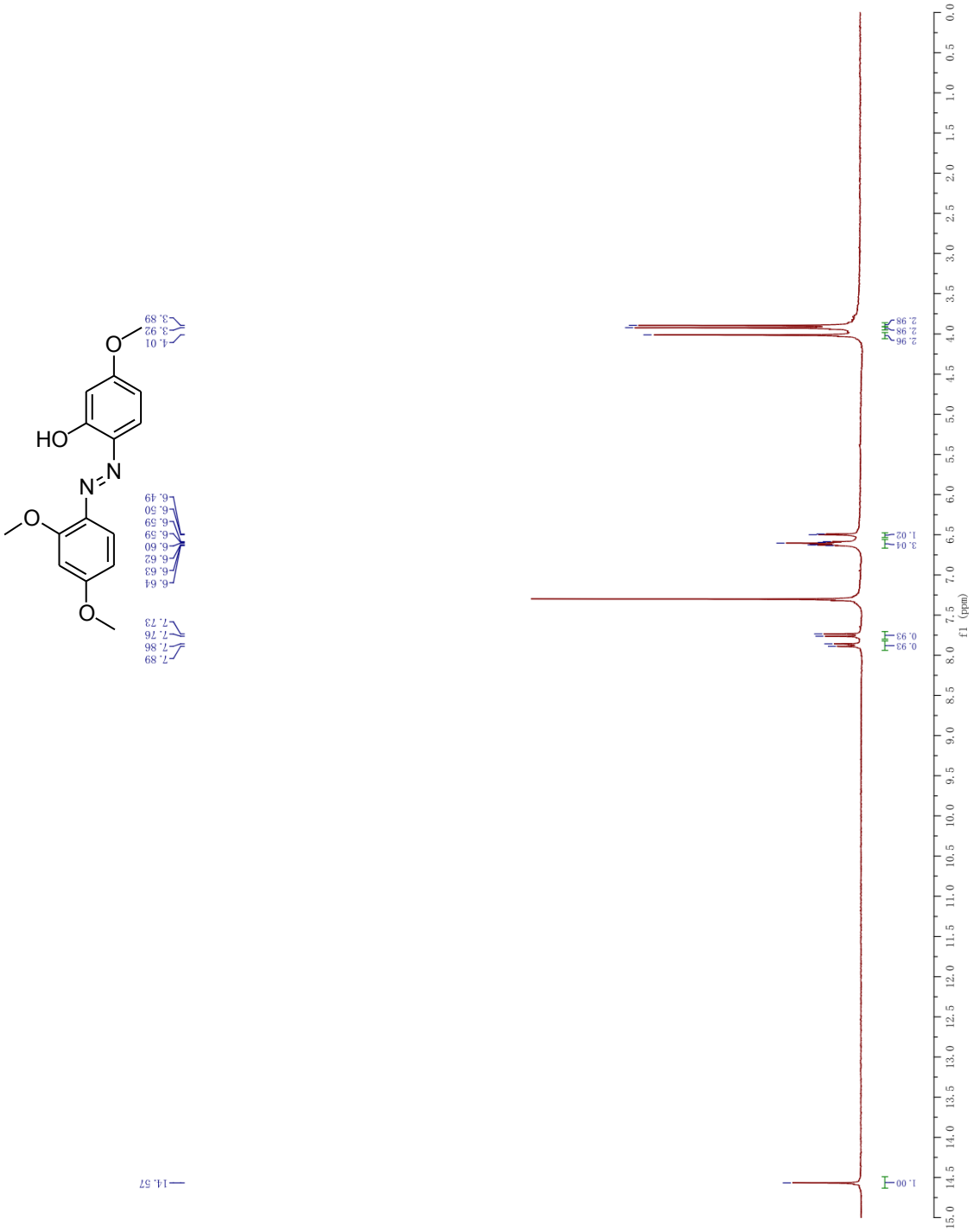

2, 4-bis((E)-(2,4-dimethoxyphenyl)diazenyl)-5-methoxyphenol (119)

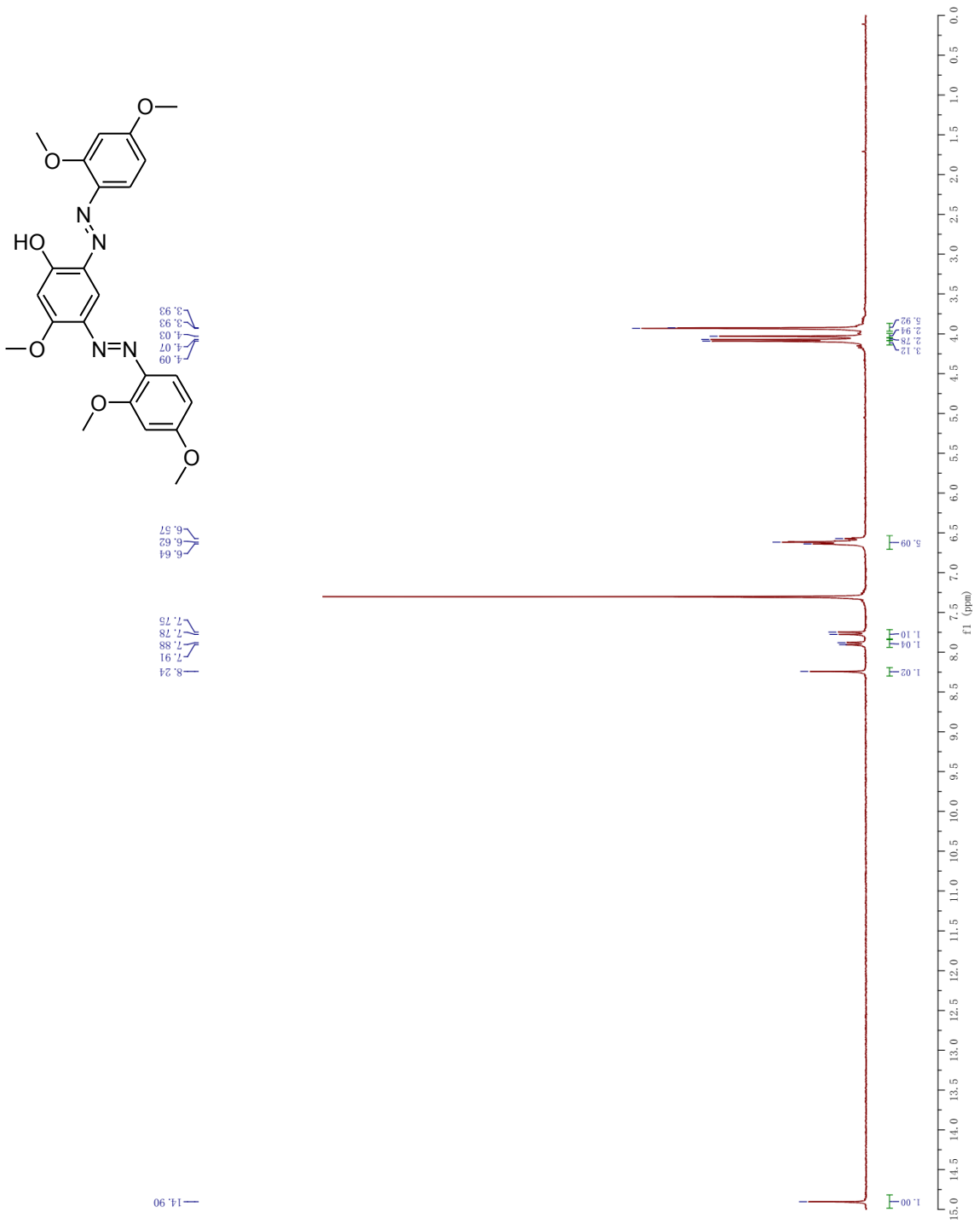

(E)-3-methoxy-4-((4-methoxyphenyl)diazenyl)phenol (121)

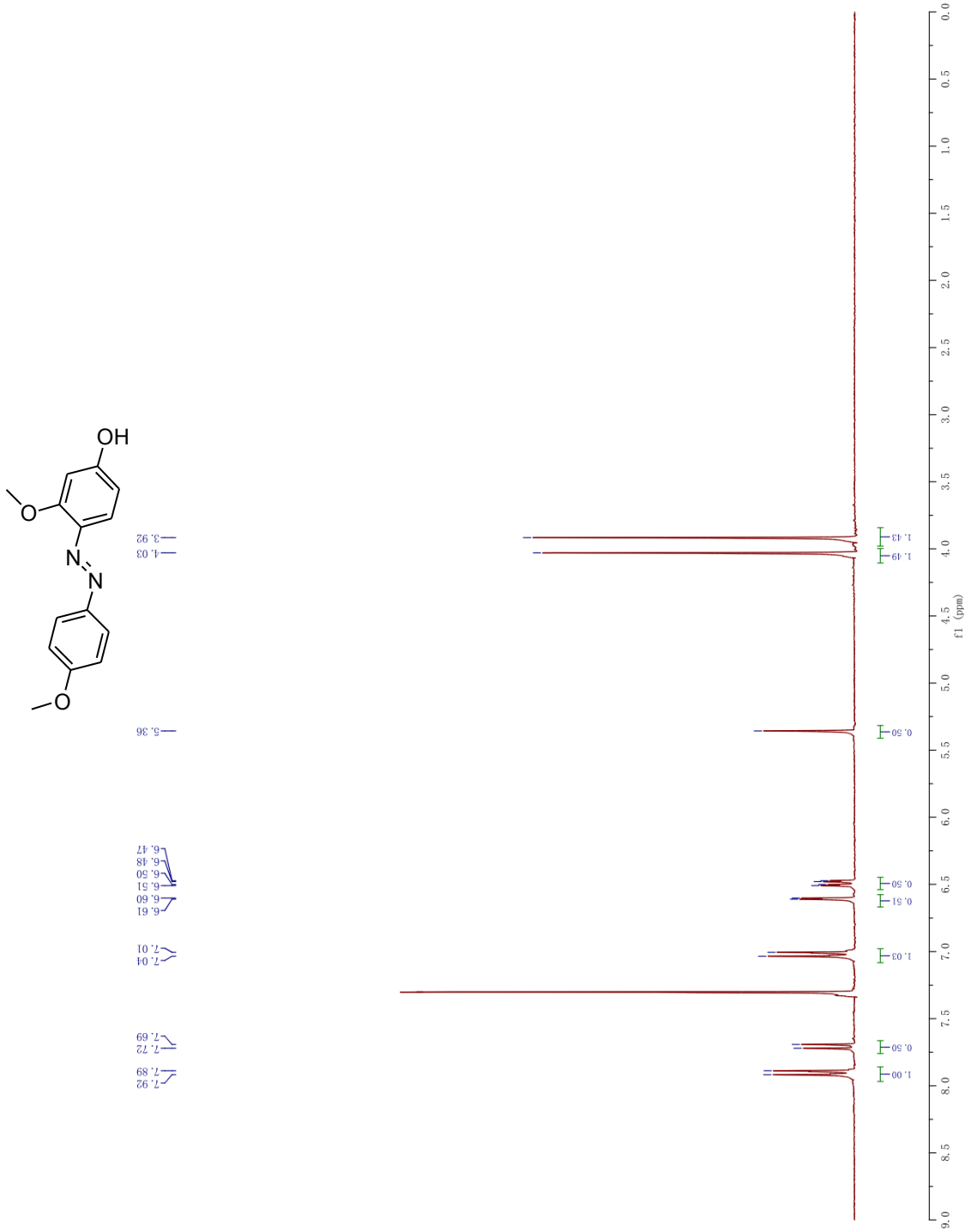

(E)-5-methoxy-2-((4-methoxyphenyl)diazenyl)phenol (122)

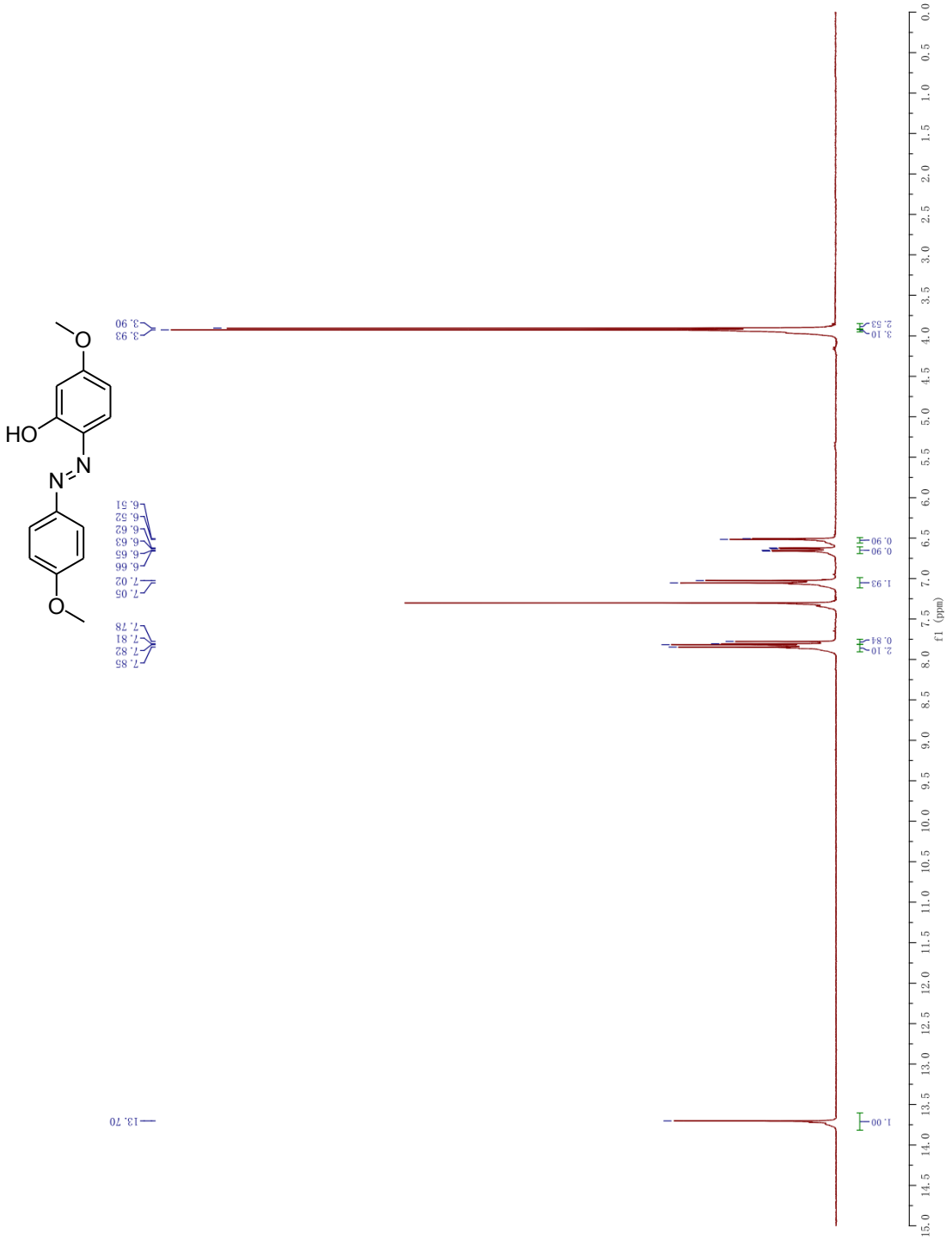

2, 4-bis((E)-(4-methoxyphenyl)diazenyl)-5-methoxyphenol (123)

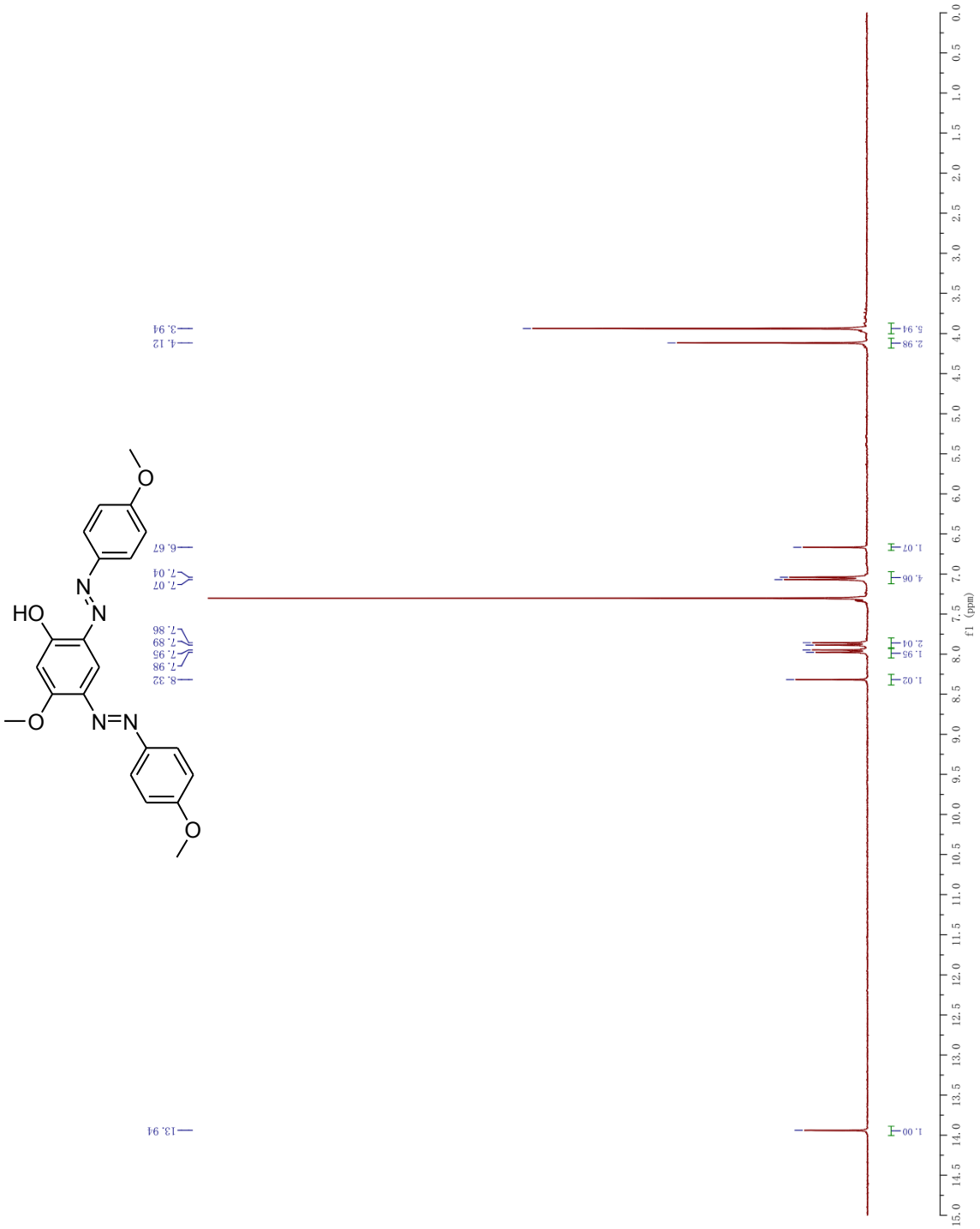

(E)-4-((4-(hexyloxy)phenyl)diazenyl)-3-methoxyphenol (125)

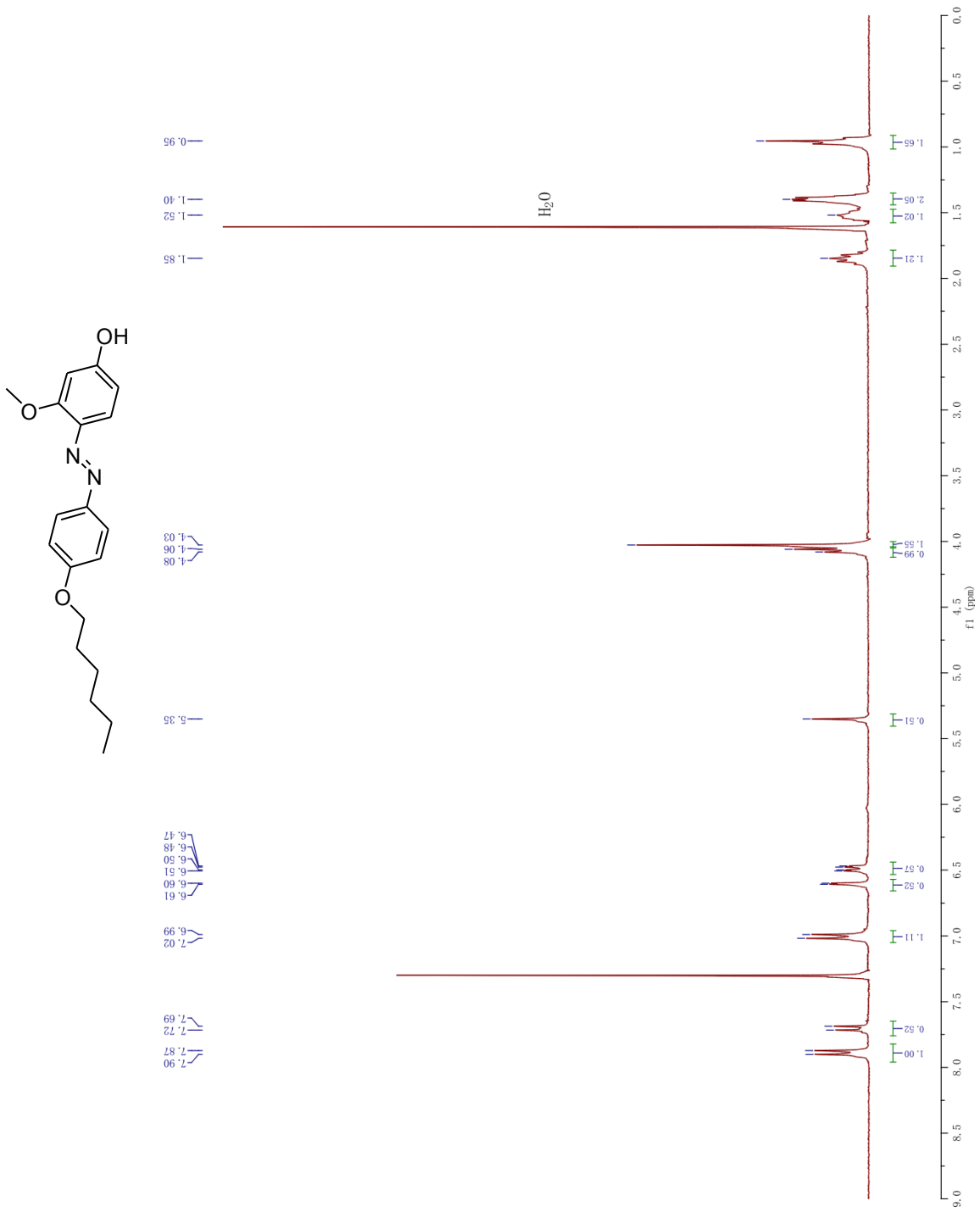

(E)-2-((4-(hexyloxy)phenyl)diazenyl)-5-methoxyphenol (126)

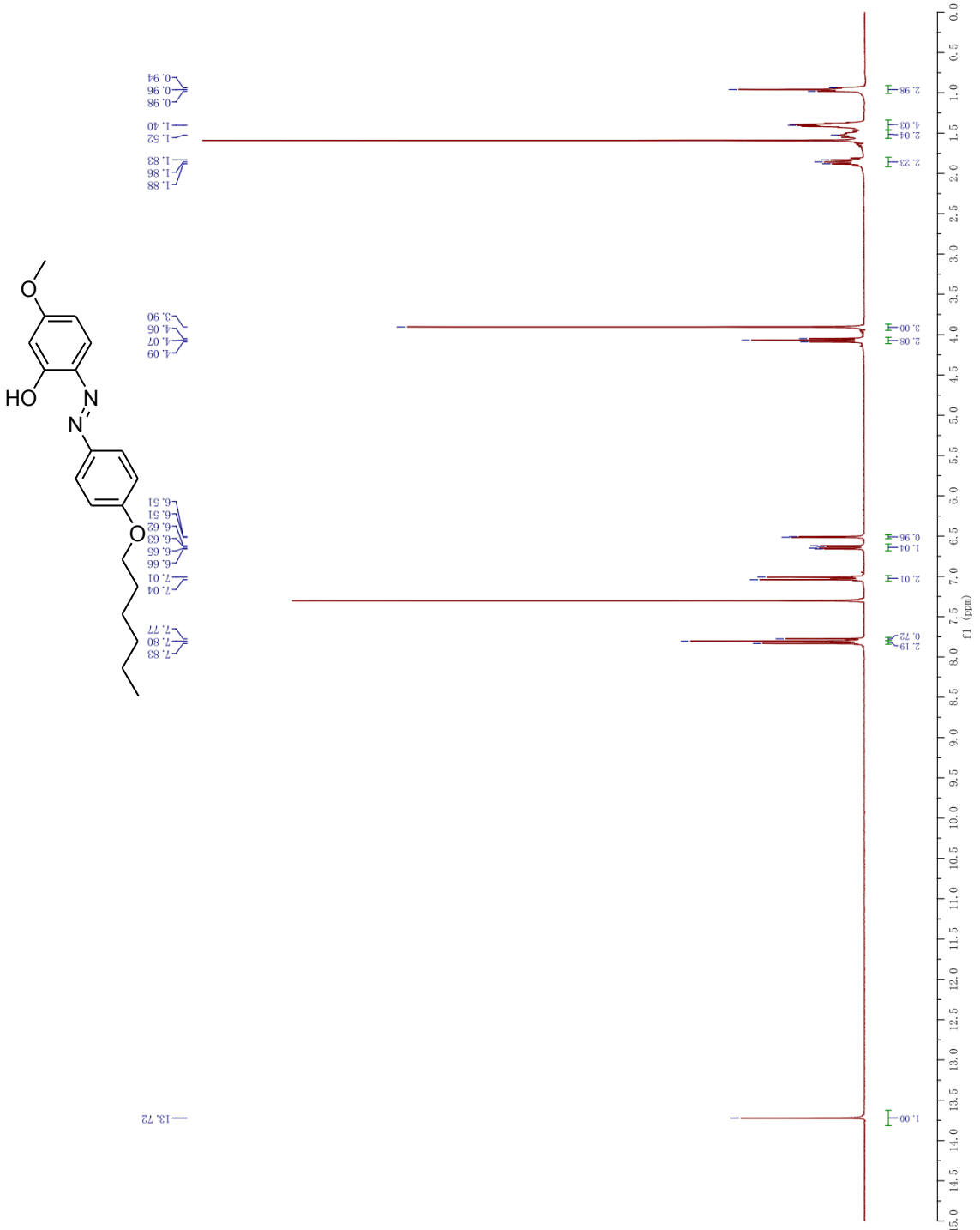

2, 4-bis((E)-(4-(hexyloxy)phenyl)diazenyl)-5-methoxyphenol (127)

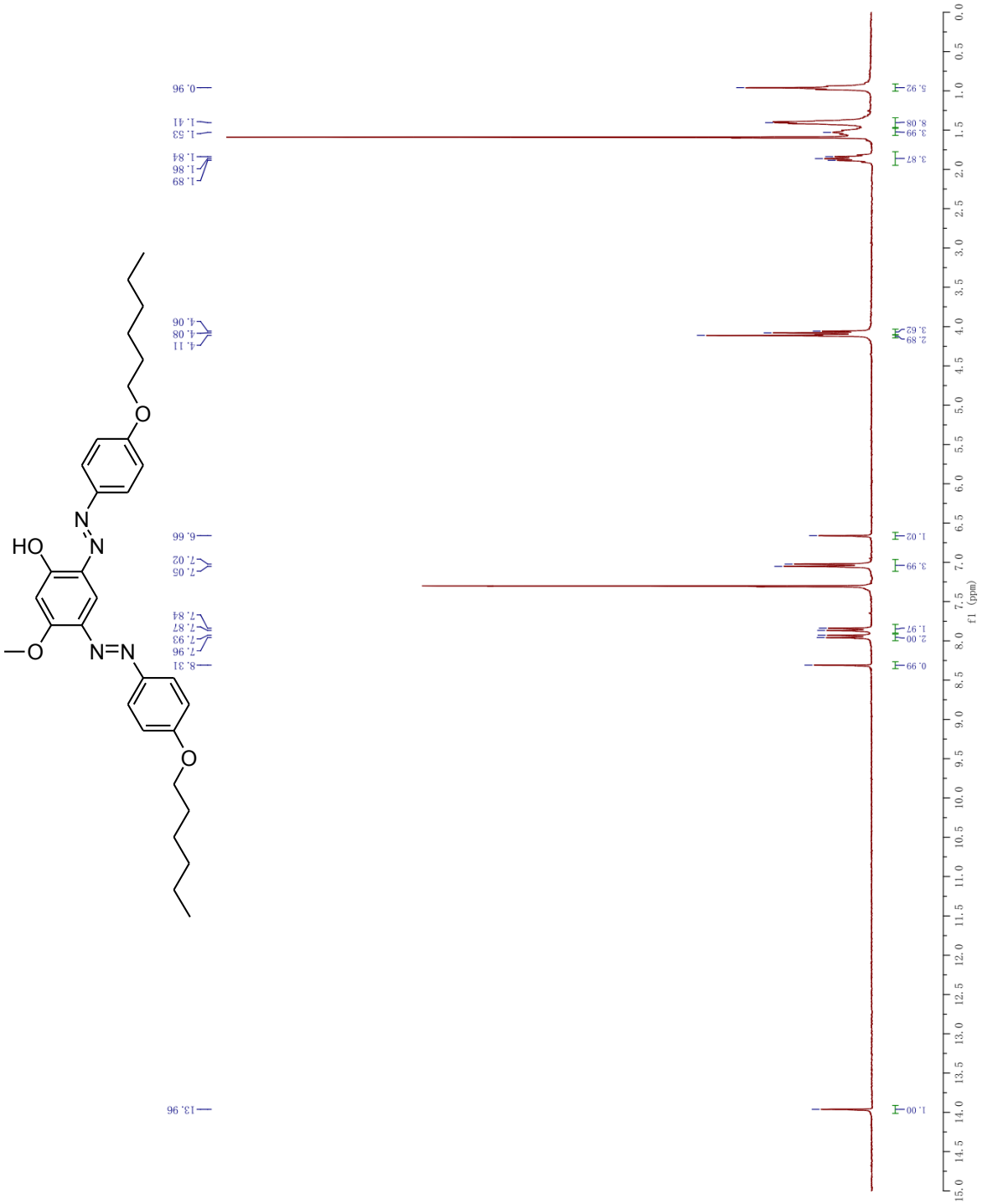

(E)-4-((4-(2-hydroxyethoxy)phenyl)diazenyl)-3-methoxyphenol (129)

(E)-2-((4-(2-hydroxyethoxy)phenyl)diazenyl)-5-methoxyphenol (130)

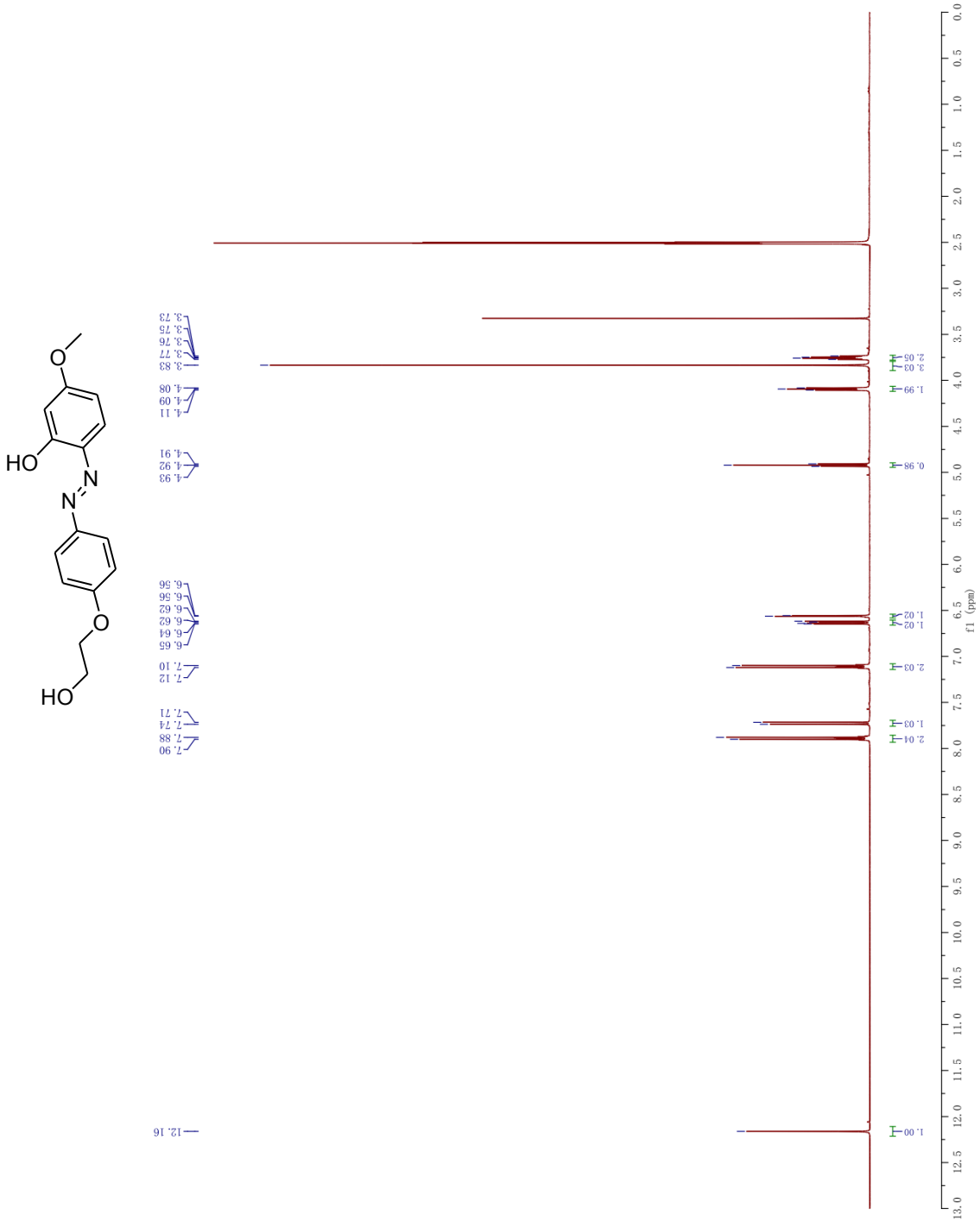

2, 4-bis((E)-(4-(2-hydroxyethoxy)phenyl)diazenyl)-5-methoxyphenol (131)

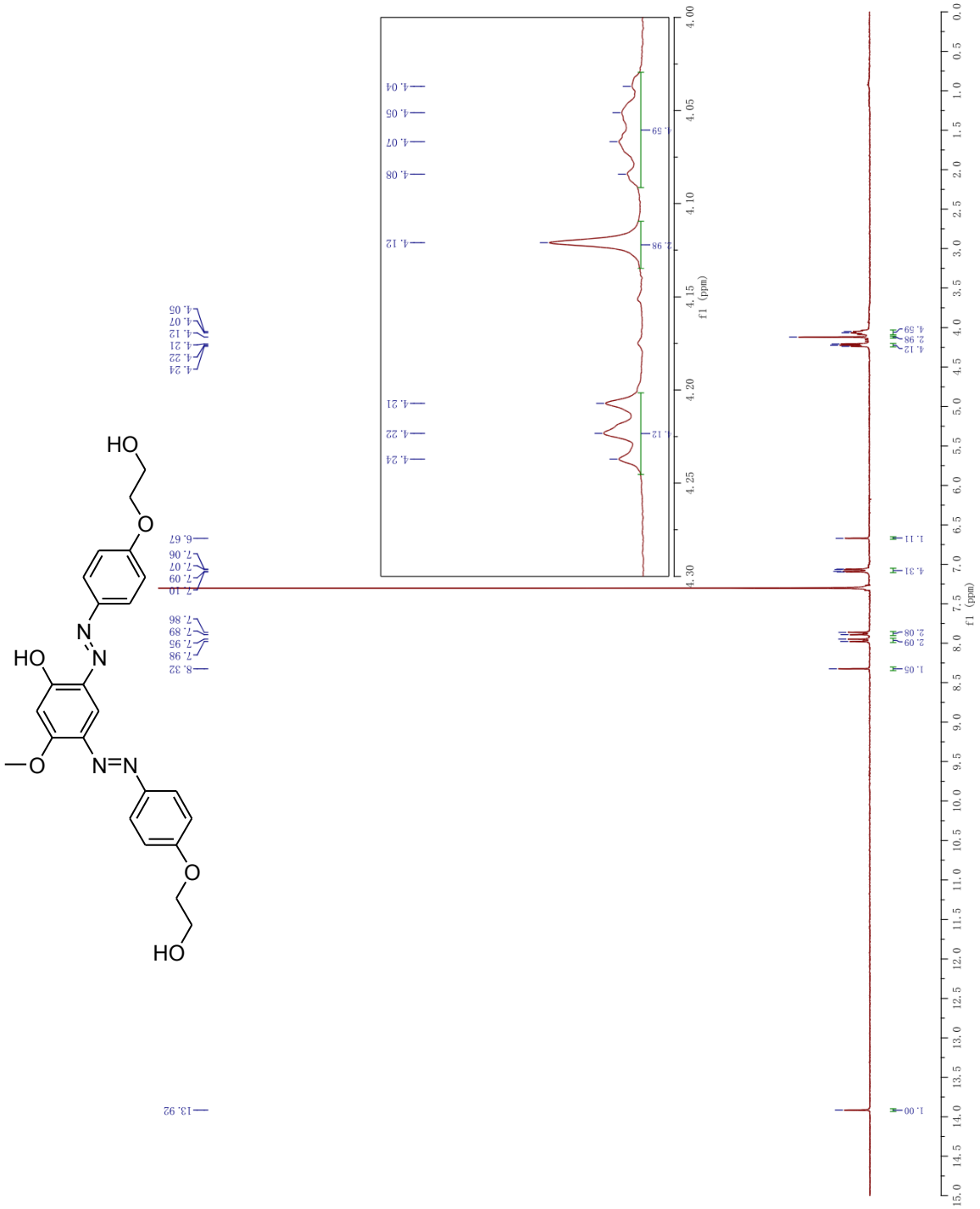

(E)-tert-butyl 4-((4-hydroxy-2-methoxyphenyl)diazenyl)benzoate (133)

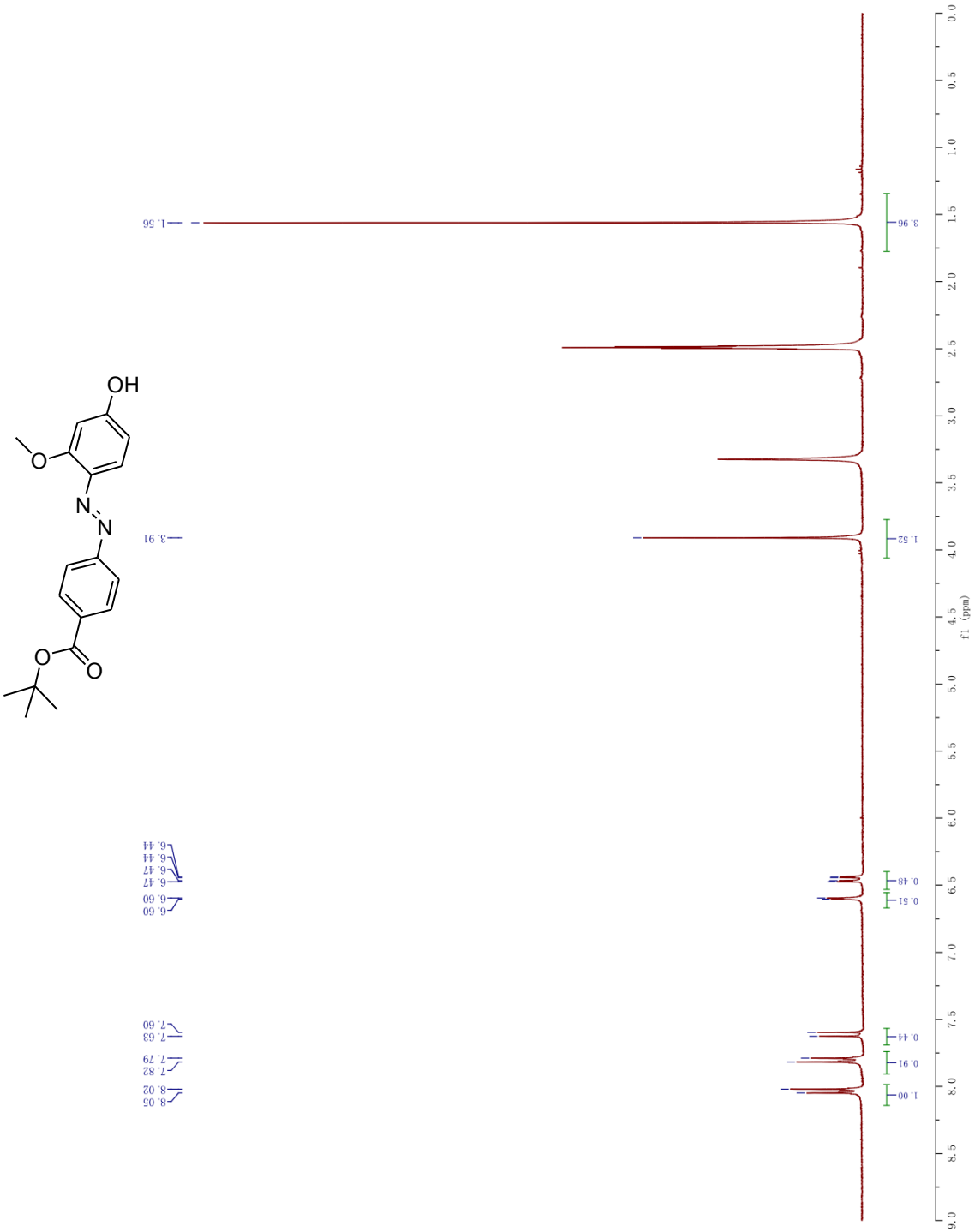

(E)-tert-butyl 4-((2-hydroxy-4-methoxyphenyl)diazenyl)benzoate (134)

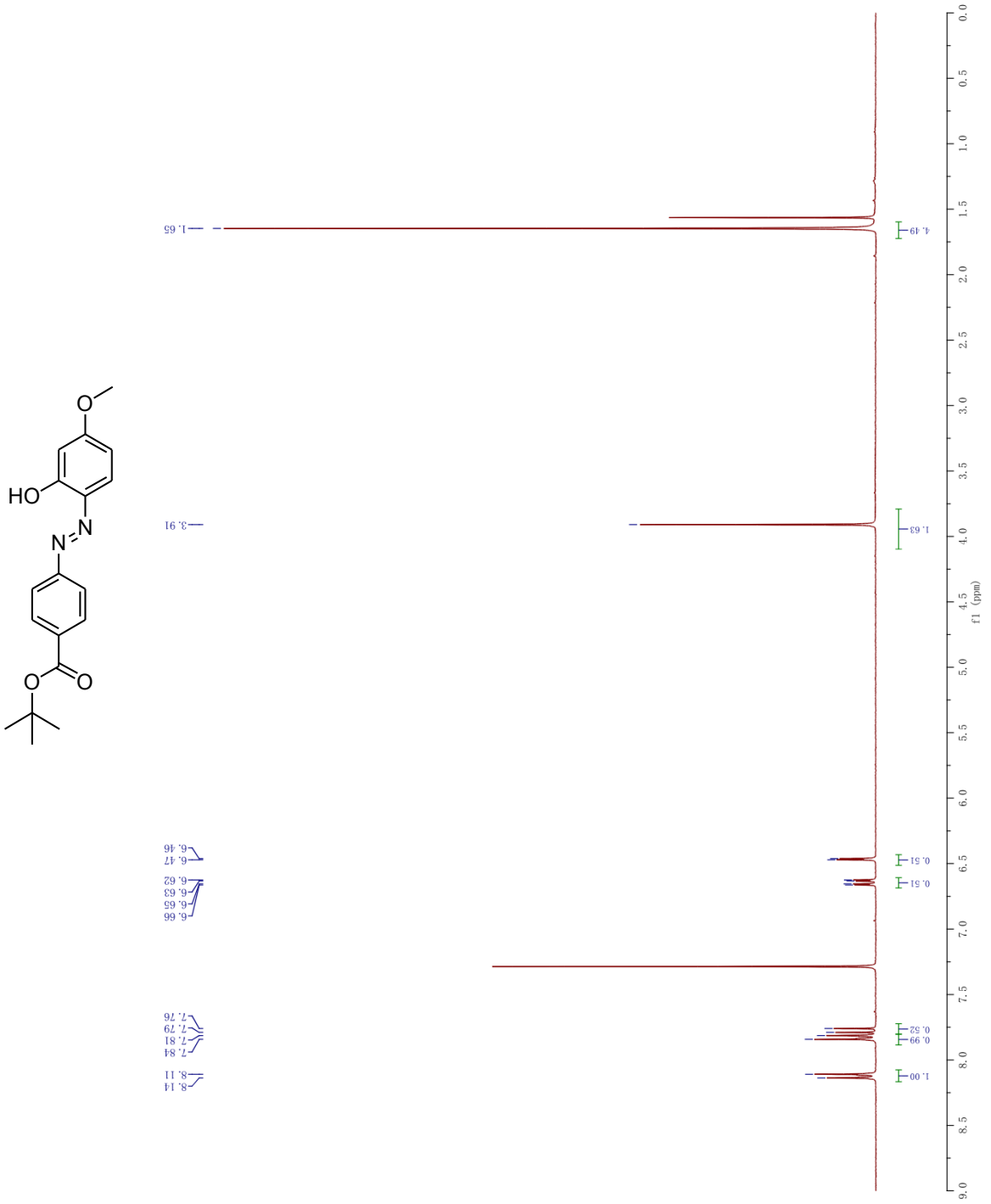

2, 4-bis((E)-(4-tert-butyl)diazenyl)-5-methoxyphenol (135)

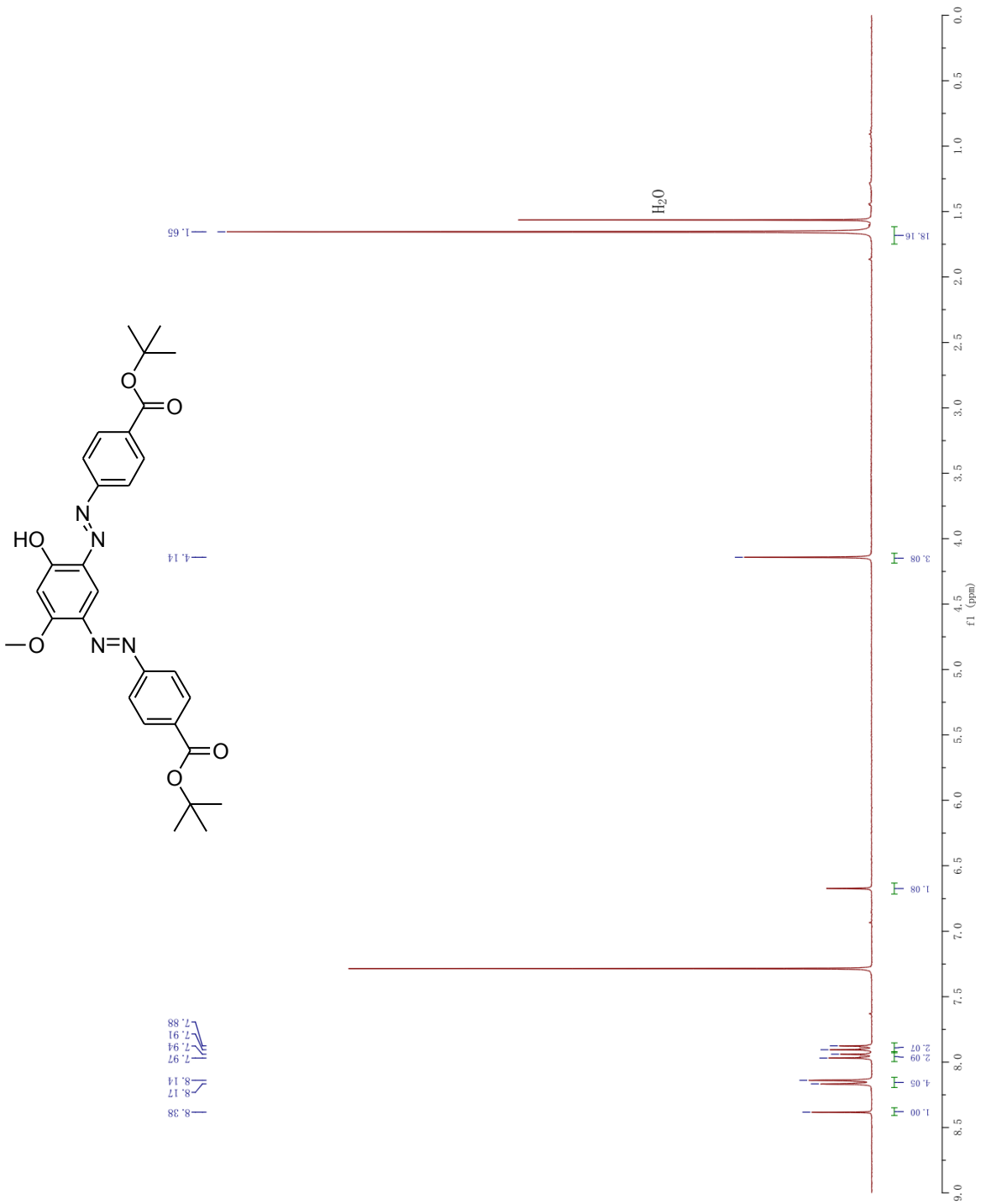

(E)-fluoro-4-((4-hydroxy-2-methoxyphenyl)diazenyl)benzoate (145)

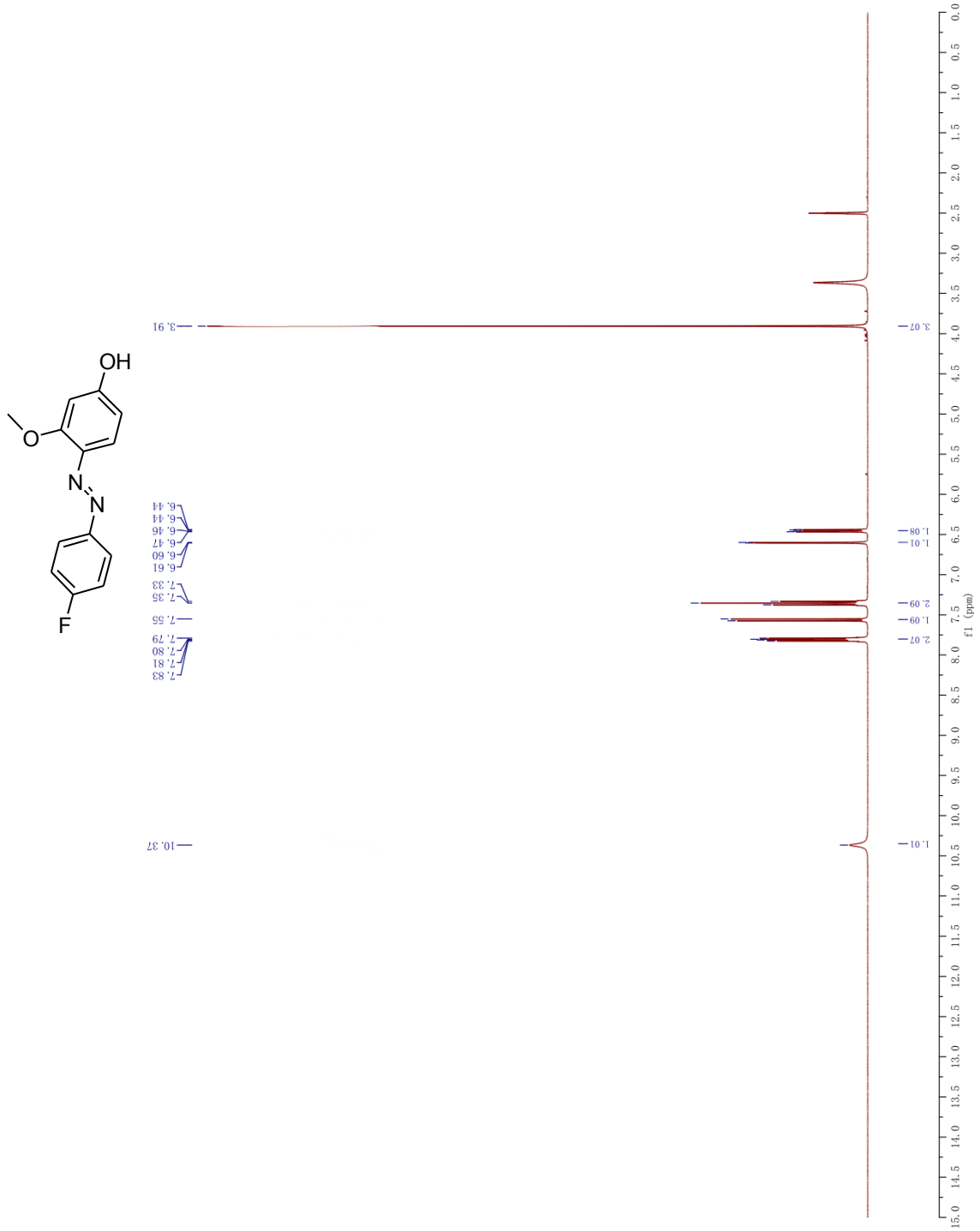

(E)-fluoro- 4-((2-hydroxy-4-methoxyphenyl)diazenyl)benzoate (146)

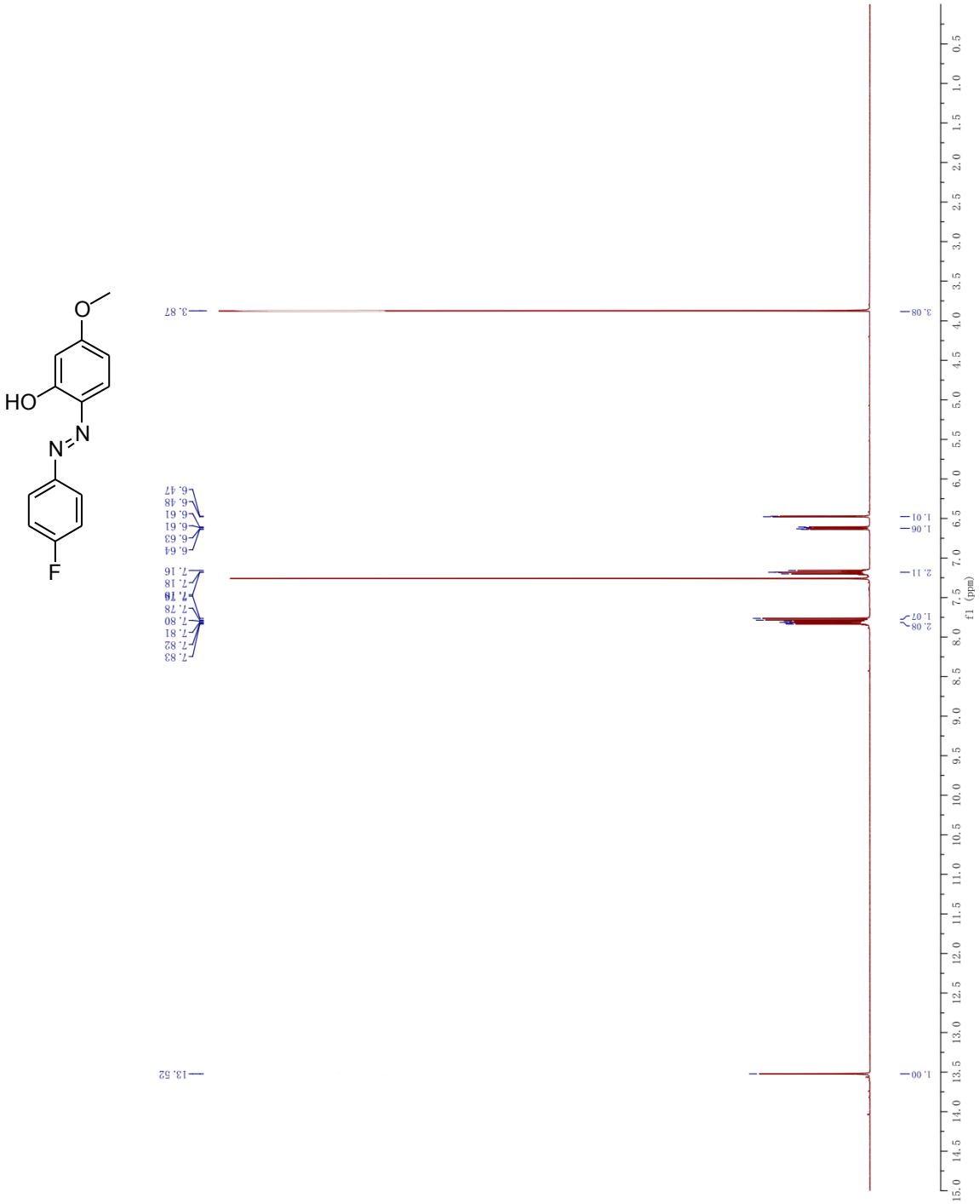

2, 4-bis((E)-(4-fluoro)diazenyl)-5-methoxyphenol (147)

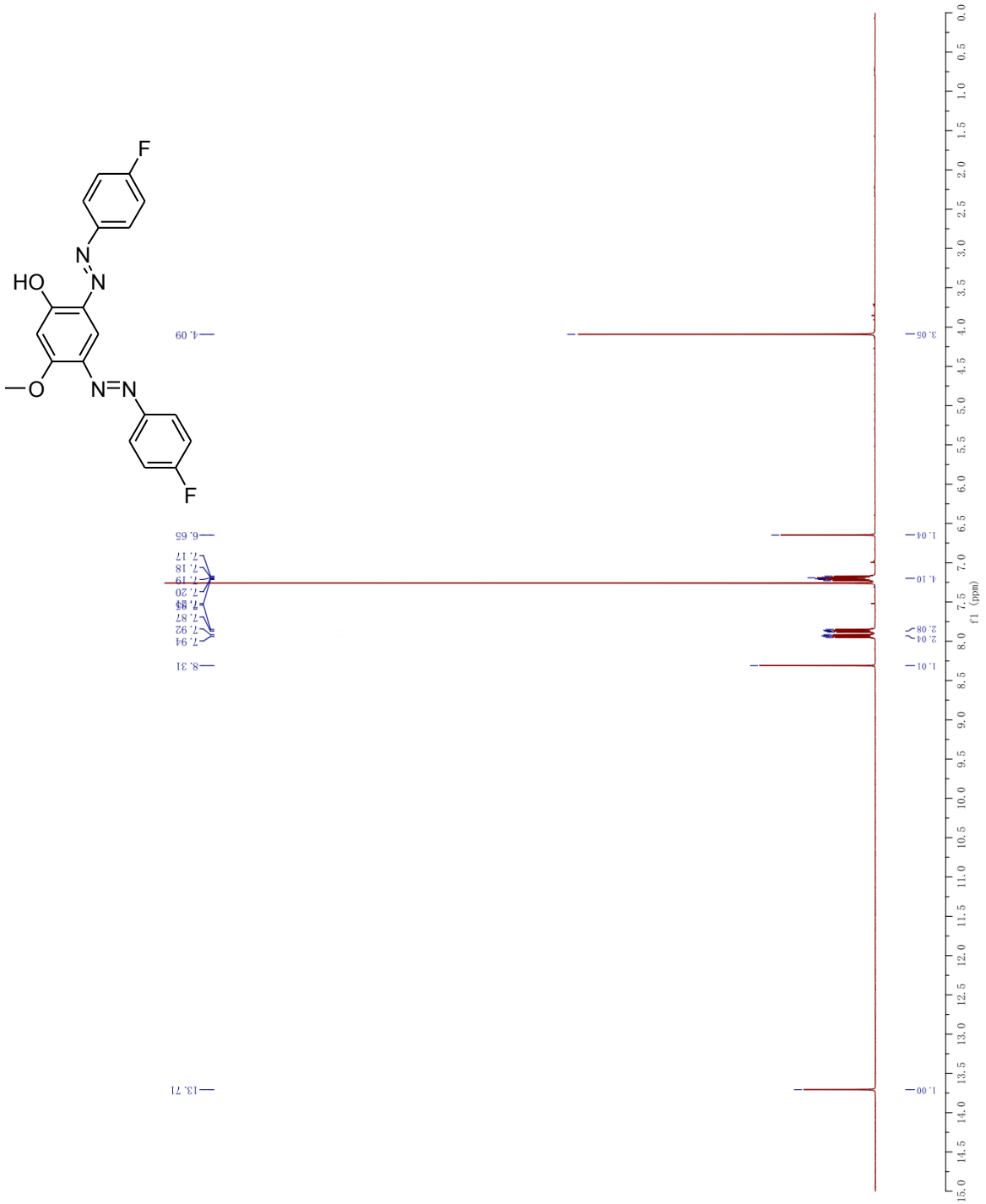

(E)-4-((2,4-difluorophenyl)diazenyl)-3-methoxyphenol (149)

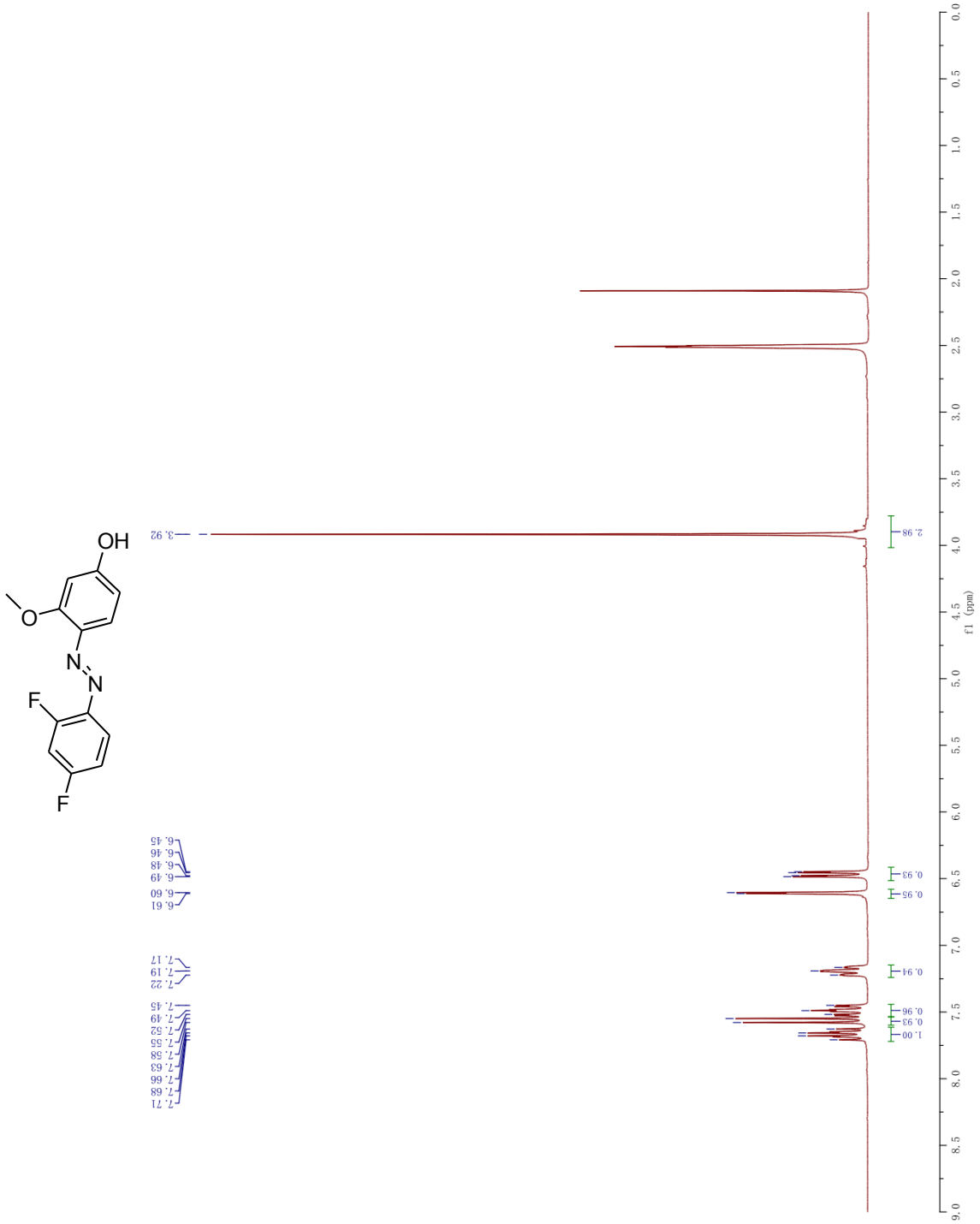

(E)-2-((2,4-difluorophenyl)diazenyl)-5-methoxyphenol (150)

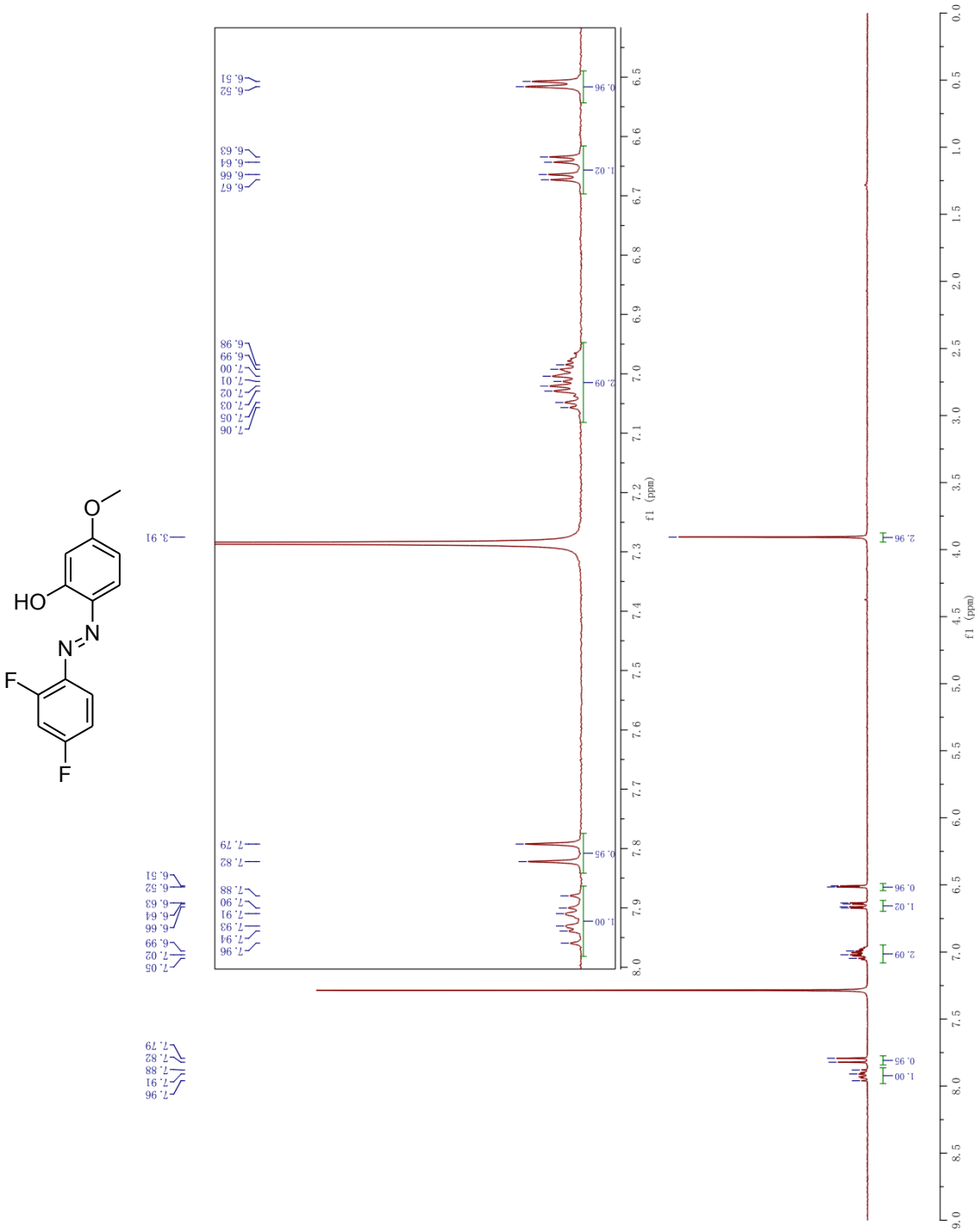

2, 4-bis((E)-(2,4-difluorophenyl)diazenyl)-5-methoxyphenol (151)

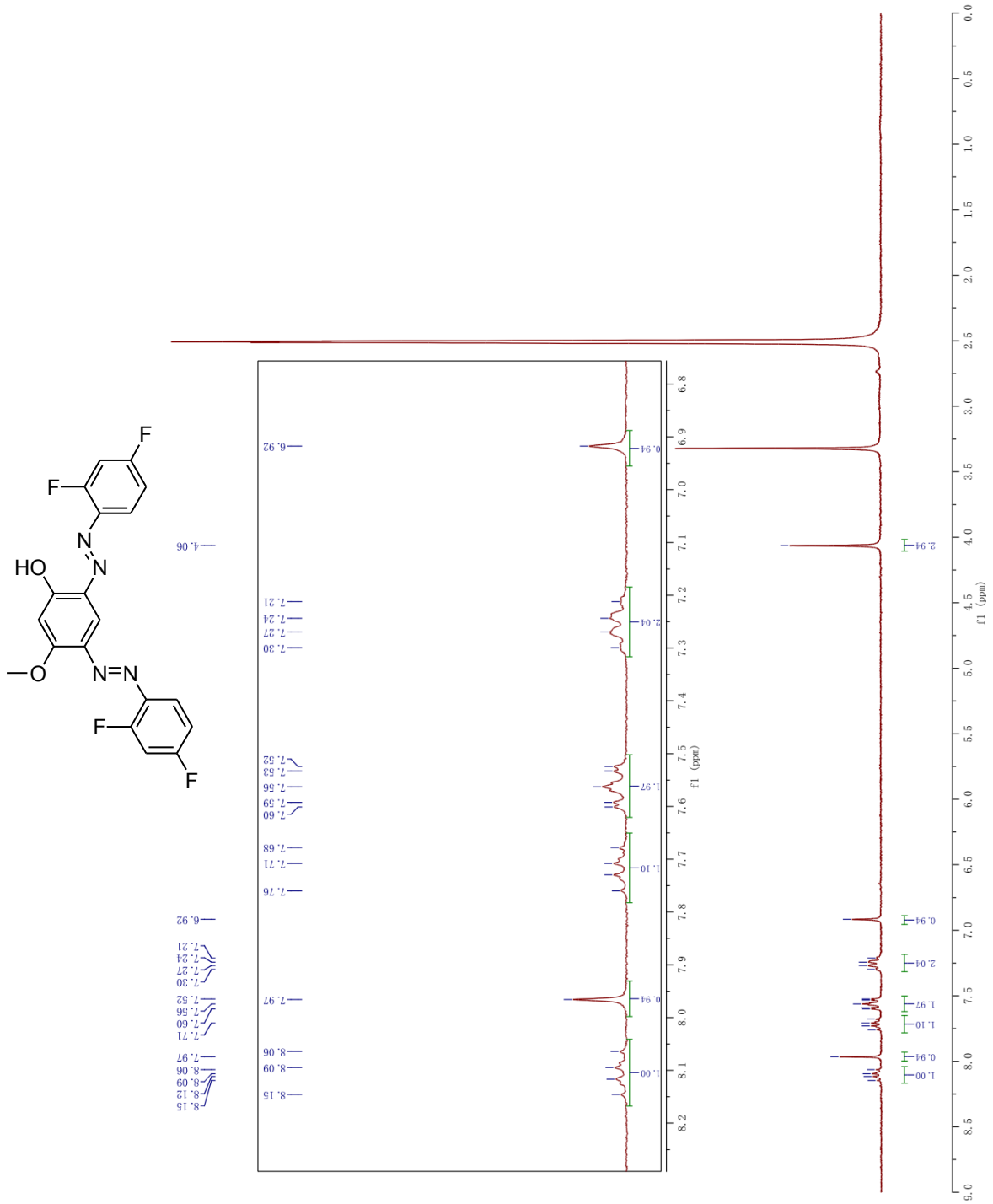

2, 4, 6-Tris-tert-butyl-phenylazo-benzene-1,3,5-triol (152)

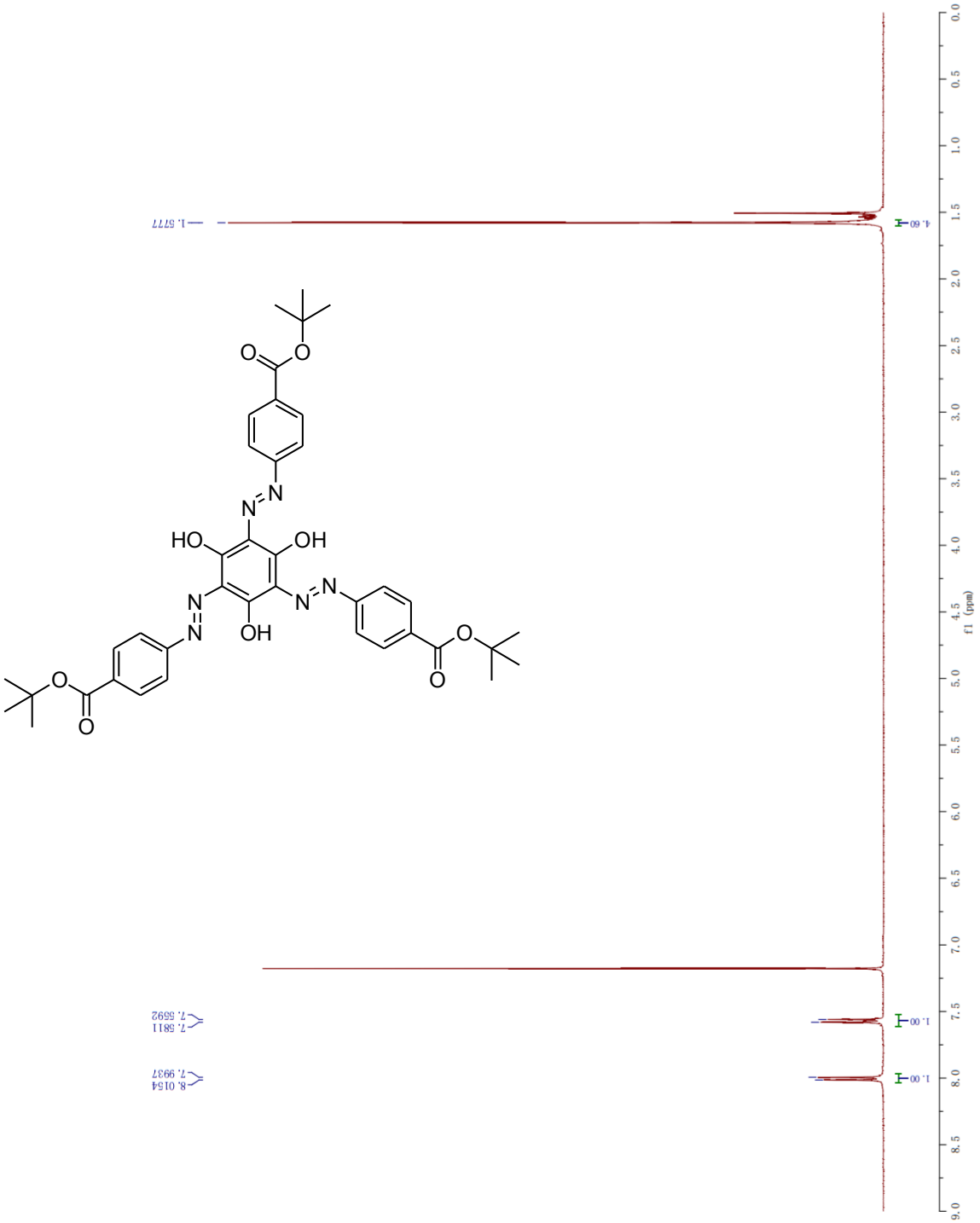

Dibenzoxadiazepines (153)

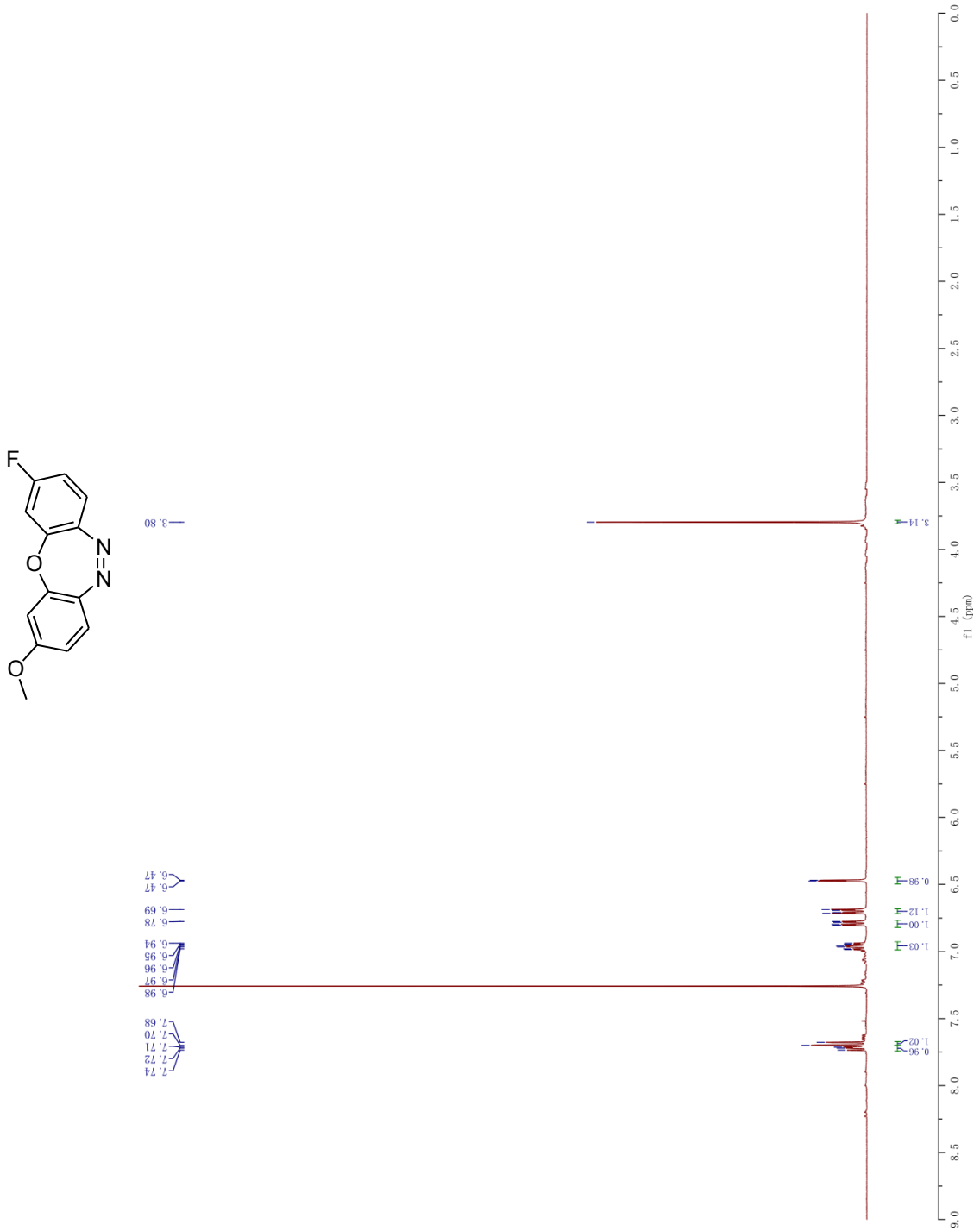

2-(2-Fluoro-phenylazo)-5-methoxy-phenol (163)

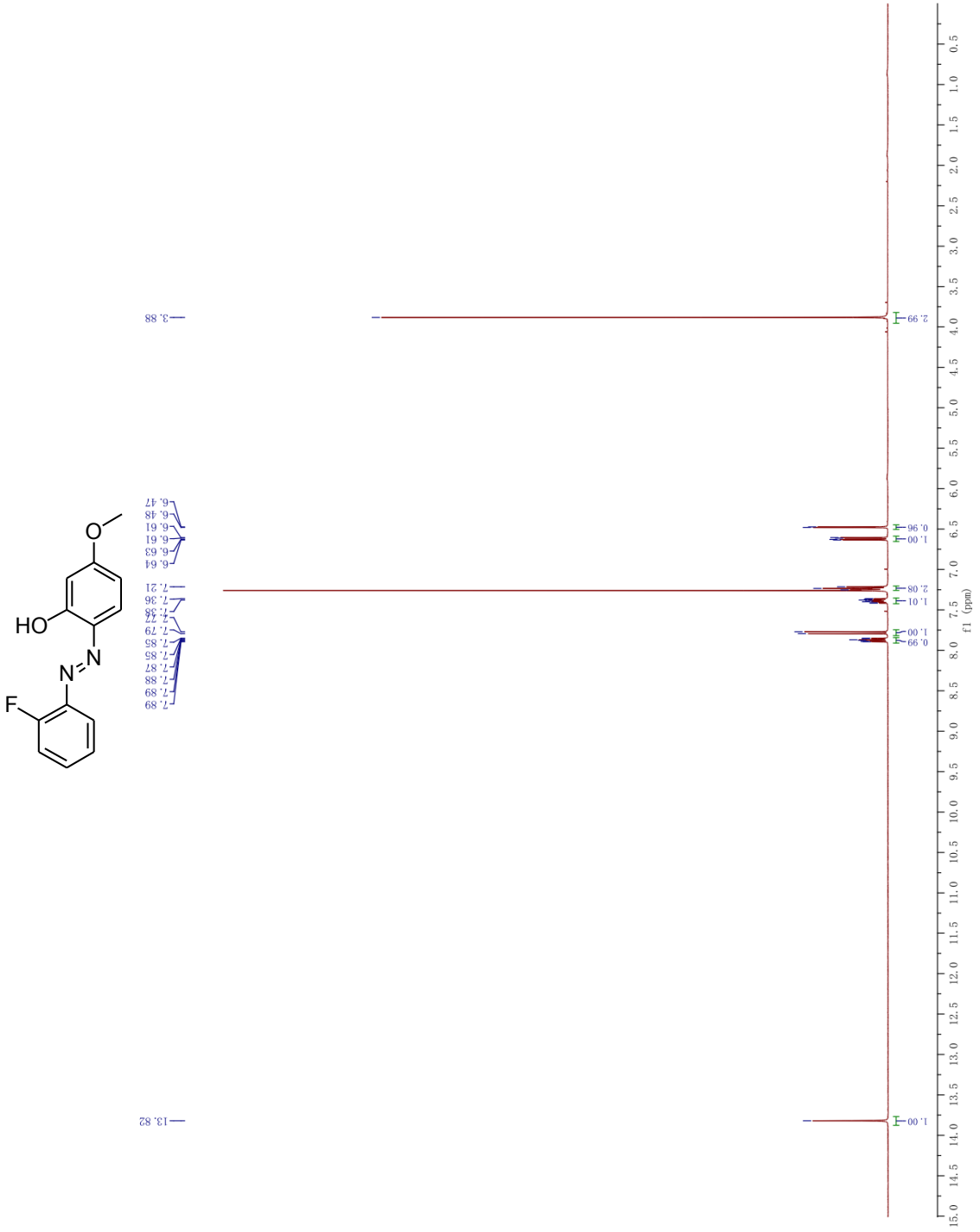

Dibenzoxadiazepines (164)

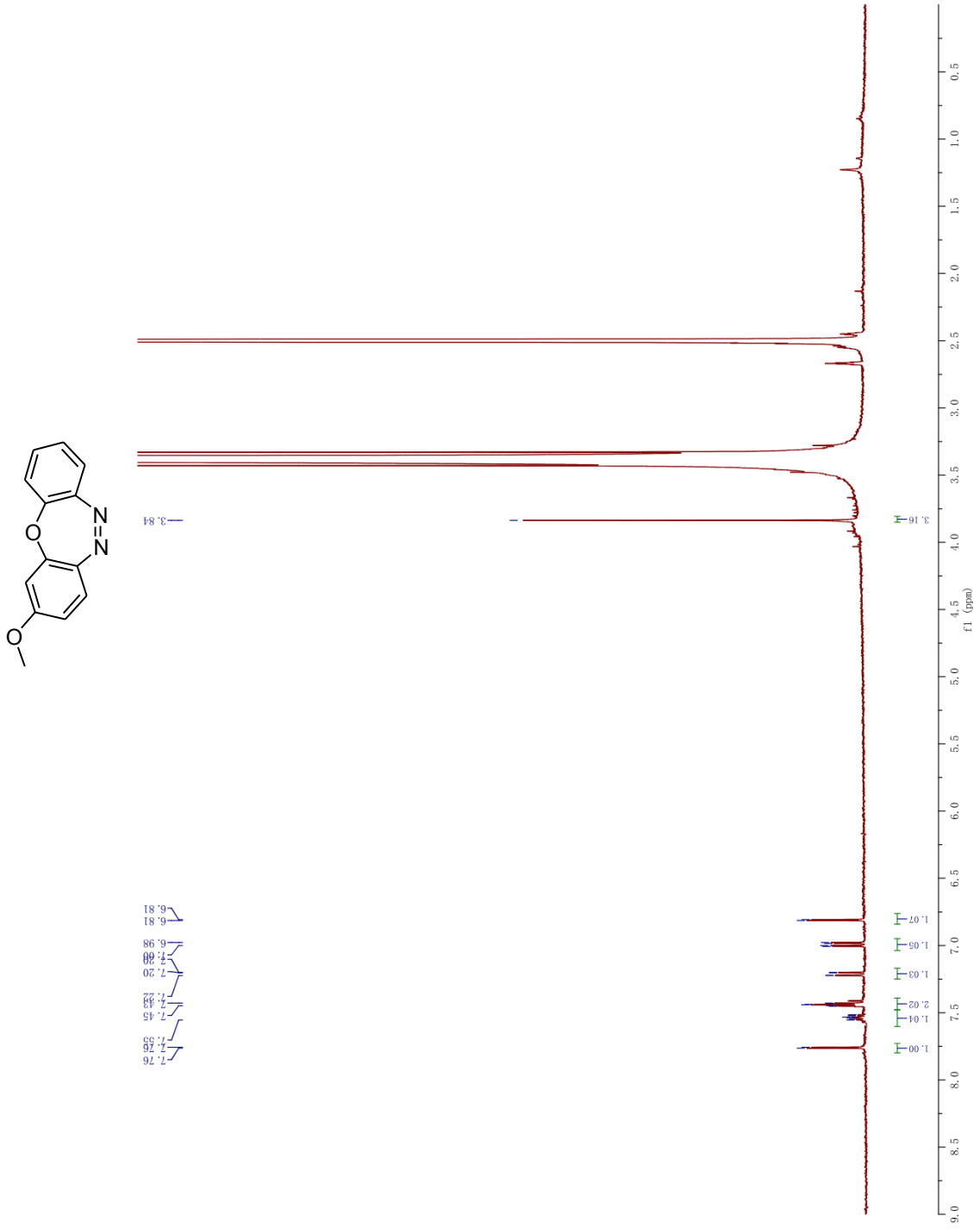

2-(2- Bromo-phenylazo)-5-methoxy-phenol (165)

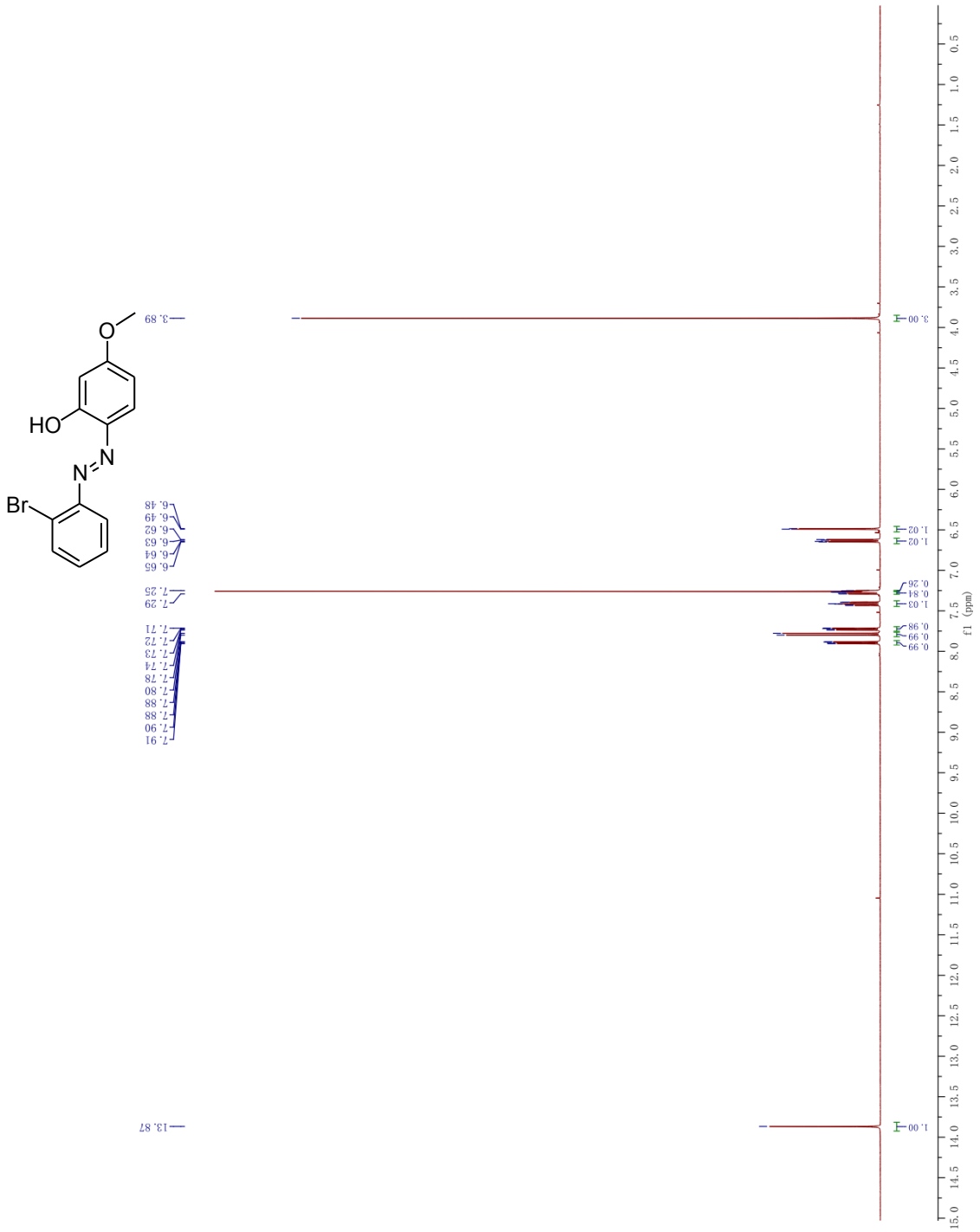

2-(2-Chloro-phenylazo)-5-methoxy-phenol (166)

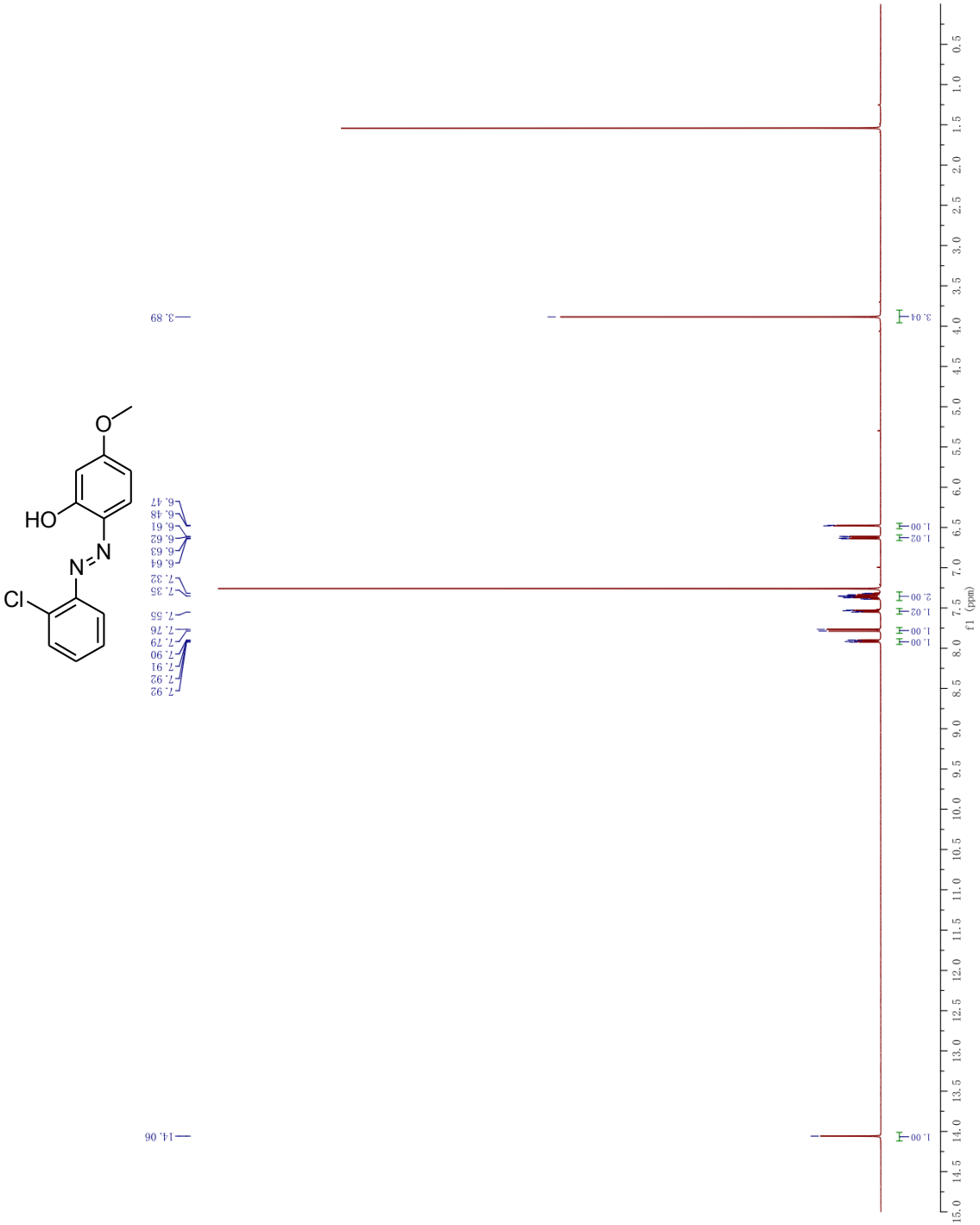

Dibenzoxadiazepine (167)

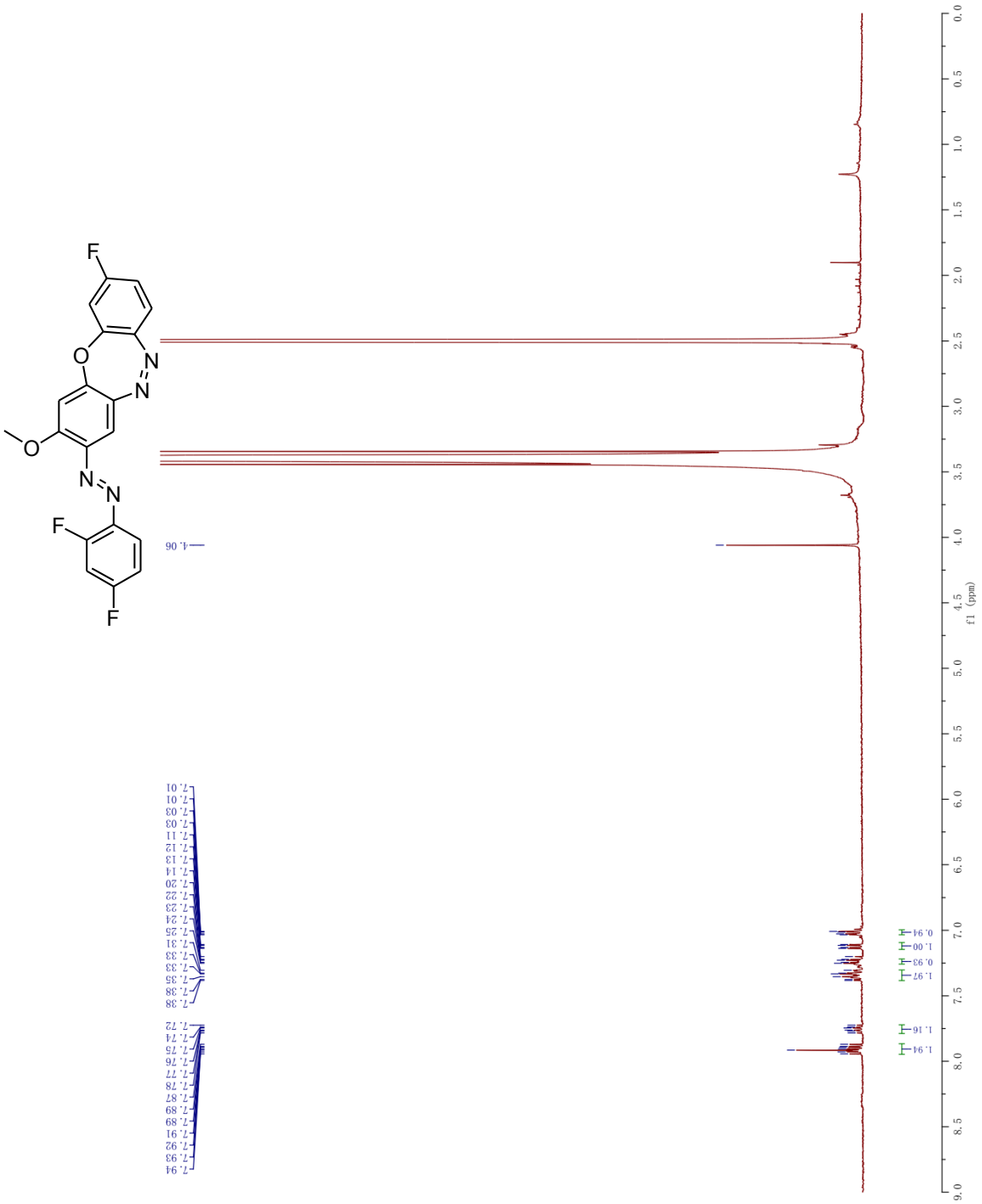

2,4-Bis-(2-Fluoro-phenylazo)-5-methoxy-phenol (168)

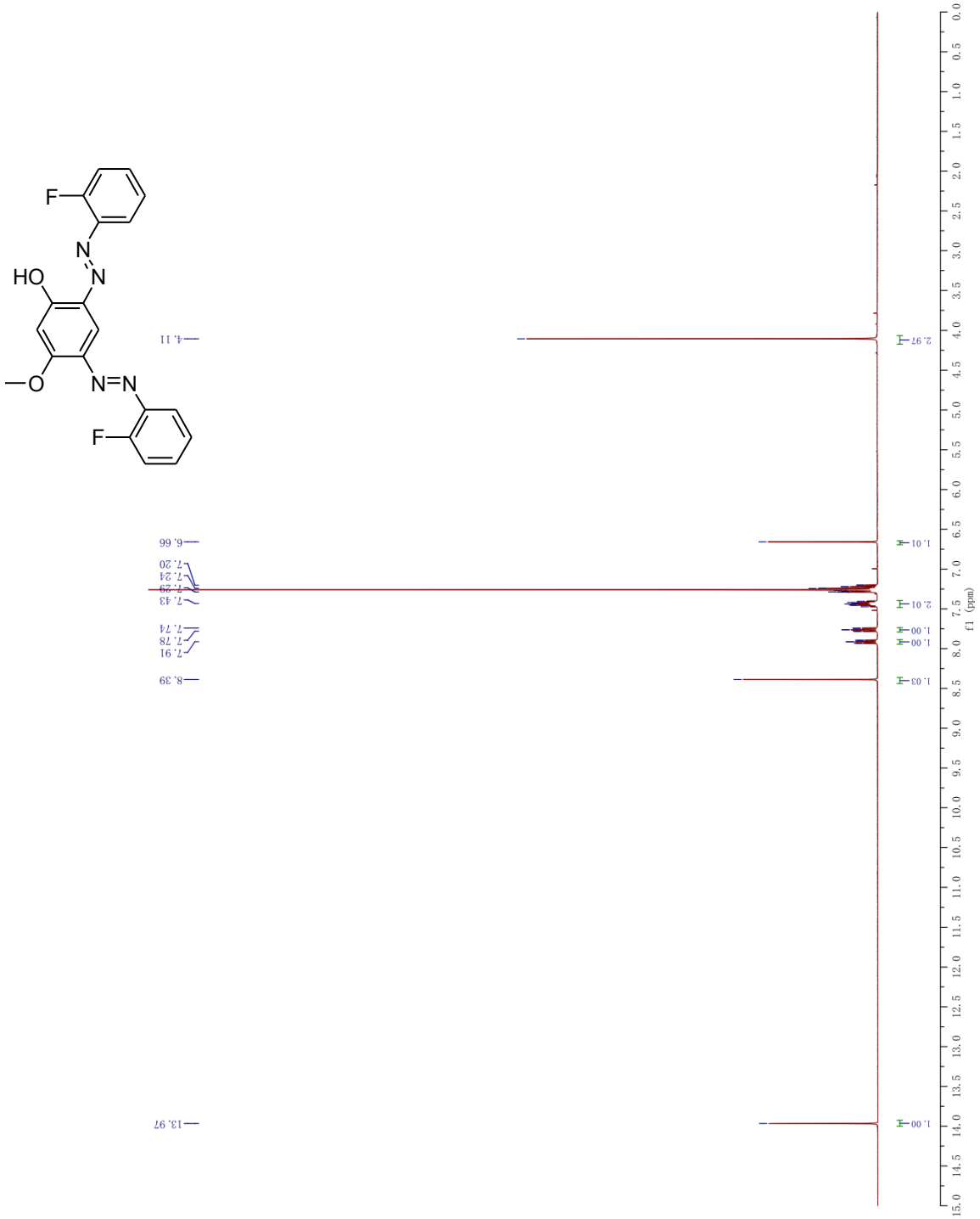

Dibenzoxadiazepine (169)

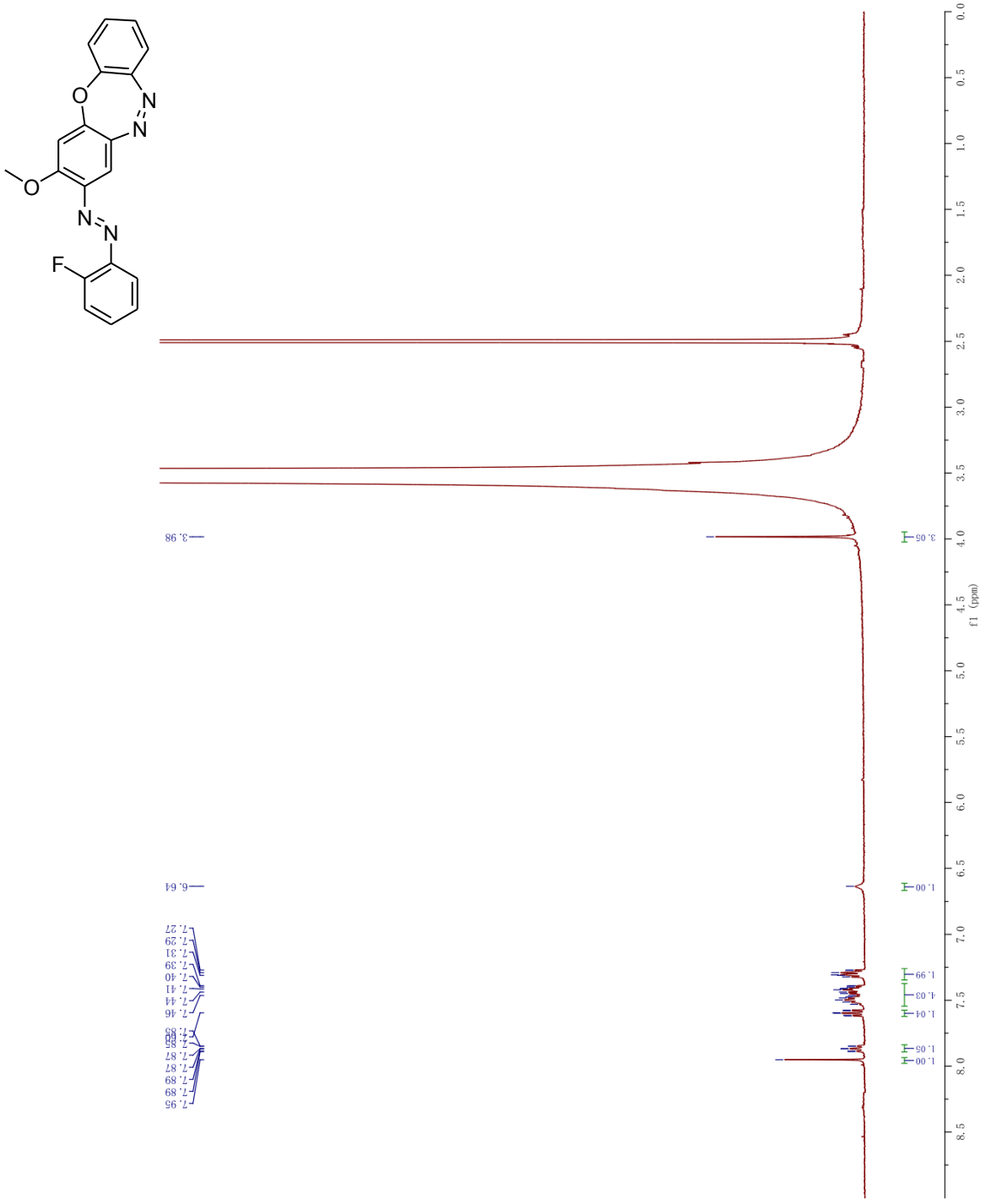

4, 6-Bis-(2,4-difluoro-phenylazo)-benzene-1, 3-diol (170)

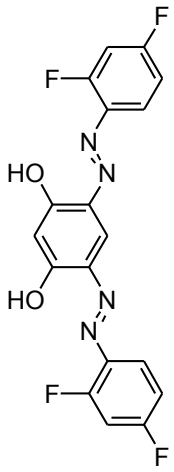

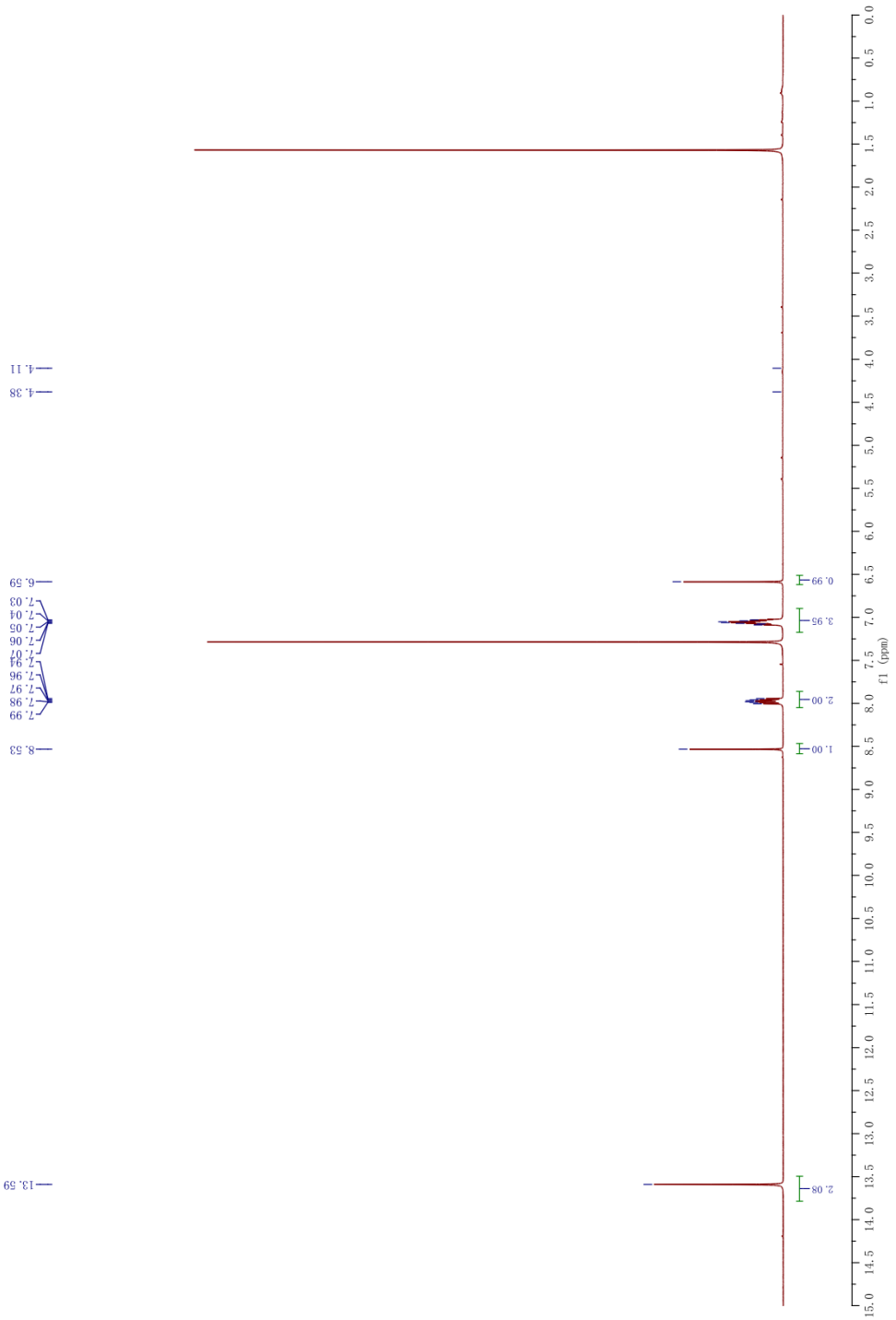

Dibenzoxadiazepine (171)

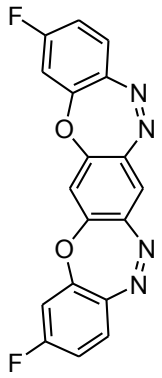

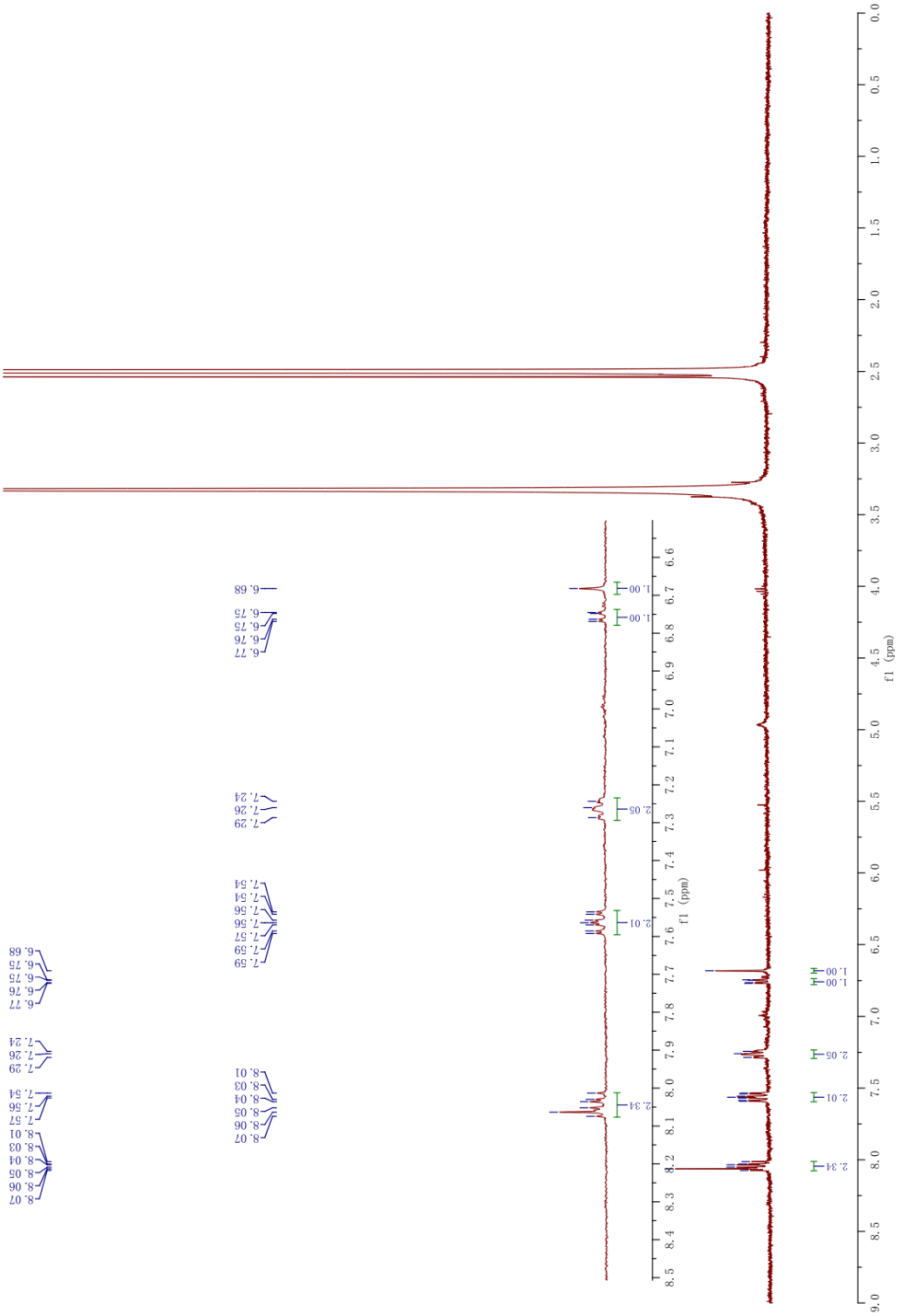

2,4-Bis-(2-Bromo-phenylazo)-5-methoxy-phenol (172)

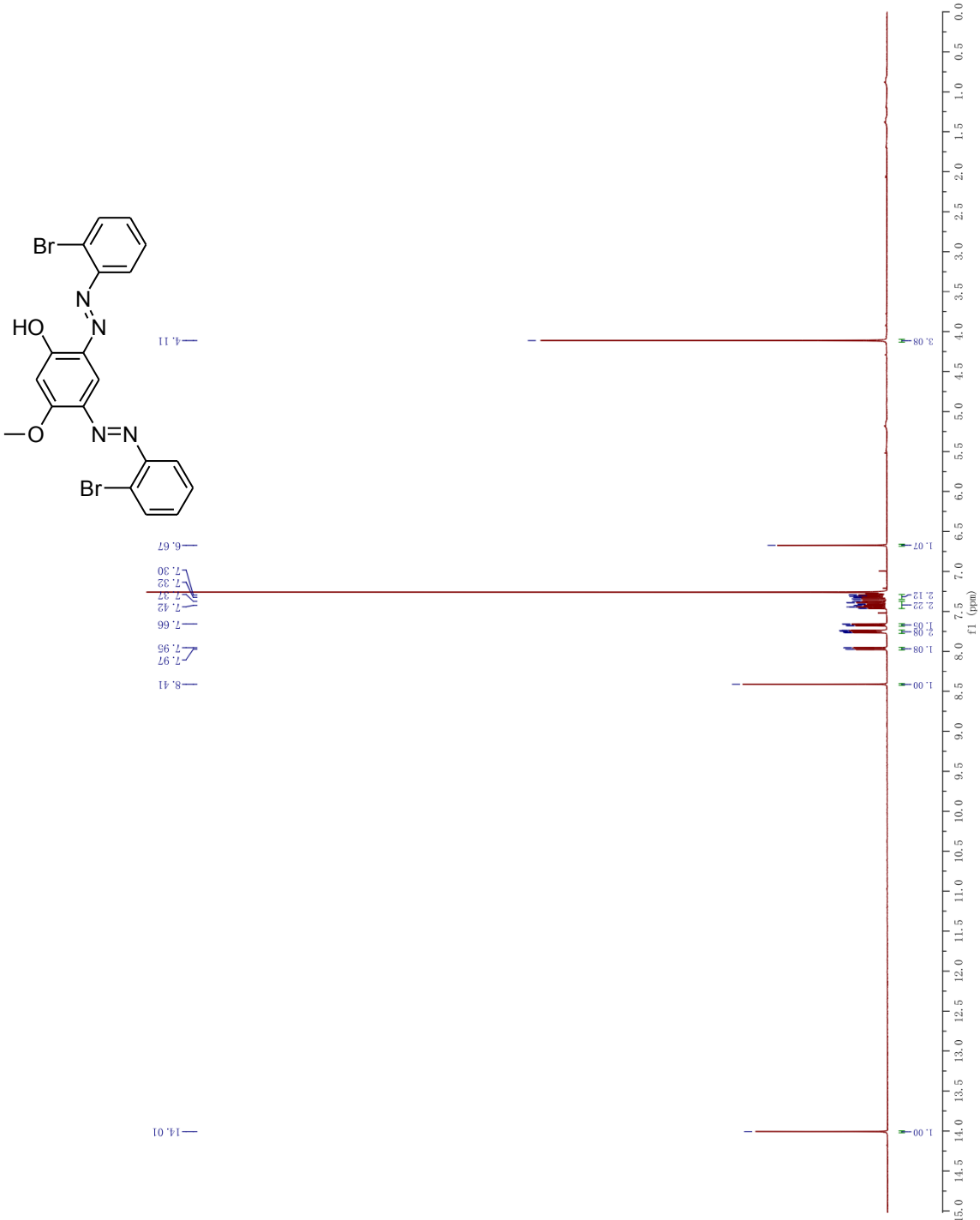

2,4-Bis-(2-chloro-phenylazo)-5-methoxy-phenol (173)

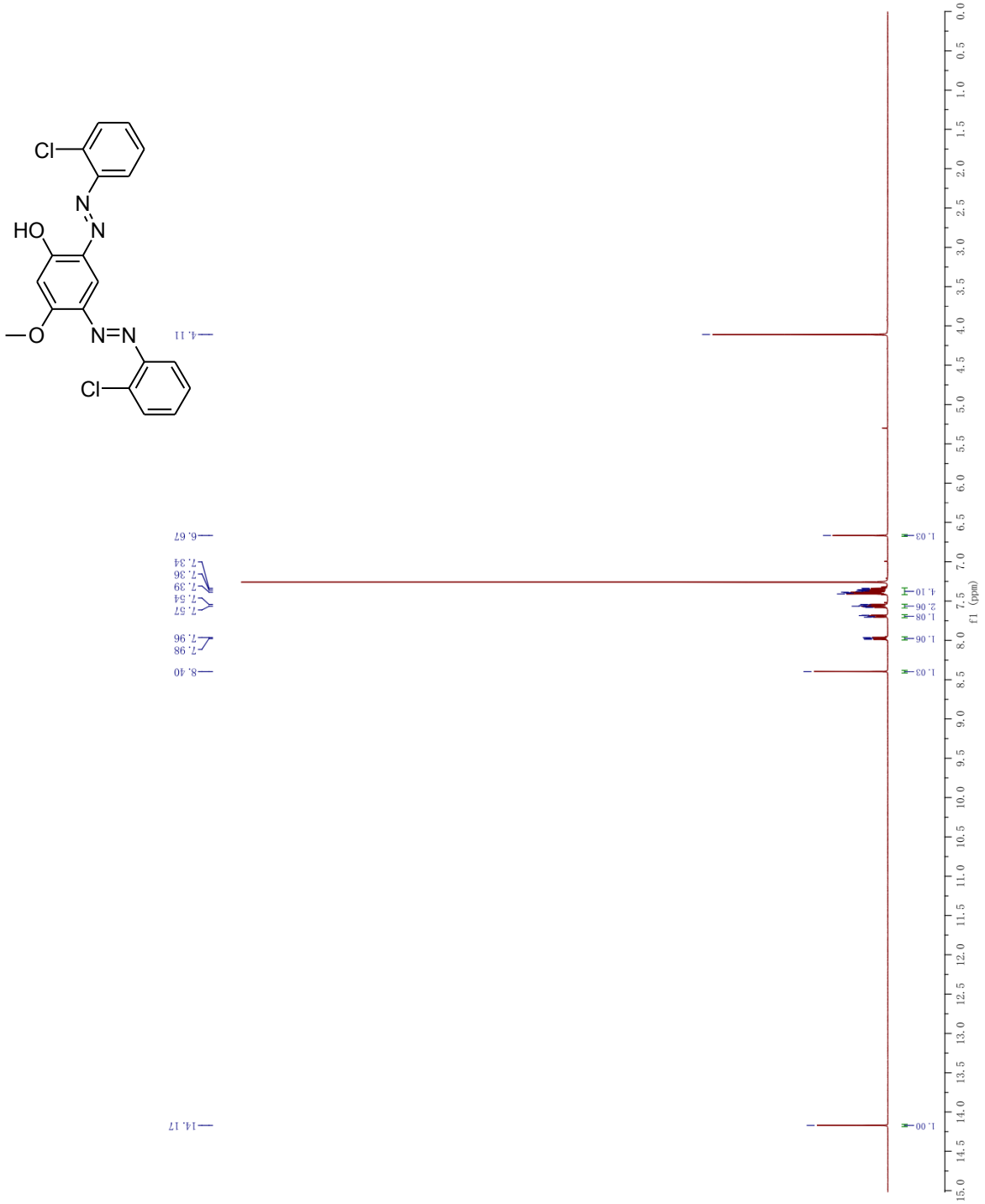

4-(2-Fluoro-phenylazo)-3-methoxy-phenol (175)

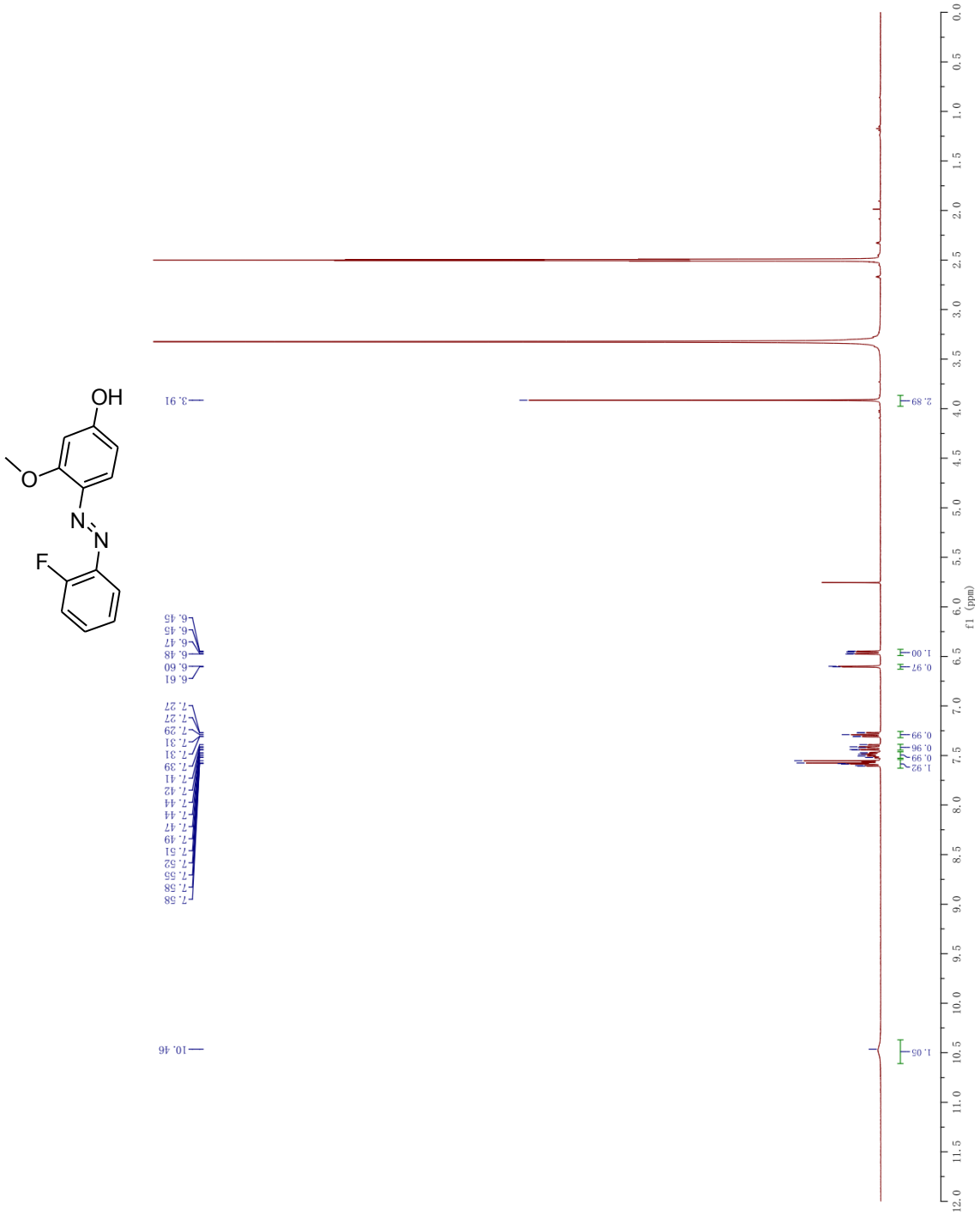

4-(2- Bromo-phenylazo)-3-methoxy-phenol (176)

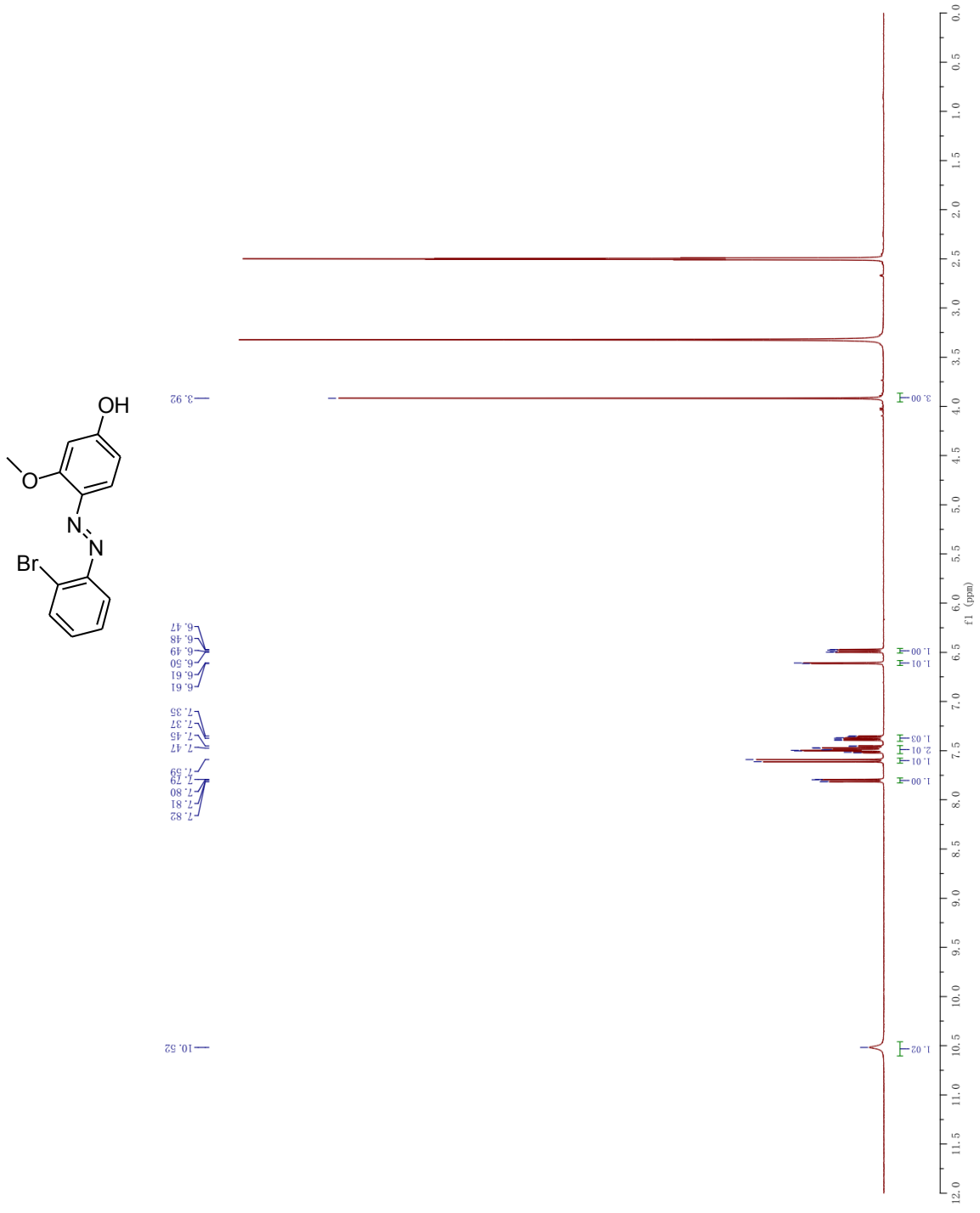

4-(2-Chloro-phenylazo)-3-methoxy-phenol (177)

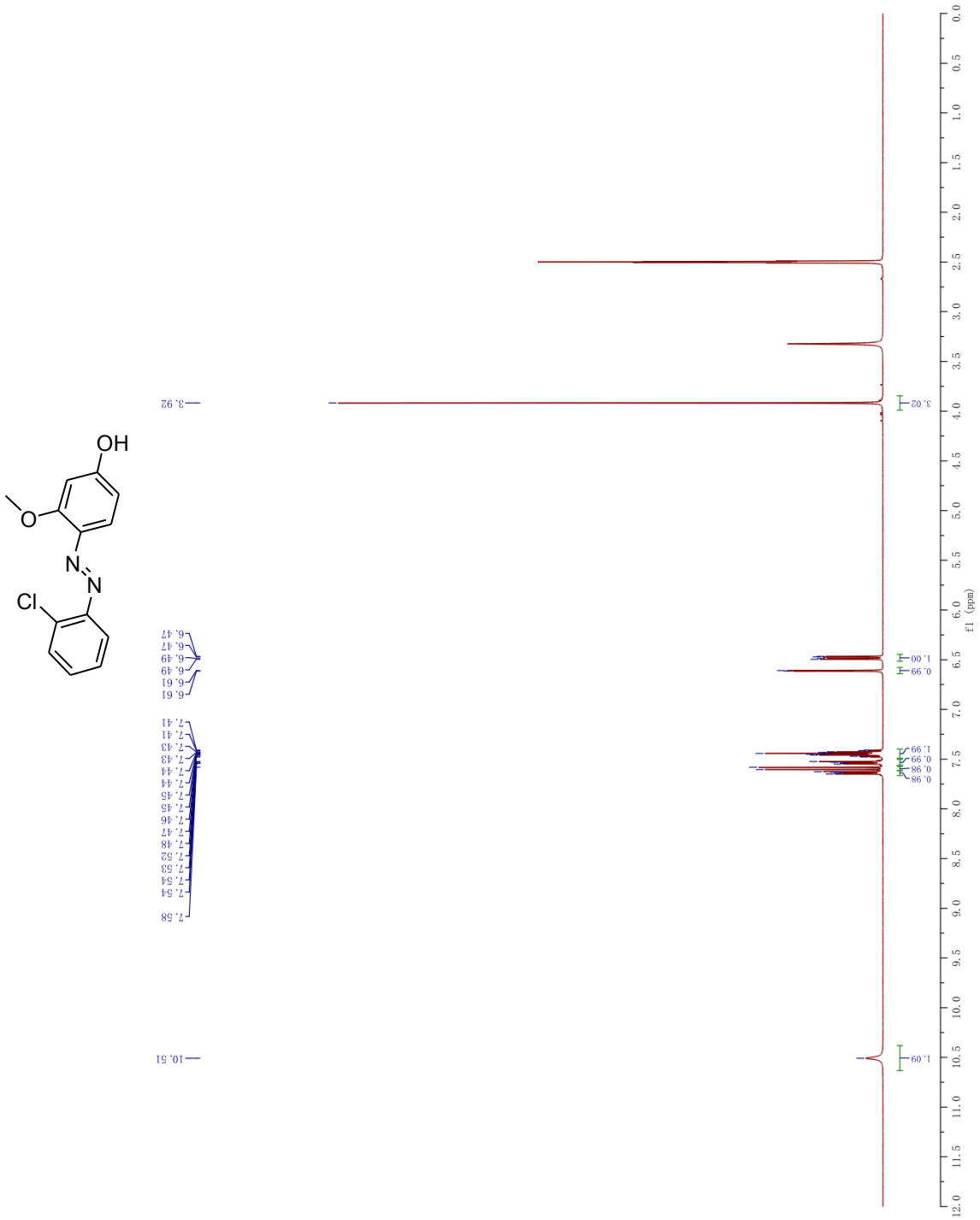

4-(2, 4-Difluoro-phenylazo)-benzene-1, 3-diol (178)

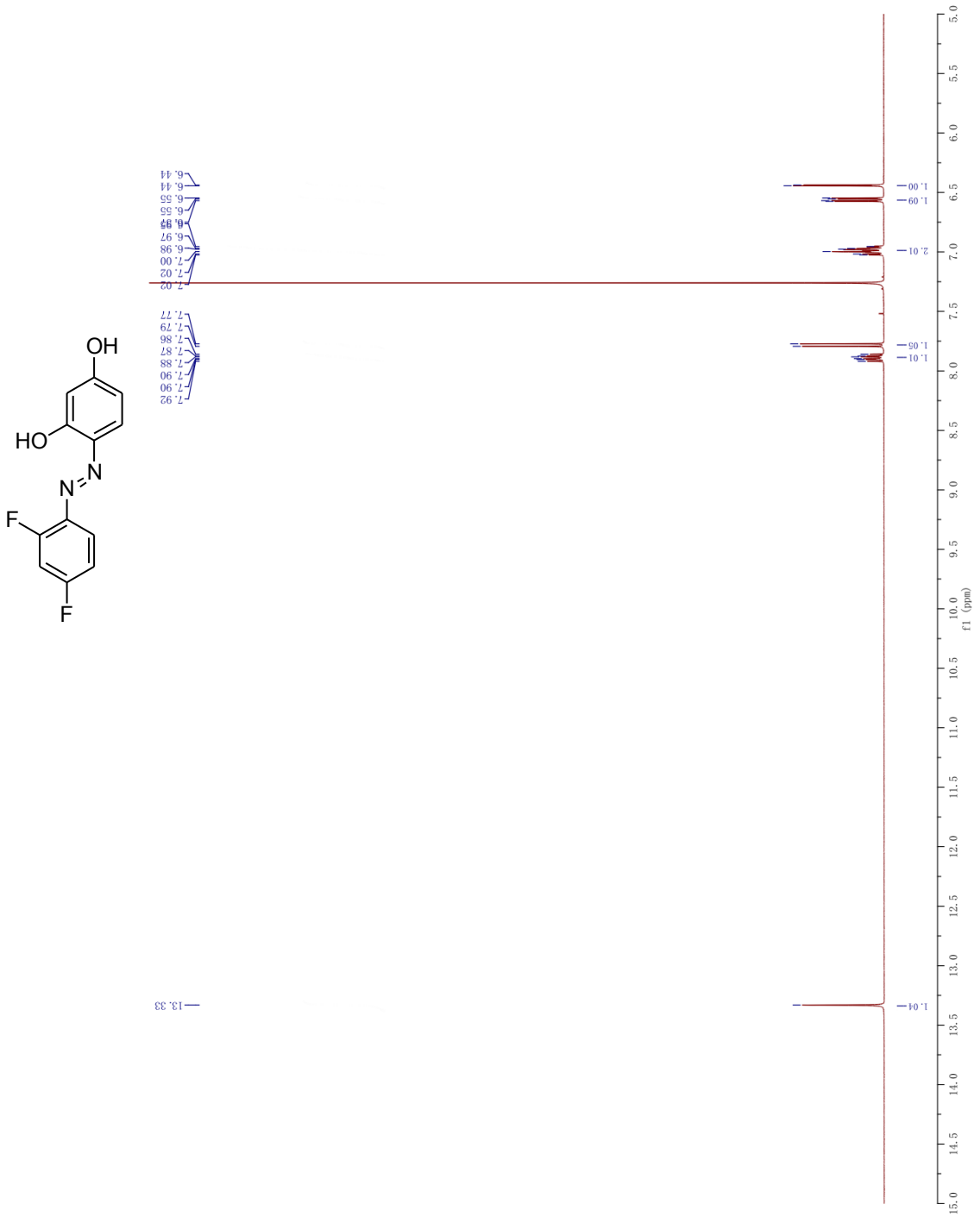

2-Methyl-acrylic acid 2-bromo-ethyl ester (182)

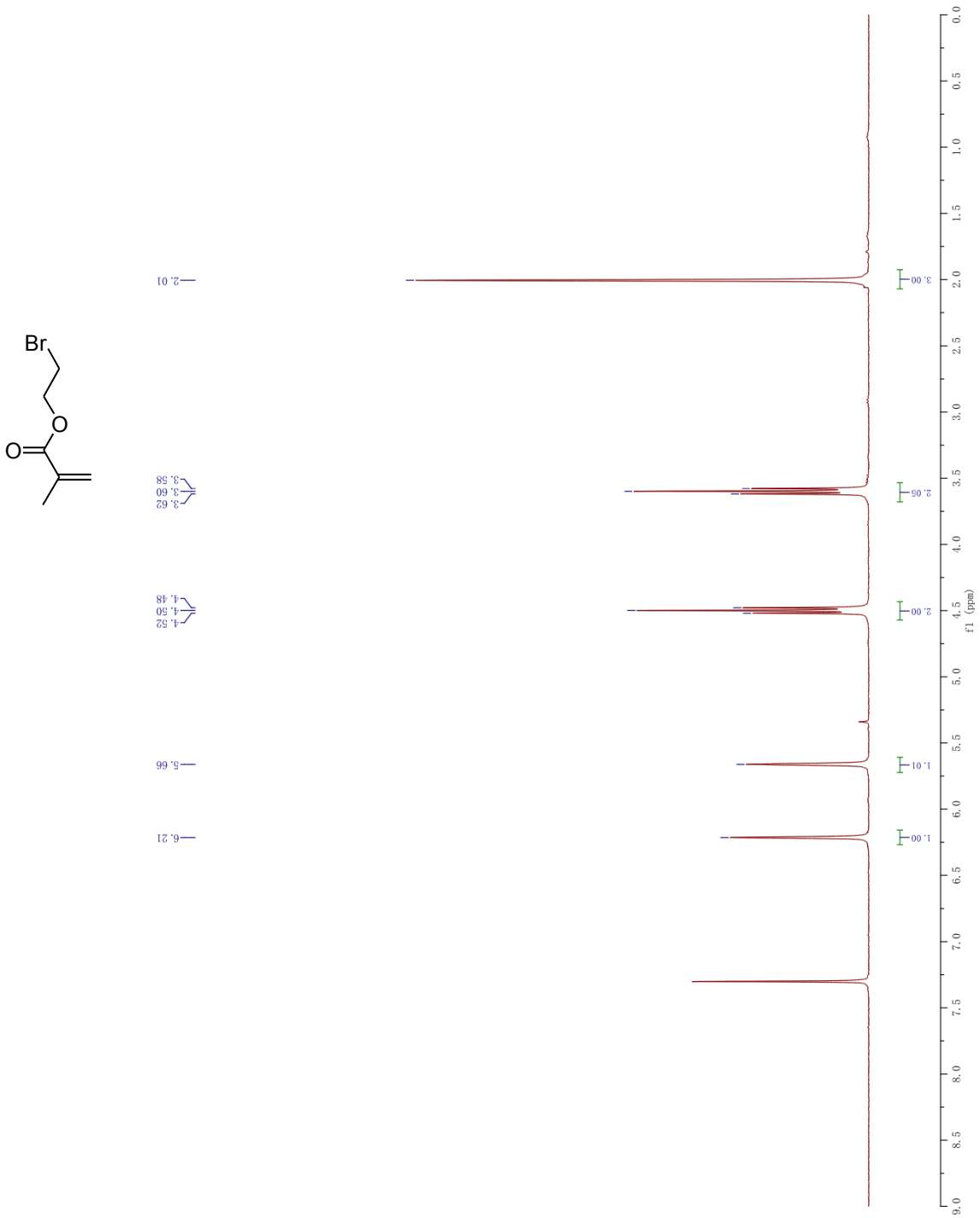

2-Methyl-acrylic acid 2-azido-ethyl ester (183)

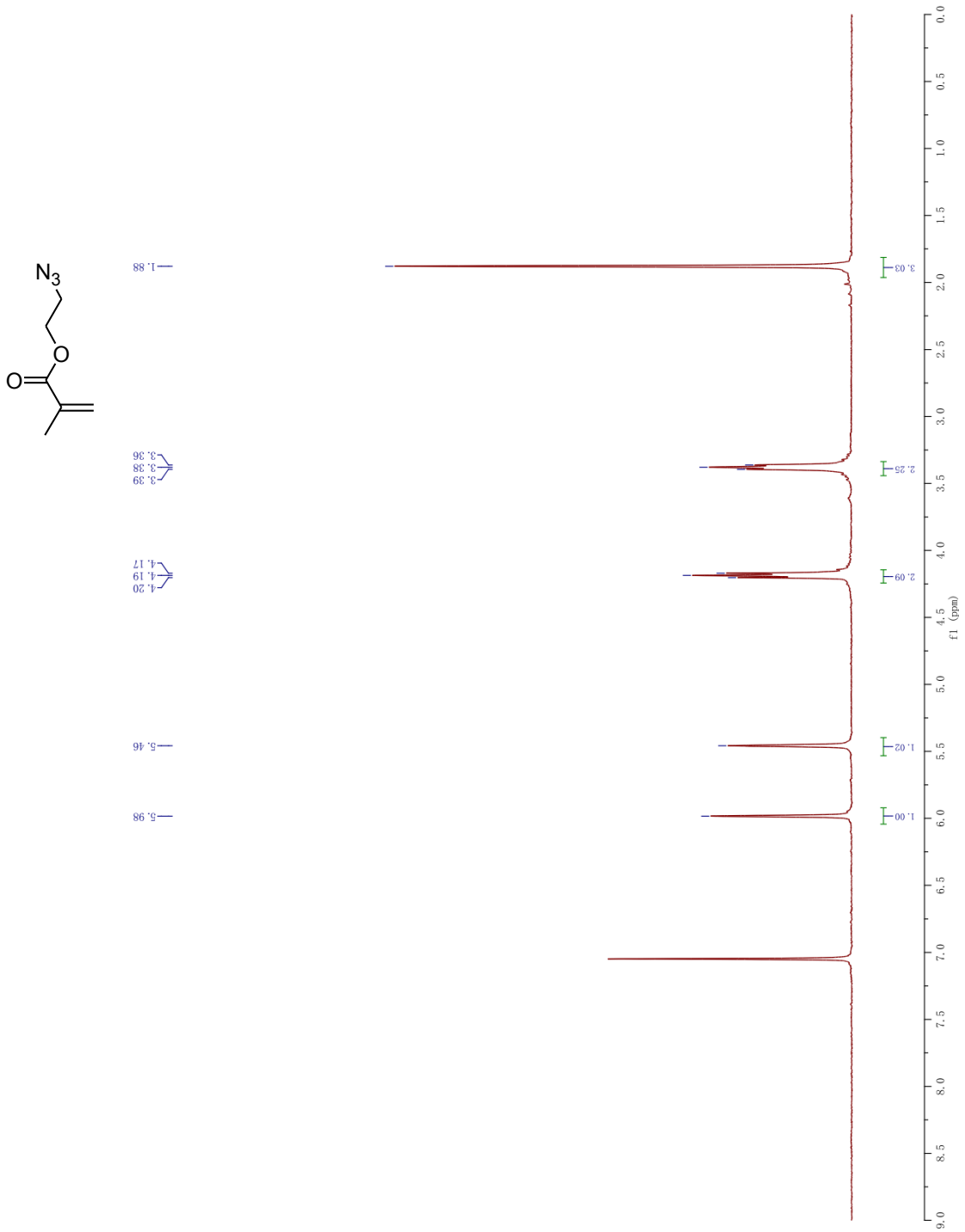

Compound 184

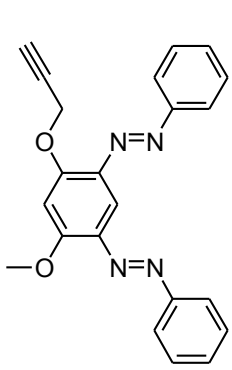

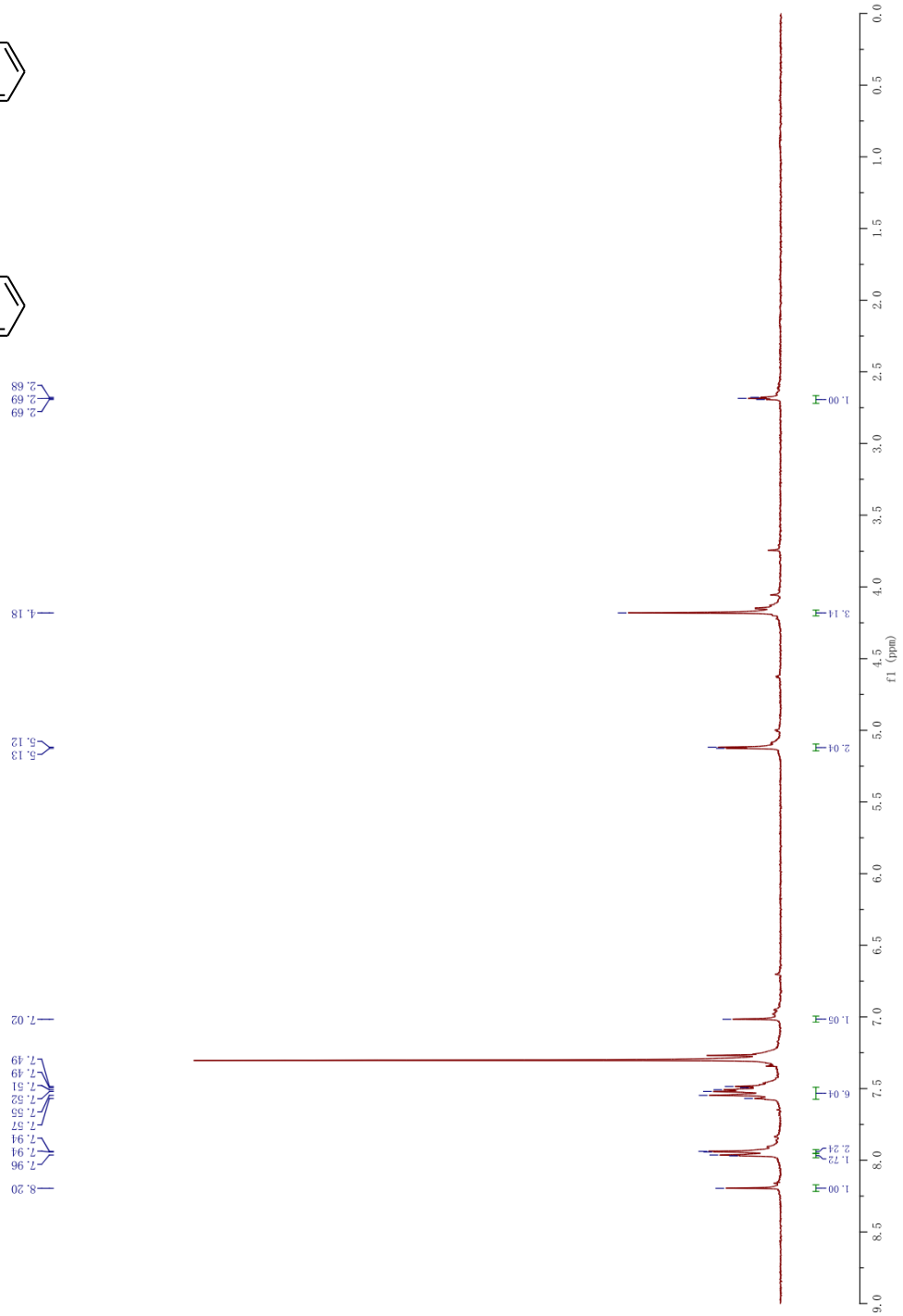

Compound 185

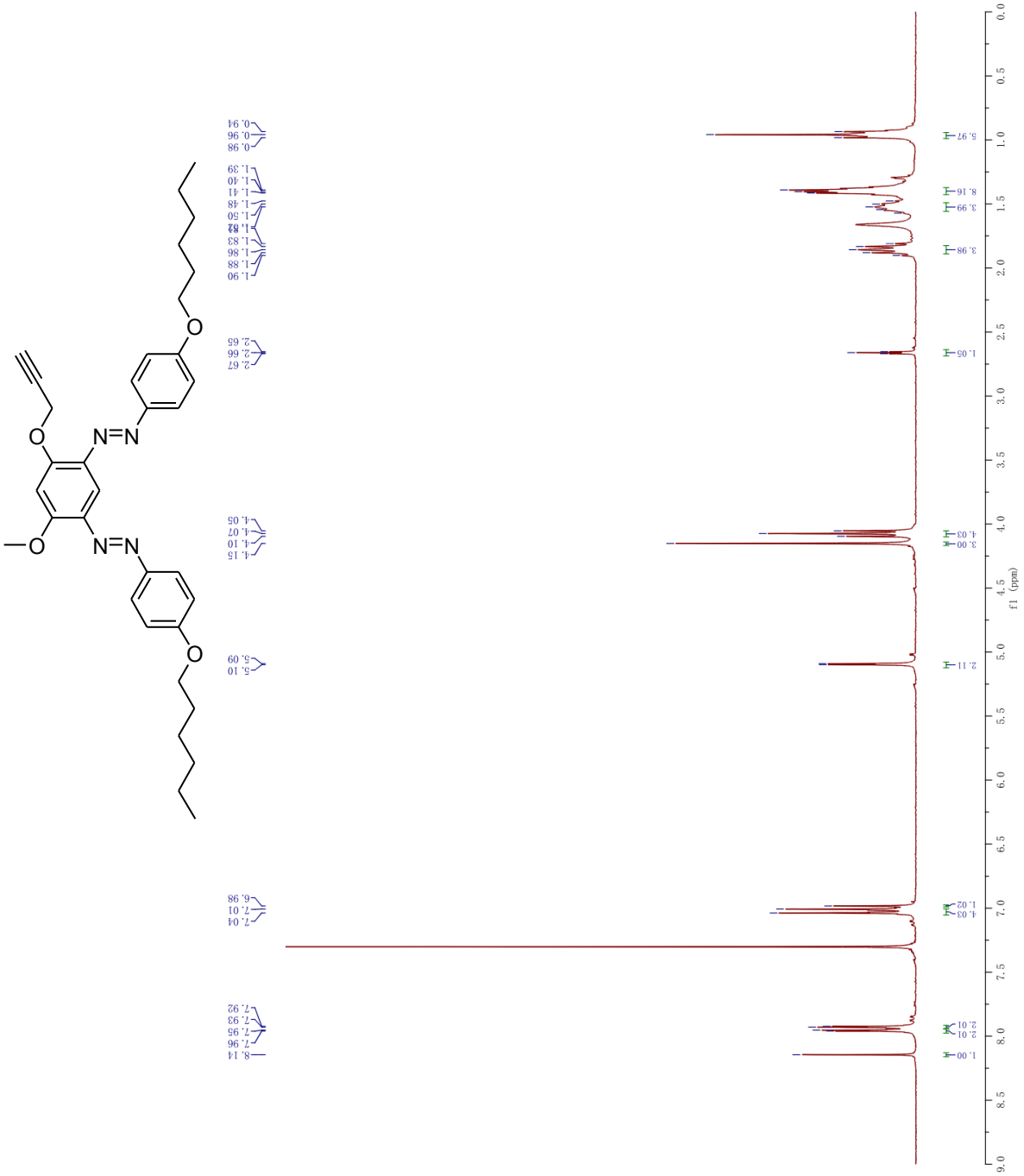

Compound 186

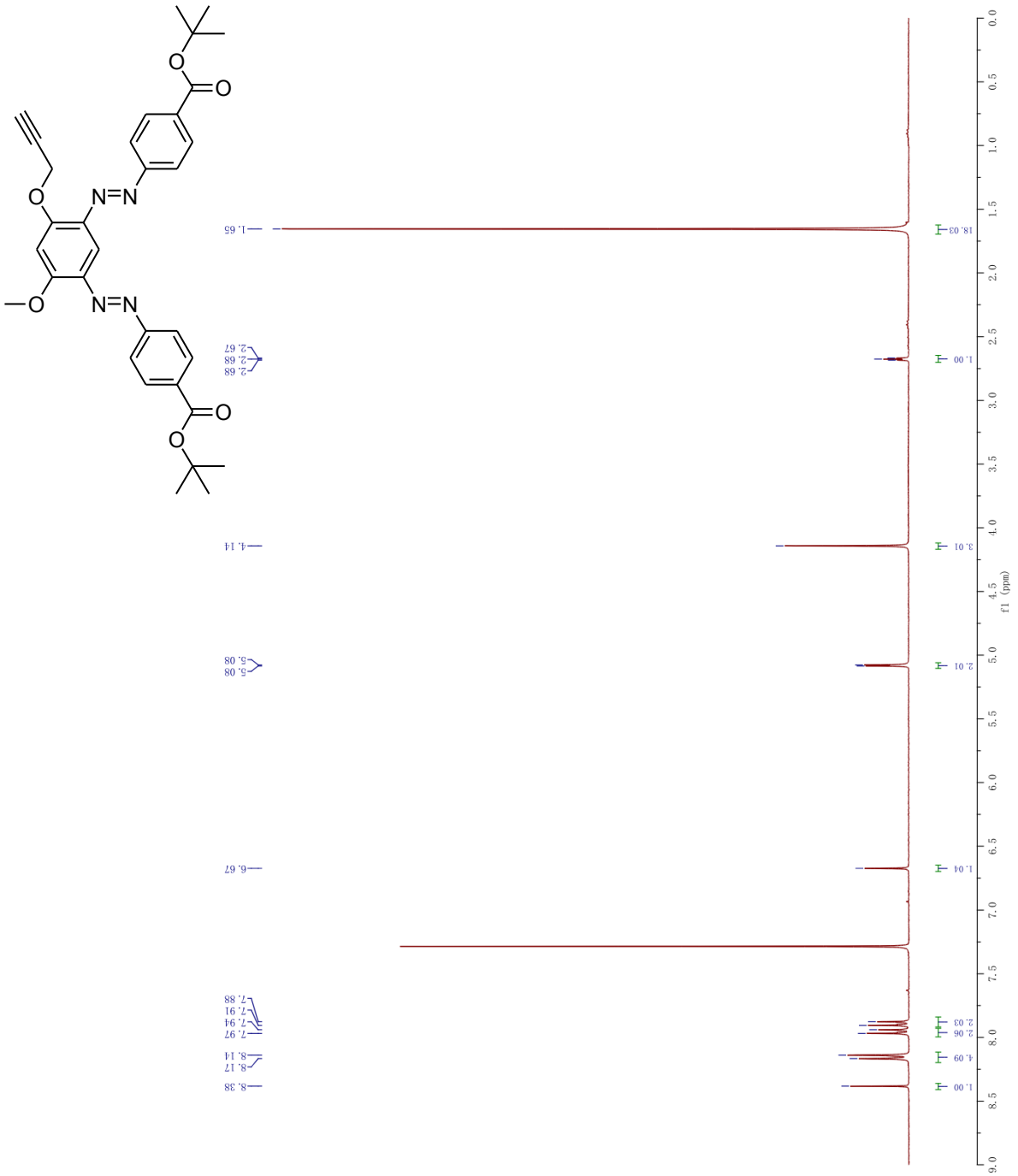

Compound 187

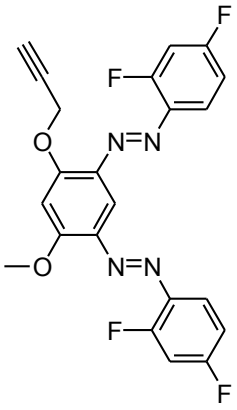

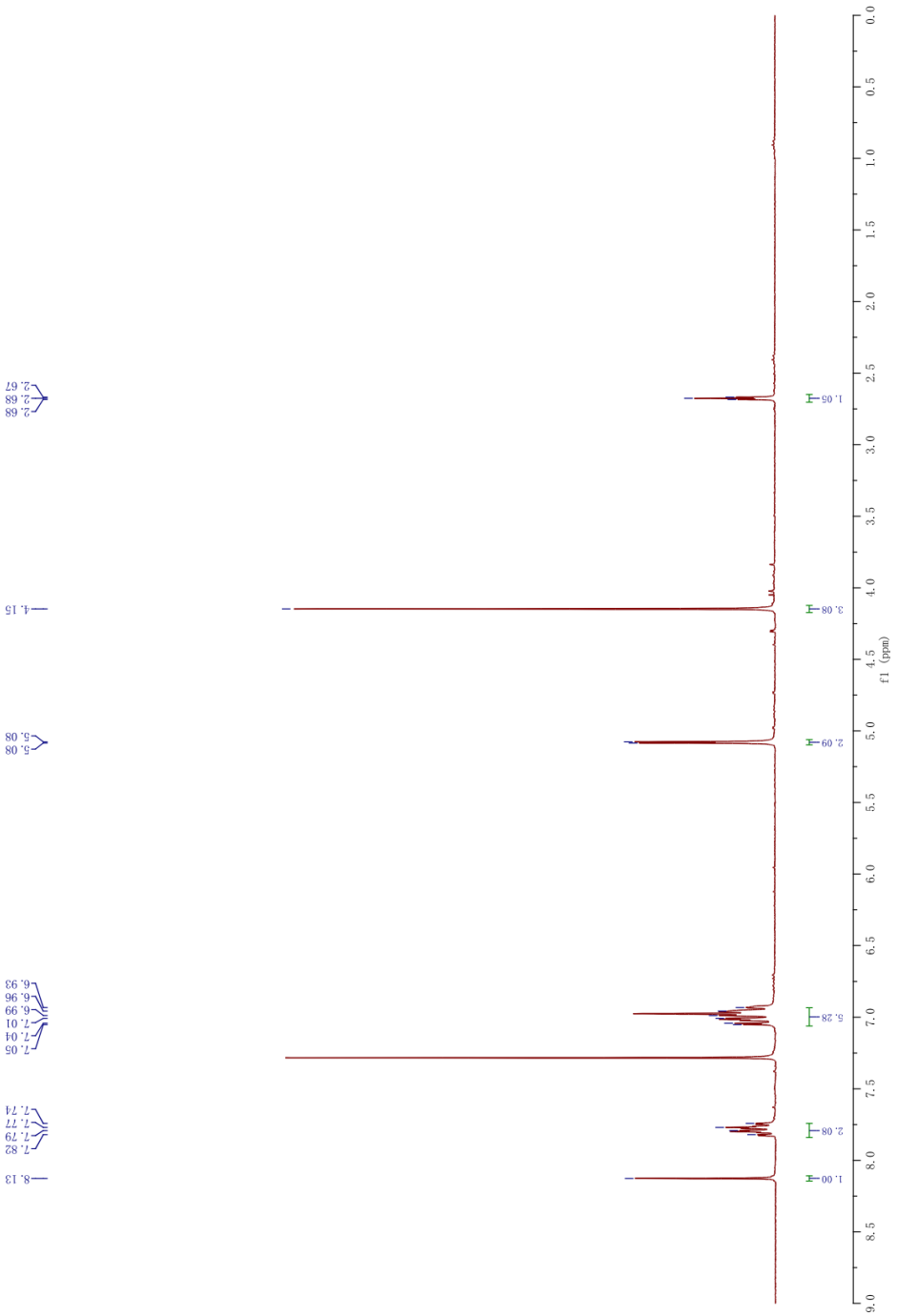

Bis-azobenzene monomer 188

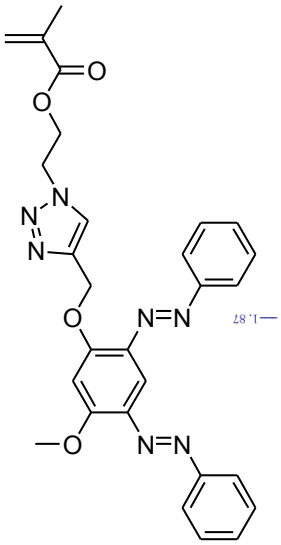

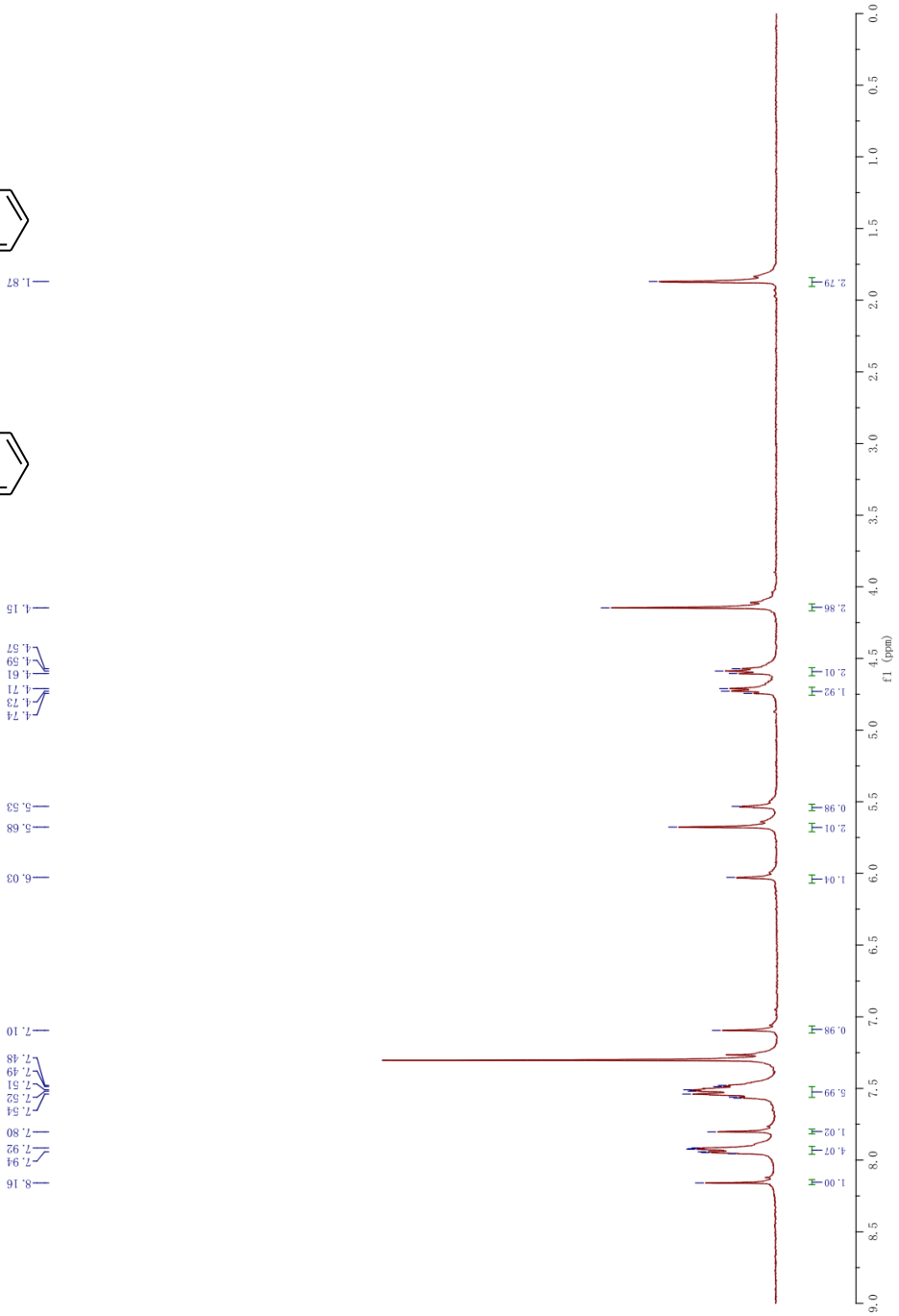

Bis-azobenzene monomer 189

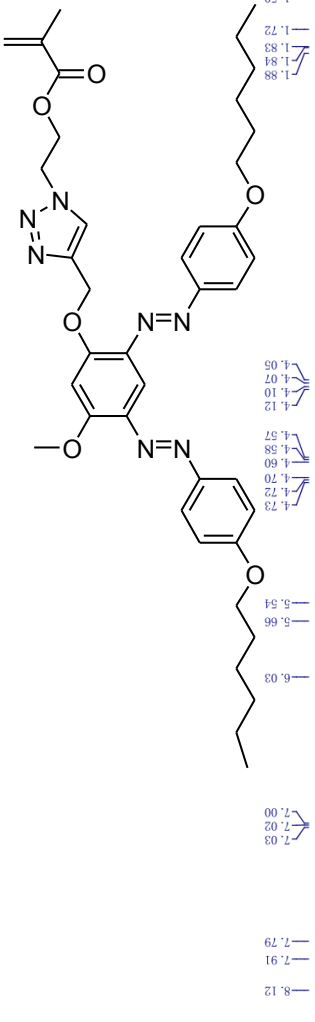

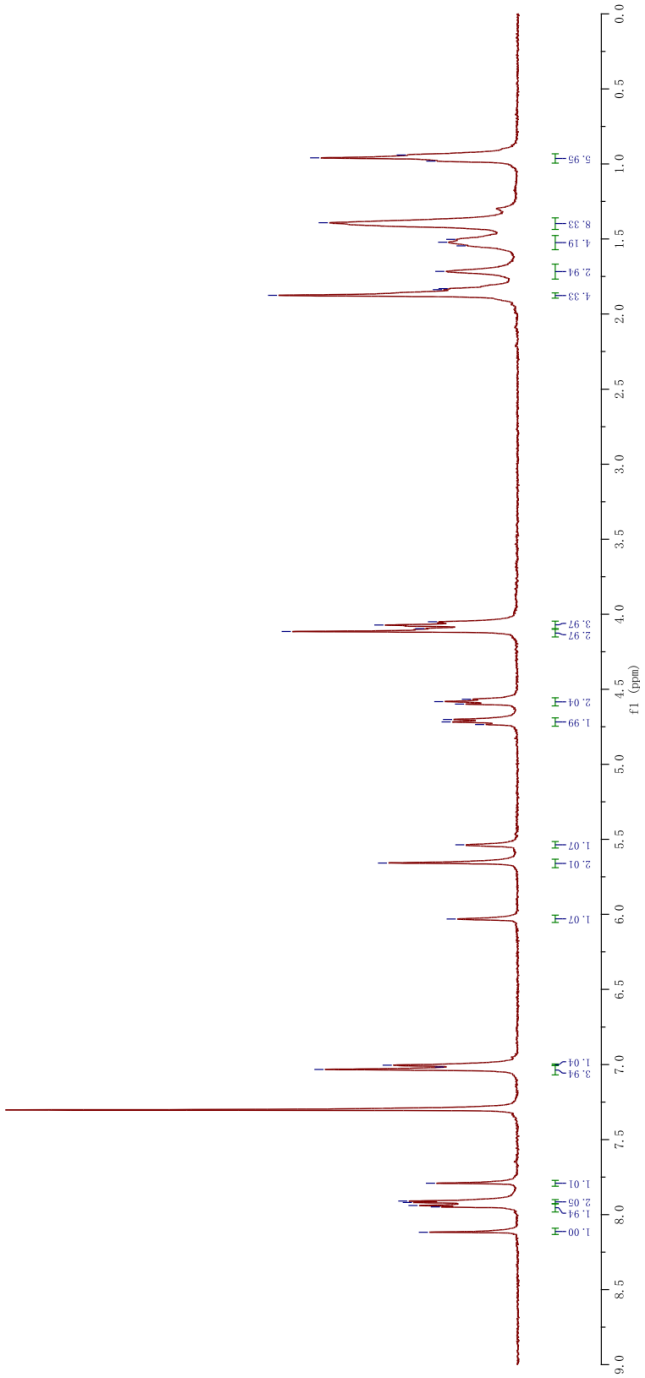

Bis-azobenzene monomer 190

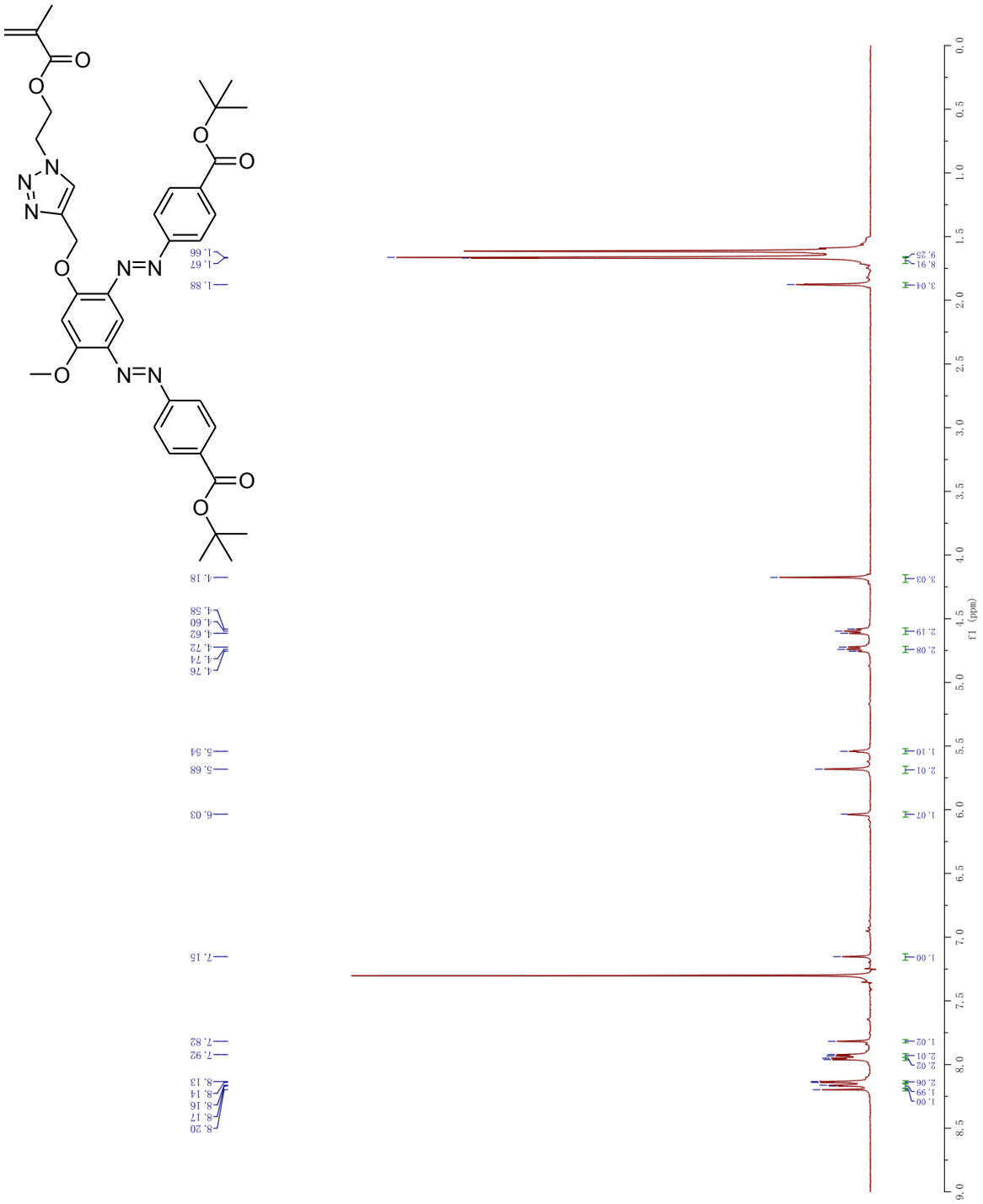

Bis-azobenzene monomer 191

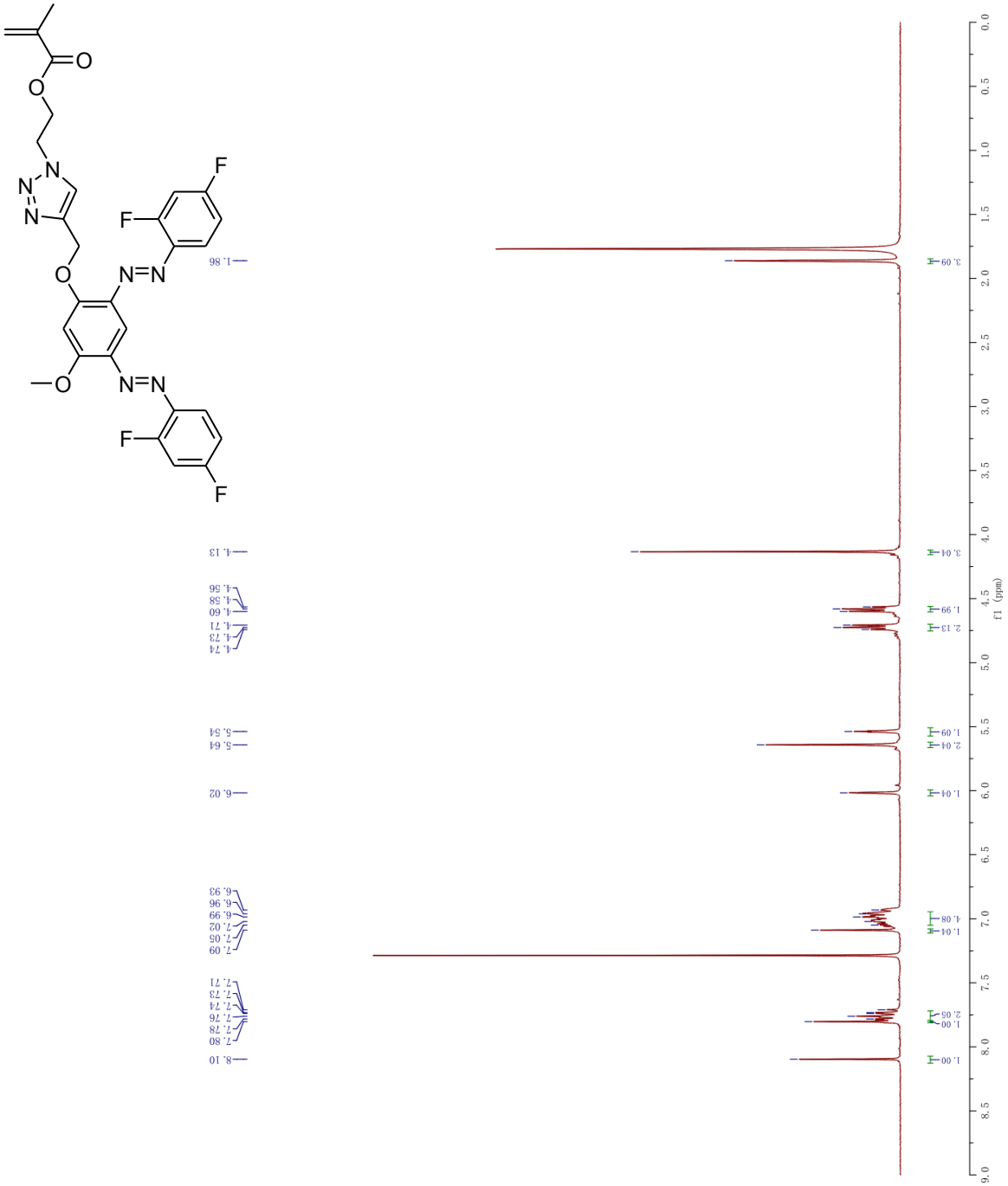

2-Hydroxymethyl-acrylic acid tert-butyl ester (194)

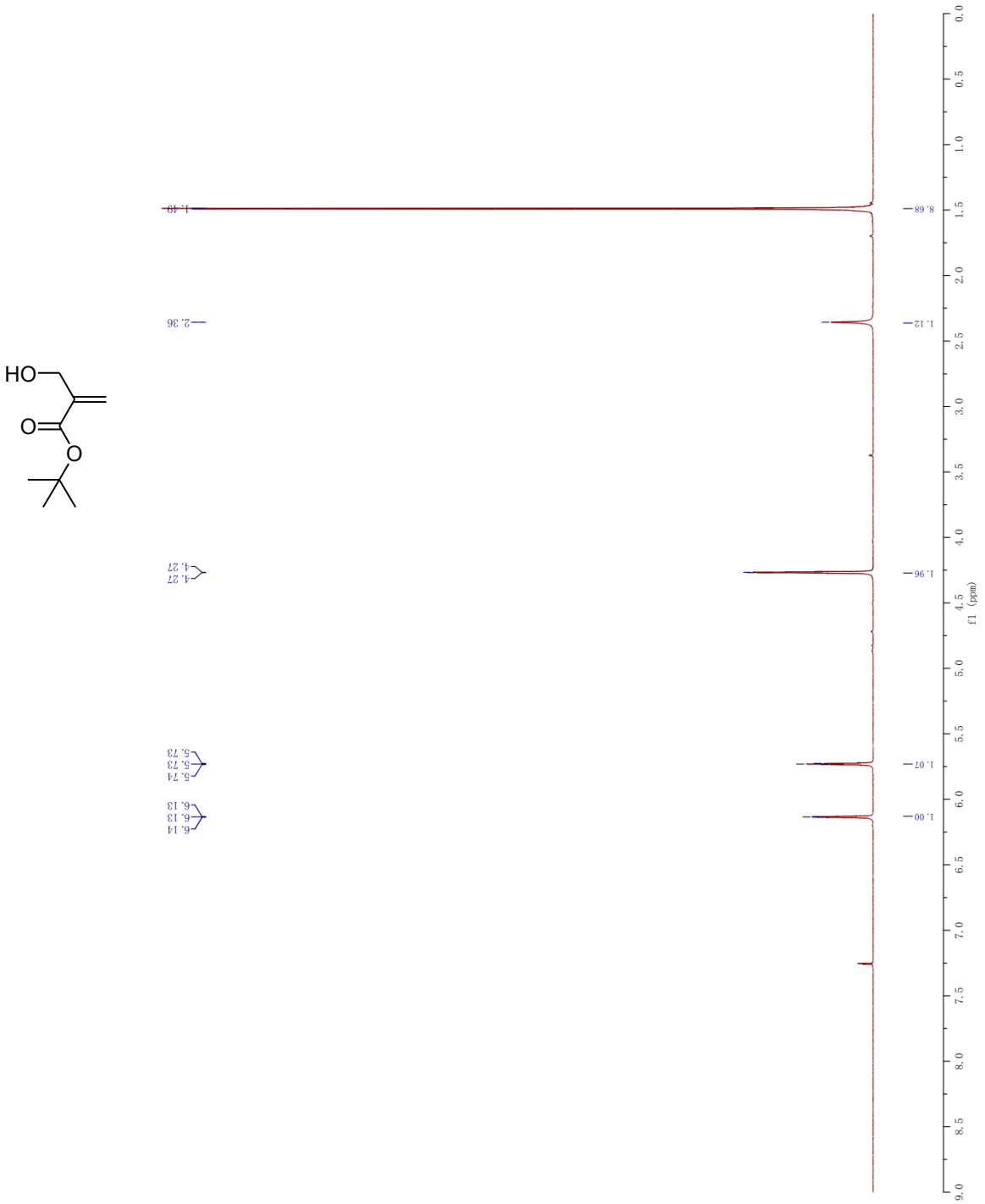

2-Bromomethyl-acrylic acid tert-butyl ester (195)

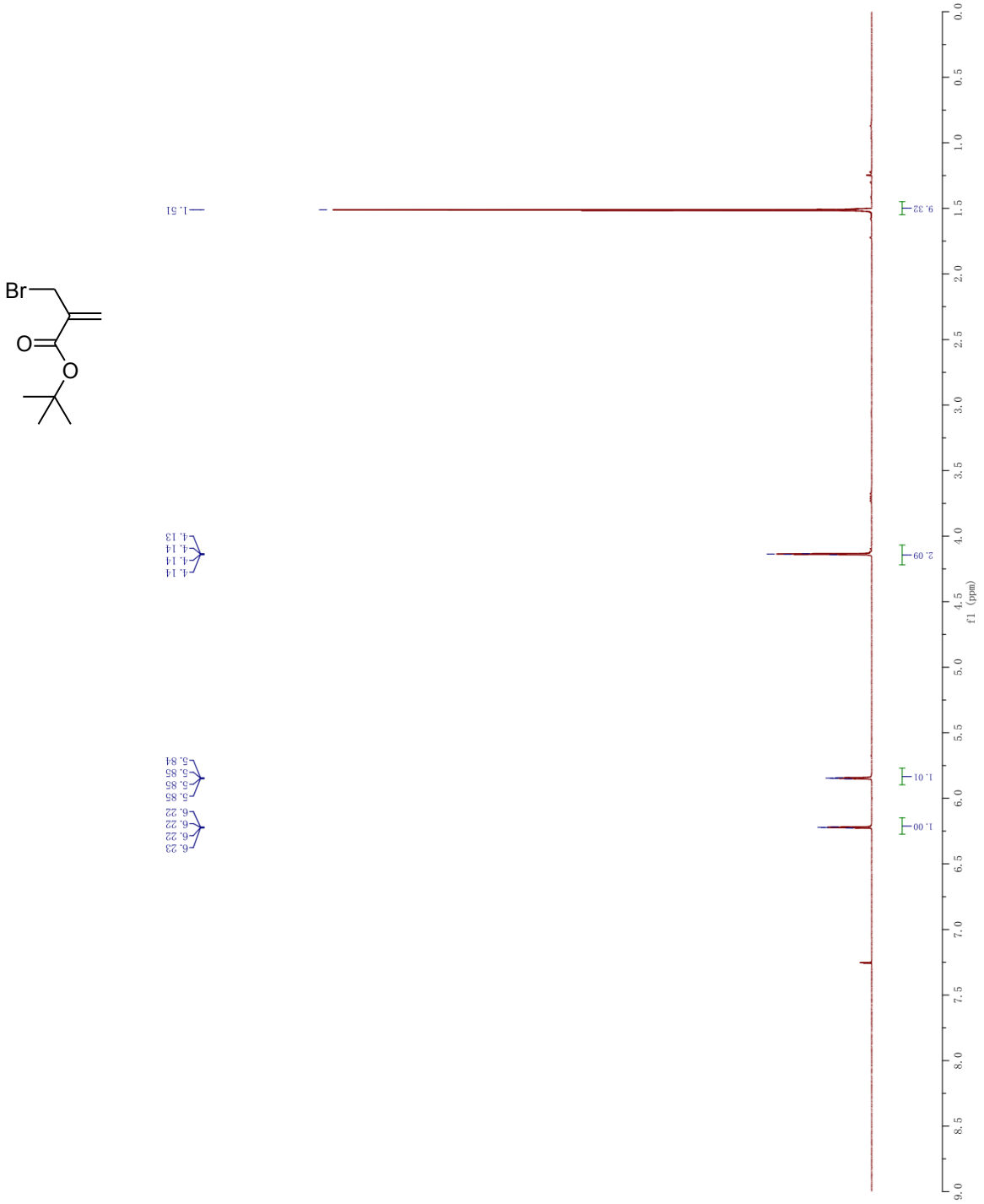

2-[4-(4-Hexyloxy-phenylazo)-3-methoxy-phenoxymethyl]-acrylic acid tert-butyl ester (196)

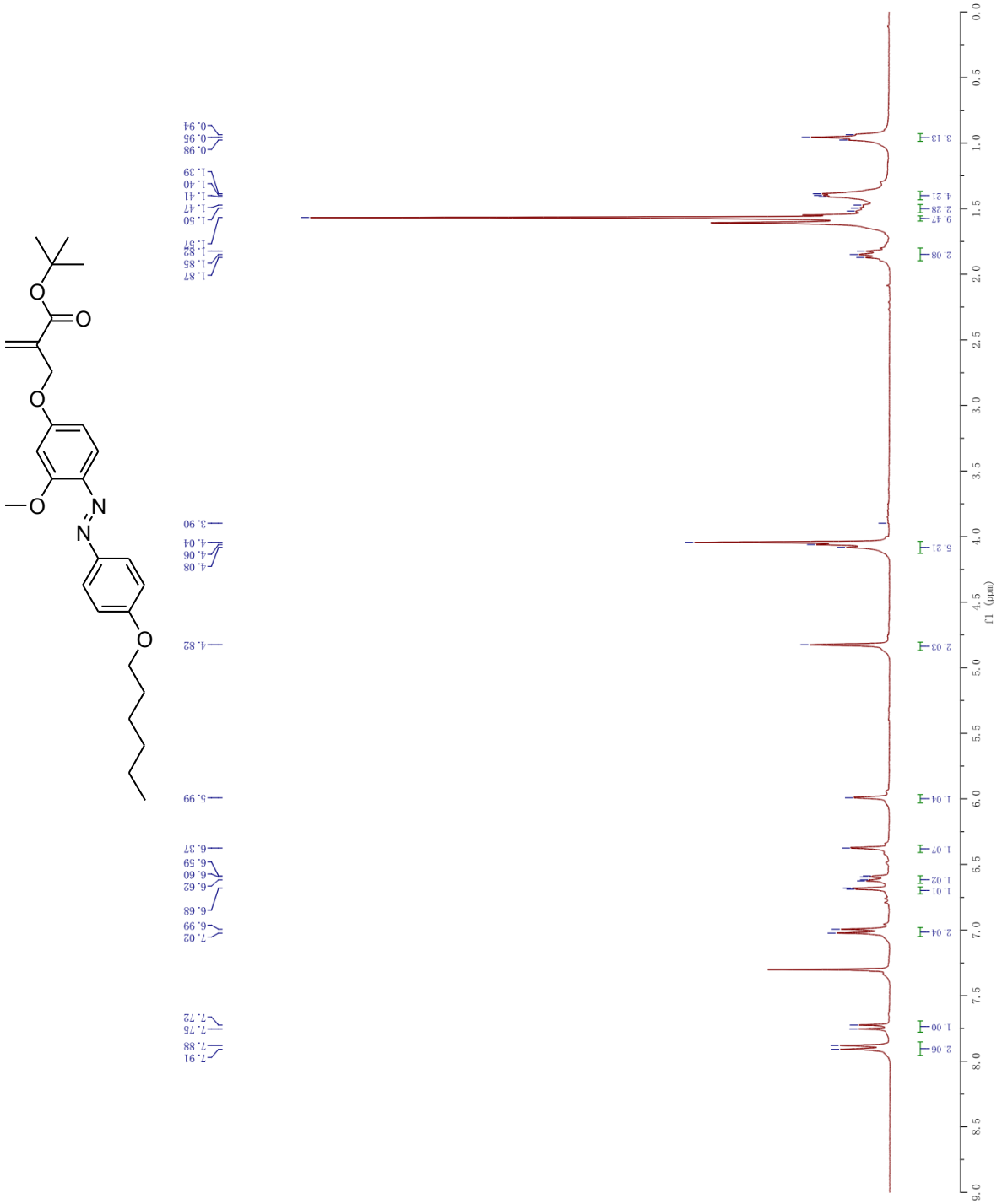

Polymer P1

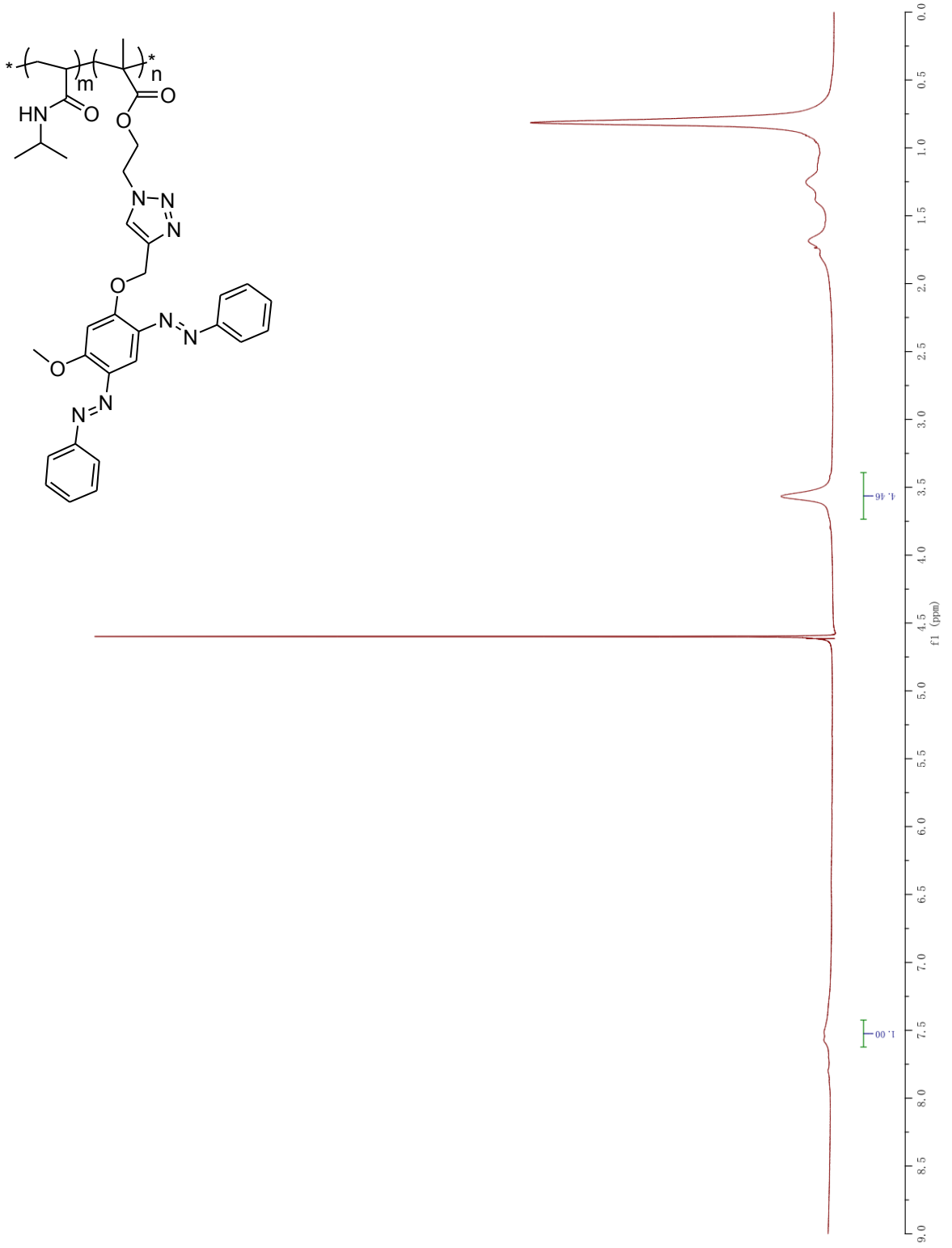

Polymer P2

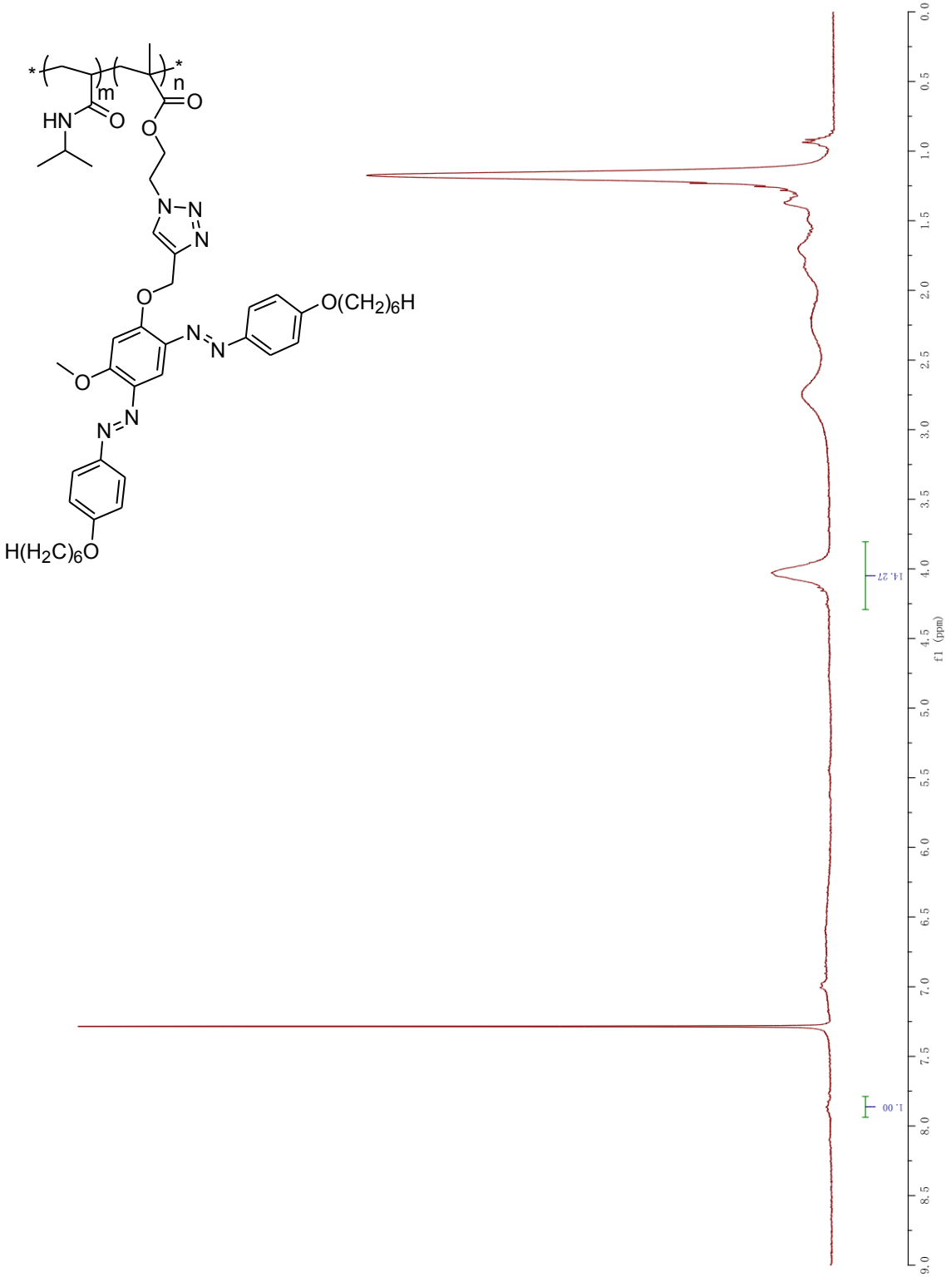

Polymer P3

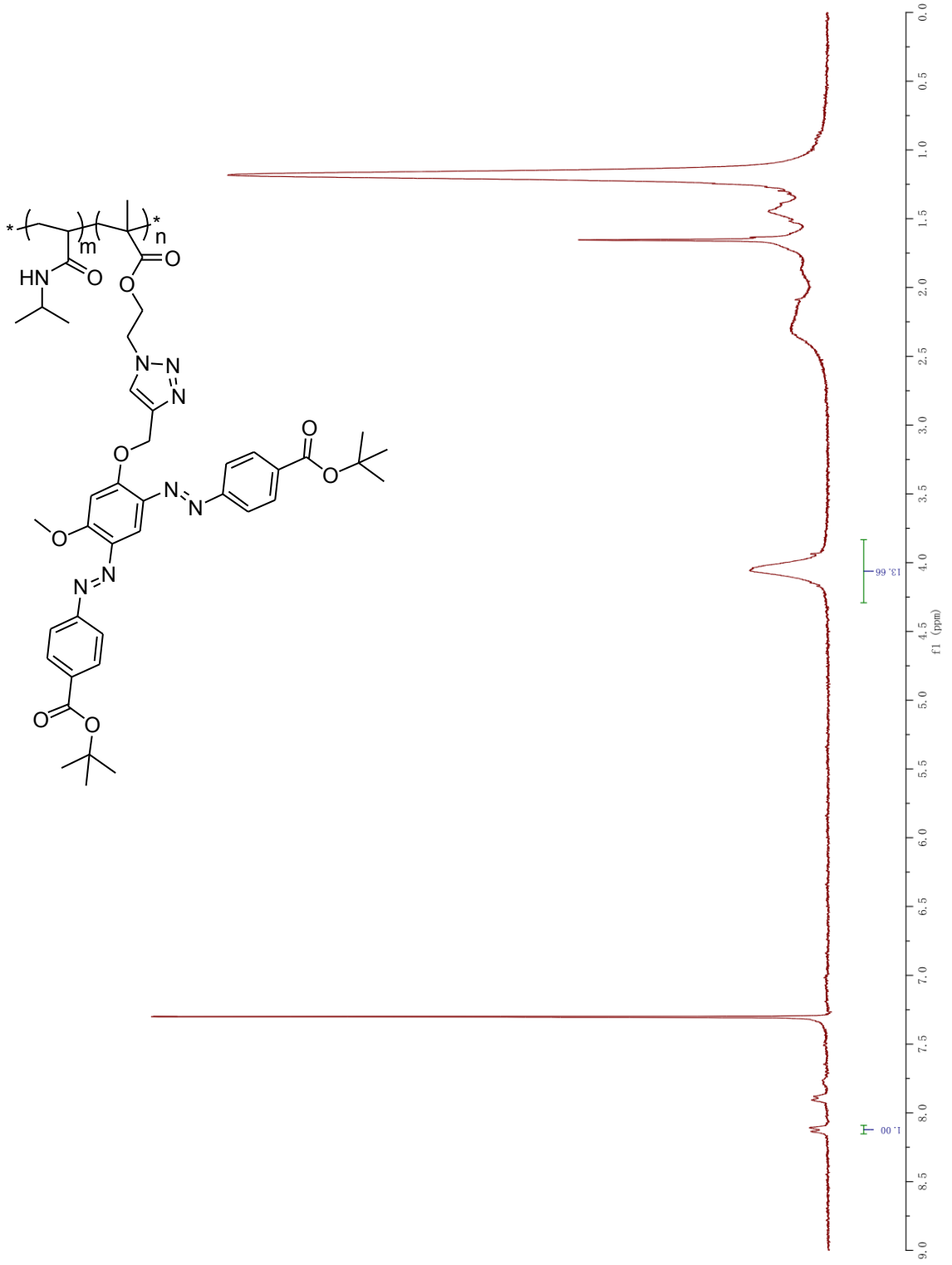

Polymer P4

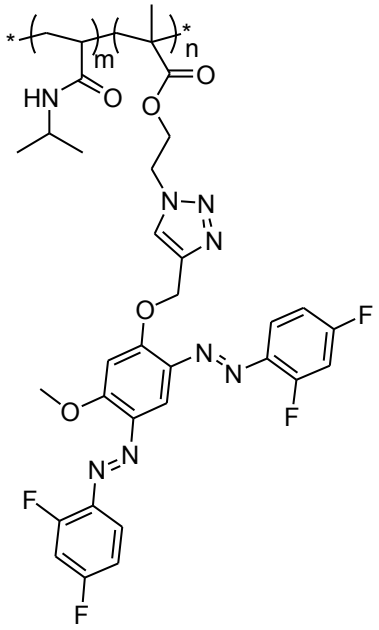

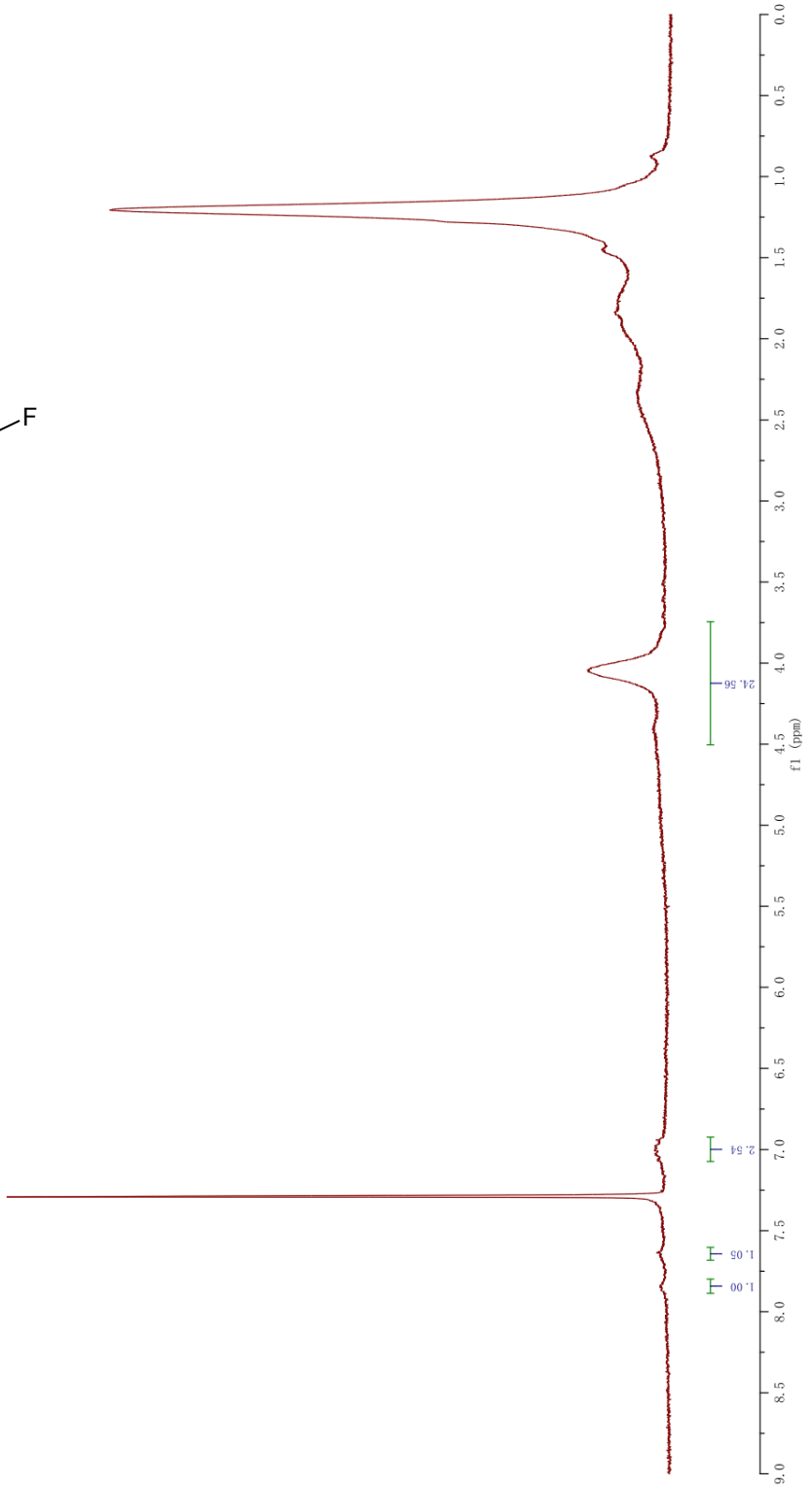

Polymer P5

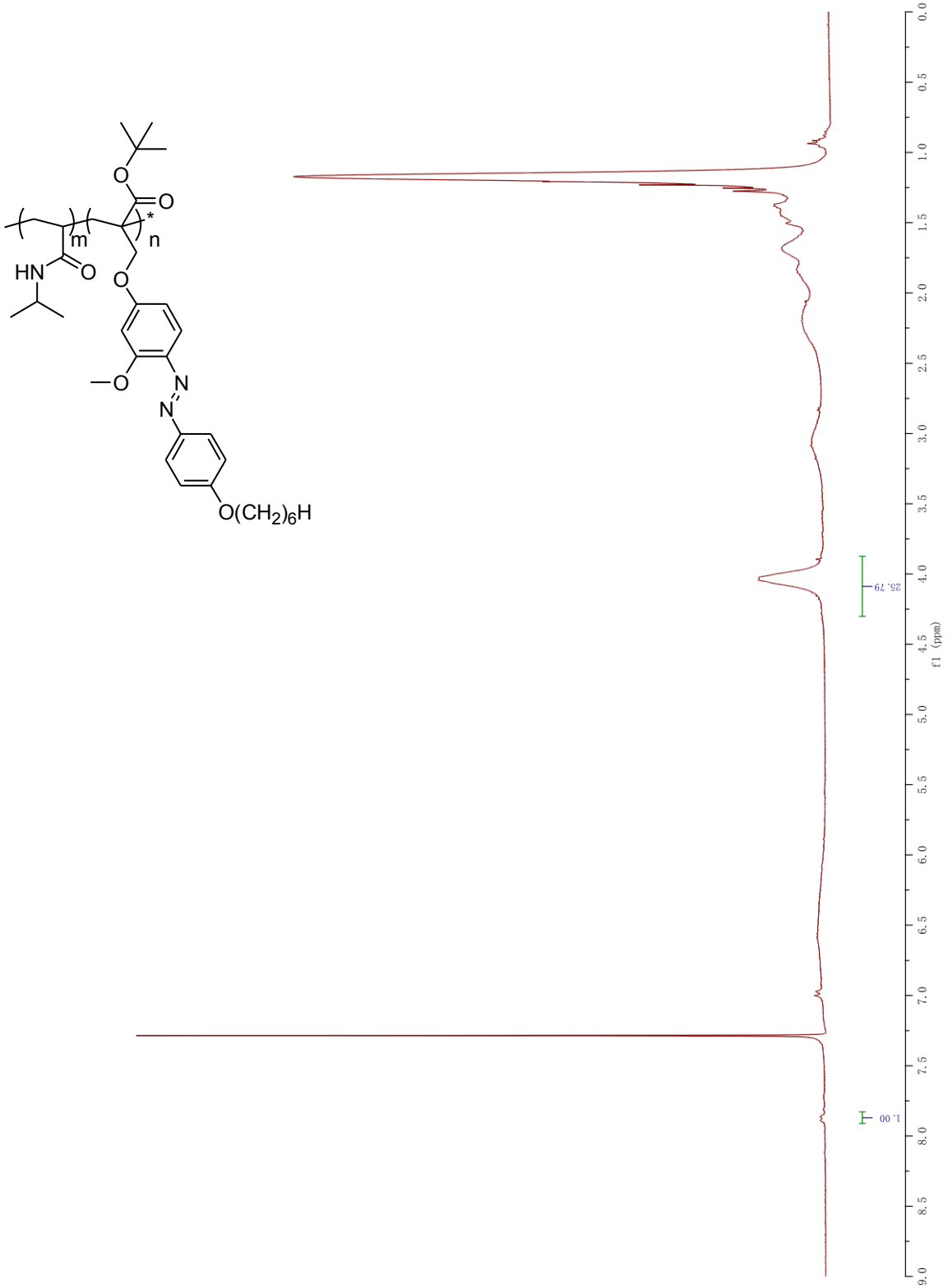

APPENDIX III: PICTURES

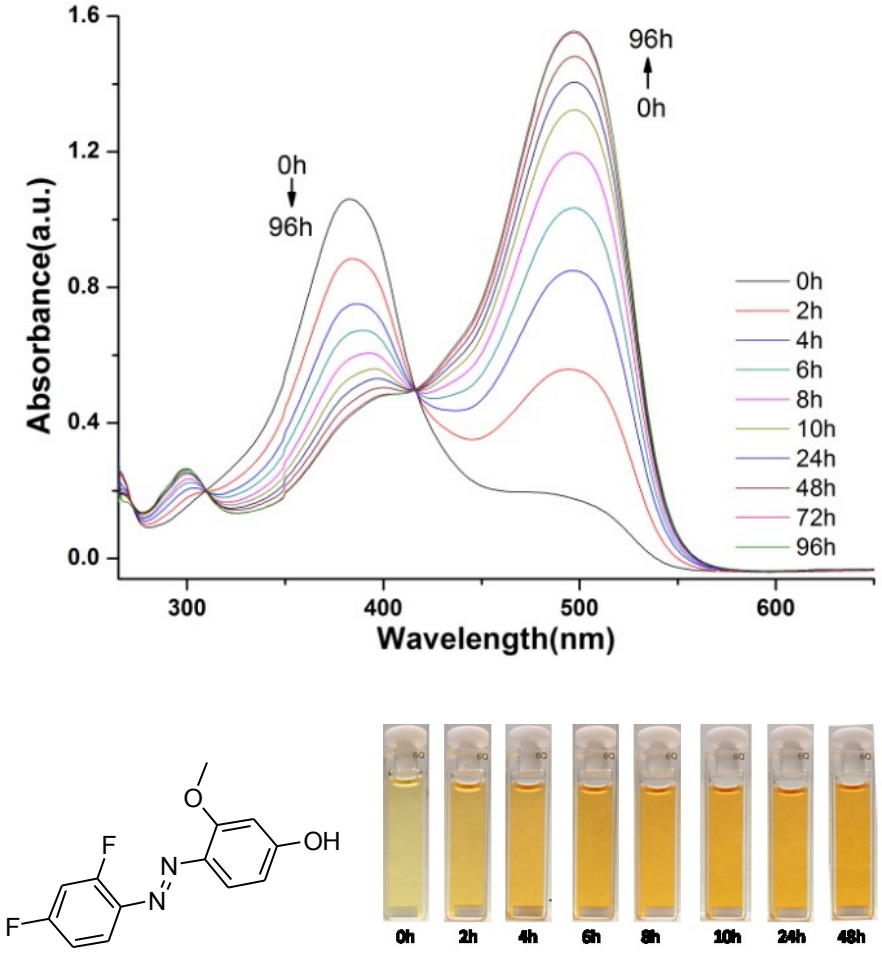

Figure S1. Top: UV-vis absorption spectra of *bis*-azobenzene **149** over time in DMAc at room temperature. The concentration of the solution is 2.5×10^{-5} mol·L^{-1}. Arrows indicate the spectroscopic changes of the absorption intensity at the maximal wavelength. Down: The chemical structure and the corresponding photographs of solution at 0h, 2h. 4h, 6h, 8h, 10h, 24h, 48h, 96h.

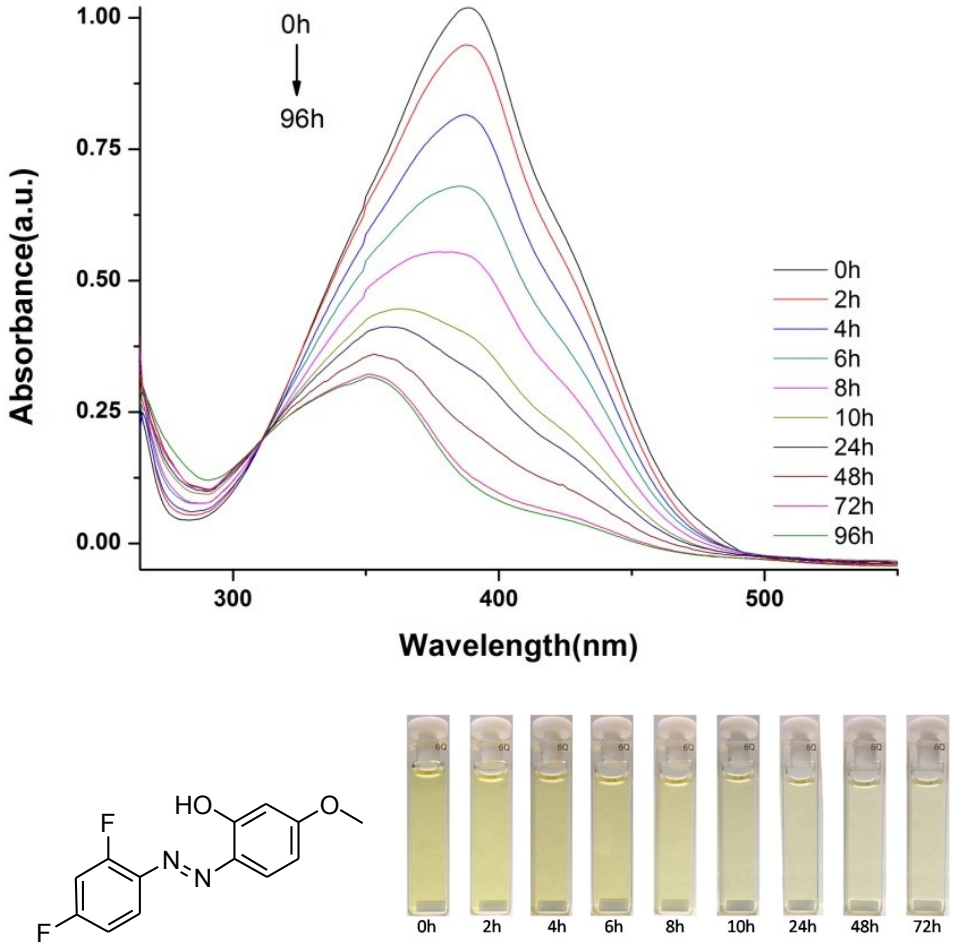

Figure S2. Top: UV-vis absorption spectra of *bis*-azobenzene **150** over time in DMAc at room temperature. The concentration of the solution is 2.5×10^{-5} mol·L^{-1}. Arrows indicate the spectroscopic changes of the absorption intensity at the maximal wavelength. Down: The chemical structure and the corresponding photographs of solution at 0h, 2h, 4h, 6h, 8h, 10h, 24h, 48h, 72h.

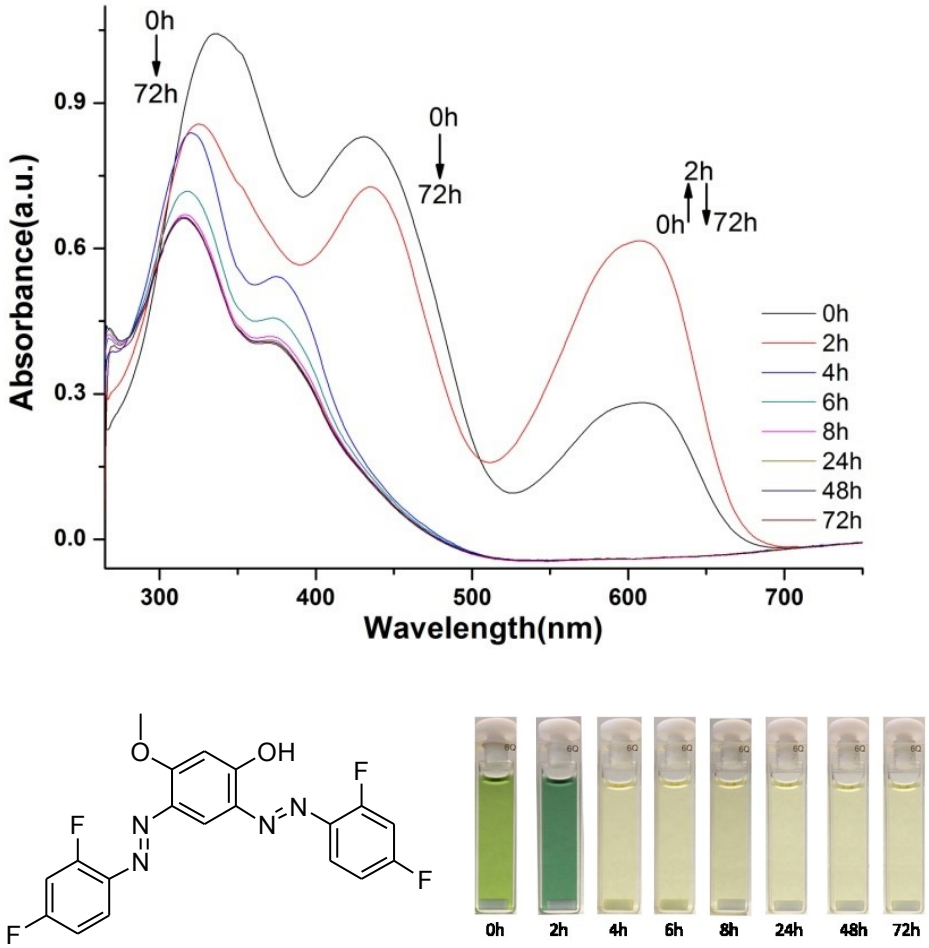

Figure S3. Top: UV-vis absorption spectra of *bis*-azobenzene **151** over time in DMAc at room temperature. The concentration of the solution is 2.5×10^{-5} mol·L^{-1}. Arrows indicate the spectroscopic changes of the absorption intensity at the maximal wavelength. Down: The chemical structure and the chemical structure and the corresponding photographs of solution at 0h, 2h; 4h, 6h, 8h, 24h, 48h, 72h.

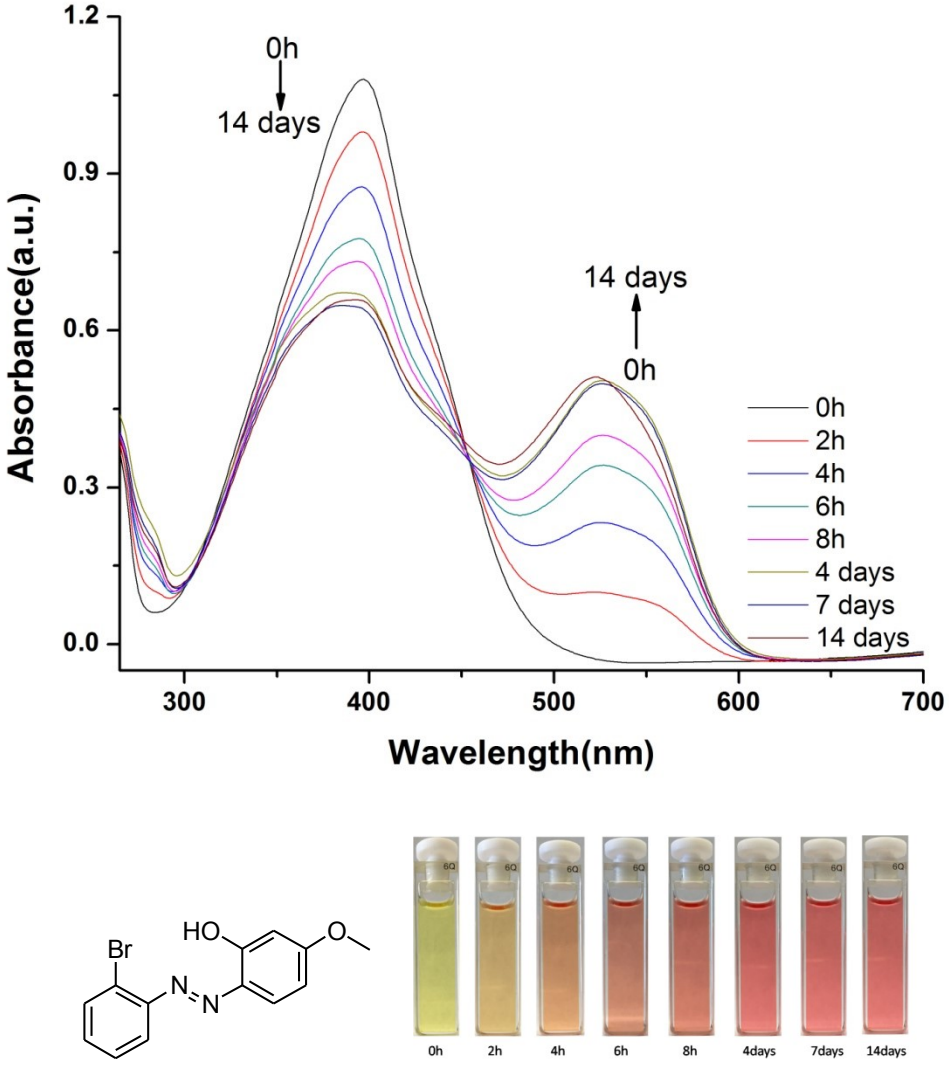

Figure S4. Top: UV-vis absorption spectra of *bis*-azobenzene **165** over time in DMSO at room temperature. The concentration of the solution is 2.5×10^{-5} mol·L^{-1}. Arrows indicate the spectroscopic changes of the absorption intensity at the maximal wavelength. Down: The chemical structure and the corresponding photographs of solution at 0h, 2h, 4h, 6h, 8h, 4 days, 7 days, 14 days.

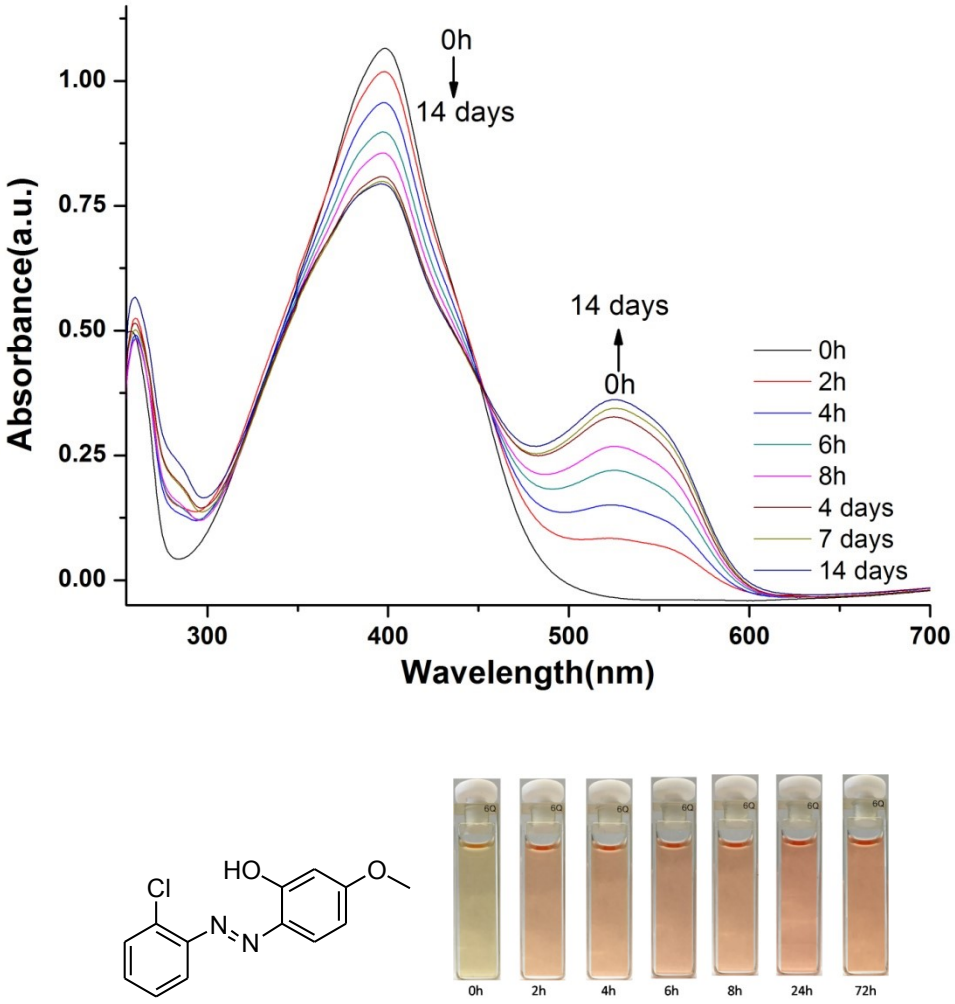

Figure S5. Top: UV-vis absorption spectra of *bis*-azobenzene **166** over time in DMSO at room temperature. The concentration of the solution is 2.5×10^{-5} mol·L^{-1}. Arrows indicate the spectroscopic changes of the absorption intensity at the maximal wavelength. Down: The chemical structure and the corresponding photographs of solution at 0h, 2h, 4h, 6h, 8h, 24h, 72h.

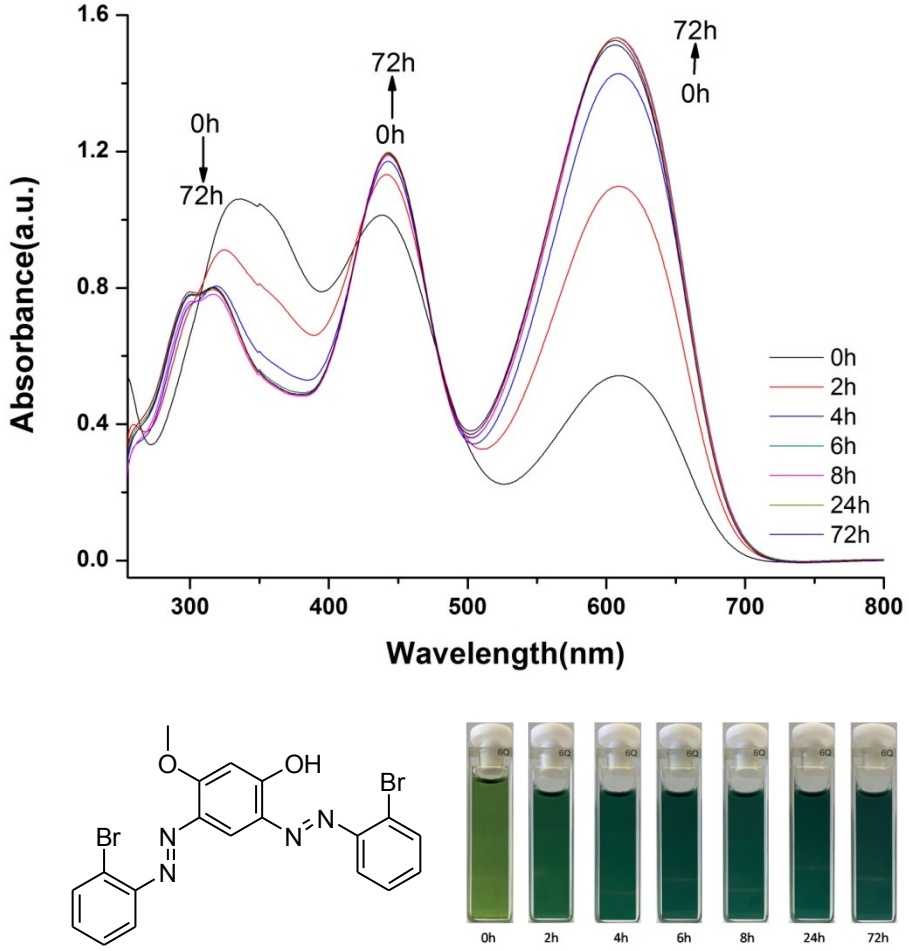

Figure S6. Top: UV-vis absorption spectra of *bis*-azobenzene **172** over time in DMSO at room temperature. The concentration of the solution is 2.5×10^{-5} mol·L^{-1}. Arrows indicate the spectroscopic changes of the absorption intensity at the maximal wavelength. Down: The chemical structure and the corresponding photographs of solution at 0h, 2h, 4h, 6h, 8h, 24h, 72h.

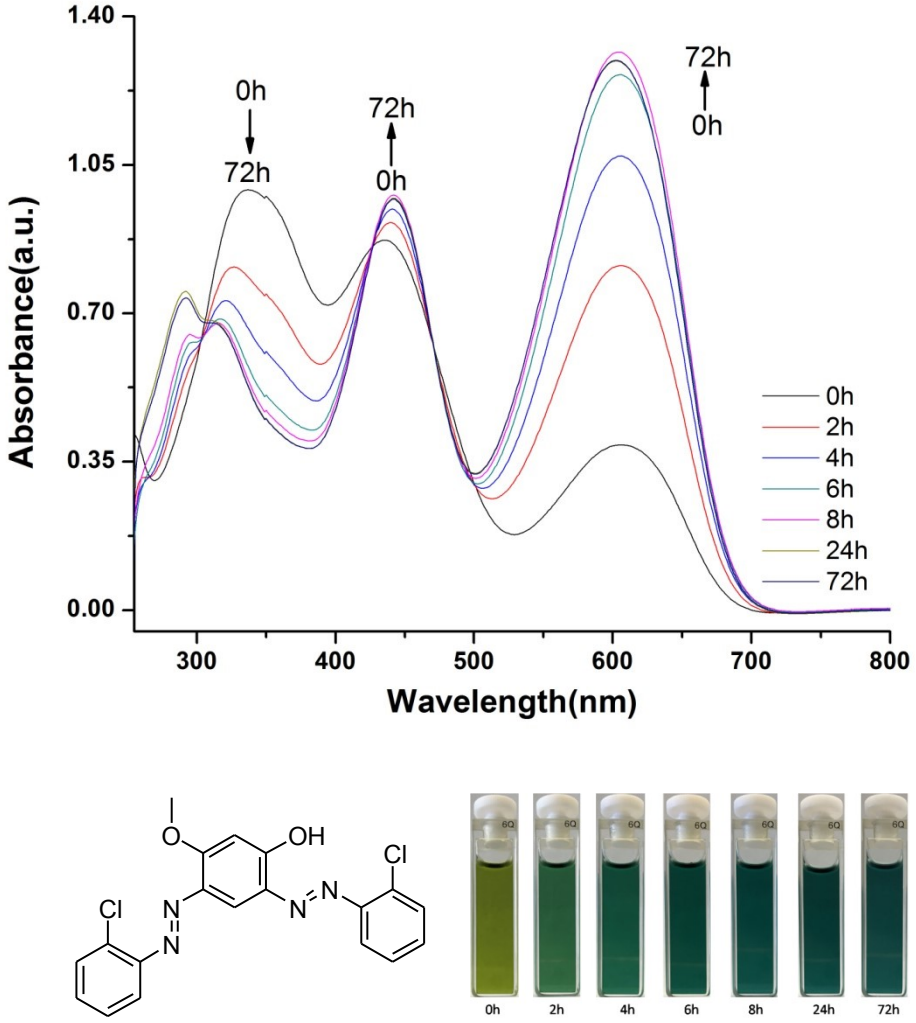

Figure S7. Top: UV-vis absorption spectra of *bis*-azobenzene **173** over time in DMSO at room temperature. The concentration of the solution is 2.5×10^{-5} mol·L^{-1}. Arrows indicate the spectroscopic changes of the absorption intensity at the maximal wavelength. Down: The chemical structure and the corresponding photographs of solution at 0h, 2h, 4h, 6h, 8h, 24h, 72h.

APPENDIX IV: X-RAY DIFFRACTION COORDINATES OF COMPOUND

(E)-3-methoxy-4-(phenyldiazenyl)phenol (99)

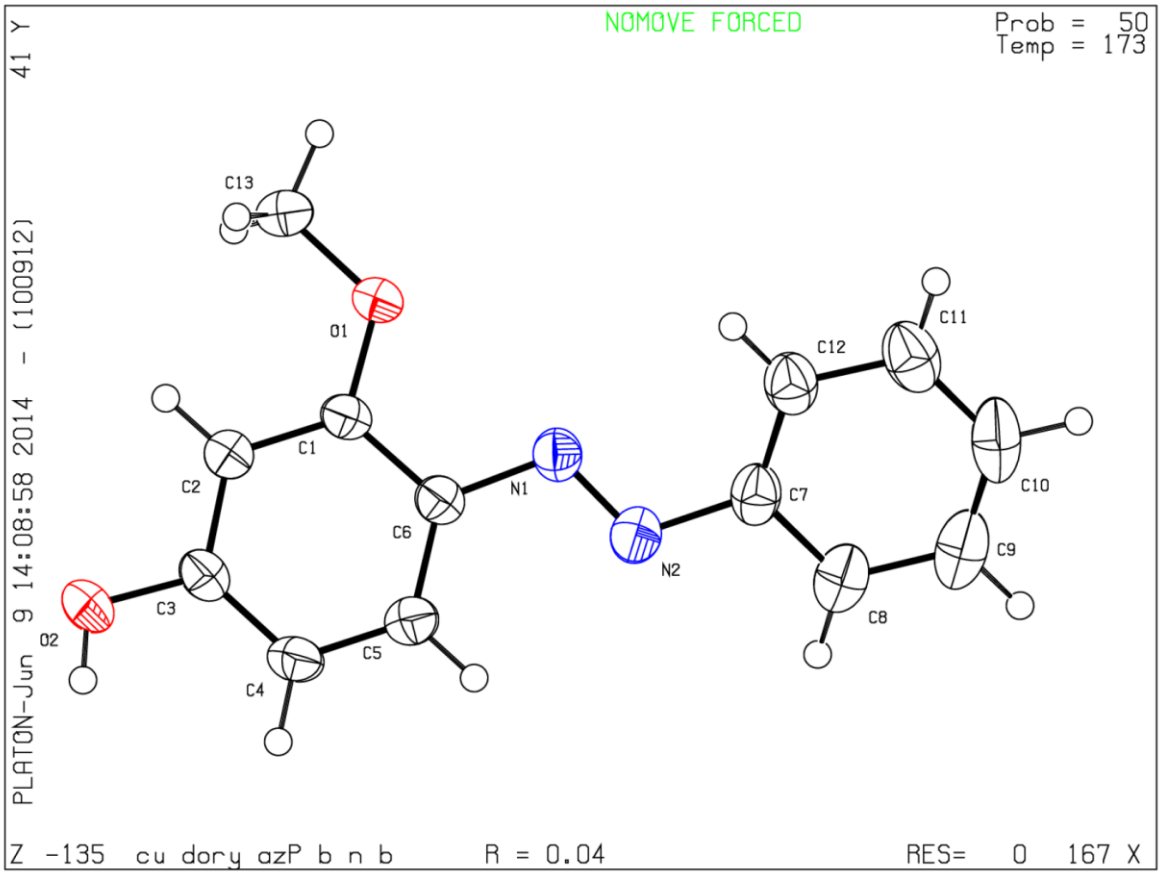

Atomic coordinates and equivalent isotropic atomic displacement parameters (Å^2)

	x/a	y/b	z/c	U(eq)
C1	0.02807(11)	0.15934(8)	0.26912(7)	0.0317(3)
C2	0.08128(12)	0.07813(8)	0.30574(8)	0.0344(3)
C3	0.03607(12)	0.98708(8)	0.28441(8)	0.0351(3)
C4	0.93647(12)	0.97639(9)	0.22798(8)	0.0387(3)
C5	0.88457(13)	0.05747(9)	0.19198(8)	0.0378(3)
C6	0.92943(11)	0.14998(8)	0.21059(7)	0.0323(3)
C7	0.75459(13)	0.30296(9)	0.07522(8)	0.0401(3)
C8	0.63538(14)	0.29417(12)	0.03825(9)	0.0502(4)

	x/a	y/b	z/c	U(eq)
C9	0.58901(16)	0.36848(14)	0.98863(10)	0.0591(4)
C10	0.66127(17)	0.44931(13)	0.97456(9)	0.0595(5)
C11	0.78100(16)	0.45789(11)	0.01026(9)	0.0530(4)
C12	0.82796(14)	0.38490(10)	0.06095(8)	0.0443(3)
C13	0.16483(13)	0.26372(9)	0.34773(9)	0.0432(3)
N1	0.88706(10)	0.23504(7)	0.17048(6)	0.0350(3)
N2	0.79358(10)	0.22123(8)	0.12267(7)	0.0407(3)
O1	0.06704(9)	0.25122(6)	0.28658(6)	0.0399(3)
O2	0.09314(10)	0.91030(6)	0.32153(6)	0.0445(3)

Hydrogen atomic coordinates and isotropic atomic displacement parameters (Å^2)

	x/a	y/b	z/c	U(eq)
H2	0.1482	1.0846	0.3451	0.041
H4	-0.0952	0.9141	0.2145	0.046
H5	-0.1835	1.0504	0.1535	0.045
H8	-0.4139	1.2377	0.0469	0.06
H9	-0.4930	1.3633	-0.0357	0.071
H10	-0.3708	1.4996	-0.0598	0.071
H11	-0.1692	1.5138	0.0000	0.064
H12	-0.0904	1.3908	0.0857	0.053
H13A	0.1357	1.2385	0.4016	0.065
H13B	0.1846	1.3325	0.3533	0.065
H13C	0.2411	1.2288	0.3301	0.065
H2A	0.0622	0.8590	0.3025	0.067

2, 4-bis((E)-phenyldiazenyl)-5-methoxyphenol (101)

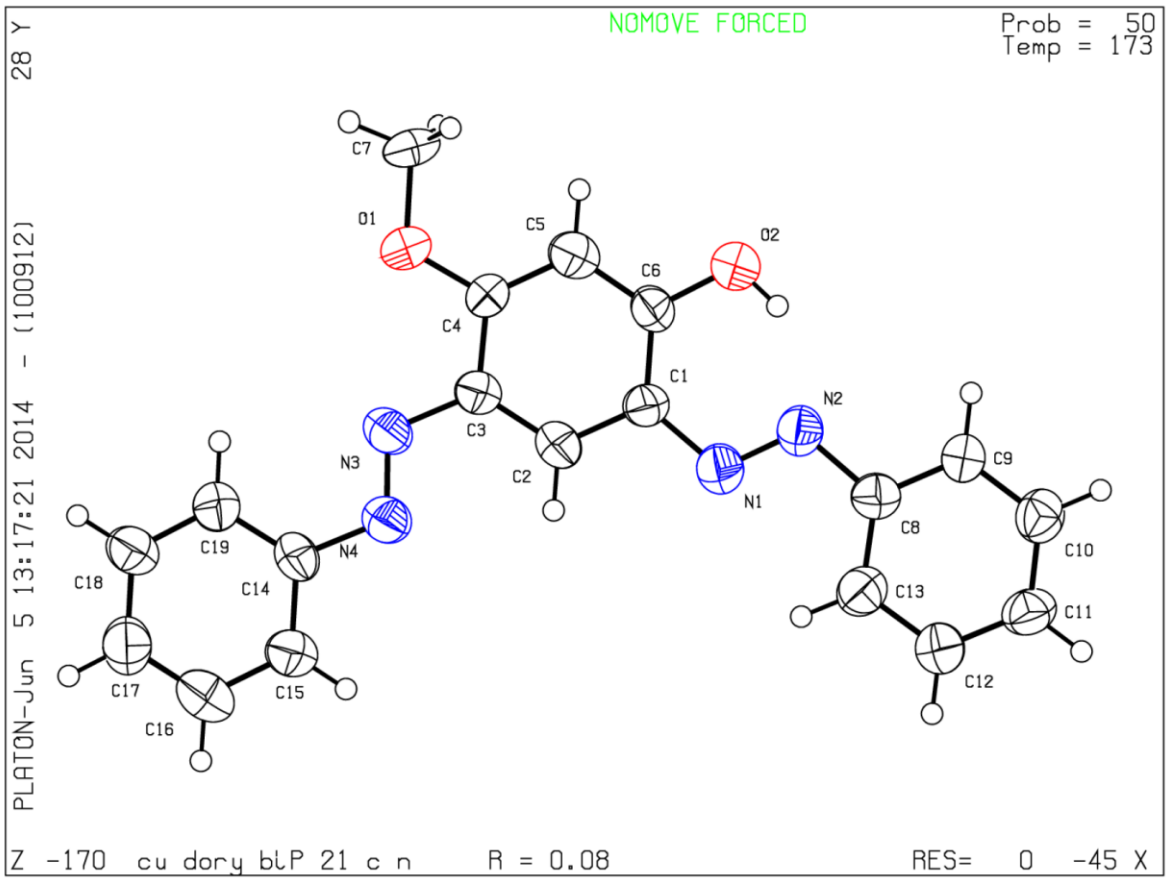

Atomic coordinates and equivalent isotropic atomic displacement parameters ($Å^2$)

	x/a	y/b	z/c	U(eq)
C1	0.6144(11)	0.5297(5)	0.3101(4)	0.0478(17)
C2	0.7616(11)	0.5405(5)	0.2562(4)	0.0521(18)
C3	0.9310(10)	0.4834(5)	0.2536(4)	0.0485(17)
C4	0.9496(10)	0.4115(5)	0.3082(4)	0.0484(17)
C5	0.8038(11)	0.3994(5)	0.3620(4)	0.058(2)
C6	0.6389(11)	0.4581(5)	0.3639(4)	0.0525(18)
C7	0.1466(11)	0.2828(5)	0.3577(4)	0.063(2)
C8	0.1628(10)	0.6548(5)	0.3532(4)	0.0507(18)

	x/a	y/b	z/c	U(eq)
C9	0.0140(10)	0.6446(5)	0.4059(4)	0.0537(18)
C10	-0.1488(10)	0.7062(5)	0.4049(4)	0.058(2)
C11	-0.1646(12)	0.7764(5)	0.3501(4)	0.0593(19)
C12	-0.0109(11)	0.7862(6)	0.2982(4)	0.063(2)
C13	0.1541(11)	0.7248(5)	0.2984(4)	0.0565(19)
C14	0.2233(11)	0.5797(5)	0.1074(4)	0.0503(17)
C15	0.1884(11)	0.6465(5)	0.0502(4)	0.059(2)
C16	0.3369(13)	0.6629(5)	0.9975(4)	0.069(2)
C17	0.5159(13)	0.6171(6)	0.0019(4)	0.067(2)
C18	0.5507(13)	0.5515(5)	0.0586(4)	0.0589(19)
C19	0.4055(11)	0.5330(5)	0.1105(4)	0.0534(19)
N1	0.4551(9)	0.5956(4)	0.3056(3)	0.0546(15)
N2	0.3244(8)	0.5862(4)	0.3574(3)	0.0522(15)
N3	0.0883(9)	0.4956(4)	0.2015(3)	0.0536(16)
N4	0.0629(8)	0.5666(4)	0.1572(3)	0.0536(16)
O1	0.1212(8)	0.3590(3)	0.3037(2)	0.0593(14)
O2	0.5024(8)	0.4448(3)	0.4183(3)	0.0656(15)

Hydrogen atomic coordinates and isotropic atomic displacement parameters (Å^2)

	x/a	y/b	z/c	U(eq)
H2	-0.2543	0.5889	0.2196	0.063
H5	-0.1824	0.3501	0.3981	0.07
H7A	0.1338	0.3087	0.4082	0.095
H7B	0.2795	0.2542	0.3516	0.095
H7C	0.0438	0.2340	0.3496	0.095
H9	-0.9772	0.5959	0.4426	0.064
H10	-1.2501	0.7005	0.4419	0.069
H11	-1.2785	0.8169	0.3481	0.071
H12	-1.0183	0.8356	0.2620	0.075
H13	-0.7428	0.7308	0.2622	0.068

	x/a	y/b	z/c	U(eq)
H15	0.0649	0.6800	0.0476	0.07
H16	0.3132	0.7067	-0.0421	0.083
H17	0.6174	0.6300	-0.0339	0.08
H18	0.6756	0.5192	0.0612	0.071
H19	0.4301	0.4879	0.1490	0.064
H2A	-0.5819	0.4893	0.4171	0.098

(E)-tert-butyl 4-((4-hydroxy-2-methoxyphenyl)diazenyl)benzoate (133)

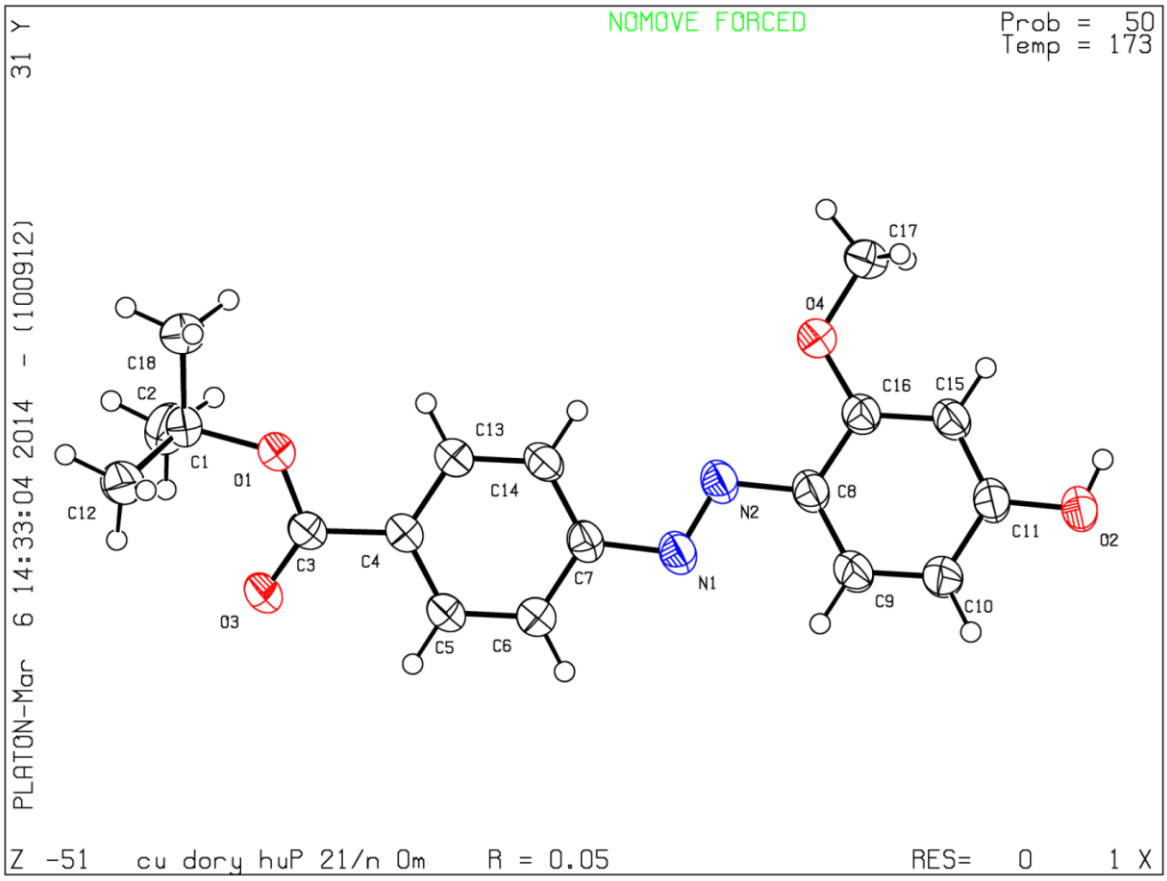

Atomic coordinates and equivalent isotropic atomic displacement parameters (Å^2)

	x/a	y/b	z/c	U(eq)
C1	0.4989(3)	0.57137(9)	0.60949(19)	0.0663(6)
C2	0.6655(3)	0.56205(7)	0.70423(15)	0.0500(4)
C3	0.6532(2)	0.44898(7)	0.69725(13)	0.0413(4)
C4	0.7770(2)	0.39555(7)	0.66142(12)	0.0384(3)
C5	0.6879(2)	0.33742(7)	0.66867(13)	0.0416(4)
C6	0.7955(2)	0.28685(7)	0.63333(13)	0.0418(4)
C7	0.9929(2)	0.29410(7)	0.58920(12)	0.0386(3)
C8	0.3544(3)	0.19529(7)	0.46883(12)	0.0418(4)
C9	0.2907(3)	0.13605(8)	0.49455(15)	0.0524(5)
C10	0.4007(3)	0.08552(8)	0.46345(16)	0.0586(5)
C11	0.5808(3)	0.09354(8)	0.40576(14)	0.0494(4)
C12	0.5755(4)	0.56928(9)	0.81198(19)	0.0738(7)
C13	0.9771(2)	0.40235(7)	0.61873(13)	0.0418(4)
C14	0.0841(2)	0.35215(7)	0.58332(13)	0.0420(4)
C15	0.6485(3)	0.15154(7)	0.37832(12)	0.0419(4)
C16	0.5349(2)	0.20263(7)	0.40846(12)	0.0393(3)
C17	0.7699(3)	0.26992(8)	0.32317(14)	0.0470(4)
C18	0.8580(3)	0.60405(8)	0.69682(17)	0.0595(5)
N1	0.0915(2)	0.23924(6)	0.55547(10)	0.0424(3)
N2	0.2514(2)	0.24874(6)	0.50128(11)	0.0425(3)
O1	0.76423(17)	0.50072(5)	0.69246(9)	0.0454(3)
O2	0.6851(2)	0.04228(5)	0.37760(12)	0.0660(4)
O3	0.47048(18)	0.44497(5)	0.72413(11)	0.0528(3)
O4	0.58595(18)	0.26080(5)	0.38283(9)	0.0471(3)

Hydrogen atomic coordinates and isotropic atomic displacement parameters (Å^2)

	x/a	y/b	z/c	U(eq)
H1A	-0.4368	0.5607	0.5432	0.099

	x/a	y/b	z/c	U(eq)
H1B	-0.5470	0.6143	0.6066	0.099
H1C	-0.6268	0.5451	0.6177	0.099
H5	-0.4475	0.3325	0.6980	0.05
H6	-0.2650	0.2472	0.6391	0.05
H9	0.1685	0.1307	0.5345	0.063
H10	0.3546	0.0456	0.4811	0.07
H12A	-0.5620	0.5471	0.8119	0.111
H12B	-0.4487	0.6128	0.8259	0.111
H12C	-0.3212	0.5526	0.8679	0.111
H13	0.0394	0.4419	0.6142	0.05
H14	0.2202	0.3570	0.5548	0.05
H15	0.7721	0.1563	0.3391	0.05
H17A	0.8993	0.2534	0.3634	0.07
H17B	0.7896	0.3138	0.3110	0.07
H17C	0.7470	0.2488	0.2542	0.07
H18A	-0.0382	0.5977	0.7591	0.089
H18B	-0.1909	0.6467	0.6952	0.089
H18C	-0.0722	0.5949	0.6314	0.089
H2	0.7898	0.0520	0.3427	0.099

(E)-tert-butyl 4-((2-hydroxy-4-methoxyphenyl)diazenyl)benzoate (134)

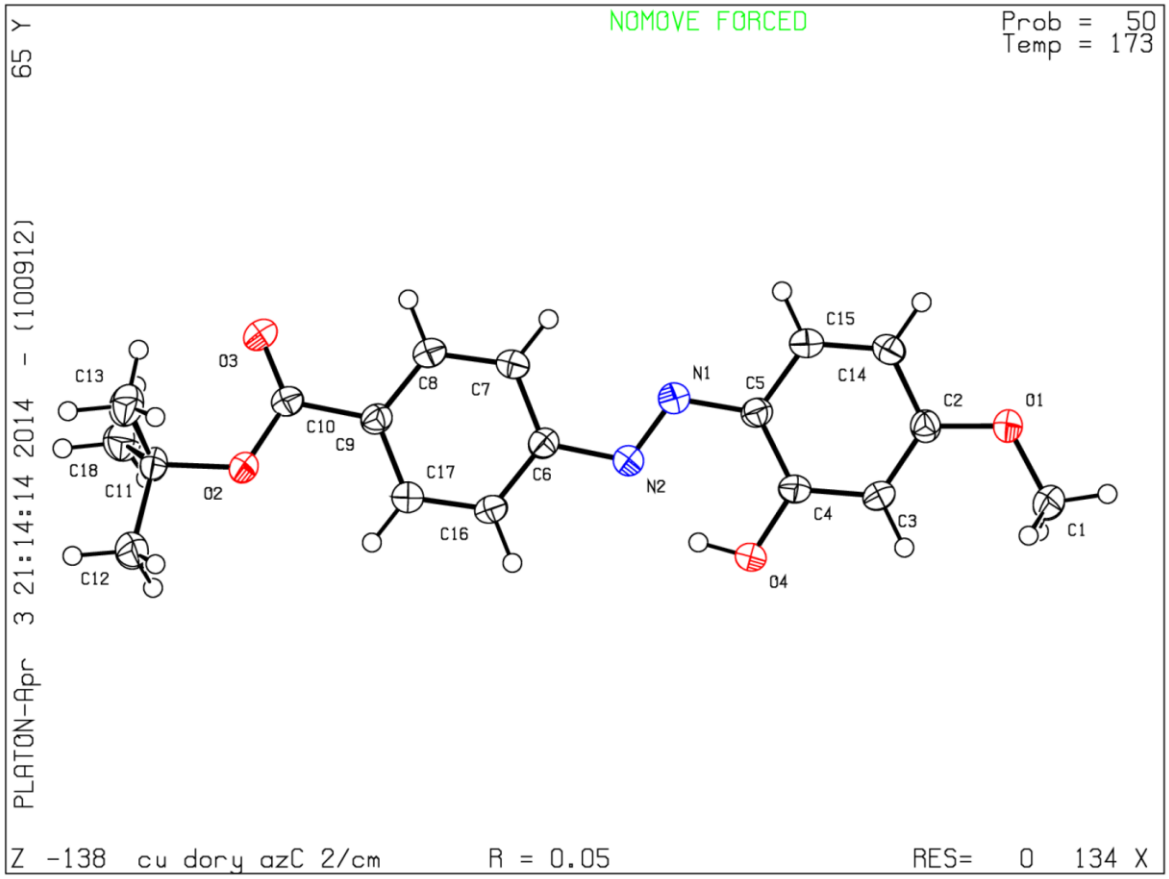

Atomic coordinates and equivalent isotropic atomic displacement parameters (Å^2)

	x/a	y/b	z/c	U(eq)
C1	0.24872(9)	0.9915(4)	0.81043(14)	0.0390(6)
C2	0.28632(8)	0.1920(4)	0.91382(13)	0.0281(5)
C3	0.28275(8)	0.0245(4)	0.96500(13)	0.0292(5)
C4	0.30145(7)	0.0469(4)	0.04045(13)	0.0274(5)
C5	0.32438(7)	0.2356(4)	0.06445(13)	0.0268(5)
C6	0.36298(7)	0.1748(4)	0.26132(12)	0.0265(5)
C7	0.38061(8)	0.3769(4)	0.28137(14)	0.0324(5)
C8	0.40111(8)	0.4085(4)	0.35451(14)	0.0324(5)
C9	0.40497(7)	0.2409(4)	0.40793(13)	0.0272(5)

	x/a	y/b	z/c	U(eq)
C10	0.42769(8)	0.2884(4)	0.48558(13)	0.0283(5)
C11	0.45785(8)	0.1175(4)	0.60596(13)	0.0305(5)
C12	0.46044(10)	0.8815(4)	0.62831(15)	0.0449(7)
C13	0.50245(9)	0.2137(5)	0.60606(15)	0.0424(6)
C14	0.30880(8)	0.3816(4)	0.93682(13)	0.0305(5)
C15	0.32746(8)	0.4019(4)	0.01033(13)	0.0303(5)
C16	0.36592(8)	0.0086(4)	0.31471(13)	0.0299(5)
C17	0.38700(8)	0.0408(4)	0.38771(13)	0.0299(5)
C18	0.43021(9)	0.2427(4)	0.65580(15)	0.0403(6)
N1	0.34418(6)	0.2766(3)	0.13764(11)	0.0285(4)
N2	0.34159(6)	0.1273(3)	0.18717(11)	0.0278(4)
O1	0.26892(6)	0.1874(3)	0.83943(9)	0.0343(4)
O2	0.43565(5)	0.1084(3)	0.52690(9)	0.0307(4)
O3	0.43744(6)	0.4683(3)	0.50682(10)	0.0402(5)
O4	0.29692(6)	0.8846(3)	0.08948(10)	0.0364(4)

Hydrogen atomic coordinates and isotropic atomic displacement parameters (Å^2)

	x/a	y/b	z/c	U(eq)
H1	0.2234	-0.0379	-0.1632	0.058
H5	0.2693	-0.1281	-0.1808	0.058
H6	0.2397	0.0065	-0.2446	0.058
H9	0.2677	-0.1039	-0.0513	0.035
H12	0.3785	0.4912	0.2452	0.039
H13	0.4128	0.5463	0.3687	0.039
H2	0.4773	-0.1970	0.5937	0.067
H17	0.4313	-0.1791	0.6247	0.067
H18	0.4745	-0.1322	0.6810	0.067
H3	0.5189	0.1938	0.6566	0.064
H19	0.4999	0.3682	0.5944	0.064
H20	0.5174	0.1415	0.5673	0.064

	x/a	y/b	z/c	U(eq)
H8	0.3110	0.4951	-0.0988	0.037
H7	0.3428	0.5300	0.0256	0.036
H10	0.3534	-0.1279	0.3011	0.036
H11	0.3892	-0.0736	0.4239	0.036
H14	0.4008	0.1843	0.6492	0.06
H15	0.4295	0.3951	0.6408	0.06
H16	0.4425	0.2295	0.7095	0.06
H4	0.3107(11)	-0.076(5)	0.1349(19)	0.055

2, 4-bis((E)-(4-tert-butyl)diazenyl)-5-methoxyphenol (135)

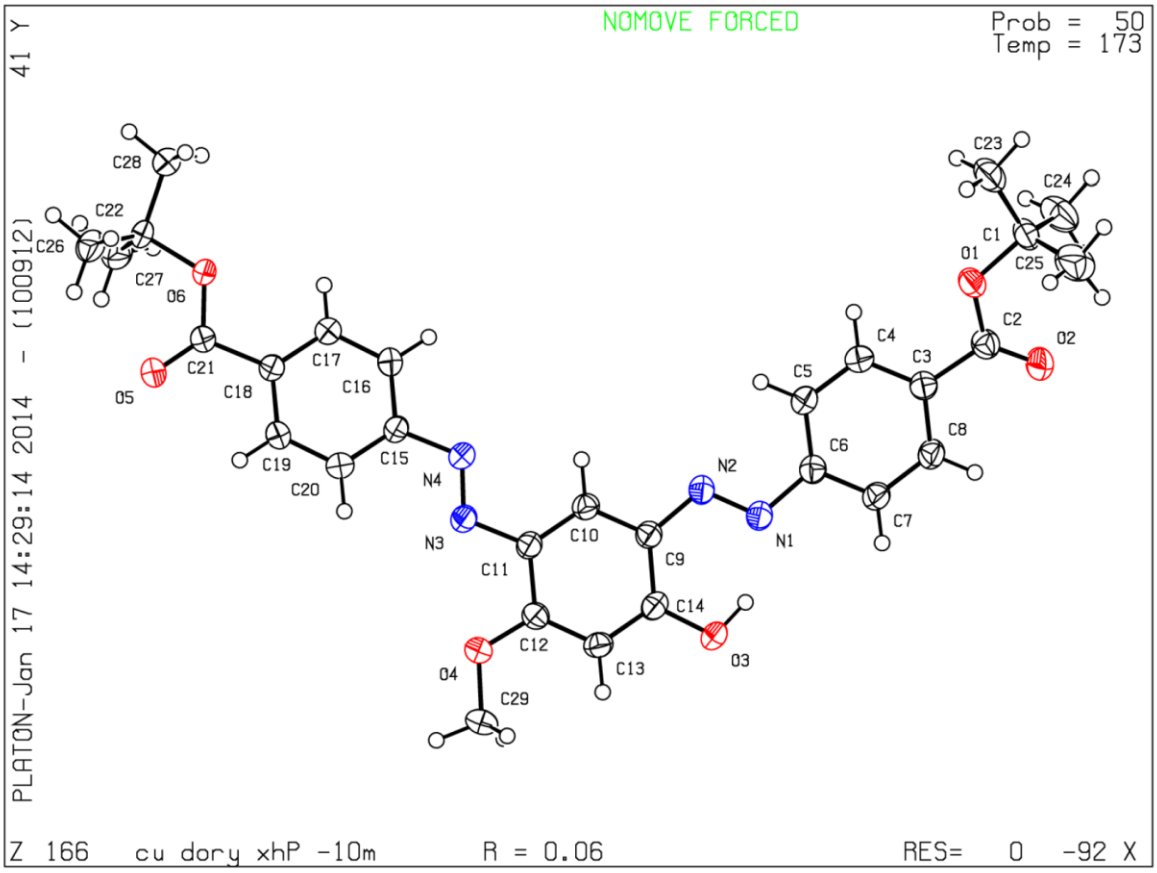

Atomic coordinates and equivalent isotropic atomic displacement parameters ($Å^2$)

	x/a	y/b	z/c	U(eq)
C1	0.2096(3)	0.63082(12)	0.80708(10)	0.0383(4)
C2	0.3741(3)	0.54595(12)	0.69741(10)	0.0355(4)
C3	0.5876(3)	0.48154(11)	0.66999(10)	0.0321(4)
C4	0.7484(3)	0.42780(13)	0.71959(10)	0.0373(4)
C5	0.9472(3)	0.37284(13)	0.69032(10)	0.0368(4)
C6	0.9887(3)	0.37157(11)	0.61029(9)	0.0306(4)
C7	0.8278(3)	0.42348(11)	0.56065(10)	0.0339(4)
C8	0.6274(3)	0.47786(12)	0.59078(10)	0.0355(4)
C9	0.5435(3)	0.22588(11)	0.58751(9)	0.0302(4)
C10	0.6998(3)	0.17351(11)	0.63843(9)	0.0307(4)
C11	0.9157(3)	0.12637(11)	0.61249(9)	0.0302(3)
C12	0.9795(3)	0.13148(11)	0.53114(9)	0.0315(4)
C13	0.8247(3)	0.18359(12)	0.47914(9)	0.0340(4)
C14	0.6086(3)	0.23010(11)	0.50582(9)	0.0317(4)
C15	0.1721(3)	0.01132(11)	0.78397(9)	0.0307(4)
C16	0.0852(3)	0.99147(13)	0.86171(10)	0.0361(4)
C17	0.2268(3)	0.93479(12)	0.91563(10)	0.0355(4)
C18	0.4556(3)	0.89743(11)	0.89159(9)	0.0312(4)
C19	0.5439(3)	0.91912(12)	0.81343(10)	0.0349(4)
C20	0.4037(3)	0.97640(12)	0.75999(9)	0.0349(4)
C21	0.6107(3)	0.82979(11)	0.94529(9)	0.0323(4)
C22	0.6318(3)	0.75697(12)	0.08241(9)	0.0333(4)
C23	0.3030(4)	0.63091(17)	0.88379(13)	0.0543(5)
C24	-0.0244(3)	0.59388(17)	0.82093(14)	0.0561(6)
C25	0.1988(5)	0.73048(15)	0.75865(14)	0.0641(6)
C26	0.8893(3)	0.76524(16)	0.08381(11)	0.0472(5)
C27	0.5951(4)	0.65718(13)	0.07107(11)	0.0467(5)
C28	0.4901(3)	0.78664(14)	0.15519(10)	0.0408(4)
C29	0.2658(3)	0.08606(13)	0.42842(10)	0.0414(4)

	x/a	y/b	z/c	U(eq)
N1	0.1943(2)	0.32145(9)	0.57478(8)	0.0320(3)
N2	0.3361(2)	0.27232(9)	0.62165(8)	0.0310(3)
N3	0.0786(2)	0.07035(9)	0.66247(8)	0.0325(3)
N4	0.0102(2)	0.06871(10)	0.73369(8)	0.0352(3)
O1	0.3889(2)	0.56196(9)	0.76990(7)	0.0395(3)
O2	0.2140(2)	0.57911(10)	0.65877(8)	0.0470(4)
O3	0.4644(2)	0.27919(9)	0.45377(7)	0.0383(3)
O4	0.1921(2)	0.08405(9)	0.50993(7)	0.0389(3)
O5	0.7881(2)	0.78202(10)	0.92293(7)	0.0468(4)
O6	0.5248(2)	0.82926(8)	0.01996(6)	0.0345(3)

Hydrogen atomic coordinates and isotropic atomic displacement parameters (Å^2)

	x/a	y/b	z/c	U(eq)
H4	-0.2793	0.4291	0.7739	0.045
H5	0.0556	0.3360	0.7244	0.044
H7	-0.1453	0.4218	0.5064	0.041
H8	-0.4837	0.5129	0.5569	0.043
H10	0.6573	0.1699	0.6928	0.037
H13	0.8676	0.1873	0.4248	0.041
H16	0.9283	0.0168	0.8780	0.043
H17	1.1674	-0.0784	0.9688	0.043
H19	1.7011	-0.1057	0.7971	0.042
H20	1.4649	-0.0081	0.7072	0.042
H23A	-0.6831	0.5653	0.9136	0.082
H23B	-0.8054	0.6749	0.9134	0.082
H23C	-0.5420	0.6526	0.8740	0.082
H24A	-1.0830	0.5940	0.7709	0.084
H24B	-1.1369	0.6358	0.8512	0.084
H24C	-1.0056	0.5278	0.8498	0.084
H25A	-0.6412	0.7461	0.7434	0.096

	x/a	y/b	z/c	U(eq)
H25B	-0.8903	0.7783	0.7892	0.096
H25C	-0.8790	0.7317	0.7119	0.096
H26A	1.9798	-0.2558	1.0373	0.071
H26B	1.9483	-0.2758	1.1303	0.071
H26C	1.9060	-0.1673	1.0848	0.071
H27A	1.4285	-0.3430	1.0660	0.07
H27B	1.6432	-0.3903	1.1160	0.07
H27C	1.6899	-0.3597	1.0238	0.07
H28A	1.5102	-0.1471	1.1589	0.061
H28B	1.5451	-0.2573	1.2010	0.061
H28C	1.3233	-0.2165	1.1527	0.061
H29A	1.1477	0.0626	0.4039	0.062
H29B	1.4169	0.0444	0.4219	0.062
H29C	1.2832	0.1525	0.4039	0.062
H3	0.335(5)	0.3077(18)	0.4818(16)	0.067(7)